63-42

WEB SUBTASK 13.009
THE RESPONSE OF SOILS
TO DYNAMIC LOADINGS, REPORT 16

EFFECTIVE STRESS vs. STRENGTH SATURATED FAT CLAY

Archie M. Richardson, Jr.

R63-20

April 1963

MIT

DEPARTMENT OF CIVIL ENGINEERING

SCHOOL OF ENGINEERING
MASSACHUSETTS INSTITUTE OF TECHNOLOGY
Cambridge, Massachusetts

Department of Civil Engineering

Research Project 63-20

THE RESPONSE OF SOILS TO DYNAMIC LOADINGS

Report No. 16 Effective Stress Versus Strength: Saturated Fat Clay

Archie Merrill Richardson, Jr.

April 1963

Contract No. DA-22-079-eng-224
with
U. S. Army Engineers Waterways Experiment Station
Department of the Army, R and D Subproject 8-S12-95-002
under Weapons Effect Board Subtask No. 13.009

Requests for copies of this report should be submitted to:
ASTIA, Arlington Hall Station, Arlington 12, Virginia

ABSTRACT

Results of a laboratory investigation of the influence of rate of strain on the effective stress-strain behavior of a remolded, saturated clay are presented and discussed. Triaxial compression tests were performed on 1½" dia. x 3" long specimens at rates of strain ranging from 1% in ½ minute to 1% in 1440 minutes. Two extreme preshear stress histories are represented, i.e. normally consolidated and heavily overconsolidated. Pore pressures were measured in all tests at the sample midheight employing a porous probe, electric pressure transducer system. In addition, base pore pressures were measured in selected tests, also with an electric pressure transducer.

The results indicate an increase in strength in the fast tests of about 12% over the slow tests in the normally consolidated and about 20% in the overconsolidated tests. The pore water pressure at failure in both normally consolidated and overconsolidated samples was lower in the fast tests. In the overconsolidated samples, evidence of a pore water migration was obtained while pore water migration appears to have had little influence on the normally consolidated samples.

In tests with increases in strain rate from slow to fast at predetermined strain levels, the evidence of a dilatancy component of the behavior of normally consolidated samples was demonstrated.

CONTENTS

CONTENTS (Continued)

CONTENTS (Contined)

CONTENTS (Continued)

CONTENTS (Continued)

LIST OF FIGURES

LIST OF FIGURES (Continued)

LIST OF FIGURES (Continued)

PREFACE

This document is the sixteenth in a series of reports issued by M.I.T. under its present contract with the U. S. Army Engineers Waterways Experiment Station. A list of the earlier reports follows this preface. The work has been carried out in the Soil Laboratories of the Civil Engineering Department. Dr. T. W. Lambe heads the soils group. This work was performed by Archie M. Richardson, Jr., formerly Instructor in the Civil Engineering Department and now Assistant Professor at Swarthmore College, under the immediate supervision of Dr. Robert V. Whitman, Associate Professor of Civil Engineering.

A documentation of the stress-strain behavior of the saturated clay utilized in this research effort over a very wide range of strain rates appears in the tenth report in this series. Report No. 10 also includes a preliminary report based on a rough draft of the present document.

PREVIOUS REPORTS

1. "Scope of Test Program and Equipment Specifications," November 1957
2. "Test Equipment for High Speed Triaxial Tests," January 1959
3. "First Interim Report on Dynamic Soil Tests," October 1959
4. "One-Dimensional Compression and Wave Velocity Tests," August 1960
5. "Pore Pressure Measurements During Transient Laodings," November 1960
6. "Effects of Rate-of-Strain on Stress-Strain Behavior of Saturated Soils," April 1961
7. "Adaptation and Use of the Boynton Device for Rapid One-Dimensional Compression Tests," June 1961
8. "Laboratory Measurement of Dilatational Wave Propagation Velocity," June 1961
9. "Shearing Resistance of Sands During Loading," May 1962
10. "Strength of Saturated Fat Clay," June 1962
11. "Triaxial Tests Upon Saturated Fine Silty Sand," September 1962
12. "Static Tests Upon Thin Domes Buried in Sand," December 1962
13. "The Dependence of Dilatation in Sand on Rate of Shear Strain," February 1963
14. "Propagation Velocity of Ultrasonic Waves through Sand," March 1963
15. "Undrained Strength of Saturated Silty Clay," March 1963

LIST OF SYMBOLS

α = slope of failure envelope on plot of $(\sigma_1 - \sigma_3)/2$ vs. $(\sigma_1 + \sigma_3)/2$

α_v = coefficient of compressibility

A = Skempton's pore pressure parameter

B = Skempton's pore pressure parameter

C_c = consolidating compressibility

C_s = swelling compressibility

c_v = coefficient of consolidation

c_e = Hvorslev's true cohesion

$\bar{c}$ = cohesion intercept in terms of effective stresses

CU = consolidated undrained

E_c = modulus of elasticity - compressing

E_s = modulus of elasticity - swelling

e = void ratio

$( )_f$ = failure value of quantity in parenthesis

ε = strain

$\frac{de}{dt}$ = strain rate

λ = pore pressure coefficient

μ_c = Poisson's ratio - compressing

μ_s = Poisson's ratio - swelling

η_v = coefficient of volume compressibility

N.C. = normally consolidated

O.C. = overconsolidated

O.C.R. = overconsolidated ratio

ρ_e = Hvorslev's equivalent consolidation pressure

σ = stress

$\bar{\sigma}$ = effective stress

t_1 = time to 1% strain (usually minutes)

t_{+1} = time to 1% additional strain (usually minutes)

$\bar{\phi}$ = angle of shearing resistance in terms of effective stresses

ϕ_e = Hvorslev's true friction angle

Chapter 1

INTRODUCTION AND BACKGROUND

A. Introduction

The following work presents and analyzes the results of an extensive series of triaxial compression tests performed on remolded samples of a saturated fat clay. These tests were performed to determine the nature of the effect of strain rate ($\frac{de}{dt}$) upon the shear resistance of this clay. Forty one consolidated undrained (CTU) tests with pore pressure measurements were performed upon samples subjected to two extreme preshear stress histories. Twenty nine tests were upon samples normally consolidated (N.C.) from a deaired slurry. In these samples the preshear effective stress was the largest stress the sample had carried since preparation of the slurry. Twelve tests were upon samples having an over-consolidation ratio of approximately 16 (O.C.R. = 16). In these samples the preshear effective stress was on the order of 1/16 of the maximum effective stress carried by the sample since preparation of the slurry.

These tests were performed at constant strain rates varying from 1% strain in 45 seconds ($t_1 = \frac{3}{4}$), to 10% strain in 24 hours, ($t_1 = 1440$). In all tests, pore water pressure was measured at the mid-height of the test sample employing a porous stone probe and a very rigid pore pressure measuring system of novel design. This system relied upon an extremely low compliance electric pressure transducer for measurement of induced pore water pressure. In addition, selected tests were performed at representative strain rates with the pore water pressure being measured at both the mid-height of the sample and at the base. These tests were performed in order to determine the existence and magnitude of any pore pressure gradient between the mid-height of the sample and the base. Water content determinations at six levels in each sample were carried out and an attempt made to correlate the observed gradients with the observed water content variation.

Using the information gathered in the manner outlined above, the results are analyzed in terms of effective stress concepts (where effective

stress equals total stress minus pore water pressure; i.e., ($\bar{\sigma} = \sigma_t - u$). The manner in which each of the effective stress components is affected by the strain rate ($\frac{de}{dt}$) is shown. Possible macroscopic mechanisms contributing to the observed effect of strain rate upon shear resistance are suggested. Results of additional tests in which the strain rate ($\frac{de}{dt}$) is varied during the course of each test are presented to support and supplement the qualitative relationships deduced from this analysis.

The work is organized for presentation in ten chapters as follows: The remainder of this first chapter gives the background material necessary for a realization of the motivations behind this work and for the attainment of perspective as to the standing of this work historically. Chapter II describes the test program and test procedure. In Chapter III are presented the results of tests upon normally consolidated samples with uniform strain rates while Chapter IV presents test results obtained in tests on normally consolidated samples where the strain rate was altered during the course of the test. In Chapter V the behavior of the normally consolidated specimens is summarized. This summary draws together and describes all the features of behavior which must be satisfied by any mechanism proposed to explain this behavior. An attempt is then made to describe this observed behavior in terms of a macroscopic and microscopic structural behavior mechanism.

The results of tests upon overconsolidated specimens tested with uniform strain rates are presented in Chapter VI and the results of tests upon overconsolidated samples in which the rate of strain was changed drastically during the course of the tests are presented in Chapter VII. Again the significant features of these tests in terms of observed behavior that must be satisfied by any proposed mechanistic theory are drawn together in Chapter VIII.

Chapter IX presents the results of all of the tests in terms of the Hvorslev "true friction" and "true cohesion" components of shear strength. (HVORSLEV, 1937). In so far as possible, the observed

relationship between shear strength and strain rate is explained in terms of change in these "true" strength-effective stress parameters. Finally, Chapter X summarizes the entire work and points up areas of weakness as avenues for further research.

In addition, there are two appendices to the work. Appendix A describes in detail the pore pressure measuring system employed in this research and presents data indicating the performance of this system. In addition it describes the author's experience gained in the development of this system. Appendix B presents and documents the results from each individual test.

B. Background

The understanding of the magnitude, nature and mechanism of the effect of rate of strain on the stress vs. strain behavior in soils is of far more than academic interest. Any attempt to utilize the results of laboratory tests in an analysis of field stability requires that the effects of the differences in rates of strain between the laboratory and the field be either slight or predictable. In general, when used in situations where these parameters are appropriate, the usual effective stress parameters $\bar{\phi}$ and $\bar{c}$ or the undrained shear strength as determined by customary laboratory tests or by field vane tests, where such laboratory or field tests are carried out within the range of convenient strain rates, give results that have been shown to be within the limits of engineering acceptability. However, certain noteworthy exceptions do occur.

At present, no analysis of stability can be made with any certainty in stiff, fissured clays. The clay shales of the prairie regions of the U. S. and Canada (for example the Bearpaw Shale) and the London Clay are two well known examples. The best that can be said at this time is that $\bar{c}$ (the intercept on the y axis of the plot of shearing resistance on the failure plane at failure vs. the effective stress on the failure plane at failure) seems to decrease with time. Thus, one of

the present day problem areas in soil mechanics is almost certainly a strain rate or at least a time problem. The other notable situation in which the use of laboratory parameters of shear strength behavior gives dubious results is found with some of the highly sensitive clays where $\bar{\phi}$ in the field is much less than laboratory tests indicate. This may or may not be partly or entirely a strain rate effect. A discussion of these situations is found in (BISHOP AND BJERRUM, 1960).

Present day concern for protective construction to resist blast effects and associated impact loading problems in foundation engineering gives the search for an understanding of the nature of strain rate effects much of its current urgency. In addition, the analysis of the stability of building foundations and slopes against stress imposed by earthquakes is currently receiving much attention. Highway and airfield pavement design and trafficability studies in general are additional areas in which the need for strain rate effect information is felt keenly. However, of much more importance is that present day parameters of stress vs. strain behavior in soils represent descriptions of observed laboratory behavior and are probably not fundamental. To begin to really understand the nature of the resistance of soils to applied stresses and the reason for the resulting strain patterns, regardless of the rate of stress or strain application, should be an underlying motive of soil mechanics research and it is hoped that the present work contributes, no matter how slightly, and thus lives up to this philosophy.

Previous research has been performed in several laboratories by numerous investigators. Most of this work has been concerned with observation of the increase of shear strength and the alteration of the shape of the shearing resistance versus strain curve with increased strain rates and a good deal of the available data concerns unsaturated (compacted) soils. (See for instance M.I.T. 1959). Tests on saturated sands with rapid load applications in which attempts were made to measure pore water pressure were begun at the Massachusetts Institute of Technology in the early part of the 1950's (M.I.T. 1954). Tests of

this nature are being performed on a much refined basis at M.I.T. today and a demonstration of the nature of the strain rate effect in sands has been made. (WHITMAN & HEALY, 1961, HEALY 1962).

Significant work with saturated clay shales and soft rock was undertaken at Harvard in the latter 1940's and early 1950's (CASAGRANDE and SHANNON, 1948) and (CASAGRANDE and WILSON, 1951). All of this early work can be found very nicely summarized in (WHITMAN, 1957a) and (WHITMAN 1957b).

Most of this research, however, has been in terms of total stress application with pore pressure measurements being attempted only in a few isolated instances and then only in saturated sands. Therefore, little light has been shed on the fundamental mechanisms contributing to the observed and documented relationship of shearing resistance to rate of strain. However, two notable studies of the relationship of effective stress parameters of shear strength behavior to rate of strain have appeared quite recently and are summarized below:

1. (CRAWFORD, 1959)

This research consisted of triaxial compression tests with base pore water pressure measurements performed upon samples of undisturbed Leda clay cut from a single block. The Leda clay is a widely distributed clay found along the Ottawa and St. Lawrence Rivers in the U. S. and Canada. It is usually highly sensitive and exhibits compression and shear strength properties indicative of a slight to moderate degree of overconsolidation.

The soil tested was rather plastic (liquid limit = 65%, plasticity index = 40%) and had a natural water content slightly above the liquid limit. Tests were performed with preshear consolidation pressures ranging from 2.0 kg./cm.^{2} to 6.0 kg./cm.^{2} where the adjudged preconsolidation load was 2.75 kg./cm.^{2}. The rates of strain considered ranged from an actual time to failure of 7.8 minutes (t_1 = 6 minutes) to an actual time to failure of 1320 minutes (t_1 = 1300 minutes).

The results of this research can be summarized as follows:

i. The deviator stress at failure increases with increasing strain rate. The absolute magnitude of this strength increase seems independent of the consolidation pressure, and therefore represents a greater percentage increase at lower consolidation pressures.

ii. The measured pore water pressure at failure (u_f) was higher in the tests with the lower strain rates, (i.e. as the strain rate increased the pore water pressure at failure decreased) in the range of strain rates considered. This decrease was slight in the slightly overconsolidated samples (σ_{cons} = 2.0 kg./cm.^{2}) and of considerable magnitude in the samples with σ_{cons} = 6.0 kg./cm.^{2}.

iii. Looked at in terms of the pore water pressure parameter A, where $A = \frac{\Delta u}{\Delta(\sigma_1 - \sigma_3)}$ (SKEMPTON, 1954), in all cases A was less in the tests with rapid strain rates (i.e., as $\frac{de}{dt}$ increased, A_f decreased).

iv. The magnitude of this decrease in A_f was sufficient to more than offset the noticed decrease in $\bar{\phi}$ (where A_f and $\bar{\phi}$ were measured at maximum $(\sigma_1 - \sigma_3)$). The value of $\bar{\phi}$ was found to be smaller at the higher strain rates than at the lower strain rates, the range being from $\bar{\phi} = 23^\circ$ in the tests at the slow strain rate to $\bar{\phi} = 17\frac{1}{2}^\circ$ in the fast test. This was accompanied by a slight increase in the cohesion intercept ($\bar{c}$) from the slow tests to the fast tests.

v. The strain rate effect in the slightly overconsolidated samples was attributed to a loss of the effects of preconsolidation with decreasing rates of strain.

vi. Evidences of gradients in the pore water pressure within the sample at the faster strain rates was noted in the post shear water content distribution. These data seem to indicate higher pore water pressures in the center of the sample than at the base.

vii. In creep type tests in which a constant deviator stress is applied and allowed to remain, the pore water pressure was seen to be a linear function of strain.

2. (BJERRUM, SIMONS and TORBLAA 1960)

This research consisted of 36 consolidated undrained tests, with pore water pressure measured in all but the most rapid tests, and 21 consolidated drained tests. The variation of the rate of strain in the undrained tests was from 100% per hour (45 seconds to 1%) to 0.0036% per hour (300 hours to 1%). The range of strain rates in the drained tests was from 1.3% per hour to .033% per hour.

The clay tested was an undisturbed, normally consolidated marine clay from Fornebu, Oslo, Norway, both less plastic and less sensitive than the Leda clay. Preshear consolidation pressures of 1.0 kg./cm.^{2}, 2.0 kg./cm.^{2} and 4.0 kg./cm.^{2} were used for both the undrained and the drained tests.

Following is a summary of the principal results obtained from this research:

i. In the undrained tests, the deviator stress at failure increased as the time to failure decreased. The absolute increase increased with increasing preshear consolidation pressure and thus differed slightly from the Leda clay.

ii. In the undrained tests, the excess pore water pressure at failure increased as the time to failure increased. It should be mentioned here that in undrained tests of as long duration as the slow tests described in this work, membrane leakage can significantly influence the measured pore water pressure.

iii. In these tests, the pore water pressure parameter A increased as the time to failure increased, but not sufficiently to account for the loss of strength.

iv. The additional loss of strength was accounted for by an observed decrease in the angle of shearing resistance in terms of effective stresses, $\bar{\phi}$, of from 30° to 25.5° as the time to failure increased. This occurred with no change in the cohesion intercept $\bar{c}$.

v. The axial strain necessary to produce failure increased as the time to failure decreased in the undrained tests and to a lesser degree in the drained tests.

vi. The maximum deviator stress in the drained tests was constant regardless of the strain rate. It was postulated that the decrease in effective stress parameters was offset by a decrease in water content due to secondary consolidation type phenomena.

In comparing and contrasting the research just described, the following summary statements may be made. As the work at the Norwegian Geotechnical Institute was confined to normally consolidated samples, this summary pertains only to such samples. In both investigations the maximum deviator stress increased as the strain rate was increased (i.e., a higher strength was attained in the more rapid tests). In both investigations the pore water pressure at maximum deviator stress and the pore pressure parameter A increased in tests with slower strain rates.

In the Canadian work the strain necessary to achieve maximum deviator stress was more or less independent of the strain rate. In contrast, the Norwegian investigation showed larger strains at failure in the faster tests. More importantly, the Norwegian work showed larger $\bar{\phi}$ values in the faster tests, while the Canadian work produced exactly opposite results (i.e., $\bar{\phi}$ larger in the slower tests). The Canadian work shows $\bar{c}$ (the τ axis intercept in a plot of shear stress on the failure plane at failure versus the effective normal stress on the failure plane at failure) increasing with increasing strain rate, while the Norwegian work suggests that $\bar{c}$ remains unchanged.

In addition, two very recent publications of the Soil Engineering Division at the Massachusetts Institute of Technology present research that paved the way for the work to be described in the following chapters. In (M.I.T. 1961) the results of rapid tests on a saturated loess and of a very preliminary series of tests on the same clay used in the research to be described, are presented. The assumption is made that the Hvorslev

parameters of shear strength behavior ϕ_e and c_e are independent of time to failure and the pore water pressures necessary at failure to produce the observed strain rate effect are deduced. In light of the present work this assumption is somewhat unjustified, but nevertheless the analyses shed light on the probable patterns of pore water pressure behavior.

(NASIM 1961) presents the results of an extensive series of triaxial compression tests with no pore water pressure measurements. These tests were performed on samples of the same clay described in the following work and prepared in a similar manner. The rates of strain employed overlapped the present work and extended to quite rapid rates. Thus the results of that research fully document the nature and magnitude of the effect of rate of strain on the total stress vs. strain behavior of this soil.

Chapter II

DESCRIPTION OF TEST PROGRAM AND TEST PROCEDURE

A. Introduction

This chapter describes the test program undertaken in the course of this work and the procedure employed in its performance. This test program consisted of a total of 43 triaxial compression tests on a single very fat clay with a permeability on the order of 10^{-9} cm./sec. Prior to shearing, the samples were subjected to two stress histories. Ten samples were overconsolidated to an overconsolidation ratio of approximately 8 atmospheres gauge and subsequently allowing rebound to approximately 1/2 atmosphere. The exact pressures used tend to differ from test to test due to the calibration difference of the several gauges used. These pressures were corrected by comparison with one accurately calibrated gauge. The remainder of the samples were normally consolidated to approximately 4 atmospheres gauge.

In general the tests were performed at rates of strain which can be grouped in two categories, fast and slow. The majority of the slow tests were performed at strain rates of approximately 1% in ten hours. ($t_1 = 600$) This strain rate is about half that which would be considered "normal" for triaxial testing with pore pressure measurements on this clay. The fast tests were performed at rates of strain on the order of 1% in one minute, ($t_1 = 1$) which is, of course, considerably more rapid than the strain rate which would be considered "normal". In addition, scattered tests performed at strain rates faster, slower, and intermediate were performed in an attempt to gain a complete picture.

Most of the tests were performed at a constant rate of application of deformation to the sample-proving ring system. This resulted, for all practical purposes, in a uniform rate of strain since the proving ring chosen was of sufficient stiffness to contribute little to the deformation. In addition, in several tests, the strain rate was changed abruptly during the course of the test. In all tests, pore water pressure was measured at the mid-height of the sample by a rather unique pore water pressure

measuring system. In selected tests, pore water pressure was measured at the base of the test sample in addition to the mid-height.

The principal results of all of the tests, the preshear history of each sample and other pertinent data are presented in Appendix B.

B. Description of Soil

The soil used for these tests was considered to be representative of a very fat clay. The soil itself was obtained from the Waterways Experiment Station of the U. S. Army Corps of Engineers, Vicksburg, Mississippi. Several shipments of this soil have been sent to the Soil Engineering Division at M.I.T. in the past several years. The preliminary series of 11 tests were performed upon assorted samples of this soil remaining from previous research efforts, primarily (M.I.T. 1959) and (NASIM, 1961). The soil used in the main series of tests was set aside from a shipment of the soil received in the summer of 1960, being "Barrel D" described in (M.I.T., 1959).

The soil used in the main series was shipped to M.I.T. in a 55 gallon drum. It had been air dried and coarsely pulverized. The sample was obtained from a typical backswamp deposit of the lower Mississippi valley. The geological history of such a deposit is described in (KOLB and SHOCKLEY, 1957). The soil is a fat clay, impermeable and quite plastic. A plot of grain size distribution of the soil used in the main series of tests is given in Figure 1. The plasticity characteristics of the soil used for the main series of tests are plotted in a Casagrande type plasticity chart in Figure 2. In addition, on this chart, are plotted the plasticity characteristics of several other shipments of this soil and references are given to the sources. Table II-1 contains a complete mineralogical analysis of a sample of the minus 74 micron fraction of the soil from a previous shipment, but there is no reason to suspect that this fraction of the soil differs in mineralogical composition from shipment to shipment. In addition, engineering properties appropriate to the soil utilized

in this research appear in this table.

C. Preparation of Samples

The preliminary series of tests, P-1S through P-9F, were performed upon samples remaining from the research described in M.I.T. (1959) and NASIM (1961). As little other than preliminary feelings and experience in setting up tests was gained from these tests, little concern is expressed regarding the exact source of each sample.

As the successful use of the device employed to measure the pore water pressure at the mid-height of the sample demands a completely saturated soil sample, and as some variation from absolute saturation was encountered with the preliminary samples, a revised method for preparation of samples consolidated from a slurry was deemed necessary. A small batch, Batch A, was prepared from a quantity of the soil in the drum to be used for this research.

Table II-1

DESCRIPTION OF THE CLAY

A. Mineralogic Composition of Minus 74μ Fraction By Weight

1.	Illite	25% ± 3
2.	Montmorillonite	25% ± 3
3.	Quartz	20% ± 3
4.	Feldspar	20% ± 10
5.	Fe_2O_3	1.9% ± 0.1
6.	Organic Matter	1.1% ± 0.1

B. Engineering Properties

1. ϕ' normally consolidated + 23° ± 2°
2. Permeability $K \approx 10^{-9}$ cm/sec.
3. Consolidation characteristics

$C_c = 0.52 \pm 0.04$, $c_v = 2 \times 10^{-3}$ $Cm^2/sec.$

(a) Preparation of Batch A

This soil was air dried and reduced to a fine powder by mechanical grinding. A quantity of deaired, demineralized water was set boiling in an enameled pail. The powdered soil was sprinkled in a very fine layer on the surface of this water, and allowed to saturate itself from the bottom and sink into the pail. The mixture was stirred with minimum disturbance with a small paddle, and the sequence of events repeated. A very small flame was maintained on the bottom of the pail as this operation proceeded, to maintain the mixture at boiling. When a slurry of the proper consistency had been obtained, it was transferred to a vacuum dessicator in the following manner:

A 1-inch layer of boiling, deaired water was placed in the dessicator. A scoop of the slurry was carefully obtained from the pail and deposited beneath this layer of water. Extreme care was taken to introduce no air bubbles, any small surface air bubbles being removed with a spatula. The slurry in the pail was gently and continually stirred. When the slurry had been entirely transferred to the vacuum dessicator, the lid was applied and the chamber over the surface of the slurry evacuated and kept evacuated for 48 hours. It was felt that in this manner any small air bubble in the body of the slurry would go into solution as the slurry cooled, but that the slurry would still not be in equilibrium with dissolved air due to the maintenance of a vacuum over its surface.

A 1-inch layer of deaired water was then placed in the bottom of a standard 4 inch diameter consolidometer which had been modified by the addition of a lucite sleeve to extend its height to 8 inches. The stone at the base of this consolidometer had previously been deaired by boiling and the bottom drainage system had been saturated. The slurry was then transferred to this consolidometer in exactly the same manner as it had been placed in the vacuum dessicator, i.e., by careful deposition beneath the surface of the layer of deaired water. When the consolidometer had been filled, the actual consolidation

load was applied in the usual manner on a Fairbanks-Morse Scale, in increments starting with 1/16 of a ton per sq. ft., and doubling until 1 ton per sq. ft. was attained. Each increment was permitted to remain three days, except the final one, which was maintained for one month. The cake of soil thus obtained was ejected from the consolidometer and stored in Mobil AB Transformer oil, an extremely inert oil, until wanted for testing. Two samples only were obtained from this Batch A.

(b) Preparation of Batch B and Batch C

As the general method of batch preparation was deemed satisfactory, a quantity of the soil sufficient for the main series of tests was taken from the shipment, air dried and finely ground. An identical procedure for the preparation of a slurry was followed. This slurry was placed in a large 9½ in. I.D. x 7 in. high Teflon-lined consolidometer (described fully in M.I.T. 1961). The consolidation pressure was applied to the top piston through transformer oil and an air-oil accumulator. The load was applied in increments as with Batch A. At the completion of consolidation, the large "cake" was ejected and stored in transformer oil until needed. Two batches, Batch B and Batch C were prepared in this manner. Approximately 20 samples could be cut from each large "cake". Although every precaution was taken to insure that the two batches, B and C, be identical, the water content from trimmings of Batch B samples averaged approximately 41%, while Batch C samples averaged about 40%. However, no immediately discernible difference in the water contents of the samples from Batches B and C was evident following testing.

D. Preparation of Individual Samples for Testing

Individual samples were cut from the large cakes of soil stored in the transformer oil as they were needed for testing. Samples were trimmed on the Norwegian Geotechnical Institute trimming frame.

This frame produces samples having a height of 8.0 cm. (3.15 in.) and a cross-sectional area of 10.0 sq. cm. (1.53 sq. in.).

Samples P-1F, P-2F, P-5S and P-6S of the preliminary series were set up as follows:

The base of the triaxial cell to be used was thoroughly deaired. It was then placed in a basin of deaired water. The level of the water in the basin was at least 2 inches above the top of the stone on the pedestal of the cell. One latex membrane was fastened to the base of the cell with a rubber "O" ring and the trimmed sample set upon the stone on the pedestal. The membrane was rolled up the sample, bringing a ring of deaired water up along with it; rolled up on the lucite top cap and secured with "O" rings. The top cap used in these tests was provided with a deaired stone and saturated drainage line leading out of the cell, so that double drainage was provided.

The membrane was grasped with the tips of a pair of longnosed pliers at mid-height and snipped in front of the pliers with a sharp pair of scissors making a small, circular hole in the membrane, and the deaired pore water pressure probe pushed horizontally into the sample through this hole. This operation was conducted beneath the surface of the water. The water level in the basin was then lowered beneath the level of the needle, and the opening cleansed with alcohol and sealed with rubber cement. Approximately 6 hours were required to permit drying of the rubber cement. The drainage lines were opened all this time, and allowed to remain open, as was the line leading from the probe. In earlier experimenting it was observed that cavitation of the water occurred in the tube leading to the probe if it were to be closed off.

The chamber of the cell was then replaced and filled with deaired water. The top half inch of the chamber was supplied with a layer of oil, the piston inserted, and the cell attached to the source of chamber pressure. Following application of the chamber pressure the tubing leading from the pore water pressure probe was blocked off.

The chamber of the cell was then replaced and filled with deaired water. The top half inch of the chamber was supplied with a layer of oil, the piston inserted, and the cell attached to the source of chamber pressure. Following application of the chamber pressure the tubing leading from the pore water pressure probe was blocked off. The progress of consolidation was checked from time to time by measuring the mid-height pore water pressure.

Two objections to this method rapidly became apparent:

1. Since no filter strips were used, an excessive time was required for consolidation of the samples. This time was in excess of 45 days.

2. As the pore water pressure probe was inserted, the sample was seen to develop a split. This split was not horizontal, but was usually quite steep, oriented at more than 60° to the horizontal. In attempt to avoid this splitting, a piece of stainless steel tubing slightly smaller in diameter than the probe was sharpened at one end, and a hole formed in the sample beneath the surface of the water before the probe was inserted. In all cases a nice core was removed with this sampling tube, but the sample split very soon after the core was withdrawn, and long before the probe was inserted.

In additional experimenting, it was found that a hole could be formed in the sample with the sample out of the water and with the stainless steel borer completely dry. If one drop of water were then to be placed in the hole thus formed, the sample split quite rapidly. This splitting represents a tension failure of the sample due to forces associated with release of the pore water tension adjacent to the hole and consequent central swelling of the sample.

One additional objection to this method of setting up the samples is the fact that only one membrane can be provided for, and the problem of membrane leakage becomes overwhelming.

To avoid the problems associated with the previously described procedure, the following system was devised and employed in setting up all of the main series of tests with only very minor exceptions as noted.

The base of the triaxial cell was modified by drilling a 0.03" diameter hole vertically through the very edge of the pedestal as described in Appendix A. The small diameter Teflon tubing from the pore water pressure probe was passed out of the triaxial chamber through this hole. The space between the outside of the tubing and the walls of the hole was sealed with an Epoxy resin. This base, stone, tubing and pore pressure probe were deaired by boiling, flushing boiling water through all tubing and drainage connections and allowing the base, in boiling water, to cool beneath a vacuum in a vacuum dessicator. With the cell base beneath water, two latex membranes were affixed to the base with "O" rings.

A hole slightly smaller in diameter and slightly shorter than the pore water pressure probe was formed at mid-height of the soil sample. This operation was performed using the stainless steel boring tool described previously, fixed in the chuck of a drill press to insure vertical alignment. The trimmed sample in the NGI trimming cradle was placed on the bench of the drill press, the hole located and formed by vertical motion. No rotation of the boring tool was permitted. The sample was then carefully and squarely sliced in half horizontally through the axis of this hole with a fine wire saw.

The bottom half of the sample was placed on the stone of the pedestal of the triaxial cell base, submerged as before in a basin of deaired water to a depth sufficient to cover by one-half inch the top of the bottom half of specimen. The porous stone probe was then placed carefully in the trough representing the bottom half of the bored hole and the top half of the sample fitted in place with the utmost care. Gentle pressure axially was then applied with the specimen cap to insure seating of the two surfaces.

A band of latex membrane 3/8 inch in width was placed over the cut, thus forming a dam insulating the region of the probe from the four filter strips which were then applied to the sides of the sample. One latex membrane was then rolled up and the water level lowered to the level of the pedestal of the cell. It is to be noted that this arrangement allows the Teflon tubing to the pore water pressure probe to spiral around the sample under the rubber membrane. A thick layer of silicone grease was then applied to the sample and the second membrane rolled up and both membranes sealed to the top cap with two "O" Rings. The cell chamber was fastened in place and filled as before.

The exceptions to this procedure are as follows:

1. Samples P-8S, P3F, P4F, P9S had only one membrane.
2. In samples OC6S, OC1F, OC2F, OC7S and OC8S, outer membrane was also rolled up under water. This was seen to be equivalent to having only one membrane as a layer of water was trapped between the two membranes and remained there during testing.

E. Consolidation in the Triaxial Cell

Following setting up the samples, the triaxial cells were connected to a source of pressure and consolidated. In the normally consolidated samples, this source of pressure consisted of Bishop type self-compensating mercury pots, (BISHOP & HENKEL, 1957). Since the available mercury pressure system was limited to 4 kg/cm^2, it was necessary in the case of the overconsolidated samples to apply the pressure through water to a water-nitrogen gas accumulator. The pressure in the nitrogen gas was controlled with a regulator. This later source of pressure was somewhat less than satisfactory. Two samples had to be discarded due to the escape of nitrogen gas bubbles from solution following diffusion through either the membrane or tube leading from the porous probe.

In the normally consolidated samples, a preliminary pressure of 30 lb./in.^{2} was maintained for approximately one hour before the entire consolidating pressure of approximately 60 lb./in.^{2} was applied. Drainage from the tube leading to the probe was closed off immediately following application of the first pressure to the chamber. Consolidation was permitted to proceed until no more than 0.1 cc. of water per day was being expelled from the sample. This occurred in seven days.

The same procedure was followed with the overconsolidated samples, up through the application of the 60 lb./in.^{2} pressure. This pressure was maintained for three days and then increased to approximately 120 lb./in.^{2}. This latter pressure was held for about a week, or until less than 0.1 cc./day was being expelled by the sample. The tubing leading to the probe was then opened and placed in a container of deaired water. This was to prevent cavitation of the water in the tubing. The chamber pressure was gradually reduced to about 7.0 lb./in.^{2}, allowing several hours in most cases for this reduction. This rebound pressure was maintained for about a week or until the criteria established above was met.

F. Testing

Following consolidation, the samples were sheared. Connection was made to the pore water pressure measuring transducer, outside the cell, as described in Appendix A, and electrical connections made to the recording equipment. The triaxial cells were placed in a Wykeham-Farrance load frame and a proving ring seated atop the piston. Two rather stiff proving rings were calibrated and set aside for this research. They were of a stiffness to strike a happy medium between accuracy and nonuniformity of strain rate due to compression of the proving ring. These rings were calibrated one against the other.

Following attachment of the pore water pressure measuring devices as described in Appendix A, check was made of the response time of the system. This was accomplished in the case of normally

consolidated samples by increasing the chamber pressure 10.0 lb./in.^{2}, recording the time to 90%, 95%, and approximately 100% response, and then reducing the chamber pressure to its original value. In all samples in the main series, essentially 100% response was obtained in 60 seconds or less. This is an excellent response for a pore pressure system when used in a clay with as low a permeability as this. It represents performance superior to that recorded by (TAYLOR, 1954) in which 100% response was attained in 10 seconds in Boston Blue Clay.

In the overconsolidated samples, the same procedure was followed, but more than 10.0 lb./in.^{2} was applied and this pressure was allowed to remain as a back pressure. If the response was less than 100% in 60 seconds, another 10 lb./in.^{2} increment was added, and this repeated until the desired response was attained. However, it was a rare occurrence indeed when the response to the first increment was unsatisfactory.

The question of whether the 60 second response represents, in part, a compression of the Teflon tubing by the chamber pressure is answered by the results of a test, appearing in Appendix A, in which increments of deviator stress were applied and the resulting response in pore water pressure measured. Here the response to a deviator stress application is seen to occur fully in about the same time as a response to a chamber stress application. The Teflon tubing is quite rigid, being in effect a thick walled cylinder, and the effect of compression of the tubing is seen to be quite small.

Compression at a constant rate was carried out until a distinct failure plane was observed, or until reasonable equilibrium of all measurements had occurred. The normally consolidated samples were usually carried to 12% strain. Following testing, the samples were dismantled and water content samples taken from six levels in the sample, with the very top and the very bottom being discarded.

Approximately 5 minutes were required for this dismantling and water content determination.

The usual question of the effects of piston friction crop up at this time. Extreme precautions were taken to have a properly fitting piston at all times. The pistons were cleaned thoroughly after each use, lubricated and checked to insure that they fell under their own weight when fitted in their bushing. Occasionally they were polished with "Noxon" as the program progressed. No notice of any reasons for concern appeared either as the tests progressed or as the data were plotted. Cells both of Norwegian Geotechnical Institute and of Clockhouse Ltd. manufacture were used, with no preference noted. However, it should be kept in mind that piston friction is a factor in all triaxial testing with external load measurement.

Chapter III

NORMALLY CONSOLIDATED SPECIMENS WITH UNIFORM STRAIN-RATE

A. Introduction

The following chapter presents and discusses the results of a series of triaxial compression tests upon normally consolidated samples of the Vicksburg clay. These tests were performed at uniform strain rates representing times to 1% strain varying from 45 seconds to 24 hours ($t_1 = \frac{3}{4}$ to $t_1 = 1440$). In some of these tests, the strain rate was "stepped" (i.e., the test was begun at one strain rate, and the strain rate was abruptly shifted at some predetermined strain to one either faster or slower). The data regarding the behavior of these samples subsequent to this "step" in strain rate are presented in Chapter IV. However, data from the earlier portions of these tests, prior to the step in strain rate, are included with the data from the tests run to completion at a constant strain rate, and are included in the summaries appearing in this chapter.

B. Presentation of Results - Normally Consolidated Samples - Uniform Strain-Rate

This section presents in summary fashion, the results of all of the tests performed upon the normally consolidated samples. Complete plots of stress versus strain, pore water pressure versus strain, obliquity versus strain and stress vector plots are presented in Appendix B.

The results of nine of the eleven preliminary tests are included in Appendix B in Figure B-1. The results of tests P1-F, P2-F, P5-S, P6-S, and P7-S are seen to be quite erratic. This is felt to be due primarily to two factors: splitting of the sample at the time of insertion of the pore water pressure probe and incomplete

consolidation of the sample. The results of tests P8-S, P3-F and P4-F are felt to be reasonably reliable, and quite interesting in themselves as will be discussed later. However, some doubt can be cast on even these tests in the preliminary series as in all but P3-F there is evidence of irregularities in the test. Test P8-S had to be stopped in the middle to correct trouble with the measuring system, and P4-F shows evidences of membrane leakage. In test P9-S an attempt was made to use a needle or probe type measuring system at a level 1/8 inch above the base in addition to mid-height. There was excessive lag in both measuring systems and the needle at mid-height appeared to be non-functioning. In summary, the results of these preliminary tests are generally not reliable. However, tests P3-F, P4-F and P8-S do point out interesting trends.

The void ratio (or water content) data following triaxial consolidation are presented in Figure 3. This data was obtained from three research efforts: that described in this thesis, M.I.T. (1959) and NASIM (1961). The majority of the data gives parallel virgin and rebound lines. The difference in placing of these lines is felt to be due to differences in water content of the slurry from which they were consolidated, and, in addition, the extreme difference recorded by the data from M.I.T. (1959) may include the effect of non-saturation. If the slightly flatter normal consolidation curve for Batches B and C is real, it no doubt represents the effect of heating the slurry. Scatter was noted in the data from all sources, and the range of scatter in the data from Batches B and C is indicated. In the performance of the research described in this work, several gages were employed for the measurement of consolidation pressure. When the gages were subsequently calibrated, slight deviations from the anticipated consolidation pressure were seen to have occurred. However, the scatter of water content data within the small range of this pressure deviation is completely random, as is

the scatter in the maximum deviator stress for any nominal consolidation pressure. However, marked differences in undrained shear strength at a given consolidation pressure occurred from one research effort to another, I.e., those appearing in this work, in M.I.T. (1959) and in NASIM (1961). These marked deviations can be directly attributed to water content variations for a given consolidation pressure from one research effort to another.

Figure 4 presents the maximum deviator stresses obtained from all tests on the normally consolidated samples ploted against the logarithm of time to 1% strain. $[(\sigma_1 - \sigma_3)$ max. vs. log $t_1]$. As tests NC9-SF, NC10-SF, NC11-SF and NC18-SFLC involved a "stepped" strain rate, and as this "step" occurred in most cases prior to the attainment of maximum deviator stress, the values of maximum deviator stress from these tests were obtained by an extrapolation of the stress vs. strain curves from these tests. In addition, data from NASIM (1961) are also shown on this plot and the slope of the deviator stress versus logarithm of time to 1% strain is seen to be identical with that of data from the current work.

The results of all of the rapid tests on normally consolidated samples are plotted in Figure 5. The deviation of test NC2-F from the average stress versus strain curve drawn in Figure 5 is felt to be due to the fact that this sample was allowed to consolidate considerably longer than the others and the effects of aging may be evident. Test NC18-SFLC was performed with a modified triaxial cell having a load measuring cell in the base. There is some question about the calibration of the load cell, and the drainage system permitting consolidation of the sample was known to leak. Tests NC3-F, NC4-F and NC5-FS will be seen to give almost identical data and have been relied upon heavily when drawing the average stress versus strain plot. Below the stress versus strain plot in Figure 5 is a pore water pressure versus strain plot. The same comments applying to the stress strain curve apply here with tests NC3-F, NC4-F and NC5-FS yielding quite consistent data.

The results of all the slow normally consolidated tests that had been consolidated to near 60 lb./in. are plotted in Figure 6. This plot represents the results of eleven tests. Unfortunately, the curves at large strains must rely heavily on the results of NC7-S. The curves as given (Figures 5 and 6), however, no doubt represent good typical curves for the rapid and slow strain rate, with NC2-F representing the only major deviation. (see Figure 5)

These average curves from Figures 5 and 6 have been reproduced in Figure 7 with the curves of stress and pore water pressure versus strain obtained from Test NC6-S superimposed. This test is assumed to be representative of a test performed at an intermediate strain rate. The average time to 1% strain as a measure of strain rate is marked on each curve.

The information presented in these average or typical curves was used to deduce the plot shown in Figure 8. This figure is a plot of the principal stress ratio ($\bar{\sigma_1}/\bar{\sigma_3}$) versus strain, with the times shown on the curve being the time to 1% strain as a measure of strain rate. This plot, in conjunction with Figure 7, presents the two components of resistance to shear stress and shows how they develop with strain. The comparison of the development of these two components is shown in Figure 9, which is a plot of $\frac{\Delta u}{\sigma_3} \Big/ \left(\bar{\sigma_1}/\bar{\sigma_3} - 1\right)$ versus strain and thus shows graphically the manner in which pore water pressure is developed in relationship to obliquity of the principal stresses as the sample is strained. In such a plot, a horizontal line indicates that both the pore water pressure (u) and the obliquity of principal effective stresses ($\bar{\sigma_1}/\bar{\sigma_3}$) are developing at the same rate. This plot can be significant in that, if Δu is taken as a measure of structural collapse with $\bar{\sigma_1}/\bar{\sigma_3}$ being a measure of the mobilization of structural resistance to displacement, then $\frac{d}{d\varepsilon}\left[\frac{\Delta u}{\sigma_3} \Big/ \left(\bar{\sigma_3}/\bar{\sigma_3} - 1\right)\right]$ is an indication of the comparative rates of structural breakdown vs. development of structural resistance.

If the sign of $\frac{d}{d\varepsilon} f(\varepsilon)$ is (−), structure is being mobilized at a faster rate than it is being broken down. If $\frac{d}{d\varepsilon} f(\varepsilon)$ is 0, structure is being mobilized and destroyed at the same rate, while if $\frac{d}{d\varepsilon} f(\varepsilon)$ is (+) structure is being broken down faster than bonds can be formed. The implications of this plot will be discussed in a later paragraph in this chapter.

Another familiar and convenient manner of looking at the development of resistance to shear displacement and pore water pressure development is presented in Figure 10. This is a plot of $\frac{\sigma_1 - \sigma_3}{2}$ as a measure of resistance to shearing and the ratio of $\frac{\bar{\sigma}_1 + \bar{\sigma}_3}{2}$ as a measure of effective stress normal to the failure plane development. Such a plot is usually termed a "stress-vector" plot. If a line be drawn on this plot starting at the chamber pressure on the x axis and extending up and to the right at an angle of 45°, such a line represents the path of total stresses during the test. The distance from a point on the effective stress path horizontally to an intersection on this 45° line represents the pore water pressure. Hence such a plot shows the interrelationship of the resistance to shear, the effective stress normal to the potential failure plane and the pore water pressure as a test progresses.

In addition, plots of maximum obliquity of principal effective stresses ($\bar{\sigma}_1/\bar{\sigma}_3$), pore water pressure (u), pore pressure parameter A ($= \frac{\Delta u}{\sigma_1 - \sigma_3}$) and probable differences between mid-height and base pore water pressure versus time to 1% strain have been developed and are presented in Figures 11, 12, 13 and 14. (Figure 11 is $\bar{\sigma}_1/\bar{\sigma}_3$ vs. t_1; Figure 12, u vs. t_1; Figure 13; A vs. t_1; and Figure 14 is $u_{base} - u_{needle}$ vs. t_1).

The other data gathered from the tests on normally consolidated samples, neglecting temporarily those tests in which the rate of strain was changed in the midst of the test, are the water content data at failure and the data on pore water pressure gradients. Every sample in the main series of tests was sliced into six slices by horizontal

cuts. A very thin slice at the bottom and at the top, if top drainage was employed, was discarded to eliminate the possibility of the water content in these areas having increased due to picking up water from the stone as the sample was dismantled. These data are listed in Appendix B on the stress versus strain curve from each individual test. The plots in Figure 15 represent an attempt at a statistical analysis of these data. In tests NC1-F, NC2-F, and NC3-F, which were all rapid tests, the water content was determined as rapidly as possible (2 to 5 minutes) following the end of shearing. Therefore, the results of these determinations probably indicate the distribution of water contents before shearing. The data from these determinations are plotted in (c) of Figure 15. All of the data were plotted in Figure 15(a) and envelopes enclosing the data were drawn. Inner envelopes enclosing 85% of the data were drawn and the average of this 85% area is plotted in 15(b). Subtracting the preshear distribution from this average leaves 15(d), [i.e. (b) - (c) = (d)], which is an indication of the possible migration of water within the samples, either during shear or following shear and while the sample was being dismantled.

In Figure 14 are plotted all of the data from tests in which the pore water pressure was measured at both the base and the mid-height of the sample. In general, two points are plotted from each such test, one being the pore pressure difference at maximum deviator stress, and the other being the maximum pore water difference occurring during the course of the test. The solid line drawn in this figure represents the best estimate of the gradients in samples of this soil that have to be contended with as they are related to the strain rate.

C. Behavior of Normally Consolidated Samples at Small Strains

The section presents and summarizes the behavior of the normally consolidated samples during the first 1% strain. These data were obtained from the stress versus strain and pore water pressure versus strain plots presented in Appendix B. The data from the individual plots were averaged numerically and summary plots of $(\sigma_1 - \sigma_3)$ versus strain and pore water pressure versus strain are presented in Figure 16. The plots presented represent the numerical average of 4 fast tests (t_1 = 1 min.) and 9 slow tests (t_1 = 500 min.). The numbers of the individual tests are listed in Figure 16. In addition to the average behavior, the range of the data is indicated in all cases.

From these averages of stress versus strain and pore water pressure versus strain data, the plots in Figure 17 were obtained. In this figure are plotted, on the basis of numerical averages, $\bar{\sigma}_1/\bar{\sigma}_3$ versus strain, the pore pressure parameter A ($\frac{\Delta u}{\sigma_1 - \sigma_3}$) versus strain and the quantity $\left[\Delta u/\sigma_3 \div (\bar{\sigma}_1/\bar{\sigma}_3 - 1)\right]$ as a function of strain, all representing behavior to one percent strain.

All of the factors acting to introduce inaccuracies into the observed magnitudes of stress versus strain and pore pressure versus strain parameters are magnified in importance when behavior at small strains is considered. During the course of this research, every precaution was exercised to insure that the data obtained were reliable and accurate, including the data describing the behavior at small strains. If it is assumed that the observed and recorded data plotted in the curves of individual tests in Appendix B are true and accurate records of actual measured quantities continuous from 0 to 1% strain, then any inaccuracy lies in interpreting just what the measured quantity represents. This assumption is, on the whole, justified. The pore water pressure in most instances was obtained from a continuous plot of pore water pressure transducer output versus either strain or time. The rate of strain of the more rapid tests was such that a sufficient number of readings of

the proving ring dial gage could be and were taken during the first one percent of strain.

In the case of deviator stress versus strain data, any inaccuracy would seem to arise from inaccuracy in the relationship of stress to strain rather in any inaccuracy in recorded value. By this is meant the effect of so-called seating errors which cause the recorded change in length to be not representative of a uniform length change over the entire sample length. In other words, the early strains might be occurring in localized zones adjacent to the base or cap of the sample. In situations where this problem was obviously present, for example NC6-S, the stress versus strain curve was corrected for this effect. Corrected areas were used in the computation of deviator stress, but this correction was quite small at less than one percent strain and any effect of inaccurate strains upon this correction would be negligible.

In addition to these seating errors, several other possibilities of sources of inaccuracies in interpretation of pore water versus strain behavior should be pointed out. Three major sources of error plague any investigator attempting to measure developed pore water pressures and the severity of these is considerably magnified at small strains. These sources of error are listed below and comments on the nature of the possible error at small strains are presented:

(1) Errors due to compliance in the measuring system. These errors are, in the main, more severe in the faster tests and doubly influence the data at small strains. Response of the pore pressure system was checked before each test, as described in Appendix A, and kept to a standard of full response in one minute or less. Therefore, the gross effect of this should be more or less constant for all tests. However, a minute bubble of air, small enough to be ineffective in introducing error into the pore water pressure observations of the slower tests at all strains and the fast tests at larger strains, could influence the observations made in the most rapid tests at small strains.

This effect would tend to lower the observed pore water pressure at small strains in the fast tests.

(2) Minute leaks in the external system. Gross leaks would be picked up in the response check before commencing the test. Such leaks would spoil any test. Minute leaks, undetected in the response check, would affect the observed pore water pressure in slow tests at all strains, but would not affect the data from fast tests. The effect would cause a lower pore water pressure to be recorded in the slow tests.

(3) Factors exist which can cause the measured water pressure to not be indicative of pore water pressure in the sample at all, but to be simply a water pressure generated by the presence of the measuring device. For example, a flexible stone on the base pedestal will obviously produce a pressure in the water in the stone or beneath it which would approach the deviator stress in magnitude. If the test was slow enough or the soil being tested was permeable enough this effect would be equalized by minute volume changes within the sample and would cause no gross inaccuracy.

In the case of the fast tests at small strains, there is the possibility of a minute void in the soil structure adjacent to the porous probe and containing water. This void filled with water could be compressed by the soil structure around it as stress was applied, and in fast tests in soils of low permeability this compression would produce pressure in the water in this void in excess of the pore water pressure in the bulk of the sample. This would cause the measured pore water pressure in the fast tests to be higher than the true value.

Considering these possibilities of error, the data plotted in Figure 16 are remarkable consistent. This is especially true of the recorded pore water pressures. In fact there is more scatter in the data from the slower tests, while the maximum scatter would be expected in the fast tests.

A careful study of the data plots presented in Figure 16 leads to the following conclusions. There can be little question that at any particular strain level in excess of 0.1%, the magnitude of the deviator stress is higher in the fast tests. The percentage increase in deviator stress in the fast tests as compared to the slow tests is much greater at low strains as compared to large strains. In fact, the actual magnitude of the excess of deviator stress in the fast tests as compared to the slow tests seems to be a maximum at approximately one percent strain. Little can be said about the modulus of the stress vs. strain curve at either strain rate at less than 0.2% strain. The secant modulus to any strain level is greater in the fast tests. However, the tangert modulus in the fast tests, while starting out greater than that exhibited by the slower tests, decreases as straining progresses at a much more rapid rate than the tangent modulus to the stress vs. strain curve of the average slow tests, and approaches the slow test tangent modulus in value at one percent strain.

The pore water pressures recorded in the slow tests are felt to be quite accurate in spite of the previously mentioned sources of error possible at small strains. It is also felt that, if any inaccuracy is affecting the observed pore water pressures in the fast tests, the effect at low strains is to make the observed values slightly lower than the true values. Considering the confidence of the author in the observed pore water pressures, the plot of pore water pressure at small strains in Figure 16 seems to indicate that there is little, if any, effect of rate of strain on the relationship between pore water pressure and strain at small strains. If any, the trend is toward slightly higher pore water pressures in the more rapid tests.

At small strains, little, if any, destruction of structure is occurring. The resistance to shear displacement is due to the mobilization of bonds or bonding forces between particles and to particle interference. This interference can be either body interference or force field interaction. It would appear that larger displacements would be necessary

to mobilize resistance due to particle interference than would be necessary to mobilize resistance due to bonding. Both of these components of shear resistance probably demonstrate a viscous type behavior. However, it is felt that the more viscous component is the resistance to displacement afforded by particle interference. In addition, it is felt that the resistance to stresses, or the stress versus strain behavior reflecting mobilization and stressing of bonds between particles, is the more elastic of the two components until straining sufficient to begin breaking bonds has occurred.

SKEMPTON (1948) at the Second International Conference on Soil Mechanics and Foundation Engineering presented a theory relating pore pressure to applied stress changes assuming elastic behavior. The relationship $u = \frac{\sigma_1 + 2\lambda\sigma_3}{1 + 2\lambda}$ where $\lambda = \frac{C_s}{C_c}$ was developed by by Skempton. $C_c = \frac{3(1-2\mu_c)}{E_c}$ is the compressibility (volume decrease per unit all-sided effective pressure increase) and $C_s = \frac{3(1-2\mu_s)}{E_s}$ the expansibility (volume increase per unit all-sided effective pressure decrease) of the soil structure. E_s and μ_s are the modulus of elasticity and Poisson's ratio operating in an unloading situation, and E_c and μ_c are the same quantities where compression is occurring. This equation can be written $u = \frac{\sigma_1 - \sigma_3}{1 + 2\lambda} + \sigma_3$ Thus the pore pressure parameter $A = \frac{1}{1 + 2\lambda}$. If the resistance of the soil structure to an increase in deviator stress is purely elastic and isotropic, with $C_c = C_s$, $\lambda = 1$ and $A = 1/3$. A value of A in excess of 1/3 would occur due to an increase in C_c or a decrease in C_s.

Since $\lambda = \frac{E_c}{E_s} \times \frac{1-2\mu_s}{1-2\mu_c}$, and increase in E_c without a corresponding increase in E_s would cause a decrease in A, while an equal

change in E_c and E_s would not change A, all else remaining constant.

In Figure 17 are plotted the deduced values of "A" versus strain. The plot of A values in the fast tests seems to indicate the possibility of A = 1/3 at very small strains, while the plot of A values from the slow tests is rather inconclusive regarding strains less than .2%, seeming to head for A values $\approx$ 1/3 at small strains. A values higher than 1/3 can be interpreted as indicating deviations from purely elastic behavior. Such deviations are seen to play more of a role in the resistance to deviator stress increases in the slower tests.

In Figure 17 are also presented plots of obliquity ($\bar{\sigma_1}/\bar{\sigma_3}$) versus strain and ($\frac{\Delta u}{\sigma_3}$) $\div$ ($\bar{\sigma_1}/\bar{\sigma_3} - 1$) versus strain. The first quantity ($\bar{\sigma_1}/\bar{\sigma_3}$) is usually taken as an indication of mobilization of structural resistance to shear displacement, while the second value, Bjerrum's parameter $\bar{A}$ (BJERRUM: 1961) is taken as an indicator of the relationship of structural breakdown. In the plot of $\bar{\sigma_1}/\bar{\sigma_3}$ versus strain, it is seen that structural resistance to shear displacement is mobilized much more rapidly in the faster tests.

As has been pointed out in a previous section, a plot of ($\frac{\Delta u}{\sigma_3}$) $\div$ ($\bar{\sigma_1}/\bar{\sigma_3} - 1$) versus strain is an indication of the relative magnitude of structural mobilization and breakdown. A horizontal slope of such a plot indicates a constant rate of structural mobilization and breakdown. A positive slope indicates an increasing rate of structural breakdown, or a decreasing rate of structural mobilization, while a negative slope indicates structure being mobilized at an increasing rate relative to structural breakdown.

The study of stress versus strain behavior and pore pressure development at small strains and its relationship to rate of strain is seen to be a promising area of future research. On the basis of the data presented the following conclusions can be drawn:

1. The resistance to shear displacement at small strains exhibits a viscous type behavior pattern.

2. Either:

(a) The resistance to compression also exhibits a viscous type behavior of such magnitude to cause the relationship between pore water pressure and strain to be unchanged with change in strain rate, or

(b) The development of pore water pressure at small strains is a function of strain and independent of both strain rate and the total stress level.

D. Behavior of Normally Consolidated Samples at Large Strains

This section presents and discusses the results of the tests on normally consolidated samples emphasizing the behavior patterns at strains in excess of 1%. Figures 4, 5, 6, and 7 summarize and average the data obtained from 17 tests on normally consolidated samples having strain rates varying from 1% in one minute (t_1 = 1 min.) to 1% in one day (t_1 = 1440 min.).

In Figure 4 maximum deviator stress is plotted versus the logarithm of time to 1% strain. Data is, of course, plentiful at the two extremes of strain rate and hence the best estimate of intermediate behavior is based on a linear logarithmic interpolation. A study of this plot and the upper plot of Figure 7 ($\sigma_1 - \sigma_3$ vs. strain) lead to the conclusion that the maximum deviator stress increases with increasing strain rate. Also, this maximum deviator stress occurs at smaller strains in the fast tests.

Figure 4 indicates that, in the range of strain rates considered, an increase in deviator stress on the order of 10% over the slow test value occurs in the fast tests. The nature of this increase in deviator stress is shown very clearly in Figure 10. If a line be drawn at a slope of $+45^{\circ}$, intersecting the x axis at the

point of origin of the particular stress vector being studied, the horizontal distance from this line, which, if no back pressure, is the total stress vector, and the effective stress vector under consideration represents the excess porewater pressure at that point of the test. A line drawn from any point on the stress vector through the origin is a measure of the obliquity of stresses at that point, or is a measure of $\bar{\phi}$ (angle of shearing resistance in terms of effective stresses). If α be the slope of a line through the origin on Figure 10, then Tan α = Sin $\bar{\phi}$. Two effects of changing the rate of strain are then seen to contribute to the increase of deviator stress at failure in the faster tests. These are: (1) a decrease in maximum obliquity as the rate of strain is increased; this would tend to produce an opposite to the observed effect (i.e., a decrease in maximum deviator stress) were it not for (2) the accompanying lower porewater pressure at failure in the faster tests. Therefore it may be said that the increase in strength accompanying an increase in rate of strain within the limits of this test program is due mainly to a decrease in porewater pressure at failure and is in spite of a decrease in $\bar{\phi}$. The magnitude of this decrease in $\bar{\phi}$ is illustrated in Figure 11 (where Sin $\bar{\phi} = \frac{\bar{\sigma}_1/\bar{\sigma}_3 - 1}{\bar{\sigma}_1/\bar{\sigma}_3 + 1}$), and the increase in porewater pressure at the lower rates of strain is shown in Figure 12. The relationship between the A factors at maximum deviator stress (SKEMPTON, 1954), where $A = \frac{\Delta u}{\sigma_1 - \sigma_3}$ is shown in Figure 13. From this figure, the increase in $A_{failure}$ with decrease in strain rate can plainly be seen.

The relationship between deviator stress and porewater pressure as the test progresses is shown clearly in Figure 18. After the initial 1% strain, the porewater pressure increases in almost direct proportion to the increase in deviator stress in the slow tests. In the fast tests, in contrast, after 1% strain (and also prior to 1%), each succeeding increment of deviator stress produces an incremental increase in porewater pressure much greater than the preceding (i.e., $\frac{d u}{d(\sigma_1 - \sigma_3)}$ increases).

The A factor, however, while higher at any strain level in the slower tests, continues to increase at more or less the same rate in both the fast and slow tests as straining progresses. These trends are clearly shown in Figure 19.

It has been demonstrated that in the samples tested in this program the effect of a decrease in the time to failure is accompanied by an increase in the deviator stress at failure. In addition, it has been demonstrated that this increase in strength is due to a decrease in the porewater pressure at failure and occurs in spite of a decrease in $\bar{\phi}$ as the time to failure is decreased.

It seems important to decide upon the mechanism by which the porewater pressure at strains in excess of 1% attains its higher level in the slower tests. Three possibilities immediately suggest themselves: (1) membrane leakage, (2) migration of porewater (i.e., pore pressure gradients), and (3) a difference in the structural behavior at rapid strain rates resulting in a lower porewater pressure. These possibilities are discussed in the ensuing paragraphs. As the following discussions with their accompanying data point out, the difference in porewater pressure is attributable to a real difference in structural behavior in the fast versus the slow tests.

(1) Membrane leakage: - Little reason exists to suspect that membrane leakage represents much of a problem in the tests in which two membranes and a layer of silicone grease were employed. Several evidences available tend to minimize this possibility. The porewater pressure versus strain curve presented for the slow tests in Figure 6 shows little change in porewater pressure from 8 to 12% strain. In time, this represents nearly one and one-half days. In addition, Tests NC 15SF and NC 16SF were brought to a failure condition and allowed to remain at constant strain for approximately four days. During this time, after the initial change in porewater pressure as straining was stopped (which was slight), the only change in

porewater pressure of any significance was a drop-off attributed to a temperature change. (The straining was stopped in the midst of a heat wave and during the night the ambient temperature dropped 20°F. as the heat wave was broken). One other bit of evidence is available. Test NC-8S (see Appendix B) was performed using Cylrex as a cell fluid. This is an inert heavy oil manufactured by the Sunocy-Vacuum Oil Company and does not attack rubber. Here again, the ambient temperature changes interfere with direct use of the test results, but if the drops in porewater pressure due to drops in ambient temperature are added onto the end porewater pressure, and a correction made as a ratio of the differences in chamber pressure between this test (66.5 lb./in.^{2}) and the average test (60 lb./in.^{2}), the equivalent porewater pressure turns out to be 40 lb./in.^{2}, or higher than that developed in the average slow test. This falls in line as test NC-8S was considerably slower than average. Therefore it seems reasonable to discard the possibility that any gross portion of the higher porewater pressure in the slower tests is due to membrane leakage.

(2) A second possibility is lowering of the mid-height porewater pressure due to migration of porewater from regions of higher pressure nearer the base. As is the case with the increase in porewater pressure that could occur due to membrane leakage, this possibility does not represent a fundamental process of soil behavior. The possibility of the existence of a porewater pressure gradient represents the little understood distribution of stresses in a triaxial test specimen. BISHOP, BLIGHT AND DONALD (1960), in a study of the effect of rate of strain on base porewater pressure measurements, have described this mechanism in the following manner:

The unequal distribution of stresses in a triaxial specimen occurs due to end restraint at the base and at the cap. End restraint has the effect in these regions of increasing the major principal stress (σ_1) slightly and considerably reducing the deviator

stress ($\sigma_1 - \sigma_3$). The basic pore pressure equation $\Delta u = B[\Delta\sigma_3 + A(\Delta\sigma_1 - \Delta\sigma_3)]$ (SKEMPTON, 1954) can be rearranged in the form $\Delta u = B[\Delta\sigma_1 - (1-A)(\Delta\sigma_1 - \Delta\sigma_3)]$. Both of the previously discussed effect of end restraint will tend to increase the porewater pressure at the base and cap over that at the mid-height of the sample unless $A > 1$. If the test is run slowly enough, the porewater pressure will be equalized throughout the length of the sample. If $A \leq 1$, the effect of this equalization will be to increase the mid-height porewater pressure over that which would be recorded in a rapid test.

Another way of looking at this same phenomenon is to liken the region of the test sample close to the stone to a consolidation test specimen with lateral restraint. In such a specimen of saturated soil, the porewater pressure set up is initially equal to the applied load. In the case of the triaxial test specimen, it would seem reasonable to expect that the porewater pressure in the region immediately adjacent to the restraining stone would equal the deviator stress at the instant of initial application. Thus, unless A was greater than 1, there would be induced against the stone a porewater pressure greater than at the center of the sample. The thickness of this region would depend on the completeness of restraint and upon the stress versus strain characteristics of the soil.

In several of the tests on normally consolidated samples, porewater pressure was measured at the base in addition to being measured at the mid-height of the sample. The results of all these measurements are summarized in Figure 14. A curve of probably typical gradient is sketched through the points on this plot. The maximum measured gradient was 5.0 lb./in.^{2} (i.e., the porewater pressure at the base of the sample was 5 lb./in.^{2} higher than at mid-height) but this measurement seems to be extreme. A more typical value would be 2.0 lb./in.^{2} higher at the base than at the midplane in the faster tests. This higher porewater pressure presumably exists in a thin zone of the

sample adjacent to the stone and rapidly grades to the mid-height porewater pressure, so it would seem inconceivable that this gradient, if allowed to be dispelled by migration of porewater, could raise the mid-height porewater pressure any significant amount. Since, at maximum deviator stress, the porewater pressure in the typical slow test is more than 5 lb./in.^{2} higher than that in the typical fast test, there would seem to be little reason to expect that porewater migration would account for any significant amount of this increase.

Additional evidence of the insignificant effect of porewater pressure gradients on the increase of deviator stress concurrent with a decrease in the time to 1% strain is given by the water content data as presented in Figure 15. These data scatter considerably and it is rather hard to draw any conclusions from them. Looking at (b) of Figure 15, one can note a suggestion of a possible migration of porewater from slices 2 and 5 to slices 3 and 4, overlooking slices 1 and 6. However, this suggestion disappears when one studies (d) of Figure 15. The best that can be said is that there is no gross evidence of any migration of porewater.

(3) The third possibility is that the lower porewater pressure in the more rapid tests is a real phenomenon resulting from the manner in which the soil structure itself responds to different rates of stress application. The author feels that one of the major contributions of this research is the demonstration of the effect of strain rate on the manner in which the soil structure resists shear displacement as manifested in the pattern of porewater pressure development.

At small strains the porewater pressure, if considered per se, appears to be independent of strain rate. It was suggested that this may be a fortuitous occurrence indicating an earlier and greater deviation from purely elastic behavior in the slower tests.

In contrast, at larger strains and presumably after a degree of structural breakdown has occurred, the porewater pressure at any strain level is higher on the slow tests.

The phenomenon of the lower porewater pressure at any strain level past 1% in the faster tests, and the higher A value in the slow tests at any strain level, can be attributed to a resistance to compression at any strain level that is time dependent and exhibits viscous behavior. If only the tests carried to completion at a constant strain rate are considered, the observed behavior follows with this explanation. However, a series of tests in which the strain rate was stepped at preselected strain levels (i.e., at certain predetermined values of strain, the strain rate was instantaneously increased or decreased) was run. The detailed results of these tests will be presented in the next chapter. However, the behavior of the porewater pressure in the tests which progressed to a strain of 2% or greater at t_1 = 500 min. before a step in strain rate to t_1 = 1 min. show a decrease in porewater pressure following this switch which seems to the author to be attributable only to some dilatent component in structural behavior.

That this dilatent component exists is shown in Figure 20. In this figure are plotted the results of four tests in which the strain rate was stepped from 1% in 500 min. to 1% in 3/4 min. In all tests where this step in strain rate occurred at strains sufficiently large to represent a reasonable degree of structural breakdown, the porewater pressure following the step in strain rate leveled off at a value lower than that existing before the step. This occurred even in the presence of a considerably higher deviator stress. The complete discussion of these tests appears in Chapter IV.

While the increase in deviator stress that has been observed with decreased time to failure in the tests on the normally consolidated samples has been attributed to the lower porewater pressure in the more rapid tests, this increase had to occur in spite of a decrease in the

angle of drained shearing resistance ϕ. This decrease is evidenced in the decrease in the principal effective stress ratio at failure as shown in Figure 11. This decrease in ϕ was also noted by (CRAWFORD, 1959) but the opposite trend was recorded by (BJERRUM, 1960). However, this decrease appears to be a real phenomenon occurring in the fat clay used in the present work.

Several mechanism have been postulated which offer explanations for this decrease in $\bar{\phi}$. One of the simplest explanations of this observation lies in attributing it to a prestress effect as illustrated in Figure 28(d). The higher porewater pressure in the slower tests, indicated by the horizontal projection of the distance x-y, results in a lower effective stress normal to the failure plane at the time of failure. The postulation of a Hvorslev line independent of strain rate is not necessary.

The author feels that in this case the relationship between effective normal stress and shear resistance reflects the relative rates of bond or resistant force link mobilization and destruction. The behavior of $\bar{\sigma}_1/\bar{\sigma}_3$ as straining progresses is illustrated in Figure 9. In this plot, the author interprets a positive $\frac{d(\bar{\sigma}_1/\bar{\sigma}_3)}{d\varepsilon}$ to indicate that resistive force links are being formed at more rapid rates than the rate of dstruction of these force links. A horizontal slope $\left(\frac{d(\bar{\sigma}_1/\bar{\sigma}_3)}{d\varepsilon} = 0\right)$ indicates bond destruction and bond mobilization are occurring at the same rate while a negative slope indicates a more rapid rate of bond destruction.

Thus, in the rapid tests, bonds are initially mobilized much faster than is the case in the slow tests. However, an equal rate of mobilization and destruction is reached at approximately 3½% strain. Following the attainment of this level, resistance force destruction occurs at a rate in excess of the rate of bond formation. However, in the slow tests, bond formation occurs at a rate in excess of bond destruction until quite large strains are reached.

If the resistance to shear displacement were largely due to particle (or micelle) interference, the behavior in terms of obliquity could be expected to be more strictly viscous and thus a higher obliquity at any strain level in the faster tests could be expected.

In Figure 9 is plotted the parameter $\left[\frac{\Delta u}{\bar{\sigma}_3} \div \left(\bar{\sigma}_1/\bar{\sigma}_3 - 1\right)\right]$ vs. strain. If Δu is a measure of structural breakdown and $\bar{\sigma}_1/\bar{\sigma}_3$ is a measure of structural mobilization, the shape of this plot can indicate much regarding the manner in which the soil structure is behaving as it mobilizes resistance to shear displacement. Two features of such a curve shed light on the behavior of the soil structure, (1) the actual value of a point on the curve at any level and (2) the slop of the curve at any point.

The value of this parameter at any strain level is an indication of how much structure has been destroyed in relationship to the amount of structural bonds being mobilized up to the strain level under consideration. For example, referring to Figure 9, at 1½% strain more shear displacement resisting bonds have been mobilized per bond destroyed in the fast tests. At 8% strain the relationship between statistical number of bonds destroyed and statistical number of bonds mobilized is about the same in both tests. However, the shape of the two curves tell much about the nature of the bond breaking versus bond formation process. In the fast tests, following 1% strain, the relationship between bond formation and bond destruction is more or less constant until a strain of about 7% has been reached. This is indicated by the horizontal slope of the curve. The positive slope of the curve for the fast tests after 7% strain indicates that the rate of bond destruction relative to bond formation is beginning to increase. In contrast, from small to large strains, the curve for the slow tests shows a negative slope, indicating bond formation at an increasing rate relative to bond destruction.

Chapter IV

NORMALLY CONSOLIDATED SPECIMENS WITH STEPPED STRAIN RATE

A. Introduction

This chapter presents and discusses the results of a series of fourteen tests on normally consolidated samples of the fat clay. These samples were prepared and set up in exactly the same manner as described in the previous chapter. The tests in this subseries differ from those of the main series only in the fact that at some predetermined strain level during the progress of each test, the strain rate was drastically changed. This series of tests was originally embarked upon with the limited objective of demonstrating the so-called "dilatency" effect, described previously, and its relationship to strain rate. It was postulated that some portions of the soil structure being strained exhibit a tendency toward collapse and thus a volume decrease (positive porewater pressure development) while other portions exhibit a tendency toward volume increase (dilatency) due to structural viscosity and thus tend to reduce the developed porewater pressure (negative porewater pressure development). Statistically, in this and most (if not all) normally consolidated soils, the dilatency effect plays a relatively minor role. However, it was felt that a rapid change in strain rate would upset the balance in these two behavior patterns and, if a lowering of porewater pressure with an accompanying increase in deviator stress would ensue, the existence of a dilatency component would be demonstrated. The data resulting from the tests at a constant strain rate can be explained (at greater than 1% strain) without postulating any dilatency effect, only attributing viscous behavior patterns to both shear displacement resistance and resistance to compression. Since it was suspected by the author that a dilatency component did exist, this series of tests was planned. In the original planning for this supplemental series of tests, the sole object was to vary the rate of strain during the course of any test and to observe the effect of this change on the

developed porewater pressure.

However, while the preliminary few tests in which the strain rate was stepped can be interpreted as clearly demonstrating the presence and importance of this structural viscosity effect on porewater pressure development in the normally consolidated samples, other effects of equal or greater importance were noted in the effect of this change in strain rate on the deviator stress. To follow up and pin down the cause of this rather significant phenomena, the scope of this supplementary test program was extended.

The effect of a step in strain rate on the deviator stress has been noted by others in the Massachusetts Institute of Technology Soil Engineering Laboratory and at other establishments. However, the rate changes were nowhere near so drastic in these cases and the change in porewater pressure had usually been overlooked. The effectiveness of the strain rate change technique in the current research is due to the ability of the novel pore pressure measuring device to rapidly (almost instantaneously in this case) detect changes in porewater pressure occurring as a result of the change in strain rate, and to detect these changes in a portion of the test specimen which is relatively unaffected by anomolies in stress distribution. Consequently, it is felt that the results of these tests stand by themselves as an important contribution to knowledge resulting from this research effort.

B. Testing Procedure

This subseries of tests involved fourteen normally consolidated samples. These tests are NC4FS, NC5FS, NC9-SF through NC17-SF, tests NC18SFLC, NC19SFLC and NC20SFLC. Some of these represent tests from the main series in which the strain rate was stepped following attainment of peak deviator stress.

Most of these tests were performed using the same load frame, triaxial cells and proving rings as were employed in the main series of tests. However, as the tests in this subseries were begun, considerable skepticism was voiced regarding the validity of the observed phenomenon of increased deviator stress with increase in strain rate. The reason for doubting the observed behavior patterns stemmed from a feeling that some frictional effect in the bushing of the piston and bushing assembly of the triaxial cell could be making a major contribution to the effect of step in strain rate upon the observed deviator stress. A careful investigation of this possibility was undertaken and is described in the next section.

In an attempt to satisfy the skepticism, several tests were set up in the cells employed in a companion research effort (NASIM 1961). The cells had been modified to provide a method of measurement of the load on the soil sample by means of a load cell inside the triaxial chamber. This load cell consisted of a lucite platten, a stainless steel piston riding in a Thompson Ball Bushing and activating an electric force transducer similar in design to those employed in measuring porewater pressure by means of the porous probe. The electronic equipment necessary for reading out the information gave considerable trouble, and there is doubt as to the calibration of the load cell and thus to the information regarding the peak values of the deviator stress. In addition, the drainage and porewater pressure measuring systems were never perfected in that leakage was known to occur. Hence, it is rather difficult to make any comparison of the gross results of these tests with those performed in the standard cells. However, there is no question that the results of changes in strain rates in tests performed in these cells gave quite similar results to tests in standard cells. A total of three tests were attempted in these cells, NC-18SFLC, NC-19SFLC and NC-20SFLC. Of these, NC-19SFLC was the most satisfactory. The deviator stress increase following the change in strain rate is the same percentage as the increase obtained using standard cells.

C. An Investigation of Stepped Strain Rate on Piston Friction

At the conclusion of each test in this series, the piston of the triaxial chamber was withdrawn to a position such that the lower end of the piston was well above the cap of the sample. The load frame was then started causing the piston to descend into the cell at the slow rate. The proving ring reading was noted. In all cases this reading in excess of that caused by chamber pressure was less than 1 lb. and in most cases considerably less than 1 lb. There was no difference between the Clockhouse Cells and the Norwegian Geotechnical Institute Cells in this regard. The speed of descent of the piston was then stepped to the fast rate. In no case was any change in proving ring reading recorded.

A Clockhouse Triaxial Cell was set up in the standard manner with the standard oil in the top and a chamber pressure of 60 lb./in.^{2} applied. A horizontal thrust of 5 lb. was applied to the piston $3\frac{1}{2}$ inches above the top of the bushing. Even with this load, less than 1/2 lb. of piston friction was noted. This was a constant value, independent of the rate of strain or of any sudden changes. In fact, the load frame was cranked by hand at a quite rapid rate and no change in the amount of piston friction was noted.

The same setup was repeated using a Norwegian Geotechnical Institute Cell. Here the piston friction with the eccentric 5 lb. force was $2\frac{1}{2}$ lb., and was again independent of strain rate and of any sudden changes in rate. These observations coupled with the results of the tests in triaxial chambers equipped for internal load measurement lead to the conclusion that while piston friction may slightly influence the gross test results, especially with the Norwegian cells, the effect of rate of strain and sudden change in rate of strain is negligible. There exists the possibility, with the Norwegian cells, of a 2 or 3% error in maximum recorded deviator stress on the gross test results.

D. Results of a Negative Step (Step Decrease) in Strain Rate

Two tests on normally consolidated samples were performed which involved a step decrease in strain rate at some strain level. The results of these two tests, NC4FS and NC5FS, are presented in Figures B-4 and B-5 of Appendix B. In test NC4FS, the test was carried to a strain of 7% at a strain rate of 1% in 45 sec. ($t_1 = \frac{3}{4}$ min.). At 7% strain, the rate of strain was decreased to 1% in 10 min. (t_1 = 10 min.), 10 minutes being the time required for 1% additional strain. The test was stopped at 7.2% strain.

In test NC5FS, the initial strain rate was again 1% in 45 seconds ($t_1 = \frac{3}{4}$ min.). At 4½% strain the strain rate was decreased to 1% in 60 min. (t_1 = 60 min.). Straining was continued at this slower strain rate until a strain level of 8½% had been attained.

Test NC-4FS contributes relatively little to this discussion as the test was stopped before the effects of the step in strain rate had reached an equilibrium state. Comparing this test with the average results of tests on normally consolidated samples leads to the following observations. Prior to the step decrease in strain rate, this sample was behaving in a manner almost identical to the average behavior for t_1 = 1 min. as shown in Figure 7 and Figure 8. At 7% strain in the average tests, the deviator stress ($\sigma_1 - \sigma_3$), porewater pressure (u) and obliquity (σ_1/σ_3) were 43 lb./in.^{2}, 32 lb./in.^{2} and 2.70 respectively in test NC-4FS. If the single test in the "average" series which represents an intermediate strain rate is taken as being comparable with the portion of NC4-FS after the step decrease in strain rate, the following comparison can be made. At 7.2% in the test representing t_1 = 20 min., Figures 7 and 8, the deviator stress, porewater pressure and σ_1/σ_3 ratio are 39.5 lb./in.^{2}, 35 lb./in.^{2} and 2.60 respectively. In test NC-4FS following the step decrease in strain rate, these values are 38 lb./in.^{2}, 33 lb./in.^{2} and 2.30 respectively. However, as will be demonstrated when the results of test NC-5FS are

discussed, these values do not represent equilibrium structural behavior following the change in strain rate.

In test NC-5FS, however, straining was continued for a sufficient period following the step decrease in strain rate to establish an equilibrium yielding condition. In this test, the strain rate was decreased from t_1 = 3/4 minute to t_1 = 60 minutes. This step decrease in strain rate was imposed at approximately 4½% strain in this test. The deviator stress prior to the step decrease was 42.0 lb./in.^{2}, the porewater pressure 30 lb./in.^{2} and the obliquity ratio 2.48 (43, 31½ and 2.52 respectively in average test). Immediately following the step decrease, these quantities were 34 lb./in.^{2}, 31½ lb./in.^{2} and 2.35 (deviator stress, pore pressure and obliquity ratio). However, further straining at the new and slower strain rate caused a rise in these same quantities (i.e., deviator stress, porewater pressure, and obliquity ratio) to 37.6 lb./in.^{2}, 35.3 lb./in.^{2} and 2.62 at 8¼% strain. (As compared with 39 lb./in.^{2}, 35 lb./in.^{2} and 2.60 in the t_1 = 20 min. test in Figure 7.)

In summary, the following description of behavior of this fat clay following a step decrease in strain rate represents in the author's opinion, the observed behavior. Following an instantaneous or "step" decrease in strain rate from t_1 = 3/4 minute to t_1 = 60 minutes:

1. The deviator stress drops to a level below that commensurate with the new strain rate and rises gradually to such a deviator stress as straining at the new rate is continued. (The deviator stress at the new or slow strain rate is lower than that attained before the strain rate step.)

2. The porewater pressure jumps slightly immediately following the step decrease in strain rate and continues to rise, attaining an equilibrium level approximating the pore pressure in a test at the slow strain rate at a constant rate of strain. (Higher than the pore pressure in a fast test.)

3. The obliquity ratio ($\bar{\sigma}_1/\bar{\sigma}_3$) drops following the step decrease in strain rate, but rises as straining continues at the new (slow) strain rate to a level approximating the obliquity ratio in a slow test at a constant strain.

E. Results of Positive Steps (Step Increases) in Strain Rate Imposed at $4\frac{1}{4}\%$ Strain in Normally Consolidated Samples

In three tests on normally consolidated samples of the saturated fat clay, step increases of varying magnitudes were imposed at $4\frac{1}{4}\%$ strain. In these tests the samples were all brought to $4\frac{1}{4}\%$ strain at the same rate, t_1 = 500 minutes. The stress versus strain, pore pressure versus strain, and obliquity ratio versus strain data for these tests, NC-9SF, NC-10SF and NC-11SF are presented in plots in Appendix B. The step increase in strain rate is given as the time required for 1% additional strain (t_{+1}). In test NC-9SF, t_{+1} = 3 minutes; NC-10SF, t_{+1} = 50 minutes, and in NC-11SF, $t_{+1} = \frac{1}{2}$ minute. Table IV-1 briefly summarizes this series of tests.

Table IV-1

TESTS WITH POSITIVE STEP IN STRAIN RATE AT $4\frac{1}{4}\%$ STRAIN

Test No.	$\varepsilon < 4\frac{1}{4}\%$ t_1(min.)	$\varepsilon > 4\frac{1}{4}\%$ t_1(min.)	Deviator Stress (lb./in.^{2})			Pore Pressure (lb./in.^{2})			Obliquity Ratio		
			Before Step	After Step	% Increase	Before Step	After Step	% Increase	Before Step	After Step	% Increase
NC9SF	500	3	37.5	45.	20%	32.3	32.8	$1\frac{1}{2}\%$	2.38	2.74	15%
NC10SF	500	50	37.5	40.8	9%	31.7	32.7	3%	2.27	2.44	$7\frac{1}{2}$%
NC11SF	500	$\frac{1}{2}$	36.5	46.6	27%	35.1	36.0	$2\frac{1}{2}\%$	2.53	2.95	$16\frac{1}{2}$%

Summary plots of the results of these three tests are presented in Figure 20. In this figure are presented plots of deviator stress, porewater pressure and obliquity ratio versus strain. In addition, a plot showing the behavior of the pore pressure parameter "A" following the step increase in strain rate is presented. This figure was derived by arriving at curves representing the average or typical behavior of these quantities up to 4¼% strain. (Actually the typical curves for t_1 = 500 minutes in Figures 7 and 8 were used. The behavior of the three tests in this series deviated from this typical behavior only to a very minor degree.) The actual observed behaviors following the step increase in strain rate were applied to these "typical" curves. For this reason, the actual magnitudes of values following the step in strain rate may differ slightly from those noted in Table IV-1; however, the percentage changes will be more or less the same.

The deviator stress, pore pressure and obliquity ratio behavior of these samples can be described as follows. All tests were brought to 4¼% strain with t_1 = 500 minutes with all measured quantities behaving quite comparable to the typical behavior portrayed in Figure 7. Behavior typical of a test at a uniform strain rate of t_1 = ½ minutes would be expected to differ only slightly from that shown as typical for t_1 = 1 minute as shown in Figure 7. Ideas of behavior typical of t_1 = 50 minutes and t_1 = 3 minutes in steady strain rate tests are not available, and the conclusiveness of the following description suffers in this regard. Following the step in strain rate, the deviator stresses rise to values about 10% higher than would have been attained in constant strain rate tests at the new strain rate and at the same level of strain. A considerable portion of this increase in deviator stress was obtained almost instantaneously in terms of strain, but additional strain on the order of ¼% in tests NC-9SF and NC-10SF and ½% in tests NC-11SF were needed to fully realize the maximum deviator stress. As

additional strain at the new strain rate was imposed, the deviator stress gradually fell to values that appear to be compatible with values that would be attained at comparable strain levels in tests having a constant strain rate equal to the post-step rate in these tests.

The porewater pressure following the step increase in strain rate in Test NC-11SF continued to rise in approximately the same manner as before the step until peak deviator stress had been reached. After the attainment of peak deviator stress, the pore pressure began falling off and, as straining at the new rate was continued, seemed to attain a value and a behavior pattern characteristic of a steady rate test at the new strain rate. In Test NC-10SF, the behavior was similar with the exceptions that a large initial jump (in comparison to NC-11SF) in porewater pressure, a subsequent leveling off until a strain-pore pressure level compatible with a steady rate test had been reached, followed by a behavior comparable to a steady rate test. Test NC-9SF exhibited porewater pressure behavior intermediate to NC-10SF and NC-11SF. Prior to the step in strain rate, the porewater pressure had been behaving typically, rising gradually. Following the step, the porewater pressure remained constant as strain was continued until a strain-pore pressure situation compatible with a steady rate test at the new strain rate had been reached.

Looked at in terms of the porepressure - deviator stress relationship, all tests exhibited a similar behavior pattern consistent with the strain rate following the step. The pore pressure parameter "A" is plotted versus strain following the step in strain rate in Figure 20. After the increase in strain rate, the A values begin dropping rapidly with additional strain, and gradually achieve a lower level. The amount of additional strain necessary to achieve this lower level increases as the new (post-step) strain rate increases. Following this drop, the A values rise to values that seem to be

comparable to those in steady rate tests at strain rates comparable with the post-step strain rate.

The measured porewater pressures following the change in strain rate would be influenced by any minor lag in the measuring system to only a very slight extent as the actual magnitude of the change to be measured is relatively small. In addition, the system is already operating under a positive pressure in excess of two atmospheres which, if looked at as a back-pressure in terms of post-step pore pressures, would tend to minimize several of the factors contributing to any slight lag in the measuring system. Hence it is felt that the porewater pressures measured following the step in strain rate are of the utmost reliability and accuracy.

Also plotted in Figure 20 is a summary of the obliquity ratio behavior exhibited in these three tests. The obliquity ratio is sensitive to slight irregularities in either pore pressure or deviator stress and thus the behavior shown is somewhat erratic. However, the gross pattern is compatible with the following description which must follow from the description of pore water pressure and deviator stress behavior following the step increase in strain rate. Following the step, the obliquity ratio jumps sharply, coming to a rather sharp peak in the tests with the most rapid post-step strain rate (NC-9SF and NC-11SF). Following the attainment of the peak, the obliquity ratios drop off and appear to reach levels compatible with those that would be achieved in steady rate tests at the post-step strain rate.

In Figure 21, the relationship between deviator stress and obliquity ratio attained following the step increase in strain rate are plotted against the logarithm of the post-step strain rate. In addition, the relationship between deviator stress at $4\frac{1}{2}\%$ strain and strain rate, and obliquity ratio at $4\frac{1}{4}\%$ strain and strain rate for typical constant strain rate tests, are shown by way of comparison.

F. Results of Tests in Which Equal Positive Steps in Strain Rate Were Imposed at Varying Strain Levels - Normally Consolidated Samples

Described in this section are a series of four tests in which a step increase in strain rate of an equal magnitude was imposed (Tests NC-13SF, NC-14SF, NC-15SF, and NC-16SF). In each case, the initial strain took place at a strain rate giving a time to 1% strain of 500 minutes (t_1 = 500 minutes). At certain preassigned strain levels, a step increase to a strain rate giving a time to 1% additional strain of 3/4 minutes was imposed. This strain rate step was imposed at progressively larger strains in each sample. In Test NC-15SF the strain rate step was imposed at 1.05% strain; in Test NC-13SF at 1.75%, NC-16SF at 4.40%, and NC-14SF at 7.25%.

The complete stress vs. strain and porewater pressure versus strain data from these tests will be found plotted in Appendix B. A summary of the behavior of these samples is presented in Figure 22. Here again the curves of deviator stress and pore water pressure at t_1 = 500 minutes (i.e., pre-step curves) are the typical slow rate curves from Figure 6. However, Tests NC-15SF and NC-16SF exhibit stress versus strain behavior almost coincident with this typical behavior. Test NC-13SF differs in both deviator stress and pore pressure only to a minor degree, being slightly high in both quantities at any strain. Test NC-14SF differs to a slightly greater extent with both deviator stress and porewater pressure being lower than typical at any strain level. In all cases, however, the numerical magnitude of the post-step increases were added to the typical curves.

All of these samples were trimmed from prisms of soil cut from Batch C. The typical curves for the fast strain rate presented in Figure 5 rely quite heavily on Batch B samples with no Batch C samples being represented. Hence, exact conclusions regarding the fast rate behavior for these samples in a steady strain rate situation cannot be drawn. However, for comparison, the typical fast curves from Figure 5 are shown in Figure 22.

In terms of deviator stress, the effect of a step in strain rate from t_1 = 500 min. to t_{+1} = 3/4 minute can be described as follows: In all cases a considerable increase occurred. The actual magnitude of this increase differed only slightly, in all four cases being 13.1 lb./in.^{2} when the step was imposed at 1.05% strain, 12 lb./in.^{2} at 1.75%, 10 lb./in.^{2} at 4.40%, and 8.5 lb./in.^{2} when the step was imposed at 7.25% strain. In each case, approximately ½% additional strain was required to completely develop the full increase in deviator stress due to the step in strain rate. This is rather hard to define in Test NC-15SF. However, a strain of ½% following the step in strain rate seems to have been required to bring the deviator stress versus strain behavior to a pattern compatible with the new strain rate. Table IV-2 following summarizes the immediate deviator stress increases following the step increase in strain rate.

Table IV-2

Deviator Stress Behavior Following Step Increase in Strain Rate - Normally Consolidated Samples

Strain Level at Step (%)	Test No.	t_1 (min.)	t_{+1} (min.)	$(\sigma_1 - \sigma_3)$ before (lb/in^2)	$(\sigma_1 - \sigma_3)$ after (lb/in^2)	$(\sigma_1 - \sigma_3)$ typical (lb/in^2)	% increase over slow rate	% in excess of typical fast rate
1.05%	NC15SF	500	3/4	29.4	42.5	41.5	45%	2½%
1.75%	NC13SF	500	3/4	33.5	45.5	42.5	36%	7 %
4.40%	NC16SF	500	3/4	38.6	48.2	43.2	25%	11½%
7.25%	NC14SF	500	3/4	40.0	48.5	42.7	21%	13½%

In addition, both the percentage increase over the pre-step deviator stress and the increase over the typical fast rate deviator stress are plotted against the strain at which the step in strain rate occurred in Figure 23.

From a study of Table IV-2, Figure 22 and Figure 23, the following conclusions can be drawn regarding the effect of the strain level at which a step increase in deviator stress is imposed and the subsequent deviator stress behavior.

1. Both the actual magnitude of the increase in deviator stress following the step in strain rate and the percentage increase is greater the lower the strain level at which the step is imposed. However -

2. The actual magnitude and the percent increase in the deviator stress over that typical for the new strain rate are less at low strains, becoming greater as the strain level at which the step in strain rate is imposed increases.

3. The exact location of a curve representing deviator stress versus strain behavior for a steady rate of strain yielding a time to 1% strain of 3/4 minute is not known. In the opinion of the author, however, the deviator stress versus strain behavior following the step in strain rate tails off to approach a behavior pattern typical of the new strain rate as straining continues at the new rate.

The pore pressure behavior following the change in strain rate is somewhat similar to the behavior described above in that it ultimately approaches the pore pressure versus strain behavior typical of the new strain rate. Immediately following the step in strain rate, the pore pressure rises above that which it would have attained if no step had occurred. As straining continues, however, the porewater pressure drops to the value it would have assumed if no rate change had occurred and approaches the level typical of the new strain rate. The change in pore pressure seems to be more fundamentally described by the behavior of the pore pressure parameter "A" following the step

in strain rate. The value of "A" in each case (with the possible exception of test NC-14SF) falls quite rapidly to a value typical of the new strain rate and thereafter exhibits values at any strain almost identical to those typical of the post-step strain rate.

The obliquity ratio versus strain behavior following the change in strain rate is of the same pattern as the deviator stress versus strain behavior. The actual magnitude of the increase is not greatly different when the shift takes place at differing strain levels. However, the percentage increase decreases as the strain level at which the step in strain rate was imposed becomes greater. The increase in obliquity ratio in excess of that typical of the new strain rate becomes progressively much greater as the step strain level increases. As post-step strain at the new strain level continues, the obliquity ratio assumes a value compatible with that expected in a steady rate test at the new strain rate.

G. Relaxation Tests - Normally Consolidated Samples

In compression testing, two types of studies can be made involving behavior during a period of stopping in the course of a test. The more common is the study of "creep" behavior following the attainment of a predetermined deviator stress. In this type of a test, following the attainment of a particular deviator stress, the deviator stress is held constant and the resulting deformation, or strain, measured as a function of time. Such a test has come to be referred to as creep test. In a relaxation test, on the other hand, following the achievement of a predetermined strain level in a compression test, the strain is held constant by varying (reducing) the deviator stress. The magnitude of the deviator stress needed to maintain this constant strain is observed as a function of time.

This section describes and presents the results of two tests on normally consolidated samples of the fat clay (Tests NC-15SF and NC-16SF) involving a period of relaxation. Both of these tests were of samples previously involved in the series of tests with a positive

step in strain rate described in the preceding section. The complete stress versus strain curves of these tests, found in Appendix B, include the relaxation and subsequent continuation of loading data.

In both of these tests, a period of relaxation for a time of approximately 10,000 minutes, at a strain level reached in identical manners (i.e., $t_1 = 3/4$ minute), were imposed upon the samples. The strain level was held within $\pm \frac{1}{10,000}$ inch by carefully observing the strain dial and correcting the load manually to maintain this constant strain. The actual strain level differed in the two samples, being $7\frac{1}{3}\%$ in NC-15SF and $9\frac{3}{4}\%$ in NC-16SF, but both strains are felt to represent approximately the same degree of structural breakdown. Following the period of relaxation, the samples were reloaded, NC-15SF at $t_{+1} = 500$ minutes and NC-16SF at $t_{+1} = 3/4$ minutes. The results of this continuation of loading are shown in the figures in Appendix B.

In Figure 24 are presented the observations of behavior in terms of deviator stress and porewater pressure. These tests were commenced in the midst of a period of hot weather (avg. temp. = 90°F). During this period, there was one day of cooler weather (avg. temp. = 70°F). This change in ambient temperature complicates the observed data to a considerable degree as is seen in Figure 24. Between points A and B in the plots in Figure 24 for both tests, a drop in ambient temperature of 20°F. occurred. This was accompanied by a significant drop in porewater pressure in both tests, (drop of 8.5 lb./in.^{2} in NC-15SF and 9.0 lb./in.^{2} in NC-16SF) and a drop in the deviator stress necessary to maintain the constant strain level (drop of 2.4 lb./in.^{2} in NC-15SF and 6.2 lb./in.^{2} in NC-16SF). The greater drop in deviator stress observed in NC-16SF may reflect the greater strain at which relaxation occurred.

One of the first items of importance shown by these tests (see Figure 24) is the apparent lack of any increase in porewater pressure as a result of membrane leakage. This observation serves to bear out the

conclusion reached earlier that membrane leakage was not a significant factor in these tests.

Following a period on the order of 10,000 minutes at these strain levels, (9500 minutes in NC-15SF and 7250 minutes in NC-16SF) straining was resumed. In NC-15SF the rate of strain following resumption of testing gave a time to 1% additional strain of 500 minutes (t_{+1} = 500 minutes) while in Test NC-16SF straining was resumed at the prerelaxation rate which gave 1% additional strain in 3/4 minute (t_{+1} = 3/4 minute). In both of these tests, deviator stresses were obtained far in excess of values appropriate to the new (post-relaxation) strain rates. In NC-15SF, the peak post-relaxation deviator stress of 43.7 lb./in.^{2} is 10½% higher than typical of a constant strain rate test having a t_1 = 500 minutes at 8½% strain. In NC-16SF, the peak post-relaxation deviator stress of 54.2 lb./in.^{2} is 30% greater than would typically occur at 10% strain in a constant strain rate test having a t_1 = 3/4 minutes. In Test NC-16SF, the post-relaxation deviator stress had every appearance of decaying to a magnitude commensurate with the new strain rate. In Test NC-15SF on the other hand, little if any decay in deviator stress occurred as post-relaxation straining was continued.

Little analysis of the pore pressure data from these two tests is possible due both to the anomolous behavior introduced by the temperature change and to the lack of extensive straining following resumption to testing. However, the data available point to the strain dependency of the porewater pressure. In both cases, following resumption of testing and the initial increase in porewater pressure, both curves of porewater pressure appear to be seeking levels appropriate to the respective rates of straining.

In terms of obliquity ratio ($\bar{\sigma_1}/\bar{\sigma_3}$), following the resumption of straining, test NC-15SF did not attain a $\bar{\sigma_1}/\bar{\sigma_3}$ ratio of a magnitude typical of the post-relaxation strain rate, but the

obliquity ratio was rising at the cessation of testing. In NC-16SF as straining was resumed at a strain rate yielding a $t_{+1} = 3/4$ sec., the obliquity ratio rose to a value far in excess of that typical for the new strain rate, but the obliquity ratio was dropping off rapidly at cessation of testing.

Chapter V

BEHAVIOR OF THE NORMALLY CONSOLIDATED SAMPLES

A. Introduction

All of the important behavior characteristics related to strain rate effect on normally consolidated samples of saturated fat clay are summarized and discussed in this chapter. Any model or mechanistic theory of shear strength behavior as related to strain rate must satisfy these observed features of behavior.

B. Summary - Effect of Strain-Rate on the Deviator Stress - Normally Consolidated Samples

The effect of the rate of strain on the deviator stress in tests on normally consolidated samples can be summarized as follows:

1. The maximum deviator stress attained in any test increases as the time to 1% strain decreases (Figure 4). This increase is on the order of 10% as the strain rate is increased from t_1 = 500 minutes to t_1 = 1 minute.

2. At any strain, the deviator stress is greater in a test with t_1 = 1 minute than in a test with t_1 = 500 minutes.

3. The magnitude of strain required to attain maximum deviator stress decreases as the rate of strain is increased (i.e., time to 1% strain decreased). At t_1 = 500 minutes, $8\frac{1}{2}$% strain was required to reach maximum deviator stress while with t_1 = 1 minute, $5\frac{1}{4}$% strain was required.

4. The maximum difference in deviator stress between a fast and a slow test (both numerical and percentage-wise) occurs at less than 1% strain (0.6%) and is on the order of 55% of the slow test deviator stress (Figures 25 and 26).

5. The increase in deviator stress is descriptively seen to occur as a result of both a steepening of the prepeak stress vs. strain curve and an elevation of the peak of such a curve and thus exhibits elements of both viscous and brittle behavior patterns.

6. As found by NASIM (1961) the greatest effect of strain rate upon maximum deviator stress occurs at rates of strain more rapid than the fast rate employed in this research.

7. The increase in maximum deviator stress within the range of strain rates considered in this research can be mainly attributed to the lower porewater pressure at failure in the faster tests.

8. If the strain rate is increased from t_1 = 500 minutes to a more rapid strain rate following the attainment of approximately 4% strain, the deviator stress immediately attains a value far in excess of that normal for the new strain rate, but decays to a value compatible with that expected in a steady rate test at the new strain rate. (Figure 20).

9. The magnitude of this excess over normal deviator stress for the new strain rate increases as the new strain rate is increased. (Figure 21).

10. If a step increase in strain rate from t_1 = 500 minutes to t_{+1} = 3/4 minutes is imposed at any strain level, a substantial increase in deviator stress occurs. (Figure 22). The actual magnitude of this increase in deviator stress decreases as the strain level at which the step in strain rate is imposed increases. (Figure 23).

11. An increase in deviator stress over what would be normal for the appropriate strain level in a steady rate test occurs as the strain rate is stepped from t_1 = 500 minutes to t_{+1} = 3/4 minutes regardless of the strain level at which such a step is imposed. However, the actual magnitude of the post-step deviator stress over that expected at a comparable strain level in a strain rate test increases as the level at which the strain rate is stepped increases. (Figure 23).

12. Following a period of relaxation at a constant strain level, the deviator stress after resumption of straining rises to a level far in excess of that normal for the post-relaxation strain rate in constant rate of strain tests.

C. Summary - Effect of Strain Rate in the Measured Porewater Pressure - Normally Consolidated Samples

The effect of strain rate on the developed porewater pressure in tests on normally consolidated samples can be summarized as follows:

1. The maximum porewater pressure developed in a test is lower at the more rapid strain rate.

2. The porewater pressure at maximum deviator stress was lower on the faster tests. (Figure 12).

3. Thus the "A" factor at failure decreases as the strain rate is increased. (Figure 13). This would happen if the pore pressure did not change as the strain rate increased.

4. Pore pressure gradients had only a minor effect on this data as did migration of porewater (i.e., internal volume change) (Figures 14 and 15). Membrane leakage was not a factor.

5. At strains, less than 1% the porewater pressure is independent of rate of strain within the strain rates considered in this research. Therefore, the pore pressure parameter "A" is greater in the slower tests at small strains. (Figure 17).

6. At any strain greater than 1%, the pore pressure in the faster tests is less than the pore pressure in the slower tests. The porewater pressure in the slower tests (t_1 = 500 minutes) rises continuously until straining ceases. In the faster tests, the porewater pressure reaches almost a "plateau" rising only 0.5 lb./in.^{2} from 6% to 12% strain.

7. The porewater pressure parameter "A" in the fast tests at any strain is a value approximately 0.2 lower than that in the slower tests. This difference in "A" between fast and slow tests remains constant as straining progresses. (Figures 17 and 19).

8. The porewater pressure following step increases in strain rate at approximately $4\frac{1}{4}$% strain from t_1 = 500 minutes to t_{+1} = 50 minutes, t_{+1} = 3 minutes and t_{+1} = $\frac{1}{2}$ minute result in the behavior shown in

Figure 20 (i.e., after an initial change, the post-step porewater pressure seeks a level commensurate with the post-step strain rate).

9. In terms of "A" factors, the post-step pore pressure behavior represents an initial drop in A. The magnitude of this drop depends upon the value of t_{+1}, increasing as the post-step strain rate becomes greater. Following this initial drop, the "A" factor rises to a value approaching that appropriate to the new strain rate.

10. Following steps in strain rate from t_1 = 500 minutes to $t_{+1} = \frac{3}{4}$ minutes at succeeding greater strain levels, the pore pressure increases immediately and subsequently drops to a level approximating that appropriate to the new strain rate. The exact post-step behavior is as shown in Figure 22.

11. In terms of "A" factor, the post-step porewater pressure behavior results in a considerable drop in "A" and a subsequent rise or leveling off to a value appropriate with the new strain rate.

D. Effect of Strain Rate on the Obliquity Ratio - Normally Consolidated Samples

The quantity $\bar{\sigma}_1/\bar{\sigma}_3$, herein termed "obliquity ratio" is a measure of the development of shearing resistance on the prospective failure planes with respect to the effective stress acting normal to these planes. If it is assumed that the observed sample strain is a shear yielding on the prospective failure planes, then the obliquity ratio is a fair indicator of the manner in which resistance to shear is being mobilized. The obliquity ratio is related to the angle of shearing resistance by the relationship $\sin \bar{\phi} = \frac{\bar{\sigma}_1/\bar{\sigma}_3 - 1}{\bar{\sigma}_1/\bar{\sigma}_3 + 1}$

This section summarizes the effect of strain rate on the observed behavior of the developed obliquity ratio. This value, of course, is completely dependent on the previously discussed externally measured quantities. However, it is felt by this author that this,

rather than deviator stress, is the fundamental quantity. The interaction of the obliquity ratio as a measure of the developed resistance to shear displacement and the developed porewater pressure give the sample its ability to resist the observed deviator stress.

The following observations summarize the effect of strain rate on the obliquity ratio. The discussion will again minimize the results of the one test representing the intermediate rate.

1. At failure (maximum deviator stress) the obliquity ratio is lower in the test with the more rapid strain rate. The obliquity ratio typical of t_1 = 1 minute at $(\sigma_1 - \sigma_3)_{max}$ is 2.55 (representing $\bar{\phi}$ of 25° 55') and that typical of t_1 = 500 minutes at $(\sigma_1 - \sigma_3)_{max}$ is 2.83 (representing a $\bar{\phi}$ = 28° 35').

2. At any strain less than 3.8%, the obliquity ratio is lower in a typical slow test (t_1 = 500 minutes). At 3.8% strain the obliquity ratio is the same in both the typical t_1 = 500 minute and t_1 = 1 minute test. However, the scanty data at intermediate strain rates suggests that this "crossover" point is not unique to all strain rates.

3. At any strain rate greater than 3.8% the obliquity ratio is higher in a typical slow test. (t_1 = 500 minutes).

4. In a typical fast test, the obliquity ratio peaks at about the same strain at which the deviator stress peaks. Following this peaking, the obliquity ratio decreases with further strain. In contrast, no distinct peak in obliquity ratio occurs in the slow test. The obliquity ratio levels off at quite large strains ($> 10\%$).

5. If, at approximately 4%, the strain rate in a slow test (i.e., t_1 = 500 minutes) is stepped, the obliquity ratio shows an immediate jump to a level higher than typical of the post-step strain rate, followed by a tailing off toward a level compatible with the new strain rate.

6. The same behavior can be expected if the strain rate is stepped from the slow (i.e., t_1 = 500 minutes) to the fast (t_1 = 1 minute) rate at any strain. The obliquity ratio shows a jump followed by a subsequent increase or decrease as straining continues to a level compatible with the post-step strain rate. However, in Figure 20, the strain rate steps at less than 3% strain produced obliquity ratios higher than would have occurred in a typical steady rate test having the post-step strain rate. This can be seen in the rather wide variation between these curves (i.e., obliquity vs. strain for steps in strain rate at less than 3% strain) and the curve given for t_1 = 500 minutes, if a "crossover" in obliquity were expected at $3\frac{1}{2}$ - 4% strain for steady rate t_1 = 1 minute and t_1 = 500 minute curves.

E. Discussion - Effect of Strain Rate on the Behavior of Normally Consolidated Samples at Small Strains

In this section is presented a discussion of the observed behavior of the normally consolidated samples at strains less than 1%. The key to the explanation of this behavior proposed by this author lies in the assumption that "bond" destruction or destruction of the interparticular forces resisting a shear deformative at these small strains is minor.

At small strains, the pore pressure is seen to be a function of the magnitude of strain and appears to be independent of the deviator stress. An admittedly crude model of this behavior is presented in Figure 28. As a shear displacement of particle A relative to particle B is effected, rotation of particle C must occur if the bonds at ① and ② are not broken. Thus, particle A must move closer to particle B inducing a pressure in any fluid filling the intervening space. If the bonds at ① and ② are not broken, it would seem that this induced pore-water pressure would be independent of the shearing stress (τ) necessary to effect the displacement, and be a function only of the tendency toward change in spacing of particles A and B, (h_1-h_2), which is in turn

a function of the horizontal or shear displacement. This is the observed behavior in terms of porewater pressure at small (i.e, $< 1\%$) strains.

If the "hinging" action of the bonds (1) and (2) is assumed to incorporate elements of "viscous" behavior, the observed behavior in terms of deviator stress can be explained. By "viscous" behavior is meant here behavior at the hinge such that the moment necessary to effect a certain angular rotation at the hinge is a function of the rate at which this rotation is caused to occur. Thus a greater shearing force is necessary to effect the same shearing displacement in a short time than in a longer time.

In summary, the observed behavior of the normally consolidated samples at small strains can be explained if it is assumed that:

1. The majority of the bonds between particles remains unbroken.

2. Some sort of a "structural viscosity" in the relative shearing displacement as modeled by the hinges in Figure 28 exists.

3. The pore pressure is a function of the tendency toward change in relative particle spacing (h_1-h_2) as shown in Figure 28, at constant volume.

4. Porewater migration or interval volume change plays a relatively minor role.

F. Discussion - Effect of Strain Rate on the Behavior of Normally Consolidated Samples at Large Strains

This section discusses and presents the author's explanation of the observed behavior of the normally consolidated samples at strains in excess of 4%. Here the key to the author's explanation of the observed behavior lies in the assumption that bonds between adjacent particles have been broken (they may be constantly breaking and reforming), and that this type of interparticular behavior described in the previous section as applying at small strains plays a relatively minor role.

In Figure 28 (b) is presented a highly idealized model representing the author's conception of the behavior at large strains in the normally consolidated samples. The rotational moment carrying capacity of the bonds (1) and (2) has been destroyed by the strain up to this time. Further displacement of particle A relative to particle B occurs by translation at the points of interparticular proximity (1) and (2). It would seem that the resistance to displacement at these points would be very much a function of the normal stress effective at these points of contact. Since this normal effective stress is a function of the induced porewater pressure and since the induced porewater pressure in the tests in which the strain rate was rapid was lower than in slower tests, it follows that the shear stress necessary to produce an additional shear displacement would become greater as the strain rate is increased, as has been observed. Therefore, the greater strength in the faster tests can be attributed to the lower porewater pressure.

This increased strength occurs in spite of an observed decrease in obliquity ratio, which is a measure of the "coefficient of friction" active at points (1) and (2) in Figure 28 (b), as the strain rate is increased. This phenomenon can be explained by postulating that the resistance of points (1) and (2) against translation and in comparison to the normal stress acting to maintain contact at these points is a function of the distance of separation at these points (which would be very small). However, as the rate at which the induced displacement occurs increases, the spacing at the points of proximity could increase due to an action somewhat akin to planing of a boat. Hence, the obliquity ratio would be expected to be lower in the more rapid tests.

This observation of decrease of obliquity ratio with increase in strain rate can also be attributed to the same phenomena causing the "pre-stress effect" which has been postulated as a portion of the explanation of an observed higher ϕ or angle of shearing resistance in undrained triaxial compression tests as compared to drained tests. (CASAGRANDE and WILSON, 1953). This effect can best be explained

by accepting as fundamental the Hvorslev Parameters of shear strength behavior and by additionally assuming that such parameters are independent of the rate of strain. The validity of the second assumption will be discussed in Chapter IX. The first assumption leads to the adoption of the line A-B in Figure 28 (d) as representing the relationship between the shear resistance on the failure plane at failure (τ_{ff}) and the normal effective stress on the failure plan at failure ($\bar{\sigma}_{ff}$) at a particular water content. The maximum pressure in terms of effective stresses acting on the potential failure plane occurred at the time of consolidation or possibly early in the test. (Actual average stress paths are shown in Figure 10). Point (x) in Figure 28 (d) represents failure in a slow test while point (y) is the corresponding point from a fast test. Since the porewater pressure is higher in the slow test, point (x) is nearer the τ axis than is point (y). A line drawn from the origin through either of these points would represent the standard failure envelope in terms of effective stresses. (OC and OD). It can be seen that since the effective stress on the failure plane in a fast test is higher due to a lower porewater pressure, the obliquity ratio (measured by $\bar{\phi}$ in Figure 20 (d)) will be lower.

The fundamental relationship in the effect of strain rate on the observed behavior of the normally consolidated samples at strains in excess of 4% is seen to be the relationship between the rate of strain and the porewater pressure at any strain. To explain the higher porewater pressure in the slower tests, a dilatency effect will be introduced using an idealized model similar to those of Figure 28 (a) and 28 (b). This is shown in Figure 28 (c). It can be postulated that at any instant, statistically, some of the displacement must be occurring in situations as shown in Figure 28 (c). If this displacement is occurring slowly, translation at the points of particular proximity can occur. However, if the resistance to such translation is of a viscous nature, a more rapid displacement of particles would lead toward a tendency of rotation

of the diagonal particle. If the resulting tendency toward increase in the particle spacing, h, is prevented by the porewater, a lower porewater pressure will be induced. Consequently, the more rapid the displacement of the particles, the lower the expected porewater pressure.

Chapter VI

OVERCONSOLIDATED SPECIMENS WITH UNIFORM STRAIN-RATE

A. Introduction

This chapter presents and discusses the results of a series of triaxial compression tests upon overconsolidated samples of the Vicksburg clay. These tests were performed at uniform rates of strain representing times to 1% strain varying from 45 seconds to 500 minutes. In some of these tests the strain-rate was "stepped" as was the case with the tests on normally consolidated samples described in Chapter IV. It was the original intent to prepare these samples by consolidation to 120 lb/in.^{2} and rebound to $7\frac{1}{2}$ lb./in.^{2}. Thus an overconsolidation ratio of 16 would be attained. However slight inaccuracies in gages (subsequently calibrated) led to OCRs varying from $15\frac{1}{2}$ to 19. (Test OC 9-S had OCR = 13. However, this test is not utilized in any analysis due to other difficulties as will be described). The OCR of each test is listed in Table VI-1. The data regarding the behavior of these samples subsequent to the change in rate of strain is described in Chapter VII. However, data from the earlier portions of these tests, prior to the "step" in strain rate are included with the data from the tests run to completion at a constant strain rate and are included in the summaries appearing in this chapter.

B. Laboratory Test Program - Overconsolidated Samples - Uniform Strain-Rate

This section presents, in summary fashion, a listing of the tests performed upon the overconsolidated samples. Complete plots of stress versus strain, pore water pressure versus strain obliquity versus strain and stress vector plots from individual tests are presented in Appendix B. Also included in Appendix B are brief descriptions of each test, including any information judged to be necessary to completely document the tests.

A total of 11 tests were performed on the overconsolidated samples. The setup of these tests is described in Chapter II as is the testing procedure. Tests OC1-F and OC6-S were on samples from Batch A as described in Chapter II, Section C. Tests OC2-F, OC3-F, OC4-F, OC5-F, OC7-S, OC8-S, and OC9-S were performed on samples from Batch B while OC10-SF, and OC11-SF were performed on samples from Batch C. There is little reason to suspect any gross deviation in the properties of the three batches of soil. However, the small differences which did exist may have considerable effect on the observed results. The nature and cause of the strain rate effect in the overconsolidated samples are rather elusive and hinge on small differences rather than on the more pronounced differences noted in the normally consolidated samples.

Considerable difficulty was experienced in the performance of Test OC9-S. This test was meant to be an extremely slow test, and was performed using Cylerex as the cell fluid. The results are obscured by seating difficulty in the piston to top cap seat and in the pedestal to internal load cell seat. In addition, the electricity was cut off to the load frame sporadically due to a faulty connection in the wiring. The results of this test are discussed, where pertinent, in light of conclusions drawn from the other tests and are not used to influence the conclusions.

All tests with the exception of Test OC8-S were performed upon samples encased in 2 rubber membranes separated by a thin layer of silicone grease. Test OC8-S, however, was performed upon a sample having 2 membranes, but without the benefit of a silicone grease layer. Since the sample was assembled under water, there was a film of water trapped between the two membranes and the effect regarding membrane leakage was to nullify the advantage to be gained from two membranes.

C. Presentation of Results - Overconsolidated Samples - Uniform Strain Rate

The following several sections present the results of the tests on the overconsolidated samples tested at a uniform strain rate. These results are presented by describing the effect of strain rate on observed stress versus strain behavior, pore water pressure versus strain behavior and conventional parameters of stress versus strain behavior deduced from these observations. (i.e., obliquity ratio and various pore water pressure parameters.) In these sections it is not the intention to pinpoint causes for the observed effect of rate of strain on these quantities, but only to describe the observed effect.

There is considerably more scatter in the data obtained from the tests on the overconsolidated samples than was the case with the normally consolidated samples. This scatter is attributed to differences in individual samples. As will be pointed out in a later section, migration of pore water to planes or zones of failure resulting in dissipation of, in this case, negative (with respect to back pressure) pore water pressure and thus tendencies toward internal volume changes in the samples were of paramount importance. The effect of strain rate on this migration of pore water probably leads to the majority of the observed effects of rate of strain on the stress versus strain behavior of these samples. Thus, as will be pointed out in following sections, the overall picture of the effect of rate of strain on stress versus strain behavior in the overconsolidated samples is obscured by the effect of rate of strain on the internal migration of pore water and the effects of this internal migration on observed behavior.

The cause of pore pressure gradients within individual test specimens is found in the stress distribution occuring as a result of the nature of the test iteself. In analysing the test results, a uniform distribution of stresses is assumed. This assumption would be valid if the sample pedestal and top cap of the triaxial test

apparatus were completly frictionless. However, this is far from the case. The resulting phenomena have been described in terms of a re-arranged pore pressure equation by Bishop et al (1960) and this has been presented in Chapter III, Section D.

The following description of this effect, while crude, is presented to point out the importance of internal pore pressure gradients in overconsolidated samples and as such will be repeated and elaborated upon in a later section. In addition, it is presented to point out that considerable scatter in data regarding the effect of rate of strain observed in these tests is probably due to differences in individual test specimens.

In a triaxial sample of saturated soil undergoing testing, the portions of the sample immediately adjacent to the stone on the pedestal and immediately adjacent to the specimen top cap are restrained from lateral expansion due to friction at the contact surfaces. In the no-lateral-strain situation, the pore water pressure induced due to an application of vertical load can be expected to be essentially equal to the vertical stress. Thus, in the thin zone adjacent to the ends of the sample, the pore pressure response to an instantly applied axial load can be expected to be essentially equal to the deviator stress $[\Delta(\sigma_1 - \sigma_3)]$ applied to the sample as a whole. In the central portion of the sample a uniform stress distribution in a horizontal plane is a reasonable assumption and here the pore pressure response to an instantaneous load is $A[\Delta(\sigma_1 - \sigma_3)]$. If A = 1, the induced pore water pressures at the sample mid-height and at the base are similar. In normally consolidated samples of clay soils, A approaches 1 and internal pore pressure gradients and resulting internal volume changes are of a minor effect. However, in overconsolidated samples with $A < 0$. it can be seen that a considerable pore pressure gradient within a test specimen is possible.

Thus, in overconsolidated samples, if a test is performed rapidly, the midplane pore pressure is the value to use in determining the effective stress controlling the shear resistance, whereas the base pore pressure would not. In this situation, little volume change is possible. If a test is performed slowly enough to allow pore pressure equalization, the measured pore pressue is inappropriate to the assigned Overconsolidation Ratio and equalization of pore pressures has led to internal volume changes. At intermediate strain rates intermediate degrees of pore pressure equalization and internal volume change have occurred. The assignment of appropriate strain rates to the extremes (i.e., no migration of pore water to complete equalization of pore water pressure) hinges on the time-compression parameters, c_v (compression) and c_v (rebound) applicable to the test specimen. These parameters are in turn a function of volume change behavior and permeability. It is felt that only minor differences in volume change behavior (as described by a_v or m_v) occurred either between batches or between individual test specimens in this test series. However, the permeability of the samples is influenced so greatly by small differences in grain size composition and particle structural arrangement that considerable differences from batch to batch and sample to sample are possible. Therefore, the observed data scatter is felt to be attributable to differences in permeability among test samples.

To sum up, it has been attempted in this section, to prepare the reader for the presentation of results which follows by pointing out that the observations are influenced more by the effect of rate of strain on internal pore water migration than by the effect of rate of strain on fundamental parameters of stress versus strain behavior, and that the importance of differences in permeability on the time rate of this pore water migration has lead to considerable data scatter.

D. Effect of Rate of Strain on the Stress Versus Strain Behavior of Overconsolidated Samples

This section presents, in a general form, the observed results from the series of tests on the overconsolidated samples performed at uniform strain rates. Complete stress versus strain and pore water pressure versus strain curves for each test appear in Appendix B.

All of the pertinent observed results are presented in Table VI-1 following:

Table VI-1

RESULTS OF TESTS ON OVERCONSOLIDATED SAMPLES

Test No.	Time To 1% Strain (min.)	$(\sigma_1 - \sigma_3)$ max. (lb./in.^{2})	$(\sigma_1 - \sigma_3)$ at $(\bar{\sigma}_1/\bar{\sigma}_3)$ max. (lb./in.^{2})	u at $(\sigma_1 - \sigma_3)$ max. (lb./in.^{2})	u at $(\bar{\sigma}/\bar{\sigma}_3)$ max. (lb./in.^{2})	M max. (lb./in.^{2})	$\bar{\sigma}_1/\bar{\sigma}_3$ max.	$\bar{\sigma}_1/\bar{\sigma}_3$ at $(\sigma_1 - \sigma_3)$ max.	ε at $(\sigma_1 - \sigma_3)$ max. (%)	ε at $(\bar{\sigma}_1/\bar{\sigma}_3)$ max. (%)	Avg. w. at Failure (%)	Batch	o.c.
OC1-F	3	28.5	23	-7.0	+3.8	-11.0	7.5	3.3	8.5	1.9	29.3	A	19
OC2-F	1.7	32.6	25	-4.1	+1.6	-9.6	4.48	3.45	7.2	1.9	30.0	B	17
OC3-F	.75	32.6	23	-5.8	+0.1	-10.6	4.15	3.45	8.4	2.2	28.6	B	16
OC4-F	1.5	33.5	24.7	-8.0	+0.1	-16.5	4.10	3.25	11.1	1.75	29.8	B	15½
OC5-FS	.75	32.5*	21.5	-6.4	+2.5	-8.0	6.4	3.5*	8.5*	1.3	29.4	B	16
OC6-S	18	27.3	17.0	-5.8	+2.6	-7.0	5.7	3.2	7.5	2.3	29.1	A	18
OC7-S	30	27	17.2	-3.2	+3.7	-4.8	4.7	3.34	5.2	1.4	30.3	B	17
OC8-S	250	24.3	19	-1.2	+1.7	-2.2	4.65	3.95	5.0	2.1	29.9	B	16½
OC9-S	3000	28.4	--	0	--	-1.0	--	--	?	--	28.4	B	13
OC10-SF	500	28.2*	20.5	-5*	+0.6	-7.5	4.30	3.5*	6.6*	2.2	29.4	C	17½
OC11-SF	500	26.5*	19.2	-4*	+1.1	-7.0	4.28	3.5*	6.0*	2.0	29.7	C	17½

*NOTE: Data extrapolated from tests with stepped strain rate.

In Figure 29 are plotted all data from tests on the over-consolidated samples performed at strain rates having times to 1% strain short enough to be grouped as "fast" tests. Average stress versus strain and excess pore water pressure versus strain are drawn using these plotted points. Test OC1-F was the only rapid test run on a sample cut from Batch A soil and hence is excluded from consideration in this plot.

In Figure 30, all data from tests considered to be "slow" tests are plotted. Data from tests OC10-SF and OC11-SF were almost coincident and were averaged. Both of these tests were tests in which a step increase in strain rate was imposed at about 4% strain. Consequently the curves beyond 4% strain are extrapolations of observed data.

From Figure 30 the following conclusions can be drawn:

1. The stress versus strain curve from fast tests rises more steeply and attains a higher deviator stress level at any strain than do stress versus strain curves from any slow test.

2. The pore pressure versus strain curve from fast test does not rise initially to quite as high positive pore water pressure levels as do curves from slow tests. Following attainment of maximum positive pore water pressure, the pore pressure in the fast tests falls off more rapidly with strain, decreases to lower negative pore water pressures and continues decreasing to larger strains than does the pore water pressure in the slow tests.

3. Fast tests attain maximum deviator stress at larger strains than do slow tests.

E. Effect of Strain Rate on Maximum Deviator Stress, Strain at Failure and Mode of Failure, Overconsolidated Samples - Uniform Strain Rate

This section summarizes the effect of strain rate upon the maximum deviator stress obtained, the strain level at the attainment of maximum deviator stress and the mode of failure observed in the tests on overconsolidated samples at uniform strain rates. These

observations are not to be construed as conclusions regarding any fundamental soil properties but are, as was pointed out in Section C of this chapeter, observations of the behavior of laboratory samples of a particular size.

In Figure 31 are plotted the maximum deviator stresses obtained in all of the tests on the overconsolidated samples. The points representing tests OC10-SF and OC11-SF are plots of values obtained by extrapolation of the stress versus strain curves following the step in strain rate. The solid line is the author's impression of the probable relationship between maximum deviator stress and rate of strain. The exact location of the intersection of the two tangents is unknown and probably hinges on local permeability deviations from sample to sample. In addition, the results of a series of tests on the same soil but at a slightly lower OCR are presented. (NASIM 1961). In the range of strain rates of Nasim's tests, the relationship between deviator stress and strain rate roughly parallel the author's.

In Figure 32 are plotted strains at maximum deviator stress versus time to 1% strain as a measure of strain rate. There is seen to be considerable data scatter. However, the solid line represents what appears to be the general trend of the data and is the author's impression of the probable relationship between rate of strain and strain at failure (i.e., maximum deviator stress). It will be seen from this figure that as the rate of strain decreases (time to 1% strain increases), the strain necessary to attain maximum deviator stress becomes less.

In Table VI-2 are listed the modes of failure of each test and, where failure planes occurred, the strain level at which these were first noted. All three batches of soil are represented in this data and the formation of failure planes is probably a phenomenon very sensitive to local variations in samples. Thus no quantitive conclusions can be drawn from this data. However, it seems obvious

that there is less tendency toward formation of failure planes in the more rapid tests. In fact, no failure planes were noted at all in the fastest tests (OCs-F, OC4-F & OC5-FS) while quite distinct failure planes were formed at relatively low strains in the slowest tests.

F. Relationship Between Rate of Strain and Pore Water Pressures, Overconsolidated Samples, Uniform Strain Rate

Presented in this section are all data obtained regarding the pore water pressures recorded in this series of tests. In all of the tests on overconsolidated samples, the pore water pressure was measured at the sample mid-height employing the probe described in Appendix A.

Table VI-2

MODES OF FAILURE-OVERCONSOLIDATED SAMPLES

Test No.	Time to 1% strain (minutes)	Mode of failure	Strain at which failure plane (%)
OC1-F	3	Bulging Failure Plane	17%
OC2-F	1.7	Bulging Failure Plane	13%
OC3-F	.75	Bulging	--
OC4-F	1.5	Bulging	none at 32%
OC5-FS	.75	Bulging	--
OC6-S	18	Failure Plane	10%
OC7-S	30	Failure Plane	9½%
OC8-S	250	Failure Plane	7 3/4%
OC9-S	3000	Failure Plane	?
OC10-SF	500	Failure Plane	6%
OC11-SF	500	Failure Plane	10%

In addition, the pore water pressure was measured at the base of the sample in tests OC1-F, OC2-F, OC3-F, OC4-F, OC5-FS, OC6-S, OC7-S and OC8-S.

In Figure 30 are plotted summary curves of pore water pressure versus strain representing all tests. The average "fast" curve represents the four fast tests as plotted in Figure 29. A study of Figure 30 leads to the following conclusions:

1. The maximum positive pore water pressure is attained at about the same strain regardless of strain rate.

2. A higher positive pore water pressure is attained at these low strains in the slower tests. However, the actual magnitude of the difference is only on the order of 1 lb./in.^{2}.

3. The pore water pressure goes negative with respect to back pressure at lower strains in the faster tests. (i.e., more strain is necessary to develop a negative pore water pressure in the slower tests).

4. The pore water pressure in the faster tests attains a much more negative value with respect to back pressure than do the pore water pressures observed in the slow tests.

5. At a certain strain, the pore water pressure in the slower tests stops decreasing and tends to remain at a constant level. However, the observed pore water pressure in the fast tests continues to become more negative to quite large strains.

The relationship between midplane pore water pressure and strain rate is shown in Figure 33. Points representing pore water pressure at maximum deviator stress and points representing the maximum pore water pressure obtained in the tests are plotted. Since the maximum negative pore water pressure attained in any test is a function of the strain at which shear plane formation occurs and is a function of the strain level at which testing was discontinued, the considerable scatter in data representing this quantity is to be expected.

The data representing pore water pressures at maximum deviator stress, as plotted in Figure 33 are remarkably consistent. The solid line in that figure represents the author's impression of the relationship

between pore water pressure at maximum deviator stress and strain rate for the overconsolidated samples. From this figure, the conclusion can be drawn that a more negative (lower) pore water pressure is attained as the rate of strain increases.

The relationship between mid-height pore water pressure and deviator stress is shown in Figure 34. The values represent typical or average values with tests OC10-SF and OC11-SF averaged for the slow values. (See Figure 30). Using the same "average" curves, the pore pressure parameter A, ($A = \frac{\Delta u}{\Delta(\sigma_1 - \sigma_3)}$), is plotted as a function of strain in Figure 35. The discontinuity in the curve representing the slow tests and occurring at about 4% strain is felt to be the start of the shifting of the strain to a zone of local yielding and thus represent the start of failure plane formation. It will be observed in this figure that no such discontinuity occurs in the curve representing the fast tests, and the A factor is gradually decreasing at a decreasing rate throughout the progress of the test.

In Figure 36, the relationship between the pore water pressure parameter A and strain rate as given by the midplane pore pressure is shown. It can be seen in this figure that the A factor tends to decrease slightly (become more negative) as the rate of strain increases.

G. Pore Water Pressure Gradients and Internal Volume Change Phenomena, Overconsolidated Samples

In this section are presented all the data regarding the differences in pore water pressure at various heights (base versus mid-height-needle pore water pressures) and the distribution of moisture content throughout individual test specimens obtained as a result of this research.

Pore water pressure was measured at both the sample base and the sample mid-height in tests OC1-F, OC2-F, OC3-F, OC4-F, OC5-FS, OC6-S, OC7-S and OC8-S, and these data are plotted with each individual

test in Appendix B. Typically, in a fast test, the mid-height pore water pressure rose more rapidly to its maximum positive value (lower than the base maximum positive value). After attaining its maximum positive value, the mid-height pore water pressure fell rapidly to a negative value (with respect to back pressure). The base pore pressure rose more slowly to a higher positive value than the midplane value, fell less rapidly, going negative at a considerably greater strain than was the case at midplane. At any strain level following an initial crossover at $\frac{1}{2}$ to 3/4% strain, the midplane pore pressure is lower than the base pore pressure. Tests OC3-F and OC4-F illustrate this typical behavior quite well.

The slow tests, typified in this case by OC7-S and OC8-S, show midplane pore pressure higher than the base pressure at strains less than $1\frac{1}{2}$% although a portion of this difference existed initially in both tests and is probably anomalous. In test OC8-S, which was slower than OC7-S, the midplane pore water pressure became slightly lower than the base pore water pressure, but the two became coincident at 8% strain and remained so to the completion of the test.

In Figure 37 are plotted all the data available in this test series regarding pore water pressure gradients, or a difference in base and mid-height pore water pressure. It can be seen that there is a good deal greater tendency for the development of gradients in the overconsolidated samples than was the case with the normally consolidated samples. This plot also demonstrates the relationship between base and mid-height pore pressures and rate of strain.

In all tests, with the exception of OC3-F, post shear water contents were determined from six levels in each sample as shown in Figure 38. The preshear, post consolidation distribution of water content is, of course, unknown. However, Nasim (1960) in tests on the same clay found an essentially uniform distribution of post consolidation water contents in his overconsolidated samples. This assumption

seems justified when the data from tests OC1-F and OC2-F are considered. In these tests, sheared rapidly and quickly dismantled, an essentially uniform water content through the sample was observed.

The water content data from the slow tests all fall within the shaded area shown in Figure 38. In addition, the water content distribution from test OC4-F in which considerable time elapsed following testing before the water contents were determined, fell within the shaded area. On the basis of the assumption of essentially uniform preshear water content, there is seen to be considerable evidence of migration of water toward the middle portion of the sample from the ends with a resulting increase in water content in the middle portion and decrease at the specimen and regions.

H. Effect of Rate of Strain on Obliquity Ratio ($\bar{\sigma_1}/\bar{\sigma_3}$) Overconsolidated Samples

This section presents and discusses the effect of strain rate on obliquity ratio as deduced from measured deviator stress and pore water pressure. In Figure 39, the $\bar{\sigma_1}/\bar{\sigma_3}$ ratios as deduced from Figure 30 are plotted against strain. The value of maximum obliquity which occurs between 1% and 2% strain is felt to be a good average as shown on Figure 39. However, as the results of individual tests are studied, this value will be seen, in the faster tests to exhibit considerable scatter. This maximum $\bar{\sigma_1}/\bar{\sigma_3}$ is quite sensitive to the maximum positive pore water pressure, and can change radically within the limits of the accuracy of pore pressure measurements in this region. It can be seen clearly from this figure that, while the faster tests, at any strain level, exhibit a higher obliquity, the $\bar{\sigma_1}/\bar{\sigma_3}$ ratio at maximum deviator stress is only slightly higher in the faster tests due to the attaining of this condition at a larger strain. This trend is illustrated in Figure 40 where, in addition to the points from the average curves, data from each test is also plotted.

In this figure are plotted both maximum obliquity ratio versus strain rate and obliquity ratio at maximum deviator stress versus strain rate. Straight lines representing possible relationships between obliquity ratios and logarithm of strain rate (time to 1% strain) have been drawn. Considerable scatter of data casts doubt on the relationship between maximum obliquity ratio and strain rate. However, obliquity ratios at maximum deviator stress seem to form a consistent pattern indicating a slight increase in obliquity ratio at failure as the strain rate increases. This trend is opposite to that exhibited by the normally consolidated samples.

I. Summary and Conclusions: Overconsolidated Samples - Uniform Strain Rate

The following conclusions drawn from observations of the behavior of the overconsolidated samples seem justified on the basis of the data available:

1. At any strain level, a faster test exhibits a higher deviator stress than a slow test.

2. Within the range of strain rates considered in this research an increase in maximum deviator stress in the more rapid tests of 20% over the slower tests occurred.

3. At any strain level, a lower pore water pressure was recorded in the more rapid tests. The pore water pressure at failure in the faster tests was much lower than that in the slower tests, partly due to the fact that the faster tests "held together" to much greater strains.

4. At any strain level, a higher obliquity ratio in terms of effective stresses ($\bar{\sigma_1}/\bar{\sigma_3}$) existed in the faster tests.

5. Thus the higher deviator stress attained in the faster tests can be attributed to a more negative pore water pressure and a slightly higher obliquity ratio at failure.

6. The above effects are observations based on the behavior of a particular size laboratory specimen. Fundamental behavior patterns were obscured by pore pressure gradients between the base of the sample and midplane. equalization of which led to internal void ratio changes in the slower tests.

7. Associated with the above phenomenon, the faster tests tended to fail by bulging, while quite distinct shear planes were observed in the slower tests.

Chapter VII

OVERCONSOLIDATED SPECIMENS WITH STEPPED STRAIN-RATE

A. Introduction

Presented in this chapter are the results of a series of three tests on overconsolidated samples, having overconsolidation ratios of between 16 and 18, which were subjected to a step in strain rate, either increase or decrease. Tests OC5-FS, OC10-SF and OC11-SF are included in this series.

B. Sample Preparation, Consolidation and Testing

The specimens tested in this series of tests were prepared, set up for testing and consolidated in the triaxial chamber in exactly the same manner as the specimens described in the previous chapter. In test OC5-FS, the sample was brought to 5.6% strain at the most rapid strain rate employed in this research, t_1 = 3/4 minutes. At this strain level, the strain rate was decreased to t_1 = 17 minutes. This test was prepared from a Batch B sample.

Tests OC10-SF and OC11-SF were prepared from Batch C samples. In these tests, the samples were brought to approximately 4% strain (4.3% in OC10-SF and 3.9% in OC11-SF) at a strain rate of t_1 = 500 minutes. At this strain level, the strain rate was instantaneously increased to a strain rate of t_1 = 3/4 minutes in both tests. In test OC10-SF, shortly following the step in strain rate, the clutch on the load frame began to slip, so the actual strain rate is unknown.

C. Presentation of Data

The data from these three tests appears in Appendix B, in Figures B-43, B-44, B-51, B-52 and B-53, and the reader is referred to these figures during the ensuing discussion. Plots of deviator stress, pore water pressure and ratio of principal effective stresses ($\bar{\sigma}_1/\bar{\sigma}_3$)

versus strain are presented. In test OC5-FS plots of both midplane and base pore pressures versus strain are presented.

In addition, the water content distribution following testing was determined in all three samples. This information is also presented on Figures B-43, B-51 and B-52 in Appendix B.

D. Test OC5-FS with Step Decrease in Strain-Rate

In test OC5-FS, the strain rate was instantaneously decreased from t_1 = 3/4 minutes to t_1 = 17 minutes at 5.6% strain. In this test, pore water pressure was continuously measured at both the sample base and the sample mid-height (via the porous probe).

From the start of the test, up to the strain at which the strain rate was decreased, the sample behaved quite similarly to the "average fast test" presented in Figure 30. The base pore water pressure at any strain level was considerably greater than the mid-height pore water pressure. The mid-height pore pressure went "negative" with regard to initial back pressure at 2.8% strain, while the base pore water pressure remained positive until after the decrease in strain rate. Prior to the change in strain-rate, the deviator stress versus strain behavior was also quite typical of the rapid rate of strain (t_1 = 3/4 minutes).

E. Effect of a Step Decrease in Strain Rate Upon Deviator Stress - Over-Consolidated Samples

Following the step decrease in strain-rate from t_1 = 3/4 minute to t_1 = 17 minutes, the deviator stress, which had nearly attained its peak at the rapid strain rate, fell abruptly from 32 lb./in.^{2} to 26.5 lb./in.^{2}, or 17%. Following this drop, the deviator stress rose steadily to a new peak of 29 lb./in.^{2} at 9% strain. This is a value about 11% below the expected peak at the fast rate (t_1 = 3/4 minutes) and occurs at a strain level similar to the expected peaking strain at the fast rate.

F. Effect of a Step Decrease in Strain Rate Upon the Observed Pore Water Pressure, Overconsolidated Samples

Prior to the step decrease in strain rate, the pore water pressure, as measured at the sample mid-height by the porous probe described in Appendix A, behaved in a pattern typical of the fast strain rate. No change in the pattern of pore pressure behavior as recorded at the sample mid-height was noted following the step decrease in strain rate. The pore water pressure as measured at mid-height did not rise to a level typical of a test at t_1 = 17 minutes performed at a uniform strain rate.

The base pore pressure measurement did change following the step decrease in strain rate. Prior to the decrease in strain rate, the base pore pressure was greater than the midplane pore pressure with the magnitude of this difference increasing. However, following the step decrease in strain rate, the base pore water pressure dropped drastically rather quickly and continued falling as straining progressed. The behavior of the base pore pressure as post-step straining continued was such as to be gradually diminishing the magnitude of the difference between it and the mid-height pore pressure. The two measurements ran parallel, with the base showing $2\frac{1}{2}$ lb./in.^{2} higher from 11% strain until cessation of testing at $12\frac{1}{2}$% strain.

This behavior of base pore water pressure illustrates nicely the phenomenon described in Section C of Chapter VI. Due to lateral restraint in regions of the sample adjacent to the base and to the end cap, a tendency toward a higher pore water pressure exists. If the equalization of this pore water pressure due to internal flow of pore water and resulting volume changes were prevented (e.g. by extremely rapid testing) the measured base pore water pressure could be expected to approach the magnitude of the applied deviator stress. However, testing at finite strain rates allows some internal flow of water to occur causing the measured pore water pressure to be always less

than the deviator stress. At the mid-height of the sample, however, lateral strains can occur, stress distribution is uniform across the sample and the pore water pressure will be $u = A(\sigma_1 - \sigma_3)$ if the test is performed rapidly. At slow strain rates, the base and mid-height pore water pressures will be equal and be greater algebraically than $A(\sigma_1 - \sigma_3)$ in overconsolidated samples (or in any situation where $A < 1$).

In test OC5-FS, at the fast strain rate a higher pore pressure is observed at the base of the sample than at the sample mid-height. Reduction of the strain rate serves to reduce the magnitude (algebraic) of the base pore water pressure by allowing time for a greater degree of internal flow of pore water to occur.

G. Effect of a Step Decrease in Strain Rate Upon the Deduced Principal Effective Stress Ratio - Overconsolidated Samples

This section presents the obliquity ratio ($\bar{\sigma}_1/\bar{\sigma}_3$) versus strain behavior deduced from observed deviator stress and midplane pore water pressure versus strain behavior. It should be emphasized that the effects of strain rate and steps in strain rate are largely a function of the degree of internal migration of pore water and thus the true strain rate effect is largely obscured.

Figure 44 of Appendix B presents deduced obliquity ratio versus strain behavior from test OC5-FS. In the early portion of the test the behavior was similar to the expected in a test performed at the fast (t_1 = 3/4 minutes) rate. The exact "typical" behavior of obliquity at small strains is a rather elusive factor as was previously pointed out. Following the step decrease in strain rate, the obliquity fell to a value below that typical of the new strain rate (t_1 = 17 minutes) at the same strain level. However, the obliquity ratio rose quickly to a value typical of uniform strain at the new strain rate and subsequently behaved similarily to test performed at a uniform strain rate of t_1 = 17 minutes.

H. Mode of Failure of Sample with a Step Decrease in Strain Rate

The mode of failure of sample OC5-FS is quite interesting. It has been observed in the main tests on overconsolidated samples at uniform strain rates that failure at slow strain rates occurred at relatively small strains by formation of a distinct failure plane. However, failure in tests at fast strain rates was by bulging with no failure plans being noticed generally at quite large strain levels.

Failure in test OC5-FS was by bulging with no failure plane being noted at cessation of testing at a strain of $12\frac{1}{2}\%$ even though the test was carried on at a slow rate of strain for a sufficient magnitude of strain to allow failure plane development.

I. Tests OC10-SF and OC11-SF with Step Increases in Strain Rate

This and the following sections of this chapter describe and present the results of two tests, performed on overconsolidated samples, in which the strain rate was "stepped" up or increased at a strain level of approximately 4%. In test OC10-FS the step increase in strain rate was imposed at 4.3% strain and in test OC11-FS at 3.9% strain.

These samples were set up and consolidated in exactly the same manner as the rest of the overconsolidated samples. Testing was instituted at a slow strain rate of t_1 = 500 minutes. At approximately 4% strain the strain rate was abruptly "stepped" to a new rate of t_1 = 3/4 minutes. Following this step in strain rate, the test was carried to completion at the new strain rate.

Some difficulty was experienced in the performance of test OC10-SF. Following the step in strain rate, the clutch of the load frame was observed to slip. Thus the exact post step strain rate is unknown. For this reason, most of the results presented in the following sections are the results of test OC11-SF. Complete stress versus strain, pore water pressure versus strain and obliquity versus strain from both tests appear in Figures 51 and 52 in Appendix B.

H. Mode of Failure of Sample with a Step Decrease in Strain Rate

The mode of failure of sample OC5-FS is quite interesting. It has been observed in the main tests on overconsolidated samples at uniform strain rates that failure at slow strain rates occurred at relatively small strains by formation of a distinct failure plane. However, failure in tests at fast strain rates was by bulging with no failure plans being noticed generally at quite large strain levels.

Failure in test OC5-FS was by bulging with no failure plane being noted at cessation of testing at a strain of $12\frac{1}{2}\%$ even though the test was carried on at a slow rate of strain for a sufficient magnitude of strain to allow failure plane development.

I. Tests OC10-SF and OC11-SF with Step Increases in Strain Rate

This and the following sections of this chapter describe and present the results of two tests, performed on overconsolidated samples, in which the strain rate was "stepped" up or increased at a strain level of approximately 4%. In test OC10-FS the step increase in strain rate was imposed at 4.3% strain and in test OC11-FS at 3.9% strain.

These samples were set up and consolidated in exactly the same manner as the rest of the overconsolidated samples. Testing was instituted at a slow strain rate of $t_1 = 500$ minutes. At approximately 4% strain the strain rate was abruptly "stepped" to a new rate of $t_1 = 3/4$ minutes. Following this step in strain rate, the test was carried to completion at the new strain rate.

Some difficulty was experienced in the performance of test OC10-SF. Following the step in strain rate, the clutch of the load frame was observed to slip. Thus the exact post step strain rate is unknown. For this reason, most of the results presented in the following sections are the results of test OC11-SF. Complete stress versus strain, pore water pressure versus strain and obliquity versus strain from both tests appear in Figures 51 and 52 in Appendix B.

J. Effect of a Step Increase in Strain Rate Upon Deviator Stress - Overconsolidated Samples

This section discusses the effect of a step increase in strain rate upon deviator stress in the overconsolidated samples. Prior to the step increase in strain rate, the deviator stress versus strain behavior in both tests OC10-SF, and OC11-SF was identical and typical of the stress versus strain behavior of the pre-step strain rate of t_1 = 500 minutes. Following the step increase in strain rate, the deviator stress jumped to a value in agreement with the deviator stress that would have been attained in a test at a uniform strain rate equal to the post-step strain rate at the same strain level. Following this, the deviator stress in test OC11-SF fell slightly and remained below the deviator stress at any strain past the strain level of the step increase. The same behavior with a much more pronounced dip in deviator stress was noted in test OC10-SF, but this excess dip in deviator stess is probably attributable to the load frameclutch slippage as discussed in the previous section.

K. Effect of a Step Increase in Strain Rate Upon Developed Pore Water Pressure - Overconsolidated Samples

One of the more interesting phenomena observed in this series of testing was the effect of a step increase in strain rate upon the observed pore water pressure versus strain pattern. Since there is some question regarding the results of test OC10-SF due to suspected clutch slippage, only test OC11-SF will be discussed here. The reader is referred to Figure 52 in Appendix B.

Prior to the step increase in strain rate, the developed pore water pressure versus strain pattern was typical of that expected in a test at a uniform strain rate of t_1 = 500 minutes. Following the step increase in strain rate, there was no discernable change in the pattern of pore pressure development. The post step pattern of pore pressure development was one of continuing decrease in pore water pressure until

cessation of testing at 10 3/4% strain.

Also presented in the bottom half of Figure 52 of Appendix B is a plot of the pore water pressure parameter A versus strain before and after the step in strain rate. The apparent behavior pattern is a follows: Prior to the step in strain rate, A is decreasing with becoming less negative and following a pattern typical of the slow rate of strain (t_1 = 500 minutes). Following the step in strain rate to t_{+1} = 3/4 minutes, the A factor assumes a constant value and holds this value until reaching a strain level appropriate to this value of A at the faster strain rate. Following the attainment of this strain level, the behavior pattern of A related to strain becomes one assumed to be typical of the rapid rate of strain.

The implications of this observed pore pressure development will be discussed in the following chapter.

L. Effect of a Step Increase in Strain Rate Upon the Effective Principal Stress Ratio ($\bar{\sigma}_1/\bar{\sigma}_3$) - Overconsolidated Samples

In this section is presented and discussed the effect of a step increase in strain rate upon the observed obliquity ratio ($\bar{\sigma}_1/\bar{\sigma}_3$) versus strain pattern as deduced from measured deviator stress and pore water pressure. It should again be emphasized that the following is an observed behavior pattern of a certain dimensioned test sample and cannot be construed to represent fundamental soil behavior as will be described in the following chapter. Here again the emphasis is upon test OC11-SF due to the suspected clutch slippage of the test frame during test OC10-SF.

Prior to the step increase in strain rate, the obliquity ratio versus strain pattern is seen to be typical of that expected in a uniform strain rate test of t_1 = 500 minutes (the reader is referred to Figure 52 in Appendix B). Incidentally, the curves of obliquity ratio versus strain from tests OC10-SF and OC11-SF are almost coincident. Following the step

increase in strain rate, the obliquity ratio jumps rapidly to a quite high level, higher in fact than any value of pre-step obliquity ratio attained, and much higher than could be considered typical of the new strain rate. As strain is continued at the new rate, t_1 = 3/4 minutes, the obliquity ratio decreases quite rapidly at a gradually decreasing rate and approaches a behavior pattern typical of the fast rate.

M. Mode of Failure - Step Increase in Strain Rate - Overconsolidated Samples

Both samples OC10-SF and OC11-SF showed distinct failure planes at cessation of testing. In test OC10-SF, a quite distinct failure plane was noted at 6% strain while in test OC11-SF no failure plane was noted until 9½% strain. Failure plane formation is typical of the slow strain rate. In test OC11-SF, the step increase in strain rate appears to have delayed the formation of a shear plane over the strain level typical of the slow strain rate.

N. Summary - Effect of Steps in Strain Rate on Observed Behavior - Overconsolidated Samples

This section summarizes the effect of step increases or decreases in strain rate upon the behavior of overconsolidated samples:

1. Deviator Stress
   (a) A step decrease in strain rate at 5% decreases the deviator stress to a level below that appropriate for the post-step strain rate. Following the step, the deviator stress rises to a level and follows a pattern typical of the new strain rate.
   (b) A step increase in strain rate at 4% strain increases the deviator stress to, but not in excess of, a value appropriate to that strain level at the faster rate. Following the step, the deviator stress follows a pattern typical of but slightly lower than that of the post-step strain rate.

2. Pore Water Pressure

   (a) A step decrease in strain rate at 5% strain appears to have no effect on the pattern of pore pressure development as measured with the porous probe at midplane. However, the base pore pressure drops drastically following the step decrease in strain rate.

   (b) A step increase in strain rate at 4% strain appears to have no effect on the pattern of pore pressure development as measured at the sample mid-height.

3. Principal Stress Ratios

   (a) Following a step decrease in strain rate at 5% strain, $\bar{\sigma}_1/\bar{\sigma}_3$ drops to a value lower than that typical of the post-step strain rate at the same strain level. However, the magnitude of $\bar{\sigma}_1/\bar{\sigma}_3$ rises as strain at at the slower rate continues, and follows a pattern typical of the slow strain rate.

   (b) Following a step increase in strain rate at 4% strain, $\bar{\sigma}_1/\bar{\sigma}_3$ rises to a value far in excess of that typical of the post-step strain rate, in fact higher than previously recorded in the test. Following this drastic jump, $\bar{\sigma}_1/\bar{\sigma}_3$ rapidly decays as straining continues, and behaves in a pattern typical of the new, fast strain rate.

Chapter VIII

BEHAVIOR OF OVERCONSOLIDATED SAMPLES

A. Introduction

This chapter sets forth explanations for the observed behavior of the overconsolidated samples as related to strain rate. The observed behavior patterns have been described in Chapter VI for tests at uniform strain rates and in Chapter VII for tests with steps in strain rate. The final sections of those two chapters present summaries of the observed behavior patterns.

However, it is not felt by this writer that the behavior patterns exhibited in the overconsolidated samples are representative of true soil behavior. Rather, it is felt that the true soil behavior patterns as influenced by strain rate are obscured by an internal volume change or pore water migration phenomenon. The effect of this migration and evidences of its occurence are presented in the following sections.

B. Stress Distribution in Triaxial Samples

In the theory of triaxial testing, a uniform distribution of stresses throughout the sample is assumed. This uniform distribution of stress would be attained if the specimen base and top cap were frictionless. However, this is not the case. In fact, at the specimen base and often at the cap of the specimen, a porous stone is employed that, at the end of testing, is usually found bonded to the specimen. Consequently, a uniform stress distribution throughout a triaxial sample is not attained. Theoretical solutions for the stress distribution in triaxial samples have been presented by D'APPOLONIA and NEWMARK (1951) and BALA (1960).

A zone of uniform stresses exists for a distance above and below a plane passed through a triaxial sample at mid-height, if the proper length to diameter ratio is maintained. The longitudinal

dimension (thickness) of this zone probably varies throughout testing and is probably a function of the σ_1/σ_3 ratio at any instant. A zone of restraint, usually assumed to be conical, exists adjacent to the specimen cap and base and extending into the sample. In fact, these two zones do not exist per se but represent boundaries of a continuous stress distribution at any instant.

The stresses on a plane adjacent to the base or top cap vary radially also. At the periphery of the sample, the minor principal stress is radial and equal to the chamber pressure and the major principal stress is vertical and related to the piston load. Thus in a differential element at the periphery of the triaxial sample stress conditions like the midplane of the sample exist.

On an element at the axis of the sample and adjacent to the base, no shear stress between the element and the base exists due to radial symmetry. Hence the principal stresses are horizontal and vertical. Since the element is restrained from outward motion, the major principal stress and the minor principal stress approach each other in magnitude and are possibly of the same order of magnitude as the major principal stress at the sample mid-height. With these boundaries, a radial distribution of stresses occurs. Thus, throughout the triaxial sample, both a radial and longitudinal distribution of stresses is attained.

C. Effect of Stress Distribution on Pore Water Pressure Distribution

Assuming an increment of piston (axial) load is applied to a triaxial specimen, the pore water pressure at any point is given by the basic pore pressure equation $u = B\Delta\sigma_3 + A(\Delta\sigma_1 - \Delta\sigma_3)$. At the mid-height of the sample, and throughout the zone of uniform stresses, the pore water pressure at the first instant of incremental load application is thus $A\Delta(\sigma_1 - \sigma_3)$, since σ_3 remains constant.

However, instantaneously at the planes of the sample base and top, the pore water pressure varies radially. At the periphery of the specimen the pore water pressure is again $A\Delta(\sigma_1 - \sigma_3)$. However, if the axial stresses are as postulated in the previous section, the pore water pressure, instantaneously, at the axis on the top and base planes is nearly $B\Delta\ (\sigma_1 - \sigma_3)$.

At the base, since a relatively very permeable stone is present, the radial distribution of pore water pressure is immediately equalized to some average value. If an initially parabolic distribution of pore water pressure varying from $A\Delta\ (\sigma_1 - \sigma_3)$ at the periphery to $B\Delta\ (\sigma_1 - \sigma_3)$ at the axis, an instantaneous average pore water pressure adjacent to the base is $(\frac{1}{15} A + \frac{8}{15} B)\left[\Delta(\sigma_1 - \sigma_3)\right]$, or approximately $(.5A + .5B)\left[\Delta(\sigma_1 - \sigma_3)\right]$ In a saturated sample, with B = 1, this becomes $(.5A + .5)\left[\Delta(\sigma_1 - \sigma_3)\right]$ Thus, if A = 1, the instantaneous average pore water pressure at the plane of the sample base (and top if a porous stone is present) should be approximately equal to the pore pressure in the uniform stress zone near the sample mid-height.

However, if $A < 1$, the pore water pressure at the sample base will be greater than the pore water at the sample mid-height. For example, if $A = \frac{1}{2}$, u at the midheight = $\frac{1}{2}$ the deviator stress increment, while u adjacent to the base = .75 times the deviator stress increment. In the case of overconsolidated soils with $A \leq 0$, the immediate pore water pressure at the specimen base due to the addition of an increment of deviator stress can be much greater than the pore pressure at the specimen mid-height. This discussion should emphasize the fact that the pore pressure gradient in normally consolidated samples with A near 1 is a minor consideration, while this pore pressure gradient assumes paramount importance in the overconsolidated samples.

D. Evidences of the Existence of Pore Water Pressure Gradients - Overconsolidated Samples

Direct measurements of pore water pressure at both sample mid-height and sample base were made in Tests OC1-F, OC2-F, OC3-F, OC4-F, OC5-FS, OC6-S, OC7-S and OC8-S. The reader is referred to plots of base and needle pore water pressures as a function of strain for each of these tests appearing in Appendix B. These tests provide direct measurement of the pore water pressure gradients as a function of strain rate.

Figure 37 presents the data from the above tests plotted against strain rate and thus shows the relationship between pore pressure gradients and rate of strain. Test OC8-S, performed at a strain rate of $t_1 = 250$ minutes, appears to have been slow enough to allow complete equalization of pore water pressure to occur.

E. Migration of Pore Water as a Function of Strain Rate

If a triaxial compression test is performed at a slow rate of strain, equalization of pore water pressures throughout the sample can occur. This results from a movement of pore water from high to low pressure areas with resulting internal volume changes. This migration occurs as the test progresses in slow tests, and can occur after cessation of testing in rapid tests. The result of this migration of pore water in overconsolidated samples would be expected to be a decrease in water content near the sample ends and an increase in water content in the middle region of the sample.

The extent of this internal volume change depends, of course, on the rate of testing and, as residual pore water pressure remains following release of axial load, on the length of time elapsing from the end of testing until water content determinations are undertaken.

F. Evidence of Internal Volume Change - Overconsolidated Samples

During the course of this test series, considerable evidence of migration of pore water leading to internal volume change was obtained. The pore pressure gradient data, of course, shows the tendency for internal volume change. In addition, as was the case with the normally consolidated samples, each test specimen was sliced into six horizontal segments following each test. This was done as rapidly as possible, the elapsed time being on the order of 5 minutes.

One missing bit of evidence is the post-consolidation, pre-shear water content distribution. NASIM (1961), on the same soil with an OCR of 16 found essentially a uniform distribution of water content at the completion of consolidation. Test OC2-F, which was one of the fastest tests, was disassembled particularly rapidly. In this case a uniform distribution of water content was obtained.

All of the post-shear water content data are plotted in Figure 38. In Figure 38 (a), the data from all of the fast tests are presented and in Figure 38 (b), all of the data from the slow tests are presented. If a uniform pre-shear water content distribution is assumed, there is seen to be some evidence of migration or internal volume change in the fast tests and overwhelming evidence of internal volume change or migration of pore water in the slow tests.

G. Relationship Between Failure Plane Formation and Pore Water Pressure

The picture of internal volume change or pore water migration is further complicated by the process of failure plane formation. In this series of tests it was noted that all of the overconsolidated samples with the exception of OC5-FS failed by shear plane formation. In addition, evidence from the M.I.T. laboratory and other soil mechanics laboratories shows that most heavily overconsolidated samples tested at conventional strain rates fail by shear plane formation.

This process also affects the measured pore water pressures. The picture of pore pressure development in overconsolidated samples probably is as follows:

As the sample is loaded and straining progresses, pore pressures are developed in the sample. At low strains, less than 2%, these are positive throughout the sample and little tendency for pore water migration occurs. As straining progresses, the pore water pressure at the midplane zone tends to be lower than at the base, for reasons already presented, and in the slow test, a migration of pore water starts internal volume change occurring. In fast tests, time is not available for this to occur.

H. Effect of Pore Water Migration and Internal Volume Changes on Observed Behavior of the Overconsolidated Samples

One of the major observations of the test series on the overconsolidated samples is that moisture redistribution occurs in the slow tests on the overconsolidated samples. This section deals with the effect of this moisture redistribution on the observed behavior of overconsolidated samples. To do this, recourse will be made to stress vector plots as shown in Figure 41.

In Figure 41, circle 1 represents the failure condition in a normally consolidated sample at a certain water content. A line drawn through the top point of this circle and the origin represents a usual normally consolidated failure line. Circle 2 is the failure circle from a test brought to the same water content as the test of circle 1, but by a different stress history (i.e., overconsolidated). A line drawn through the top point of the two circles represents a failure line for the water content of these two tests as shown by HVORSLEV (1937). A family of lines parallel to this "Hvorslev" line can be drawn for other water contents.

A "stress vector" representing the progression of $\frac{\sigma_1 - \sigma_3}{2}$ versus $\frac{\bar{\sigma}_1 + \bar{\sigma}_3}{2}$ as the overconsolidated sample is strained is shown. This stress vector rises, in a pattern dictated by the manner of mobilization of obliquity of effective stresses on the potential failure plane and the pattern of development of pore water

pressure, to the failure line. The stress vector rides along this "Hvorslev" failure line as the further development of negative pore water pressure increases the effective stress on the failure plane. At some point no more increase in effective stress is possible due either to cavitation of the pore water, migration of pore water to a failure zone and/or failure plane formation. At this point the stress vector breaks away from a "Hvorslev" failure line and tends to progress horizontally until a "failure" occurs.

The relationship of rate of strain to this process is diagrammed in Figure 42. In this Figure, the assumption is made that a "Hvorslev" line is non-time dependent. "Hvorslev" lines for several water contents are shown. Stress vectors from slow and fast tests are shown. In region A, the exact path of the stress vector is probably time dependent. In this investigation the data obtained is sketchy as quite small strains are involved, and thus no conclusions can be drawn regarding any "structural viscosity" effect on either principal effective stress ratio or pore pressure development.

The stress vector from a slow test will rise through region A to a "Hvorslev" line appropriate to the water content in the portion of the sample in which yielding is occurring. Depending on the degree of slowness, this may or may not be the initial water content of the sample as a whole. The sample reaches this line somewhere between 1.5% and 2% strain. The pore pressure has not, as yet, gone negative.

Upon reaching a "Hvorslev" line appropriate to the water content at that instant in the zone that is yielding (i.e., the middle portion of the sample), the stress vector tends to progress along this "Hvorslev" line until a flow of water internally in the sample increases the water content. At this point, point 1 on Figure 42, the stress vector breaks away from the failure line and tends more toward a horizontal path as the moisture content in the yielding zone becomes increasingly greater. The stress vector, reaches a peak

at a situation where the rate of migration of water to the yielding zone is the same as the rate of development of negative pore pressure, and as this rate of migration becomes great enough with respect to the development of negative pore water pressure, the stress vector path assumes a downward trend. As failure plane formation retards any further development of pore water pressure, migration of water to the failure zone decreases the effective stresses and the stress vector turns back toward the origin.

In the case of a fast test, the stress vector path may reach a higher "Hvorslev" line, the one appropriate to the initial uniform sample water content if the test is rapid enough, as the time necessary for migration is not available. This failure line will be followed by the stress vector for a distance until either failure of the soil structure in the yielding zone has occurred, or time has elapsed allowing internal volume change to occur. Hence the higher strength in the faster tests seems probably to be mainly due to less internal volume change. This results in: 1. The forcing of yielding to occur at a lower water content (i.e., reaching a higher "Hvorslev" line) and, 2. the forcing of yielding to occur longer at this lower water content with the development of more negative pore water pressure and the resultant increase of effective stresses (i.e., progression further up a "Hvorslev" line).

That this does occur is demonstrated by the actual stress vector paths observed in this series of tests. In Figure 43, the stress vector paths from all of the fast tests have been reproduced while those from the slow tests appear in Figure 44. These stress vectors have been summarized in Figure 45. The stress vector paths from all fast tests fall within the shaded zone. The slow tests present a close enough grouping of stress vector paths to allow a single typical stress vector path to be drawn. That the processes described in this section do in fact occur is felt to be clearly shown by Figure 45.

I. Conclusions

The behavior of the overconsolidated samples has been discussed in this chapter. Theoretical analyses have been presented to show that pore pressure gradients could exist in overconsolidated triaxial compression samples and thus migration of pore water and consequent internal volume changes during testing could occur.

Experimental evidence of differences in pore water pressures between the base of overconsolidated triaxial samples and the sample mid-heights have been presented and the relationship of these pore pressure differences to strain rate has been shown. Thus the presence of pore pressure gradients has been demonstrated experimentally. Results of moisture content determinations have been presented to show that internal volume changes have occurred, and that this moisture content redistribution is related to the strain rate.

The effect of this internal volume change tendency upon the relationship between stress versus strain behavior and rate of strain has been shown by use of stress vector path plots on "Hvorslev" yield criteria plots. Thus it has been shown that behavior similar to that experimentally observed in the overconsolidated samples could be attributed to internal moisture content redistribution or internal volume change.

On the basis of this evidence, the conclusion is drawn that the observed behavior of overconsolidated samples can, to a large degree, be attributed to internal migration of pore water producing internal moisture content redistribution. This is a result of pore pressure gradients which exist in triaxial samples, and to a great degree in overconsolidated samples, as a consequence of non-uniform stress distribution (end restraint) and failure plane formation phenomena.

The effects of rate of strain upon fundamental parameters of shear strength behavior in the overconsolidated samples are thus assumed to be obscured to a great extent by effects relative to sample geometry and the triaxial test itself.

Chapter IX

ANALYSIS IN TERMS OF HVORSLEV PARAMETERS

A. Introduction

This chapter presents an analysis of the observed behavior in uniform strain rate tests and in two tests with a step-increase in strain rate, in terms of shear strength parameters advanced by HVORSLEV (1937). These parameters of shear strength behavior were introduced in Section H of the preceding chapter. In brief, HVORSLEV proposed two parameters of shear strength, one termed "true angle of internal friction" (ϕ_e), and the other termed "true cohesion" (c_e). These represent the angle of shearing resistance and cohesion intercept of samples tested at varying stress histories, but identical failure water contents.

The analyses performed in this chapter use a method of determination of the true friction angle and true cohesion presented by BISHOP and HENKEL (1957).

B. Tests with Uniform Strain Rate

In this section the failure (i.e., maximum deviator stress) shear strength behavior as related to strain rate is analyzed in terms of "Hvorslev" parameters for those tests performed at a uniform rate of strain. Data used in the determination of the appropriate "Hvorslev" parameters are listed in Table IX-1.

These data are normalized using an equivalent pressure (p_e) as suggested by Hvorslev. This equivalent pressure in this case is the triaxial chamber pressure required to produce the water content of the test specimen in a normally consolidated sample. The equivalent consolidation pressure (p_e) was determined from the virgin consolidation branch of the Batch B and Batch C consolidation plots of Figure 3. The equation of this average Batch B and C virgin consolidation curve is $w\ (\%) = 41.8 - 18.05\ (\log p - \log 10)$. Thus p_e was calculated using $\log \frac{p_e}{10} = \frac{41.8 - w\ (\%)}{18.05}$.

Table IX-1

DATA FOR DETERMINATION OF HVORSLEV PARAMETERS AT FAILURE [i.e. $(\sigma_1 - \sigma_3)_{max}$]

Test No.	σ_3 (lb/in^2)	$(\sigma_1 - \sigma_3)_{max}$ (lb/in^2)	W_{avg} %	P_e (lb/in^2)	u_f (lb/in^2)	$\bar{\sigma}_3$ (lb/in^2)	$\frac{\bar{\sigma}_3}{P_e}$	$\frac{\bar{\sigma}_1 - \bar{\sigma}_3}{2P_e}$	t_1 (minutes)	Class
NC1F	117.6	82.2	23.4	104.5	62.0	55.6	.532	.394	2	F
2	58.5	47.5	27.6	61.0	29.4	29.1	.476	.390	1	F
3	59.0	42.5	29.6	47.4	31.0	28.0	.590	.449	3/4	F
4FS	59.0	44.5	28.9	51.8	31.8	27.2	.525	.428	3/4	F
5FS	58.5	42.8	28.8	52.5	29.0	29.5	.563	.408	3/4	F
6S	60.5	39.5	28.8	52.5	34.4	26.1	.500	.376	20	I
7S	60.0	40.0	29.1	50.5	38.2	21.8	.432	.396	350	S
8S	66.5	47.4	26.4	71.4	39.0	27.5	.385	.332	1500	S
9SF*	59.0	39.3	27.6	61.2	34.6	24.4	.399	.321	500	S
10SF*	61.0	38.5	27.8	59.6	33.0	28.0	.470	.323	500	S
11SF*	59.8	37.0	28.3	60.6	35.5	24.3	.400	.305	500	S
14SF*	58.5	39.5	28.0	58.2	35.2	23.3	.400	.339	500	S
16SF*	60.5	39.5	28.3	60.6	36.2	24.3	.401	.326	500	S
17SF*	61.0	39.8	27.5	62.0	38.0	23.0	.372	.321	1000	S
OC1F	6.0	28.5	29.3	49.1	-7.0	13.0	.265	.290	.3	F
2F	7.0	32.6	30.0	45.1	-4.1	11.1	.246	.362	1.7	F
3F	7.2	32.6	28.6	53.8	-5.8	13.0	.241	.302	.75	F
4F	7.5	33.5	29.8	46.2	-8.0	15.5	.336	.364	1.5	F
5FS*	7.5	32.5	29.3	48.0	-6.4	13.9	.290	.339	.75	F
6S	6.4	27.3	29.1	50.5	-5.8	12.2	.242	.270	18	I
7S	7.0	27.0	30.3	43.4	-3.2	10.2	.235	.311	30	I
8S	7.0	24.3	29.9	45.5	-1.2	8.2	.180	.267	250	S
10S*	6.6	28.2	29.4	48.6	-5.0	11.6	.238	.290	500	S
11S*	6.7	26.5	29.7	46.7	-4.0	10.7	.229	.283	500	S

Notes: * = Tests extrapolated
S = Slow
F = Fast
I = Intermediate

The resulting normalized data are plotted in Figure 46. From the resulting plots, the values of ϕ_e and c_e were determined and are listed on this Figure. In the upper portion of Figure 46 are plotted $(\sigma_1 - \sigma_3)/2p_e$ vs. $\bar{\sigma}_3/p_e$ for the tests of this research that could be deemed fast tests. All of these tests had a strain rate in excess of that producing 1% strain in 2 minutes (i.e., $t_1 \leq 2$ min.). A moderate degree of scatter exists. A best fit line was drawn through the plotted data points.

In addition, in the upper half of Figure 46 are plotted data from three tests (one normally consolidated and 2 overconsolidated) representative of an intermediate strain rate. The t_1 from these tests varied from 18 to 30 minutes.

In the bottom half of Figure 46 are plotted data from the slow tests. These data represent all tests having a rate of strain slower than that necessary to produce 1% strain in 250 minutes (i.e., $t_1 \geq 250$ min.). Many of these data points represent extrapolations of tests involving step increases in strain rate and are thus noted. Here again a best fit line was drawn through the test data.

C. Effect of Strain Rate on the Hvorslev True Friction and True Cohesion

Using the data plotted in Figure 46, the magnitudes of the Hvorslev shear strength parameters from the fast and slow tests were determined. The magnitudes of ϕ_e and c_e were also determined from the intermediate strain rate test data. However, it is felt that the limited data available invalidates these values. Tabulated in Table IX-2 following are the results of this determination.

Table IX-2

EFFECT OF STRAIN RATE
ON THE HVORSLEV SHEAR STRENGTH PARAMETERS

Strain Rate	ϕ_e	$\frac{c_e}{p_e}$
t_1 2 minutes	11° 45'	.218
t_1 250 minutes	11° 45'	.180

In can therefore be concluded that the observed increase in strength in the fast tests occurs as a result of a lower pore water pressure in the faster tests and an increase in the "true cohesion" with increase in strain rate with the "true friction" being independent of strain rate, when the shear strength behavior is discussed in terms of Hvorslev parameters.

It should be emphasized that ϕ_e and c_e were determined in the conventional manner using the average water content for the sample as a whole. Since it was concluded that migration of pore water played such an important role in the behavior of the over-concolidated samples, these values are not representative of fundamental shear strength behavior. If the true water content at the failure zone were known, this value could have been used to determine φ_e. In Figure 46, the effect of this on the fast test data would be negligible and in the slow tests, the effect would be to shift the points plotted from the overconsolidated tests up and to the right. Since these are the data points at the lower left of the plot, the effect of this shift would be to increase the y intercept while decreasing the slope of the best fit line. Since c_e/p_e is a function of both the y intercept and the slope of the line

on such a plot, the magnitude of this value would be relatively unchanged by this shift. However, ϕ_e would be lowered to a noticeable degree.

Hence it can be concluded that, in terms of fundamental shear strength behavior, the effect of an increase in strain rate is to increase both the "true cohesion" and the "true angle of internal friction."

D. Effect of a Step Increase in Strain Rate on the Hvorslev Shear Strength Parameters

An attempt to determine the effect of a step increase in strain rate upon the observed Hvorslev shear strength parameters is presented in this section. This determination is based on data from only two tests, NC16SF and OC11SF and suffers considerably from the lack of sufficient data. In addition, the step increase in strain rate in these tests occurred at strain levels differing by about 1%. The data used in this analysis are listed in Table IX-3 and are plotted in Figure 47.

Here again the magnitude of p_e was determined from the average water content of the entire sample as determined at the conclusion of testing. The results of the analysis made on this basis are presented in Figure 47. From these limited data it appears that the effect of a step increase in strain rate is to increase both ϕ_e and c_e/p_e. However, additional straining tends to reduce both ϕ_e and c_e to values more commensurate with the new strain rate as evidenced by the 10% strain data.

Table IX-3

DATA FOR COMPUTING HVORSLEV PARAMETERS DUE TO CHANGE IN STRAIN RATE

Test No.	σ_3	$\sigma_1 - \sigma_3$	p_e	u	$\bar{\sigma}_3$	$\bar{\sigma}_3/p_e$	$\frac{\bar{\sigma}_1 - \bar{\sigma}_3}{2 p_e}$
at 3.9% Strain							
Before Change							
NC16SF	60.5	37.8	60.6	33.8	26.7	.441	.312
OC11SF	6.7	25.1	46.7	-1.5	8.2	.175	.269
at 4.9%							
After Change							
NC16SF	60.5	48.2	60.6	33.8	26.7	.441	.398
OC11SF	6.7	31.3	46.7	-2.6	9.3	.198	.335
at 10%							
NC16SF	60.5	44.3	60.6	31.8	28.7	.473	.366
OC11SF	6.7	31.5	46.7	-7.0	13.7	.293	.337
Typical at 4.9% Fast							
NC16SF	59.7	43.4	60.6	31.5	28.2	.465	.358
OC11SF	7.3	32.0	46.7	-3.5	10.8	.231	.342

E. Conclusions

No firm conclusions can be drawn from the foregoing analysis due both to scatter of data and the influence of migration of pore water in the slow overconsolidated tests. It appears that the values of ϕ_e and c_e are related to the rate of strain. If determined in the

conventional manner, ϕ_e at failure is relatively unaffected by the strain rate in tests with uniform rate while c_e is higher in the faster tests. However, if the water content existing at failure in the actual zone of failure were known and used in the analysis, it would appear that both ϕ_e and c_e would be a function of strain rate and would be greater in tests at a more rapid strain rate.

This observation is borne out by the tests with a step increase in strain rate. However, the lack of sufficient data severely hampered this analysis.

Chapter X

SUMMARY AND CONCLUSIONS

A. Objectives of Research

The research described in the preceding chapters was instituted for the purpose of determining the cause, in terms of fundamental contributors to stress versus strain and shear strength behavior, of the strain rate effect in a saturated fat clay. The effects of rate of strain upon the shear strength and observed stress versus strain behavior of the particular fat clay employed have been shown by NASIM (1961). However, that investigation, while covering a larger range of strain rate than that covered by the program described herein, suffered in that only total stresses were considered (i.e., no pore water pressures were measured) and thus no deductions could be made regarding the causes of the observed behavior.

Consequently the program of research described in this paper was undertaken with the determination of the cause, in terms of effective stresses, of the effect of rate of strain on the stress versus strain behavior of a fat clay as its principal objective.

B. Summary of the Research Program

The research program described in the proceding chapters consisted of a total of 31 triaxial compression tests on a fat clay having a liquid limit of 60% and a plasticity index of approximately 32%. The predominant clay mineral constituents of the clay are illite and montmorillonite.

These tests were performed at rates of strain varying from that necessary to produce 1% strain of a 3.15 inch high sample in 45 seconds (t_1 = 3/4 minutes) to that rate of strain producing 1% strain in 24 hours (t_1 = 1440 minutes). In 17 of the tests, a step in strain rate was imposed at some predetermined strain level.

Twenty of the tests were upon normally consolidated samples, 19 of which were consolidated to a triaxial cell pressure of 60 lbs./in^2. In 14 of these tests on normally consolidated samples, a step in strain rate was imposed. Eleven tests were upon samples having an overconsolidation ratio of approximately 16. Three of these overconsolidated samples involved steps in strain rate at predetermined strain levels.

In all of the tests, the pore water pressure was measured in the zone of the sample in which yielding was occurring. This was accomplished by employing a small porous probe inserted into the sample at sample mid-height. This probe was connected by a length of very small, exceptionally noncompliant teflon tubing to a quite rigid electric pressure transducer and the output of this transducer was monitored by an X-Y plotter.

In addition, in several tests, the pore water pressure was also measured at the base of the test specimen and thus some measure of the distribution of pore water pressure throughout the test specimen was obtained.

The post shear distribution of water contents throughout each test specimen was obtained as rapidly as possible at the completion of each test. This was accomplished by slicing each test specimen into six horizontal slices and determining the water content of each slice.

C. Significance of Research

The following three sections summarize what is thought, by the author, to represent the significant results of this research. Three features of this research stand out: (1) A pore pressure measuring system capable of measuring the pore water pressure at the sample mid-height in tests having a strain rate in excess of that necessary to produce 1% strain in 1 minute was developed. Techniques necessary for the successful utilization of this system were perfected. (2) In the range of strain rates considered, the cause, in terms of effective stress behavior, of the observed strain rate effect in the normally consolidated

samples was determined. (3) The results of the test program on the overconsolidated samples showed the presence of and demonstrated the importance of internal migration of pore water leading to internal volume changes. This process was shown to contribute substantially to the observed effect of strain rate on the stress versus strain behavior.

D. Pore Pressure Measuring System

The pore water pressure measuring system and the techniques for its utilization are described fully in Appendix A. Briefly, the system as finally perfected, consisted of a porous stone probe 1/8 inch in diameter and 3/4 inch long, inserted into the specimen at mid-height. This probe connected to a length of fine teflon tubing .01 inches I.D. by .03 inches O.D. The tubing spiraled around the test specimen beneath the rubber membranes but over the filter strips and passed out of the triaxial chamber through the pedestal of the triaxial cell. This tubing connected to a minute volume chamber into which was threaded a very rigid electric pressure transducer.

The response of this system in a triaxial sample submitted to an increase in all around pressure (chamber pressure) was 100% in less than 1 minute which, considering the low permeability of the clay, is considered exceptional. The development of this rapid response system capable of measuring pore pressures at the middle zone of the samples was the key to the successful completion of this research.

E. Strain Rate Effect in the Normally Consolidated Samples

It was demonstrated in this research that the deviator stress achieved at any strain level in a triaxial compression test on normally consolidated samples of the saturated fat clay was higher in tests with more rapid strain rates. At failure (i.e., maximum deviator stress), this higher deviator stress in the fast tests was shown to be primarily due to a lower failure pore water pressure in these tests. In fact,

the angle of shearing resistance in terms of effective stresses, $\bar{\phi}$, was shown actually to be slightly lower in the fast tests.

At strains less than 1%, the higher deviator stress in the fast tests was shown, on the other hand, to be attributable to a higher principal effective stress ratio ($\bar{\sigma_1}/\bar{\sigma_3}$) with the pore pressure at these low strain levels being independent of strain rate.

The migration of pore water due to pore water pressure gradients existing during testing of normally consolidated samples and resulting in internal volume changes was shown to be a minor factor in contributing to the strain rate effect observed in normally consolidated samples.

The existence of a "dilatency" component of pore water pressure development in the normally consolidated samples was shown to exist and to be time dependent by tests with step increases in strain rate.

F. Strain Rate Effect in the Overconsolidated Samples

As a result of this research on the fat clay, it was shown that the major portion of the observed strain rate effect on the observed stress versus strain and pore water pressure versus strain behavior is a function of internal volume change or moisture content redistribution phenomena. This internal volume change is due to migration of pore water to equalize pore pressure gradients set up by the irregular stress distribution in triaxial samples.

The reason for a tendency toward a higher base than mid-height pore water pressure in overconsolidated samples was demonstrated. The dissipation of this pore pressure gradient is a time dependent phenomenon and thus contributes heavily to the observed strain rate effect and would lead to the dependency of the observed strain rate effect upon sample geometry.

The author feels that the results of the test program on overconsolidated samples of the fat clay demonstrates that in searches for fundamental explanations of stress versus strain behavior, tri-

axial test data on heavily overconsolidated samples is to be severely suspected. It is up to any future investigator to demonstrate that internal volume change phenomena is not influencing his test results.

G. Conclusions

The cause, in terms of effective stress behavior, of the strain rate effect on triaxial compression samples of this fat clay has been determined. The existence of similar phenomena in other clay soils needs to be demonstrated. The tools necessary for this demonstration are available.

Further work is necessary particularly on overconsolidated samples of this and other clays. Testing techniques eliminating end restraint in these samples could be developed. The fundametal behavior and strain rate effect of these samples has yet to be demonstrated.

The pore water pressure measuring system developed in the course of this research is a valuable research tool and should lend itself to further investigations of fundamental stress versus strain behavior of clay soils.

BIBLIOGRAPHY

BALA, A. 1960: "Stress Conditions in Triaxial Compression," Journal of the Soil Mechanics and Foundations Division of the ASCE, Vol. 86, December 1960, pp 57-84

BISHOP, A. W., ALPAN, I., BLIGHT, G. E. and DONALD, I. B., 1960: "Proceedings ASCE Research Conference on the Shear Strength of Cohesive Soils," pp 503-532 and 1027-1042

BISHOP, A. W., and HENKEL, D. J., 1957: "The Measurement of Soil Properties in the Triaxial Test," Edward Arnold, London

BJERRUM, L. 1961: Lecture Series in Spring of 1961 at M.I.T.

BJERRUM, L. 1954: "Theoretical Investigations on the Shear Strength of Soils," Publication No. 5 of the Norwegian Geotechnical Institute, Oslo, 1954

BJERRUM, L., SIMONS, N., and TORBLAA, I. 1960: "The Effect of Time on the Shear Strength of a Soft Marine Clay," Publication No. 33 of the Norwegian Geotechnical Institute, Oslo

CASAGRANDE, A., and WILSON, S., 1951: "Effect of Rate of Loading on the Shear Strength of Clays and Shales at Constant Water Content," Harvard Soil Mechanics Series No. 39, Cambridge, Massachusetts

CASAGRANDE, A., and SHANNON, W. L. 1948: "Stress Deformations and Strength Characteristics of Soils Under Dynamic Loads," Second International Conference on Soil Mechanics and Foundation Engineering, Rotterdam, Vol. 5

CRAWFORD, C., 1959: "Influence of Rate of Strain on Effective Stresses in a Sensitive Clay," Annual Meeting of ASTM, Atlantic City, June 1959

D'APPOLONIA, E., and NEWMARK, N. M., 1951: "A Method for Solution of the Restrained Cylinder Under Axial Compression," Proceedings of the First U. S. National Conference of Applied Mechanics, ASME, 1951, pp 217-226

HEALY, KENT A., 1962: "Dependence of Dilation on Rate of Shear Strain," M.I.T. Doctors Thesis, Department of Civil Engineering

HVORSLEV, M. J., 1937: Thesis at Vienna Abstracted in "The Shearing Resistance of Remolded Cohesive Soils," Proceedings of the Soils and Foundations Conference of the U. S., Engineers Department, Boston, Massachusetts, 1938

KOLB, C. R., and SHOCKLEY, W. G., 1957: "Engineering Geology of the Mississippi Valley," Transactions of the ASCE, Vol. 124, p 633

M.I.T., 1954: "The Behavior of Soils Under Transient Loadings," Report No. 3 to the Office of the Chief of Engineers, U. S. Army

M.I.T., 1959: "Dynamics No. 3, First Interim Report on Soil Tests," Report to U. S. Army Engineers Waterways Experiment Station

M.I.T., 1961: "Dynamics No. 6, Effect of Rate of Strain on Stress Vs. Strain Behavior of Saturated Soils, "Report of U. S. Army Engineers Waterways Experiment Station

NASIM, N. M., 1961: "Laboratory Investigation of the Effect of Rate of Strain on the Shear Strength of a Saturated Clay," M. S. Thesis, Department of Civil Engineering, M.I.T.

SKEMPTON, A. W., 1948: "A Study of the Immediate Triaxial Test on Cohesive Soils," Second International Conference on Soil Mechanics and Foundation Engineering, Vol. I. Rotterdam, 1948

SKEMPTON, A. W., 1954: "The Pore Pressure Coefficients A and B," Geotechnique Vol. No. 4, pp 143-147

TAYLOR, D. W., 1954: "Review of Research on Shearing Strength of Clay at M.I.T., 1948-1953," Report to U. S. Army Waterways Experiment Station

WHITMAN, R. V., 1957a: "Testing Soils with Transient Loads," Conference on Soils for Engineering Purposes, ASTM, Mexico City, p 243

WHITMAN, R. V., 1957b: "The Behavior of Soils Under Transient Loadings," Proceedings of the Fourth International Conference on Soil Mechanics and Foundation Engineering, London, 1957 Vol. I, p 207

WHITMAN, R. V., and HEALY, K. A., 1961: "Shearing Resistance of Sands During Rapid Loadings," Publication No. 114 of the Soil Engineering Division M.I.T.

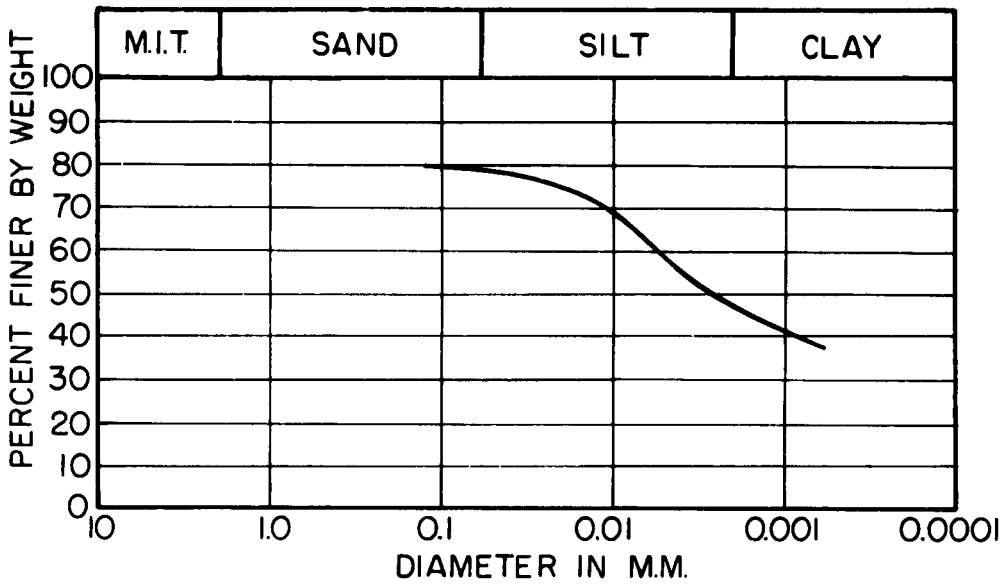

FIGURE 1 GRAIN SIZE DISTRIBUTION
VICKSBURG FAT CLAY

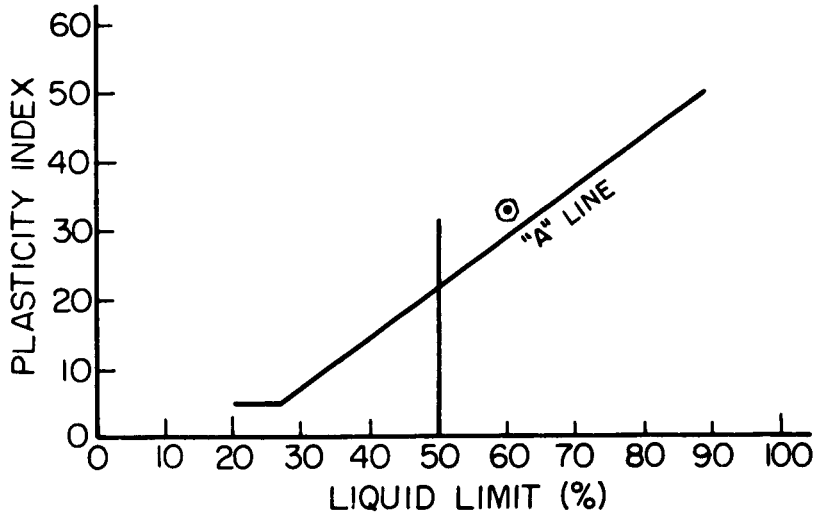

FIGURE 2 PLASTICITY CHARACTERISTICS
VICKSBURG FAT CLAY

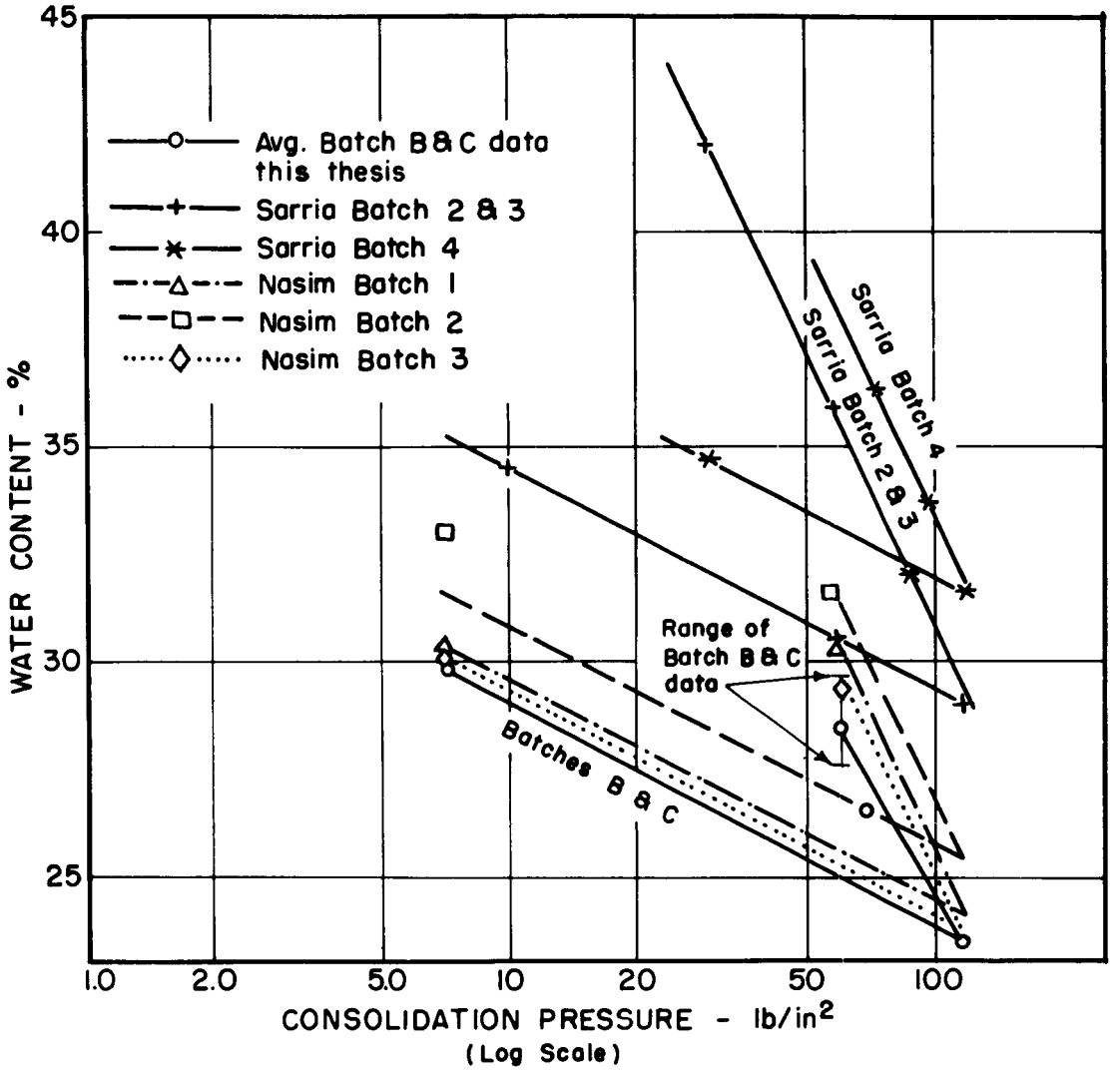

FIGURE 3 SUMMARY PLOT - CONSOLIDATION CHARACTERISTICS OF VICKSBURG FAT CLAY

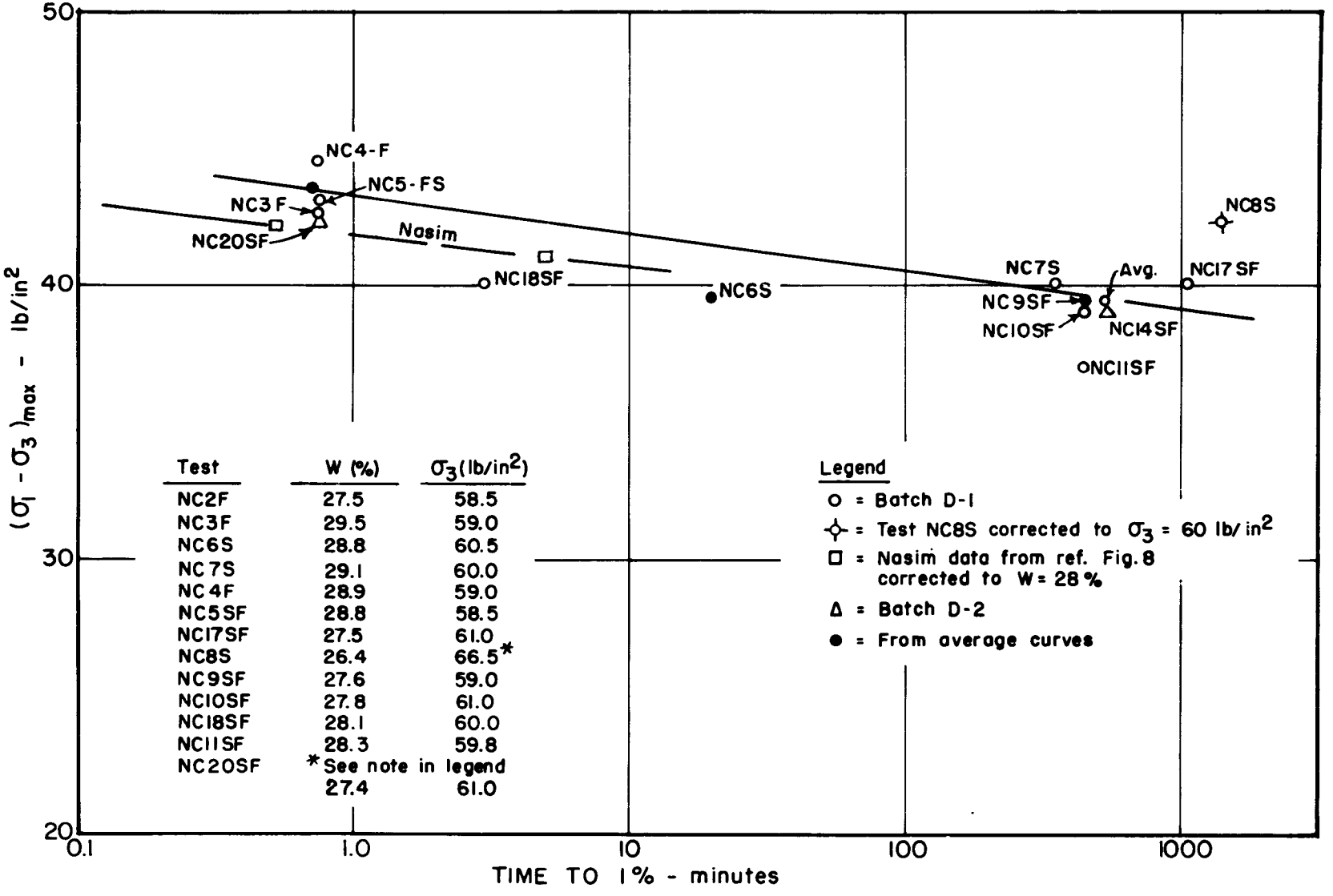

FIGURE 4 MAXIMUM DEVIATOR STRESS vs STRAIN RATE
NORMALLY CONSOLIDATED SAMPLES

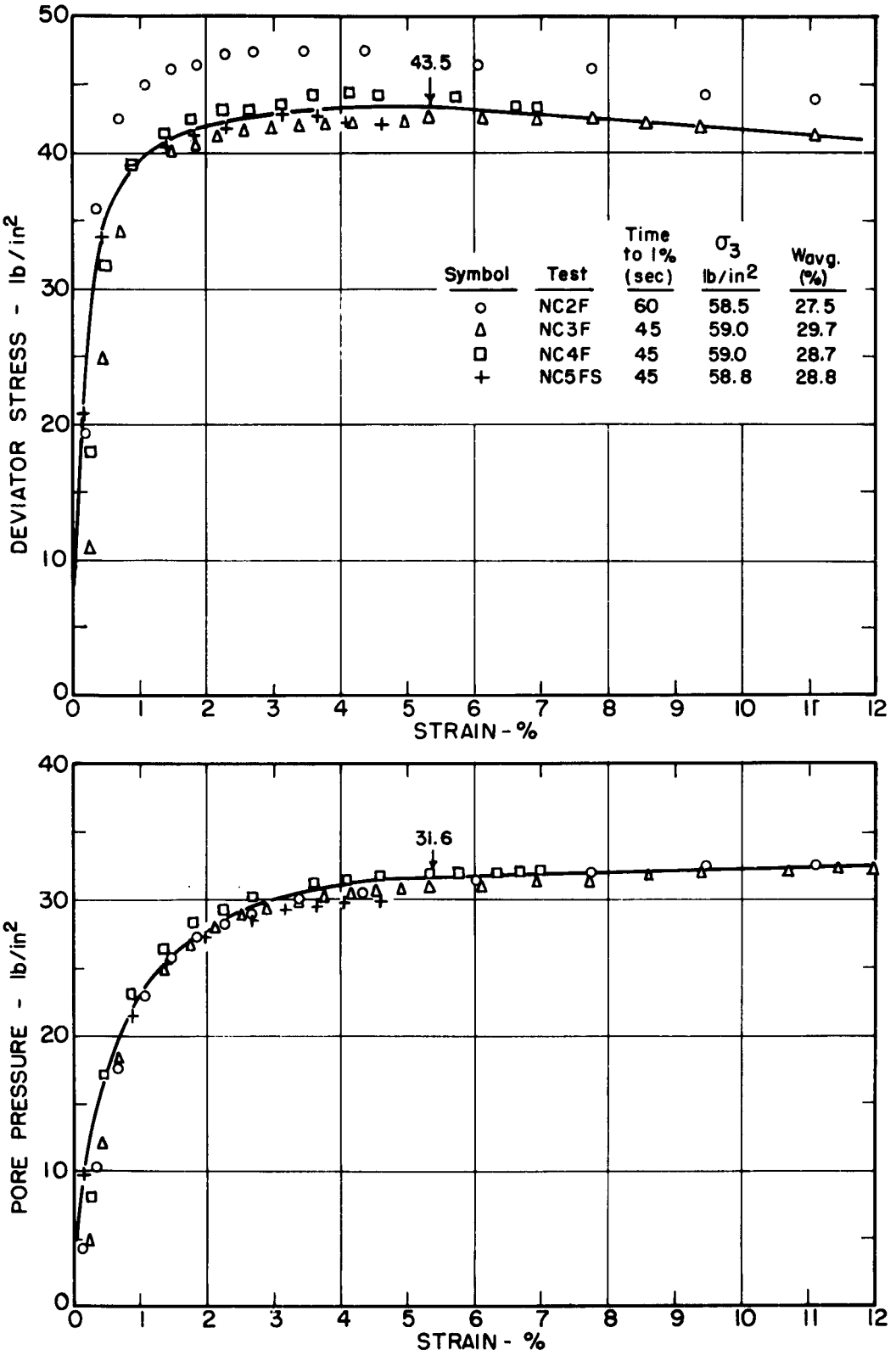

FIGURE 5 SUMMARY PLOT - FAST TESTS - NORMALLY CONSOLIDATED SAMPLES

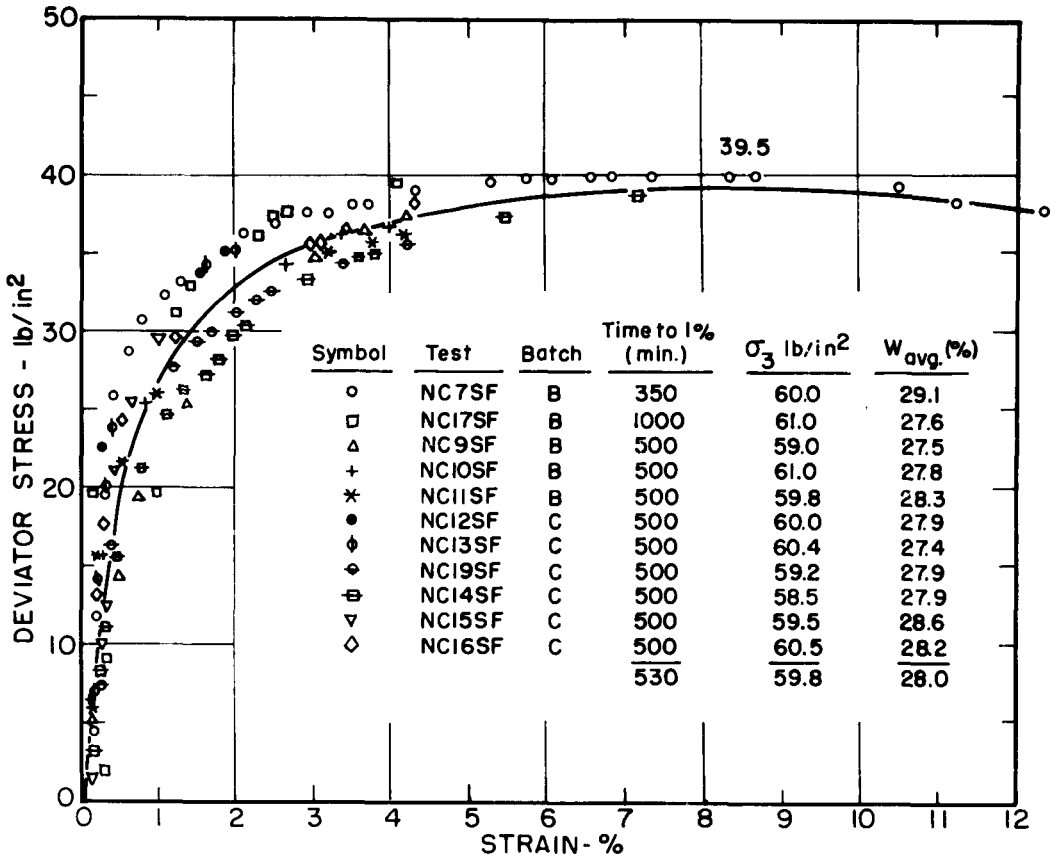

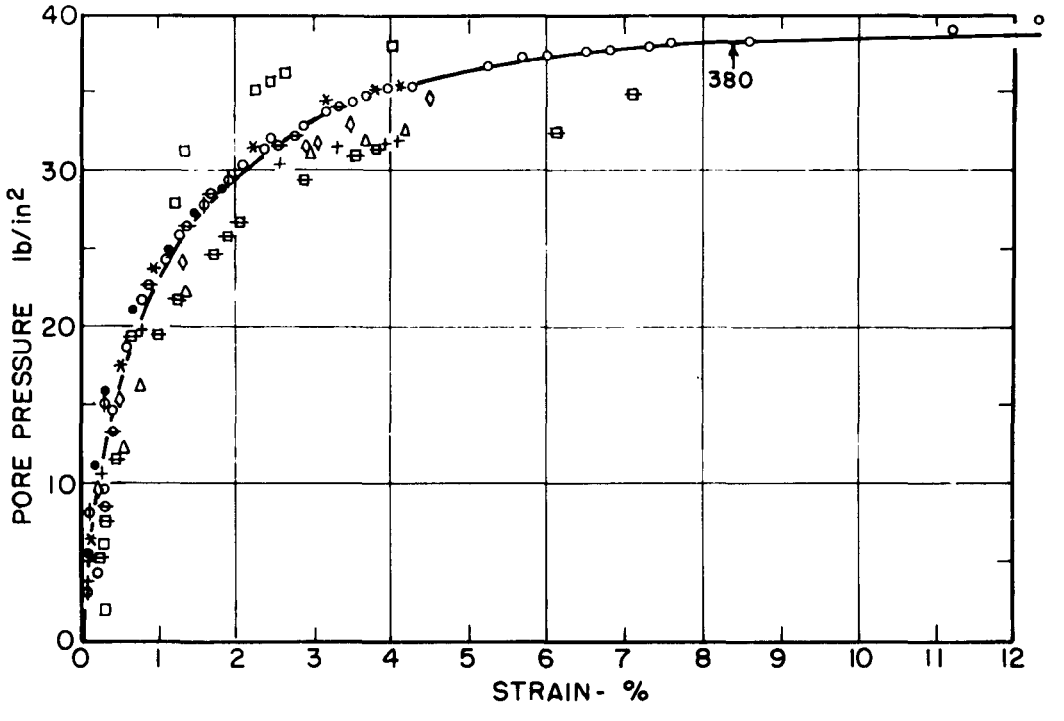

FIGURE 6 SUMMARY PLOT - SLOW TESTS - NORMALLY CONSOLIDATED SAMPLES

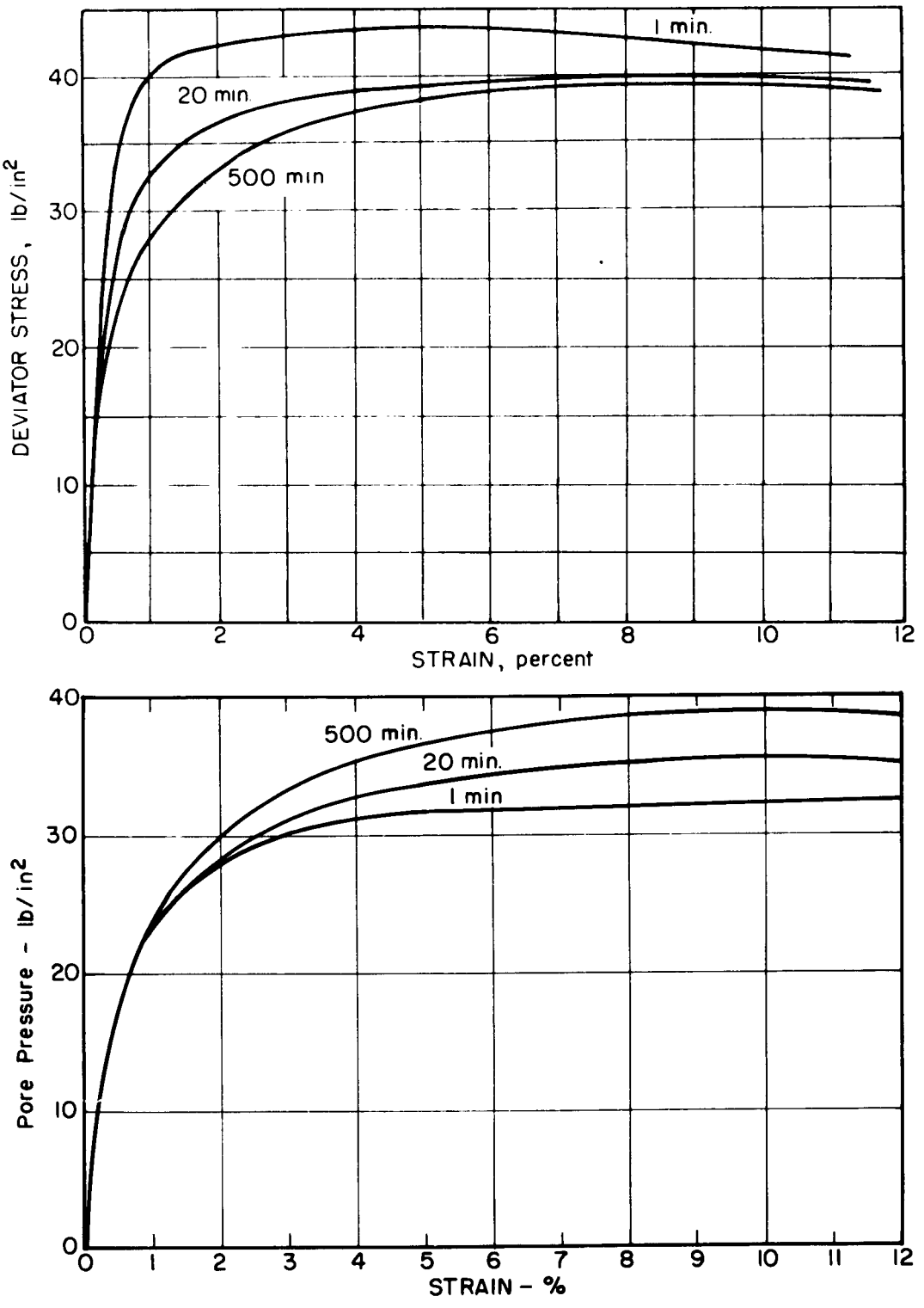

FIGURE 7 AVERAGE DEVIATOR STRESS AND MIDHEIGHT PORE PRESSURE vs STRAIN BEHAVIOR NORMALLY CONSOLIDATED SAMPLES

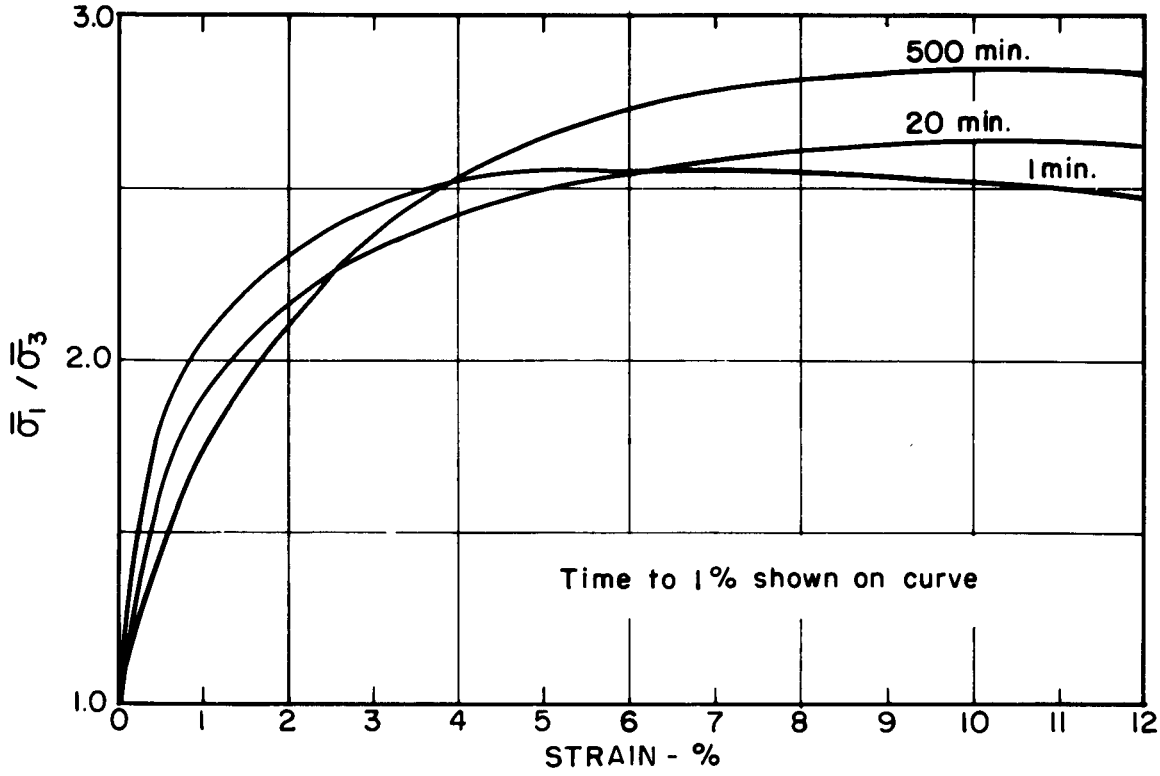

FIGURE 8 OBLIQUITY RATIO vs STRAIN
NORMALLY CONSOLIDATED SAMPLES

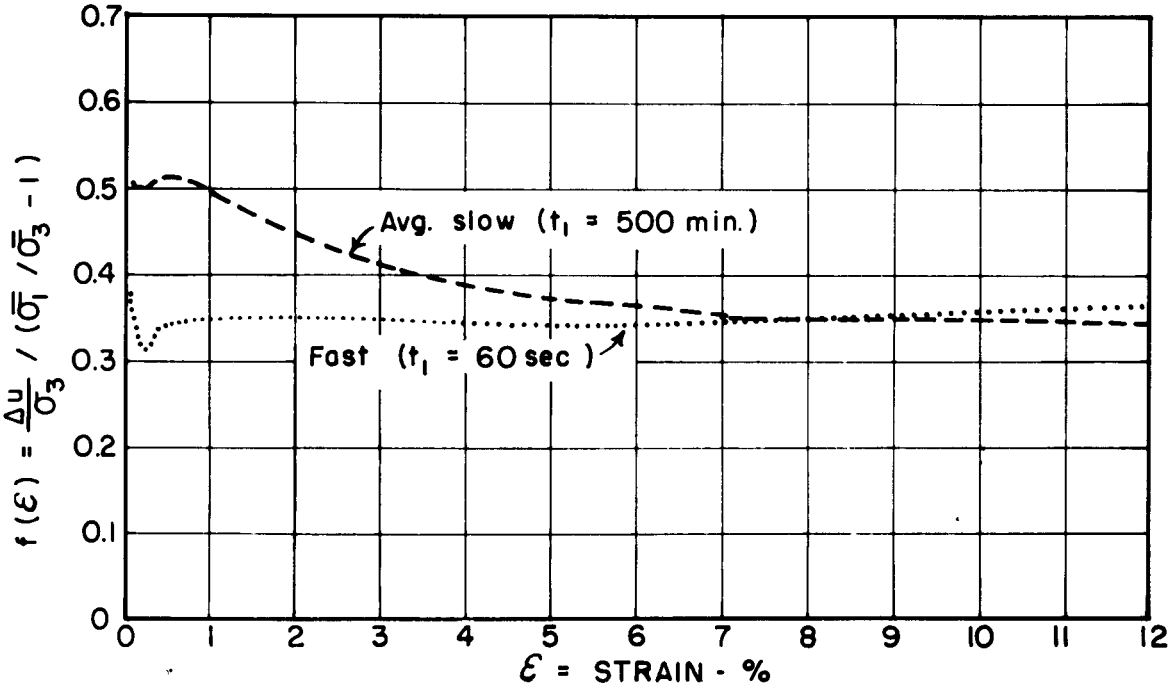

FIGURE 9 RELATIONSHIP BETWEEN PORE PRESSURE & OBLIQUITY RATIO - NORMALLY CONSOLIDATED SAMPLES

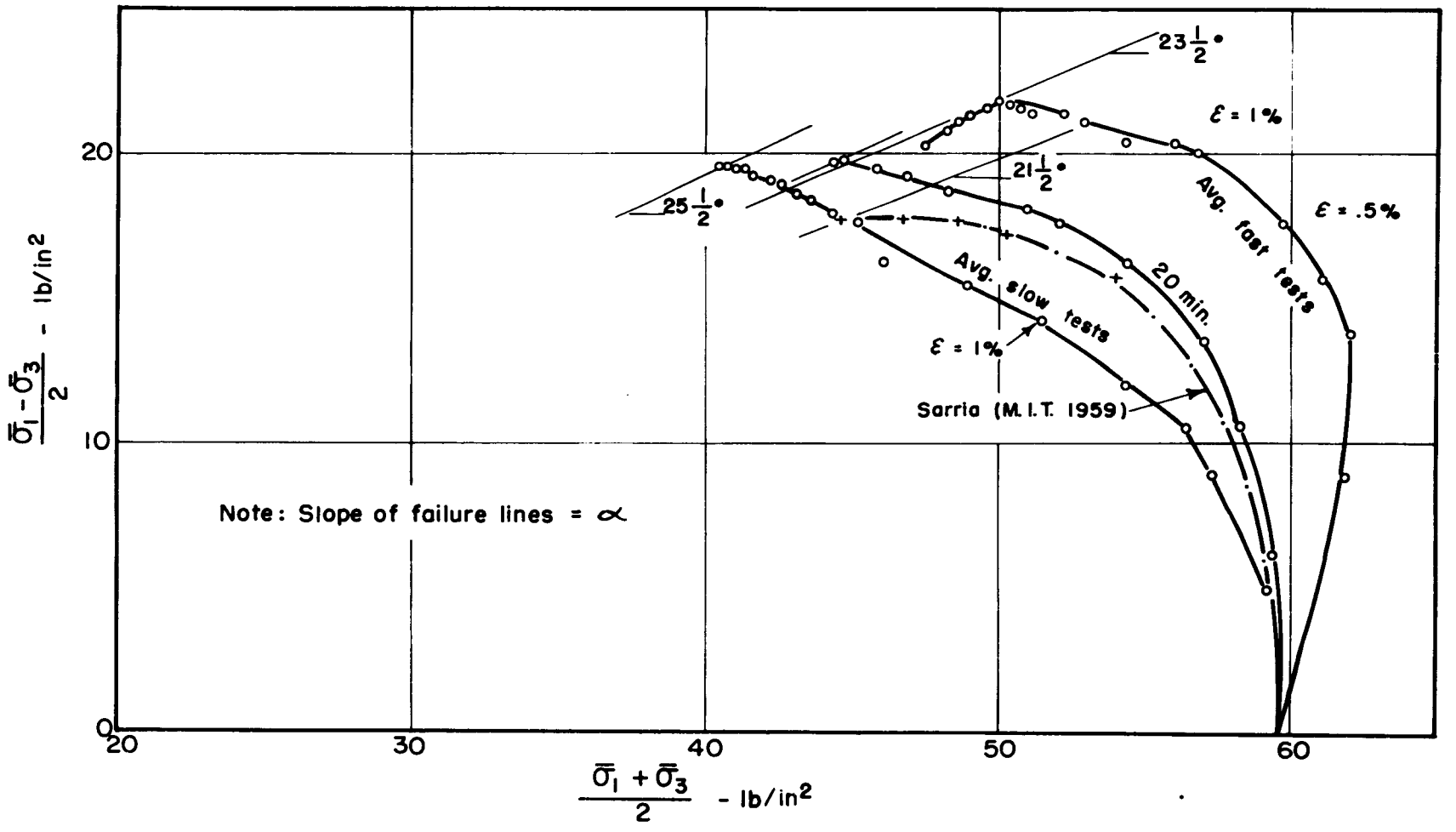

FIGURE 10 STRESS VECTOR PATHS - NORMALLY CONSOLIDATED SAMPLES

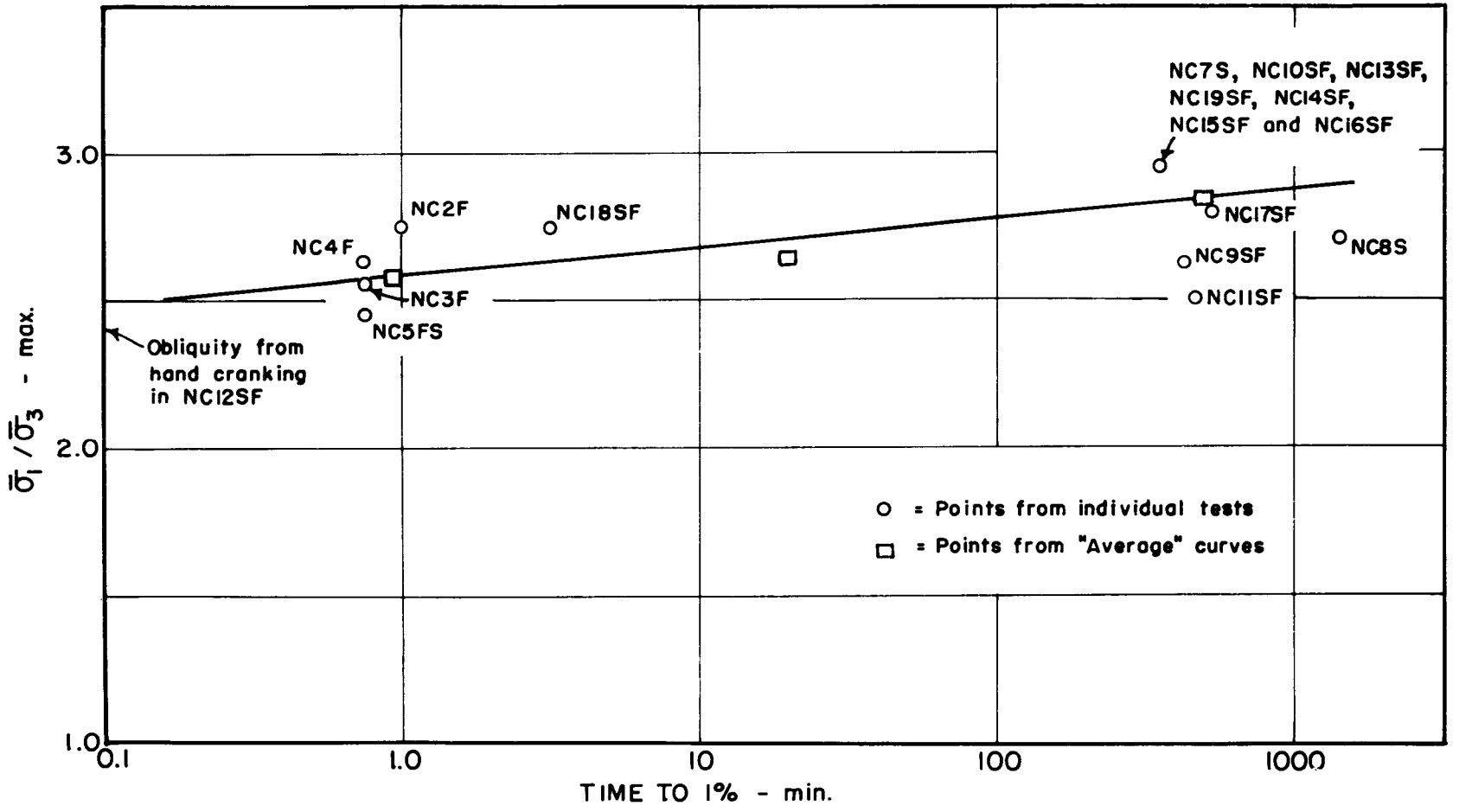

FIGURE II MAXIMUM OBLIQUITY RATIO vs STRAIN RATE
NORMALLY CONSOLIDATED SAMPLES

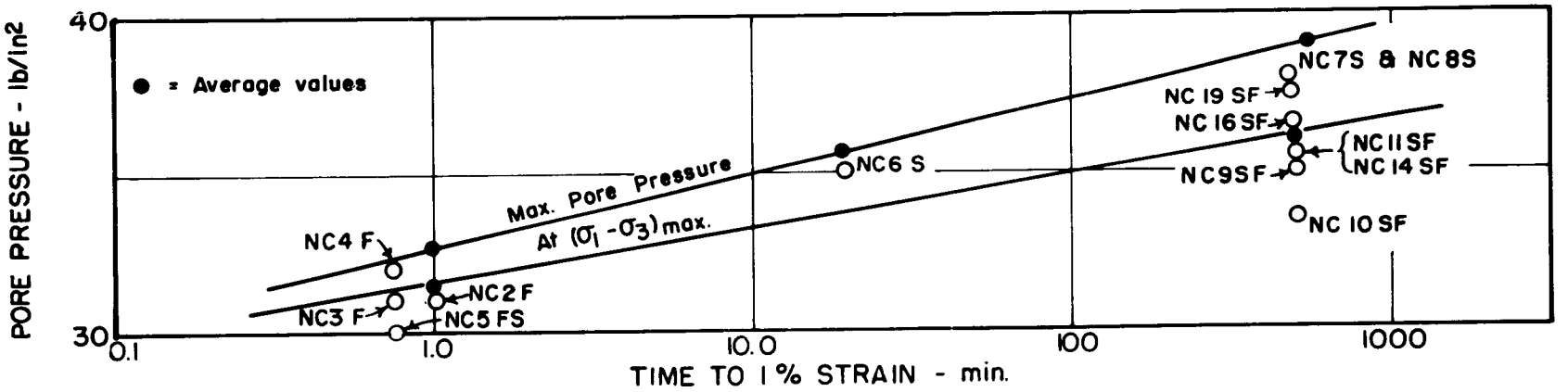

FIGURE 12 PORE WATER PRESSURE vs STRAIN RATE
NORMALLY CONSOLIDATED SAMPLES

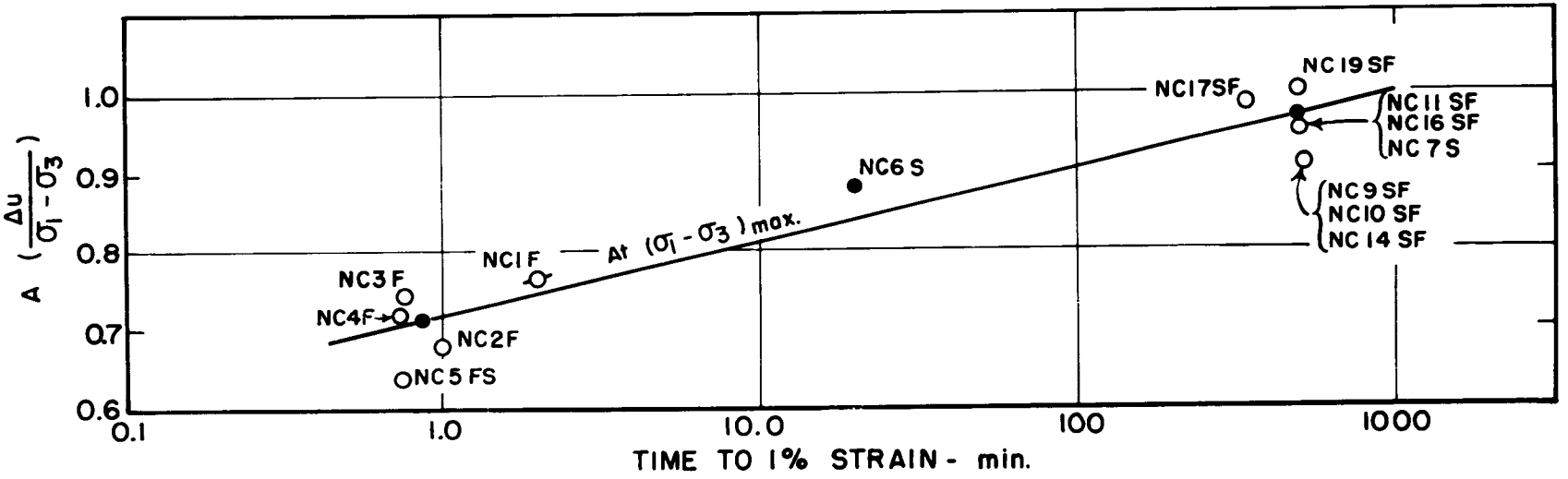

FIGURE 13 PORE PRESSURE PARAMETER A vs STRAIN RATE
NORMALLY CONSOLIDATED SAMPLES

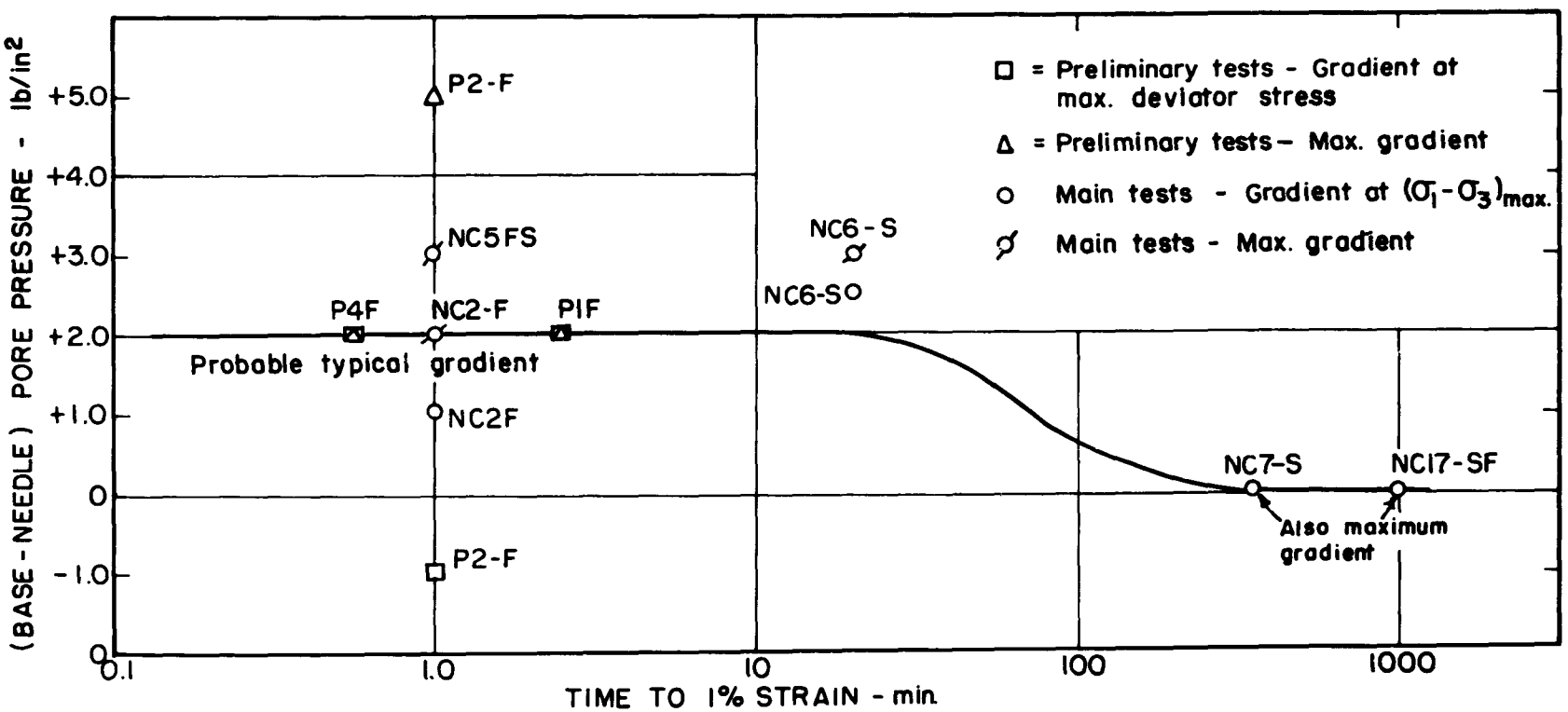

FIGURE 14 PORE PRESSURE GRADIENT vs STRAIN RATE
NORMALLY CONSOLIDATED SAMPLES

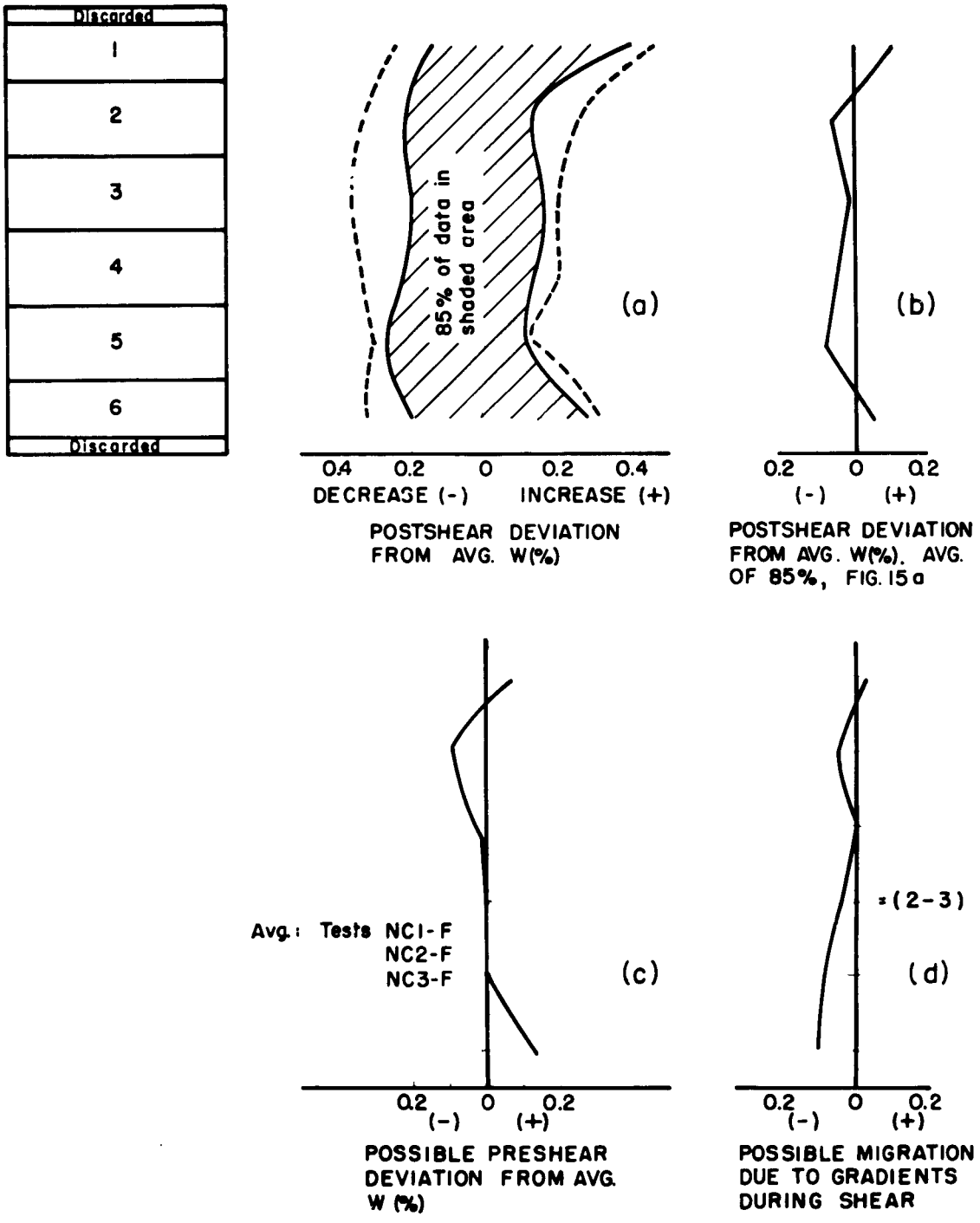

FIGURE 15 SUMMARY OF WATER CONTENT REDISTRIBUTION DATA NORMALLY CONSOLIDATED SAMPLES

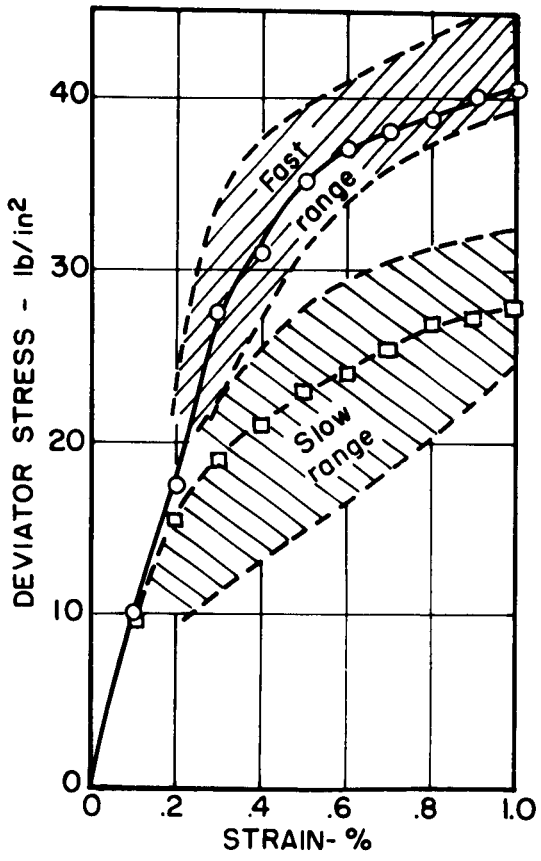

$(\sigma_1 - \sigma_3)$ vs STRAIN

Fast Tests	Slow Tests
NC2F	NC7S
NC3F	NC9S
NC4F	NC10SF
NC5FS	NC11SF
	NC12SF
	NC13SF
	NC14SF
	NC15SF
	NC16SF

Note: Shaded areas show range of data

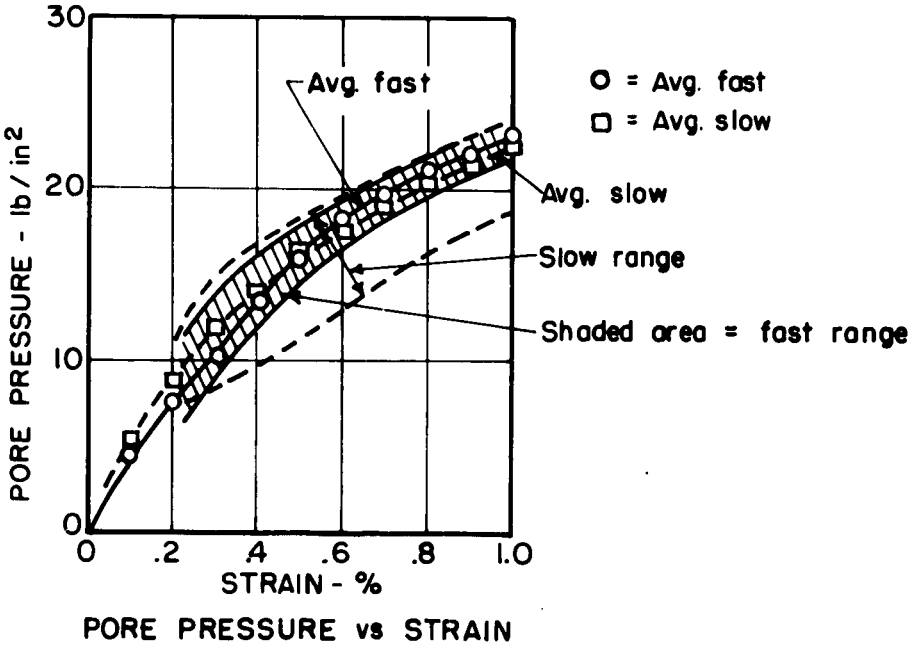

PORE PRESSURE vs STRAIN

FIGURE 16 SUMMARY - BEHAVIOR AT SMALL STRAINS NORMALLY CONSOLIDATED SAMPLES

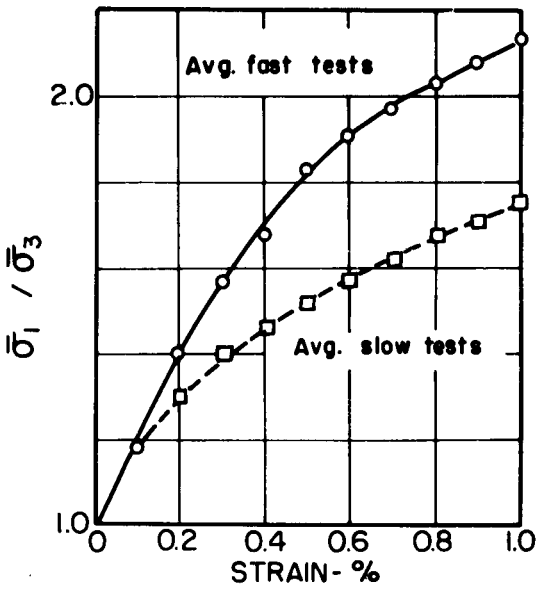

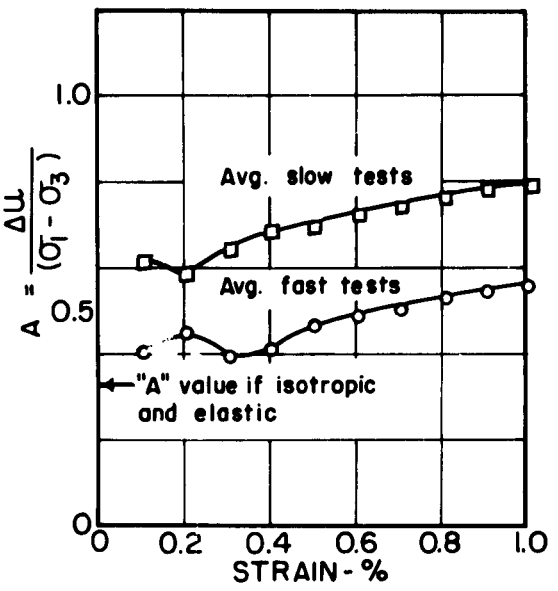

Note: Tests averages are listed in Figure 16

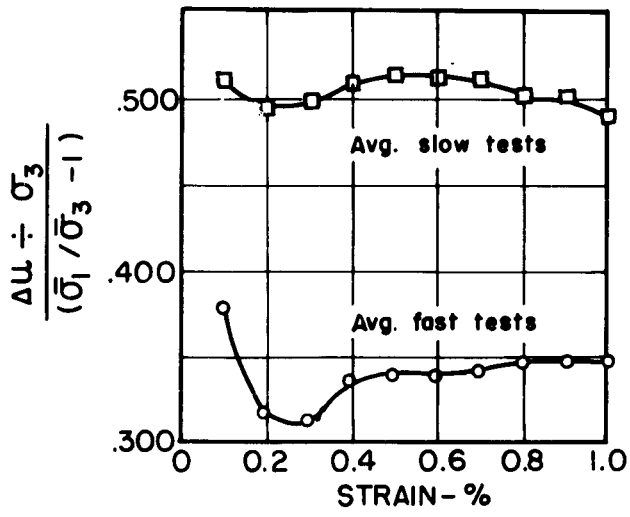

FIGURE 17 SUMMARY - BEHAVIOR AT SMALL STRAINS (cont'd)

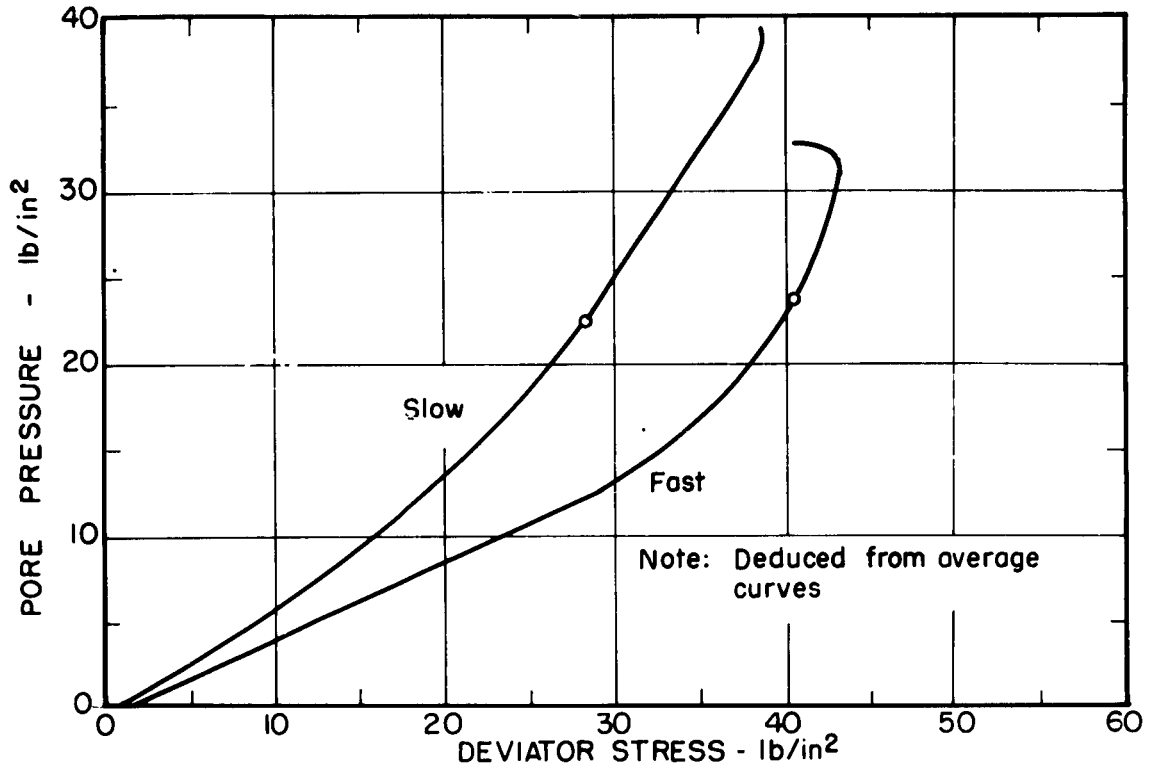

FIGURE 18 PLOT OF MIDHEIGHT PORE PRESSURE vs DEVIATOR STRESS - NORMALLY CONSOLIDATED SAMPLES

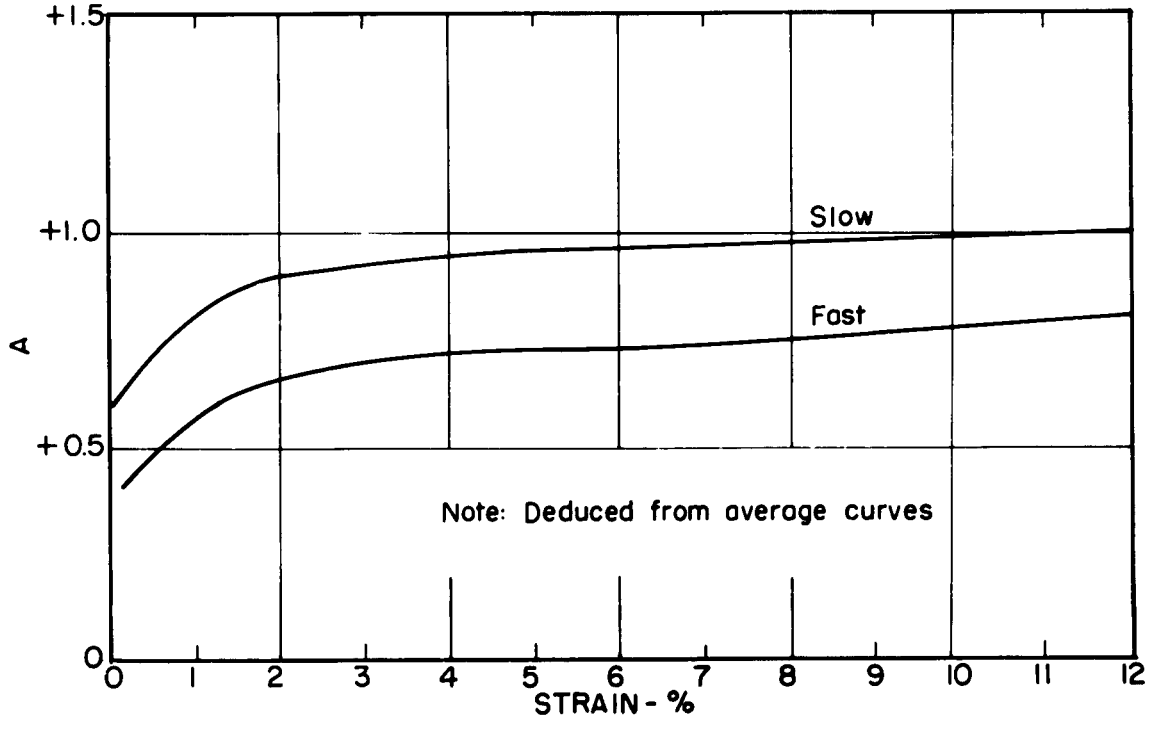

FIGURE 19 PLOT A vs STRAIN - NORMALLY CONSOLIDATED SAMPLES

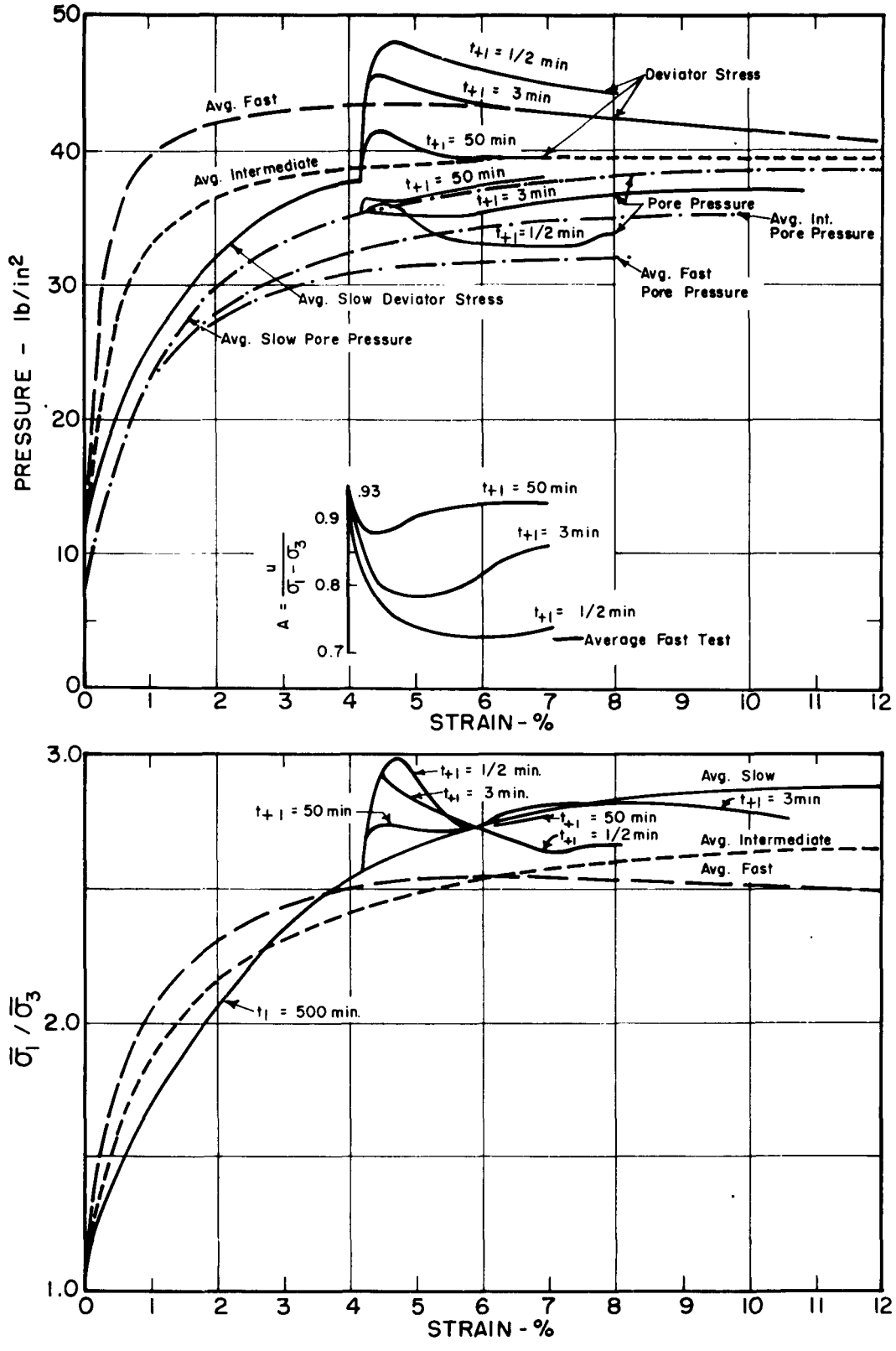

FIGURE 20 SUMMARY PLOT - TESTS WITH STEP INCREASE IN STRAIN RATE AT 4% STRAIN

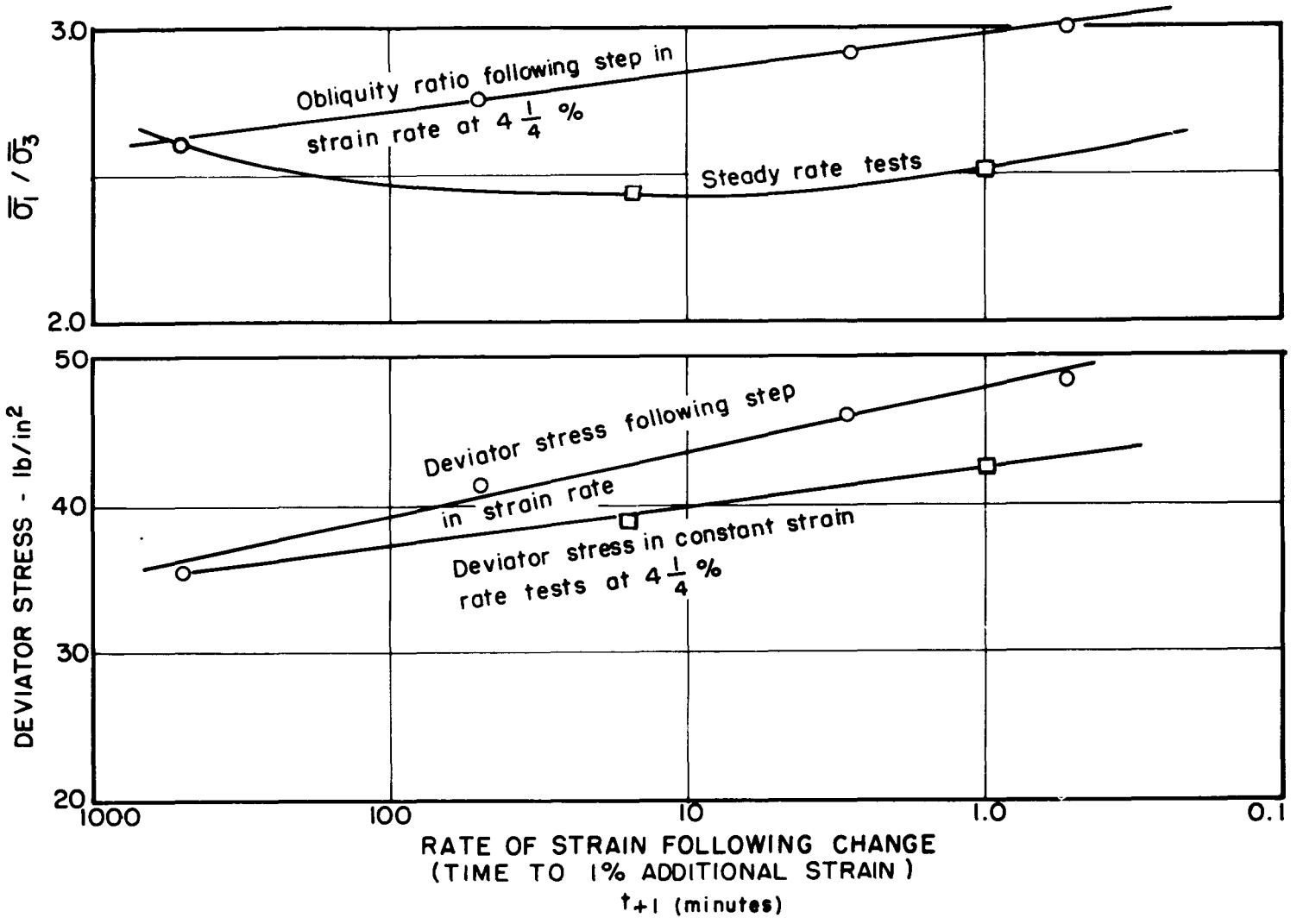

FIGURE 21 RELATIONSHIP OF POST STEP σ_1 / σ_3 AND $(\sigma_1 - \sigma_3)$ TO STRAIN RATE FOLLOWING STEP INCREASE IN STRAIN RATE - NORMALLY CONSOLIDATED SAMPLES

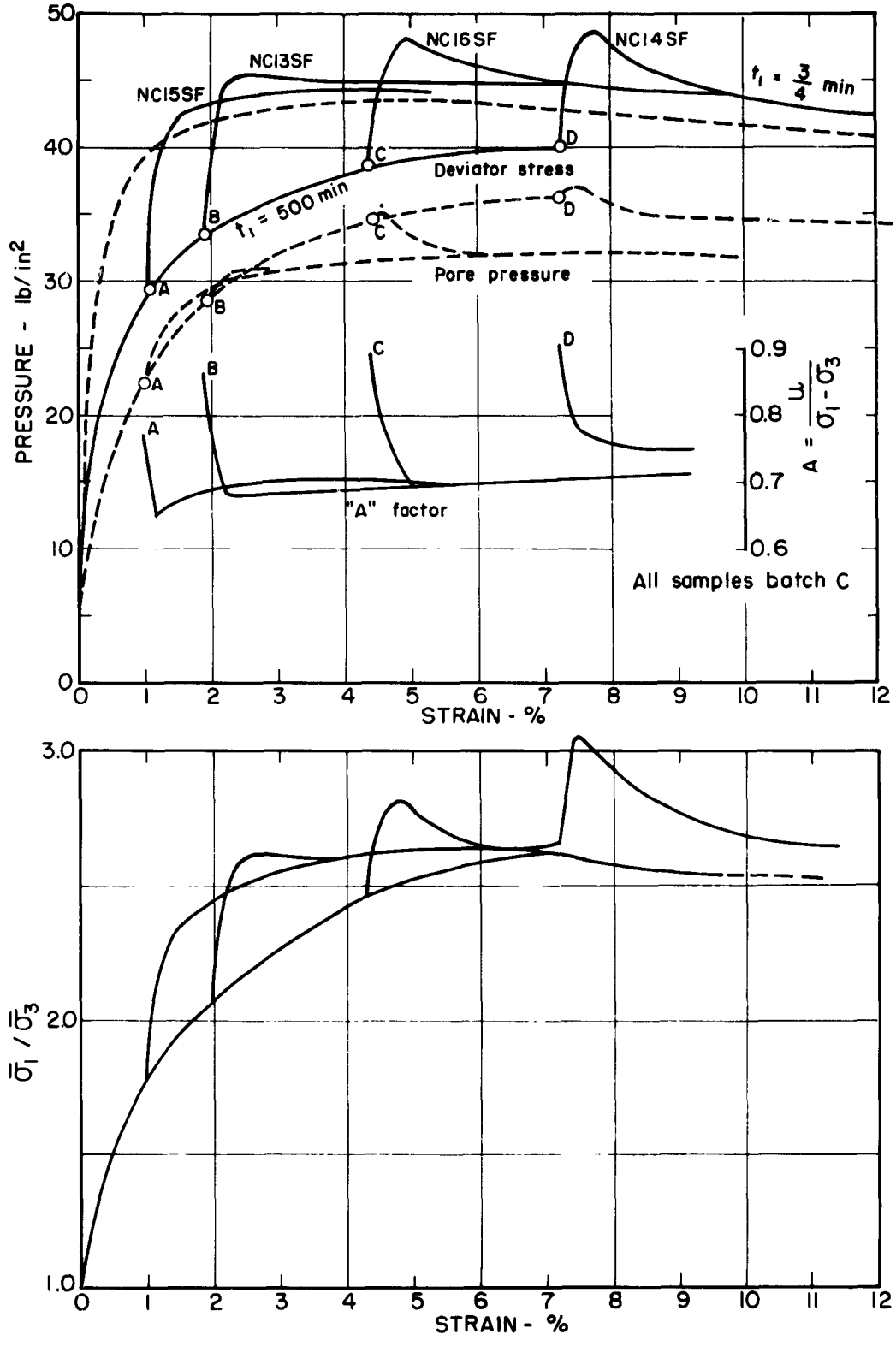

FIGURE 22 SUMMARY PLOT - TESTS WITH STEP INCREASE IN STRAIN RATE AT VARYING STRAIN LEVELS NORMALLY CONSOLIDATED SAMPLES

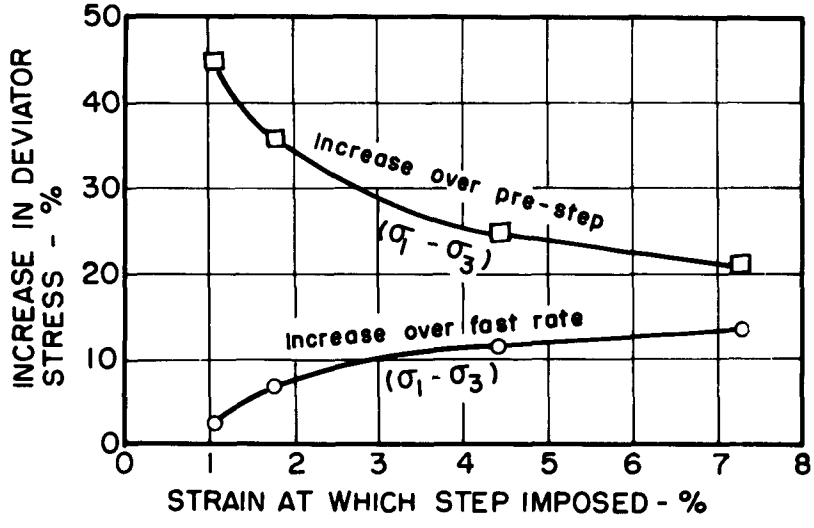

FIGURE 23 DEVIATOR STRESS BEHAVIOR FOLLOWING STEP INCREASE IN STRAIN RATE FROM t_1 = 500min. TO t_{+1} = 3/4 min. - NORMALLY CONSOLIDATED SAMPLES

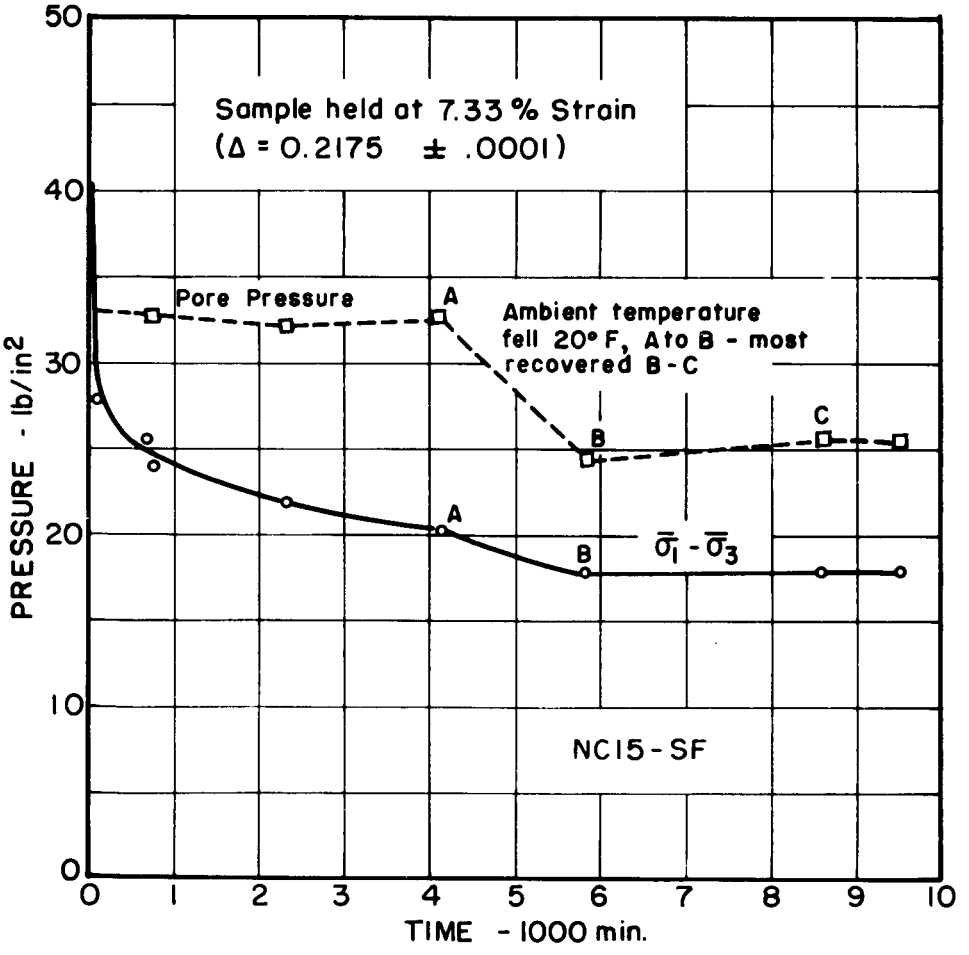

FIGURE 24a RELAXATION BEHAVIOR - NORMALLY CONSOLIDATED SAMPLES

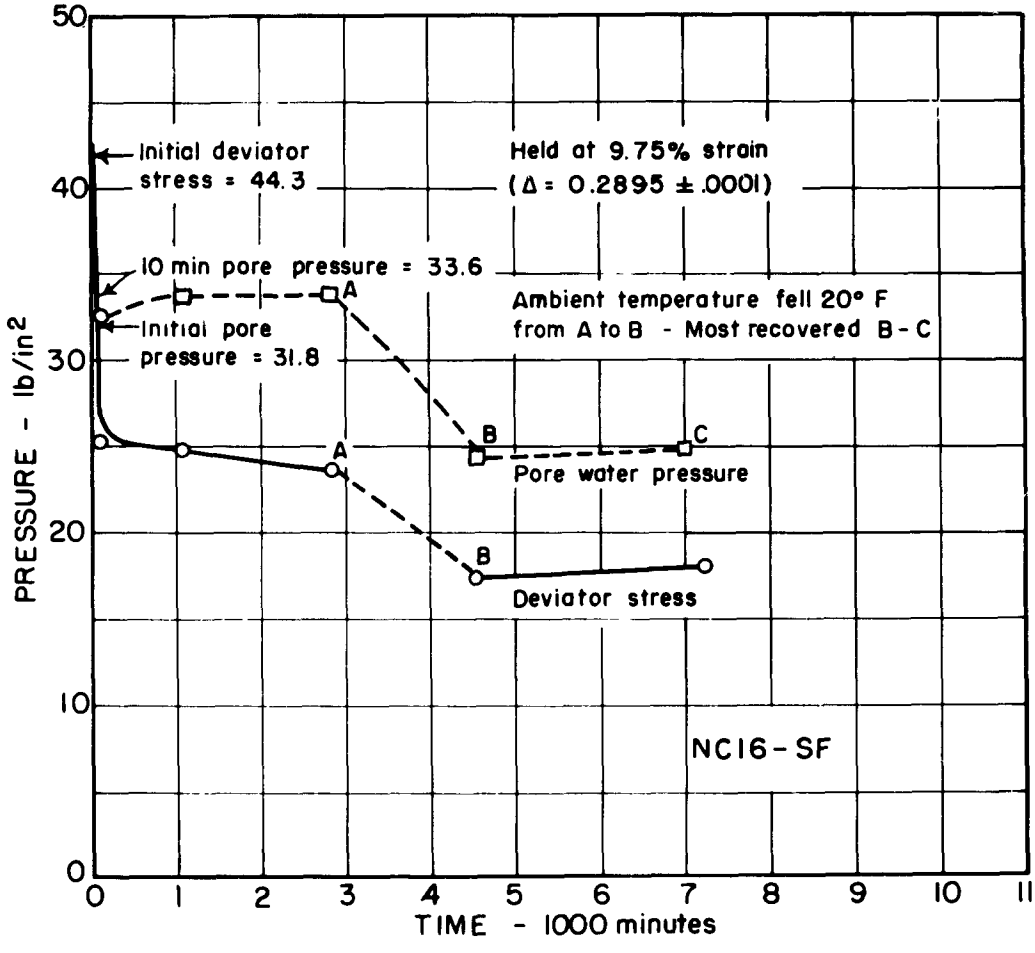

FIGURE 24b RELAXATION BEHAVIOR - NORMALLY CONSOLIDATED SAMPLES

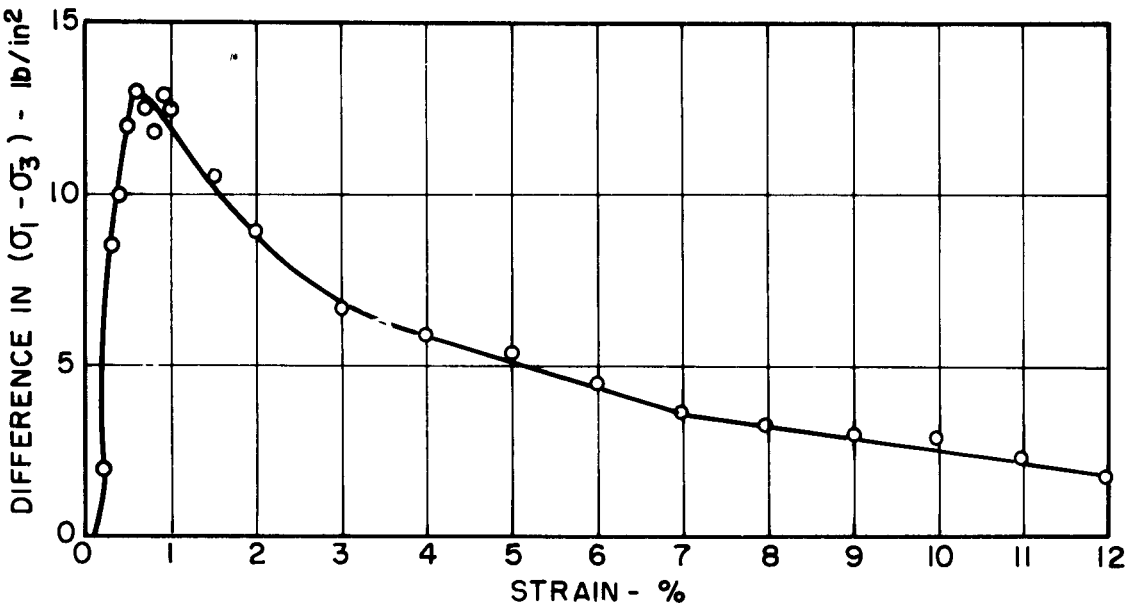

FIGURE 25 $[(\sigma_1 - \sigma_3)\ t_1 = 1\ \text{min.} - (\sigma_1 - \sigma_3)\ t_1 = 500\ \text{min.}]$ vs STRAIN

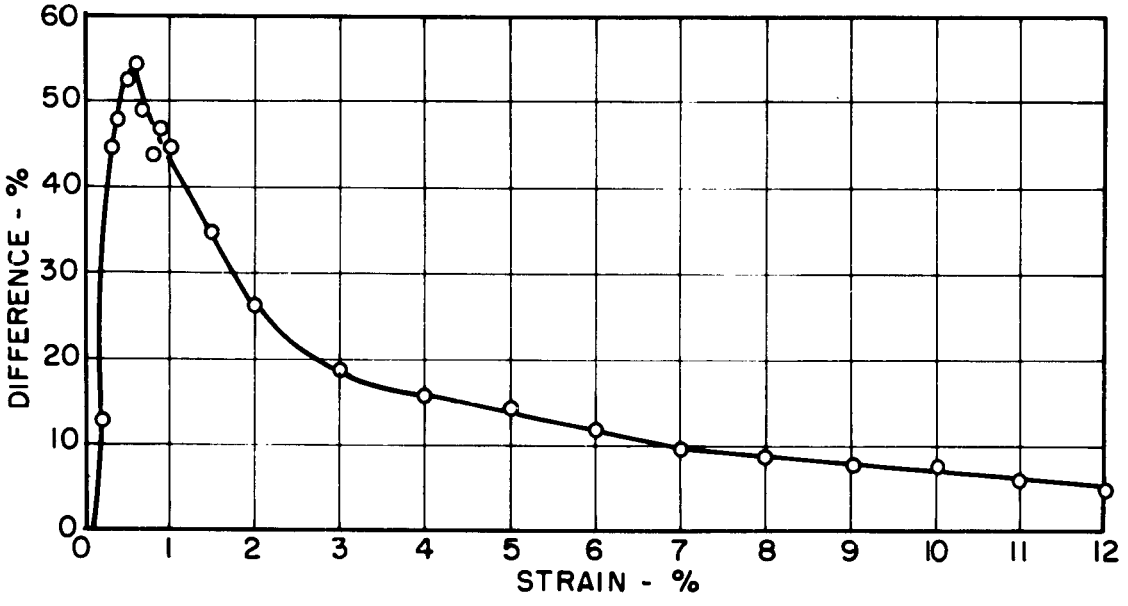

FIGURE 26 % INCREASE IN $(\sigma_1 - \sigma_3)$ FROM $t_1 = 500$ min. TO $t_1 = 1$ min. vs STRAIN

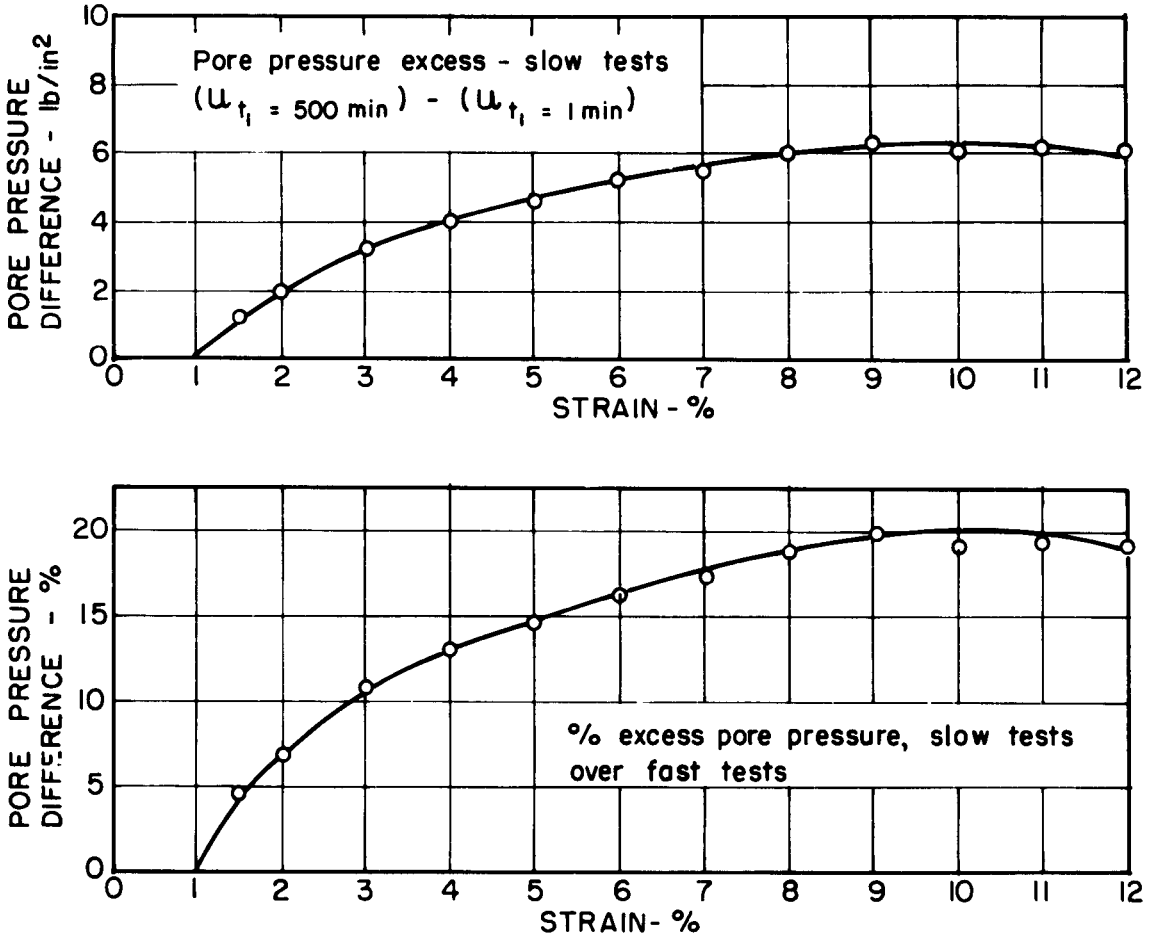

FIGURE 27 PORE PRESSURE DIFFERENCE - SLOW AND FAST TESTS vs STRAIN

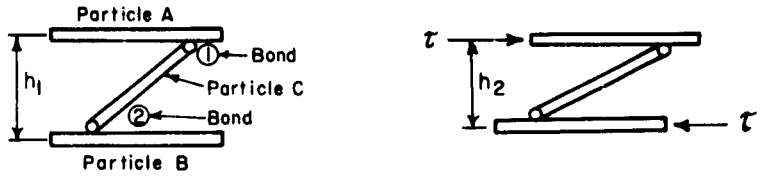

(a) IDEALIZED SMALL STRAIN BEHAVIOR MODEL

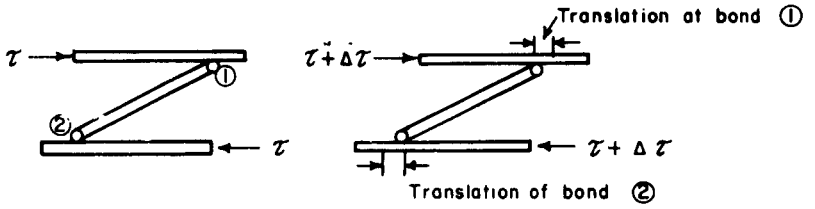

(b) IDEALIZED LARGE STRAIN BEHAVIOR MODEL

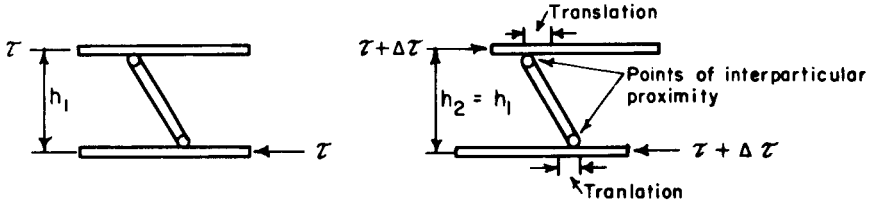

Slow displacement

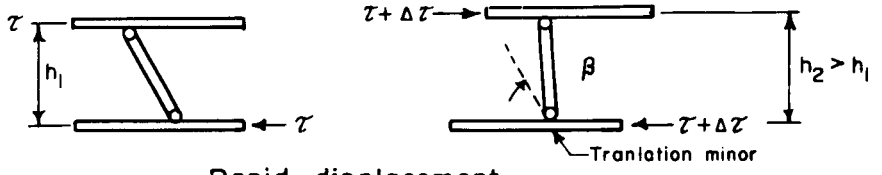

Rapid displacement

(c) IDEALIZATION OF "DILATANT" BEHAVIOR COMPONENT

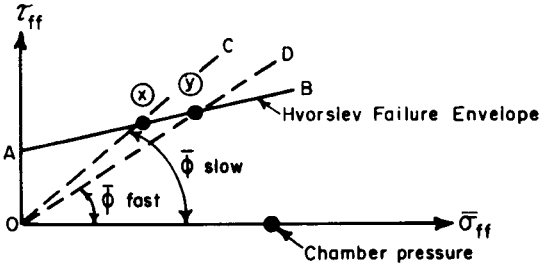

(d) EFFECT OF "PRESTRESS" ON OBLIQUITY RATIO

FIGURE 28 IDEALIZED BEHAVIOR MODELS - NORMALLY CONSOLIDATED SAMPLES

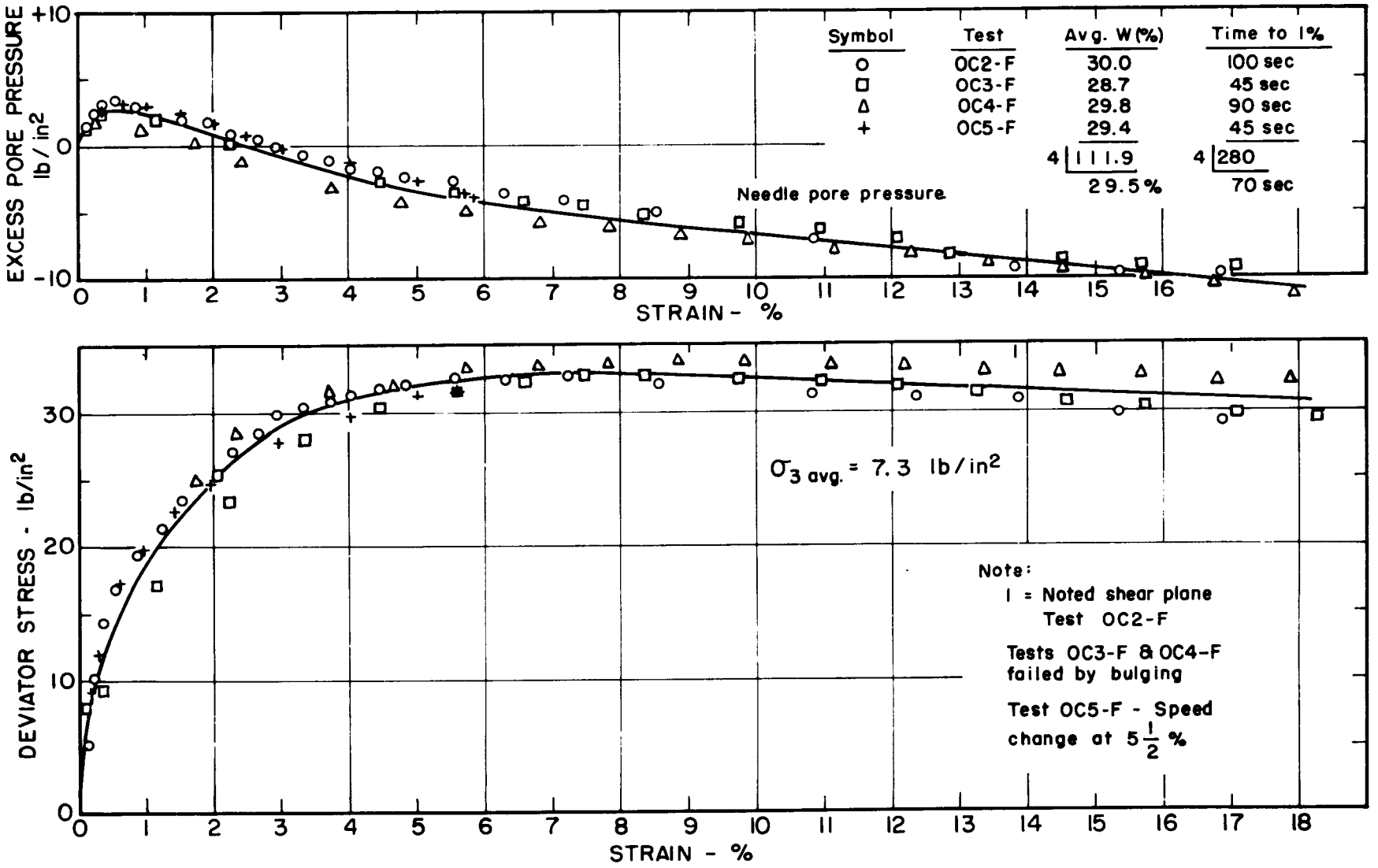

FIGURE 29 SUMMARY PLOT - FAST TESTS - OVERCONSOLIDATED SAMPLES

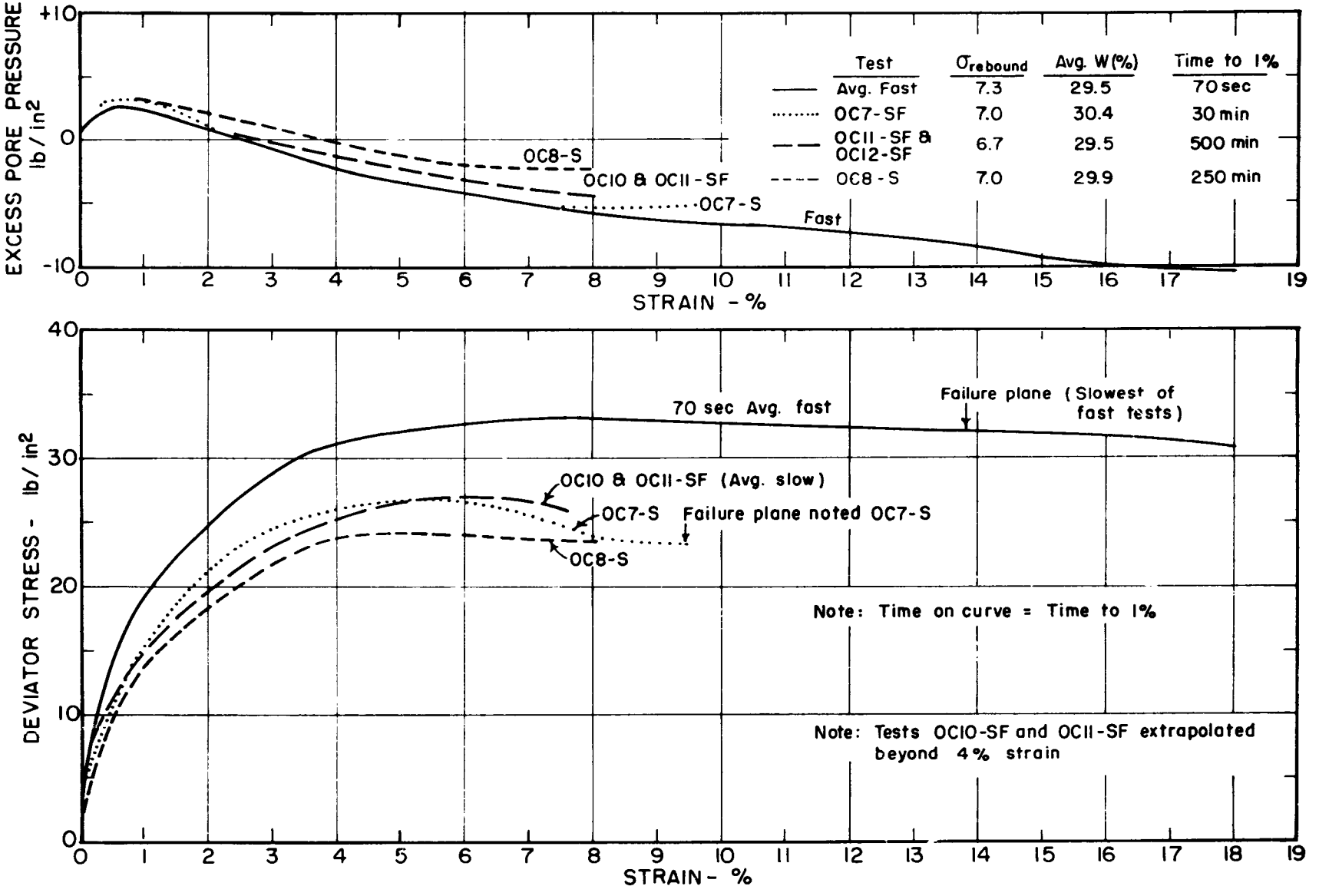

FIGURE 30 SUMMARY PLOT - ALL TESTS - OVERCONSOLIDATED SAMPLES

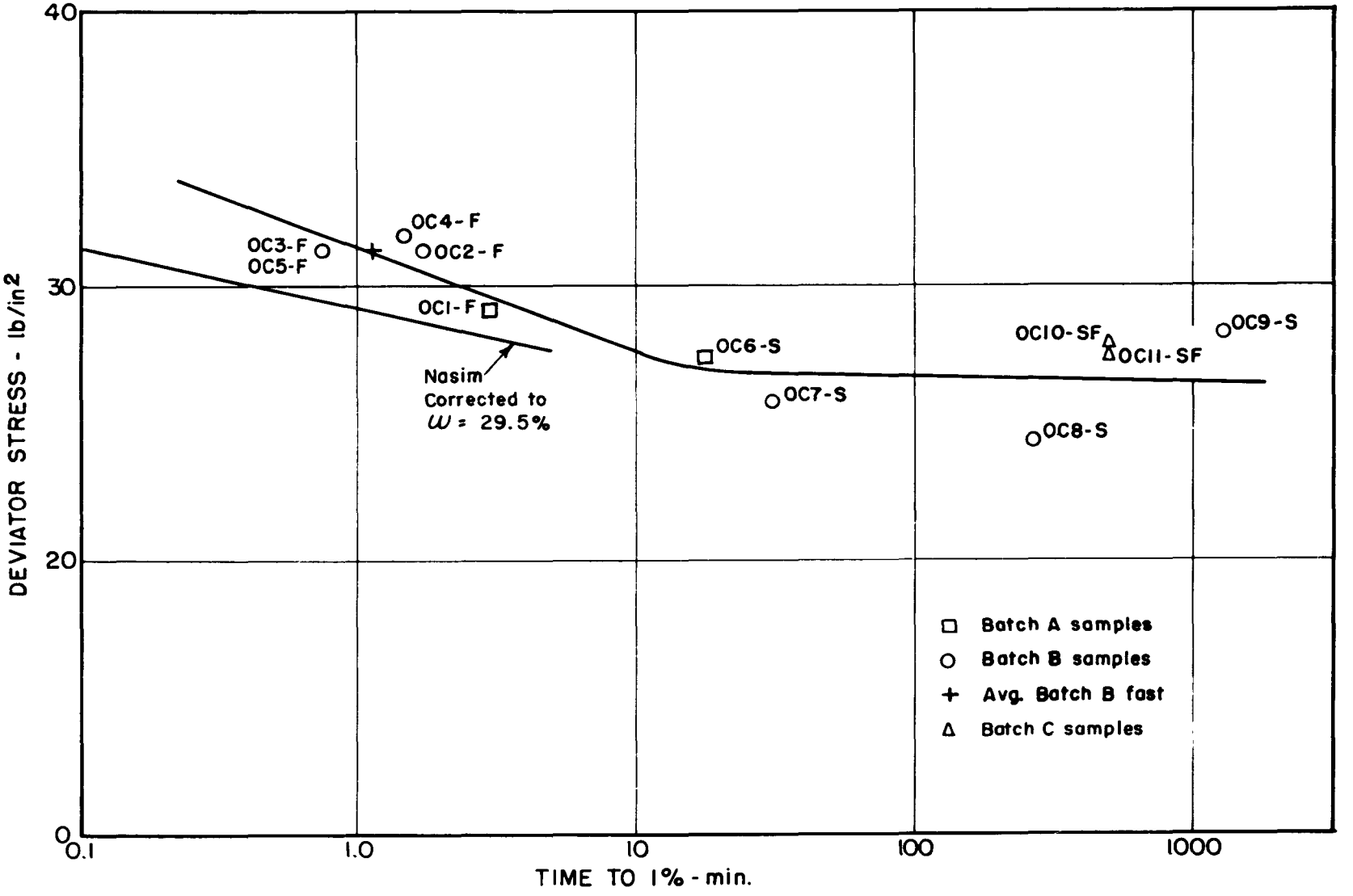

FIGURE 31 MAXIMUM DEVIATOR STRESS vs STRAIN RATE - OVERCONSOLIDATED SAMPLES

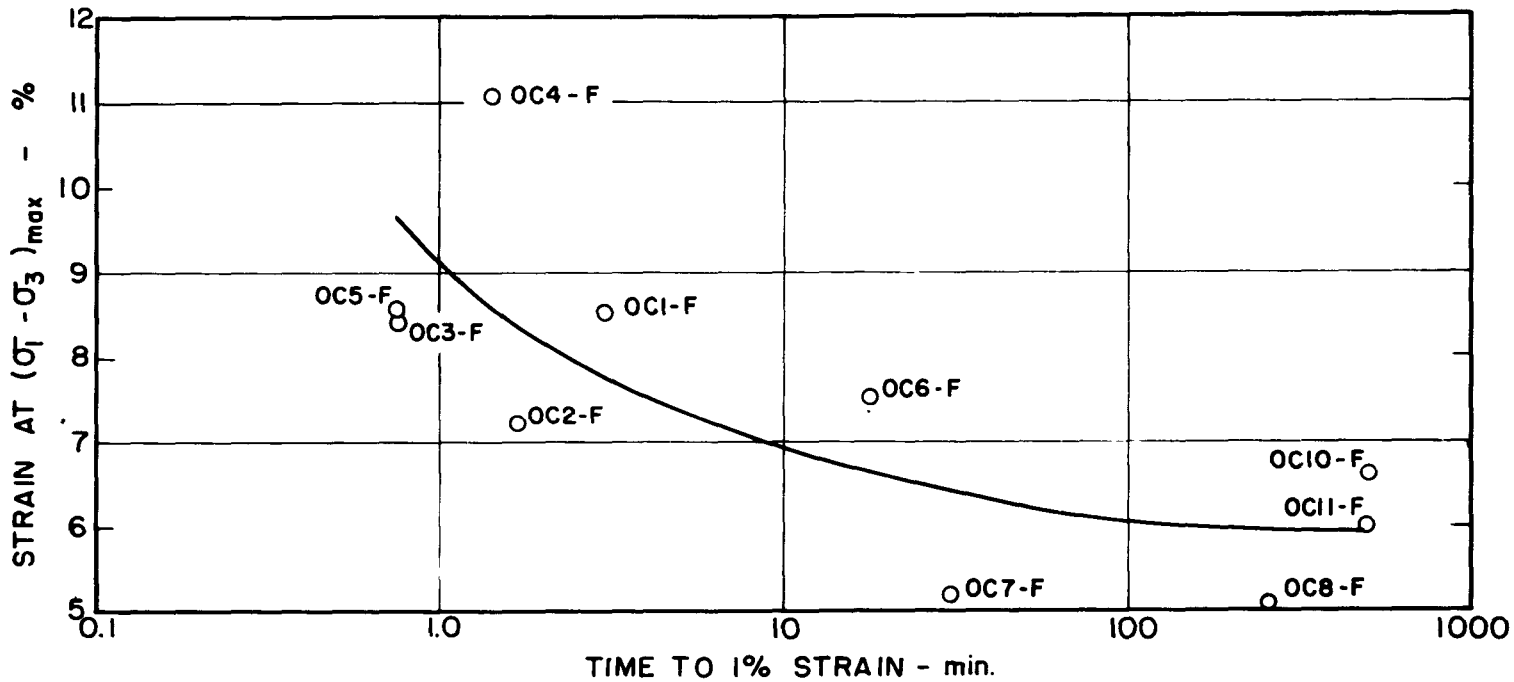

FIGURE 32 STRAIN AT $(\sigma_1 - \sigma_3)_{max}$ vs STRAIN RATE - OVERCONSOLIDATED SAMPLES

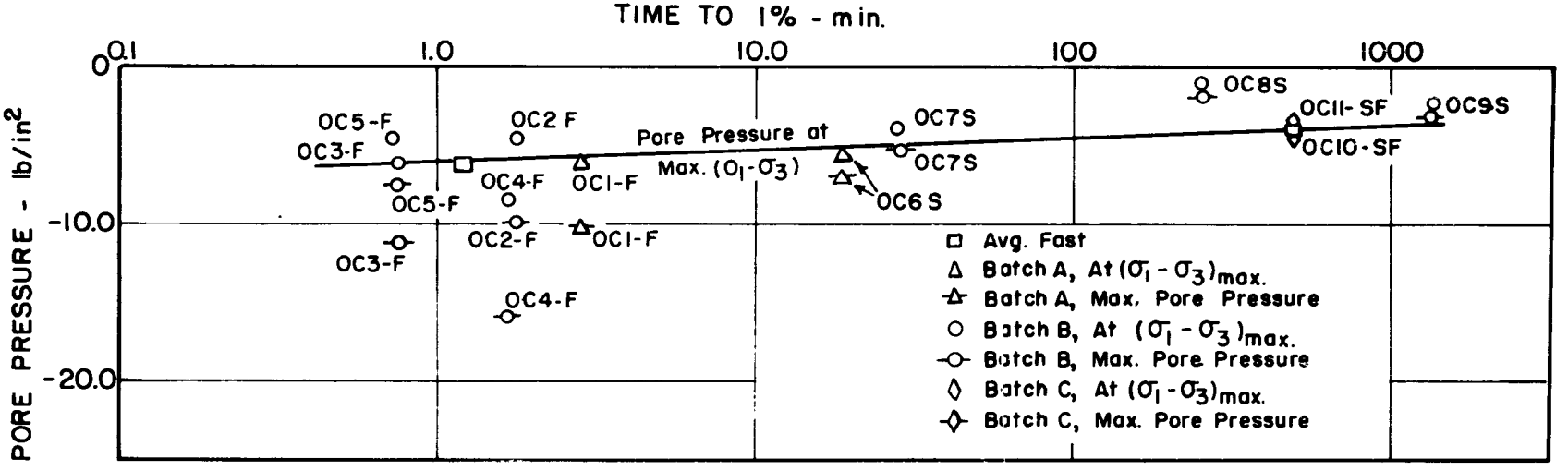

FIGURE 33 MIDPLANE PORE PRESSURE vs STRAIN RATE - OVERCONSOLIDATED SAMPLES

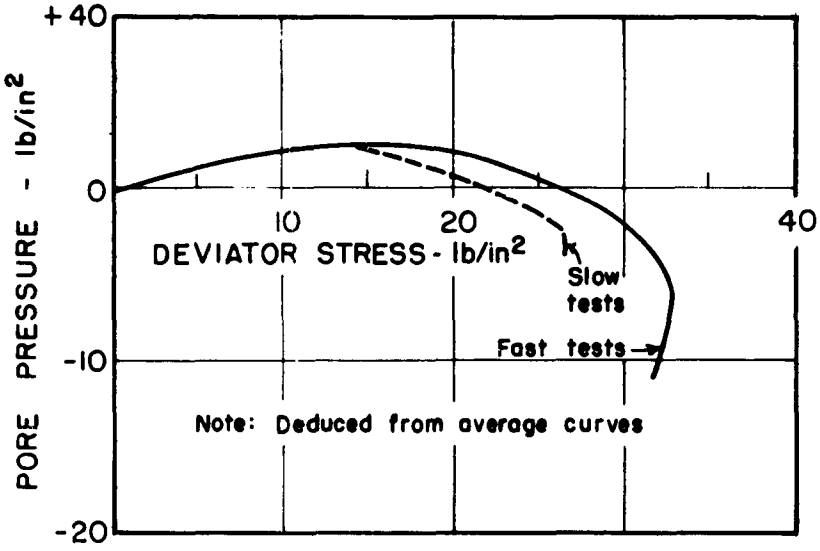

FIGURE 34 MIDHEIGHT PORE PRESSURE vs DEVIATOR STRESS OVERCONSOLIDATED SAMPLES

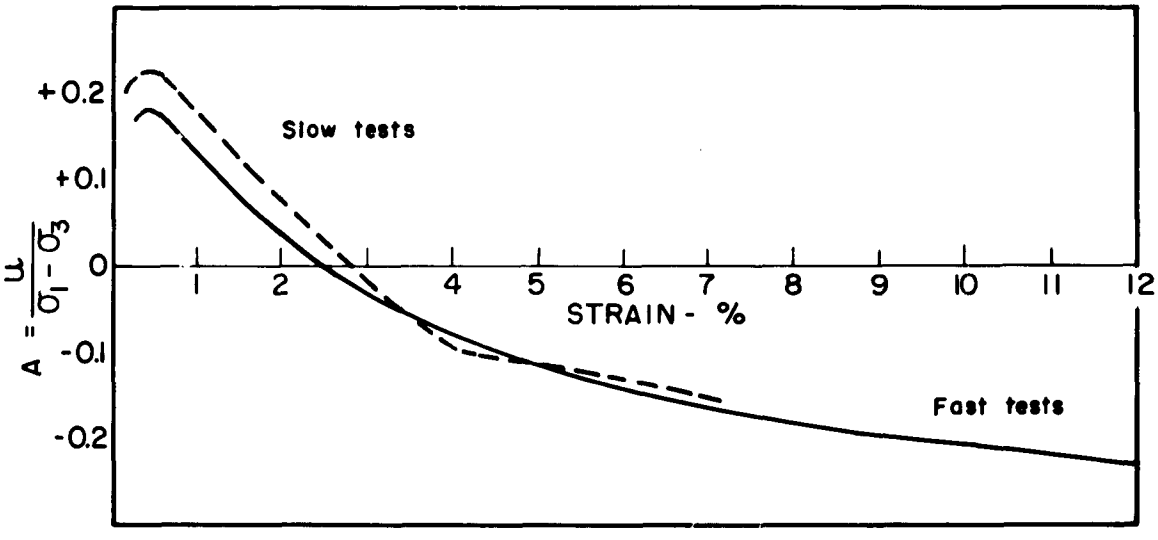

FIGURE 35 PORE PRESSURE PARAMETER A vs STRAIN OVERCONSOLIDATED SAMPLES

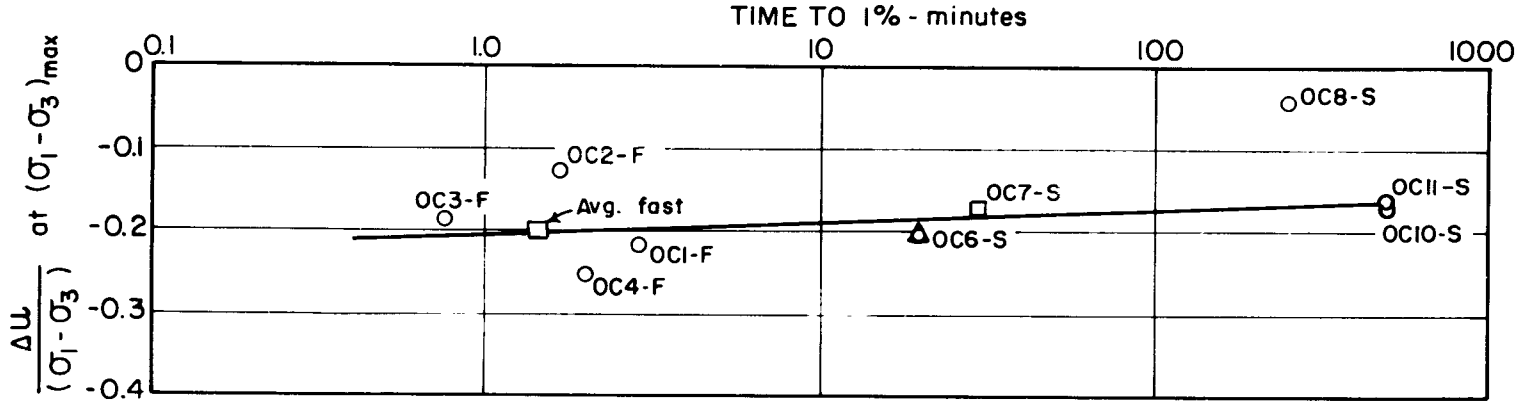

FIGURE 36 A AT $(\sigma_1-\sigma_3)_{max}$ vs STRAIN RATE - OVERCONSOLIDATED SAMPLES

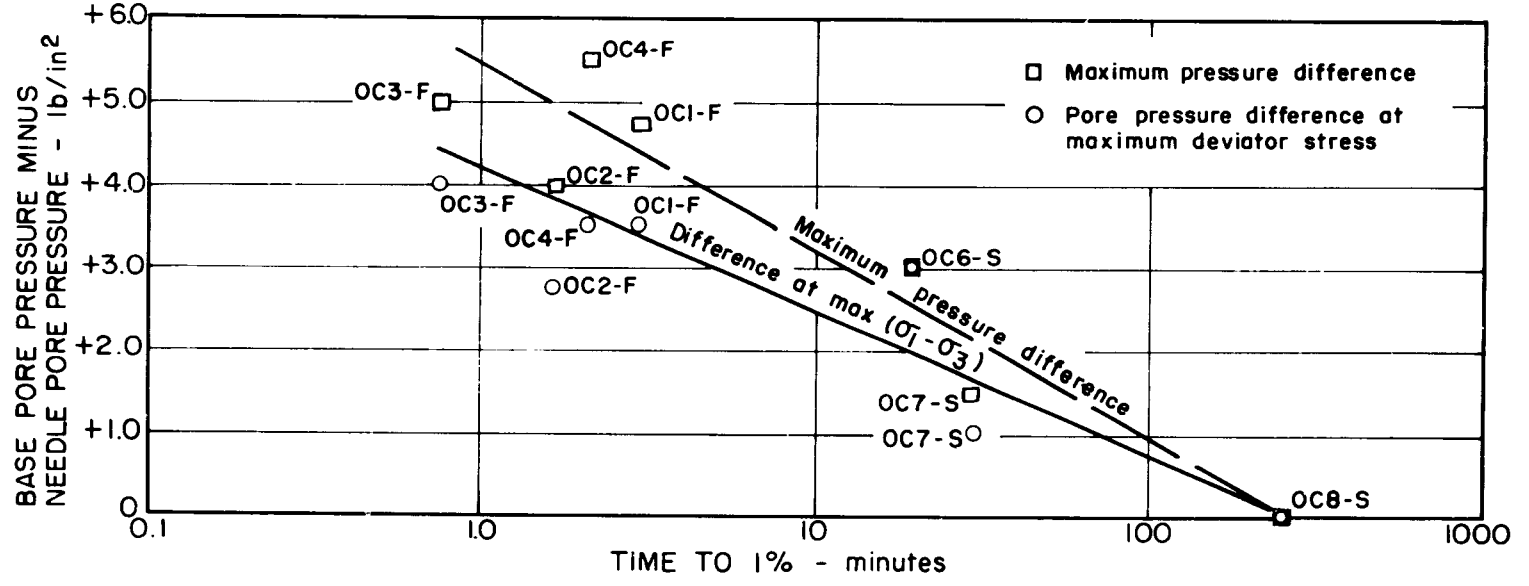

FIGURE 37 PORE PRESSURE GRADIENT vs STRAIN RATE - OVERCONSOLIDATED SAMPLES

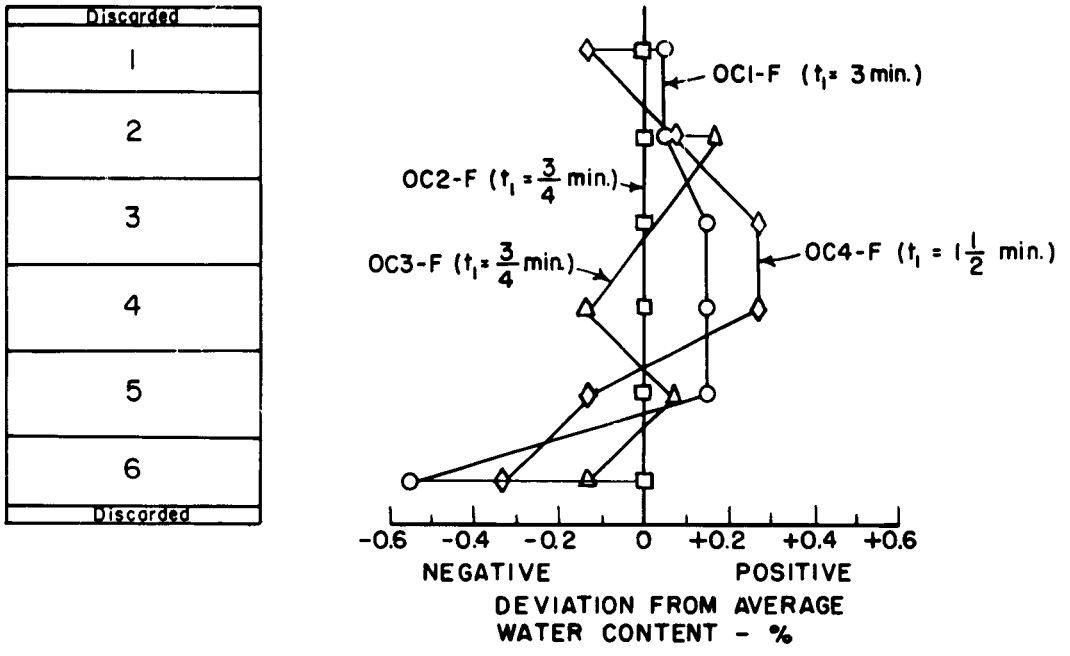

(a) FAST TESTS

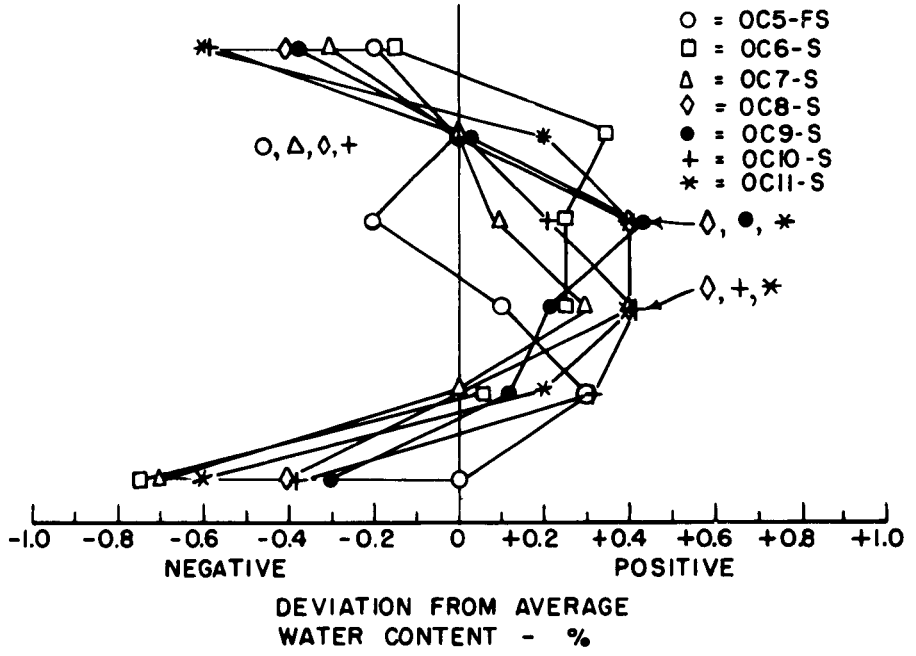

(b) SLOW TESTS

FIGURE 38 POST SHEAR DISTRIBUTION OF WATER CONTENT OVERCONSOLIDATED SAMPLES

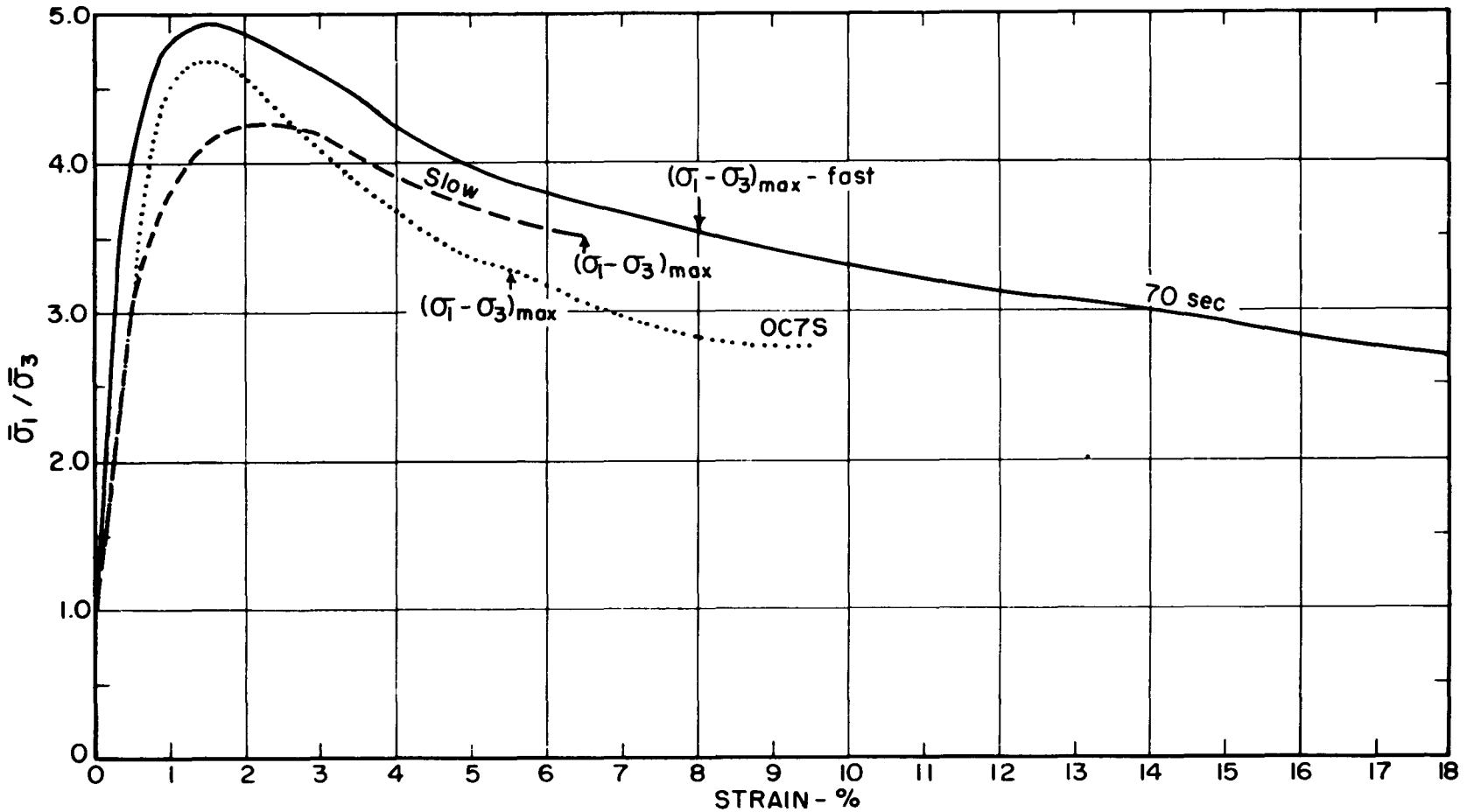

FIGURE 39 OBLIQUITY vs STRAIN RATE - SUMMARY - OVERCONSOLIDATED SAMPLES

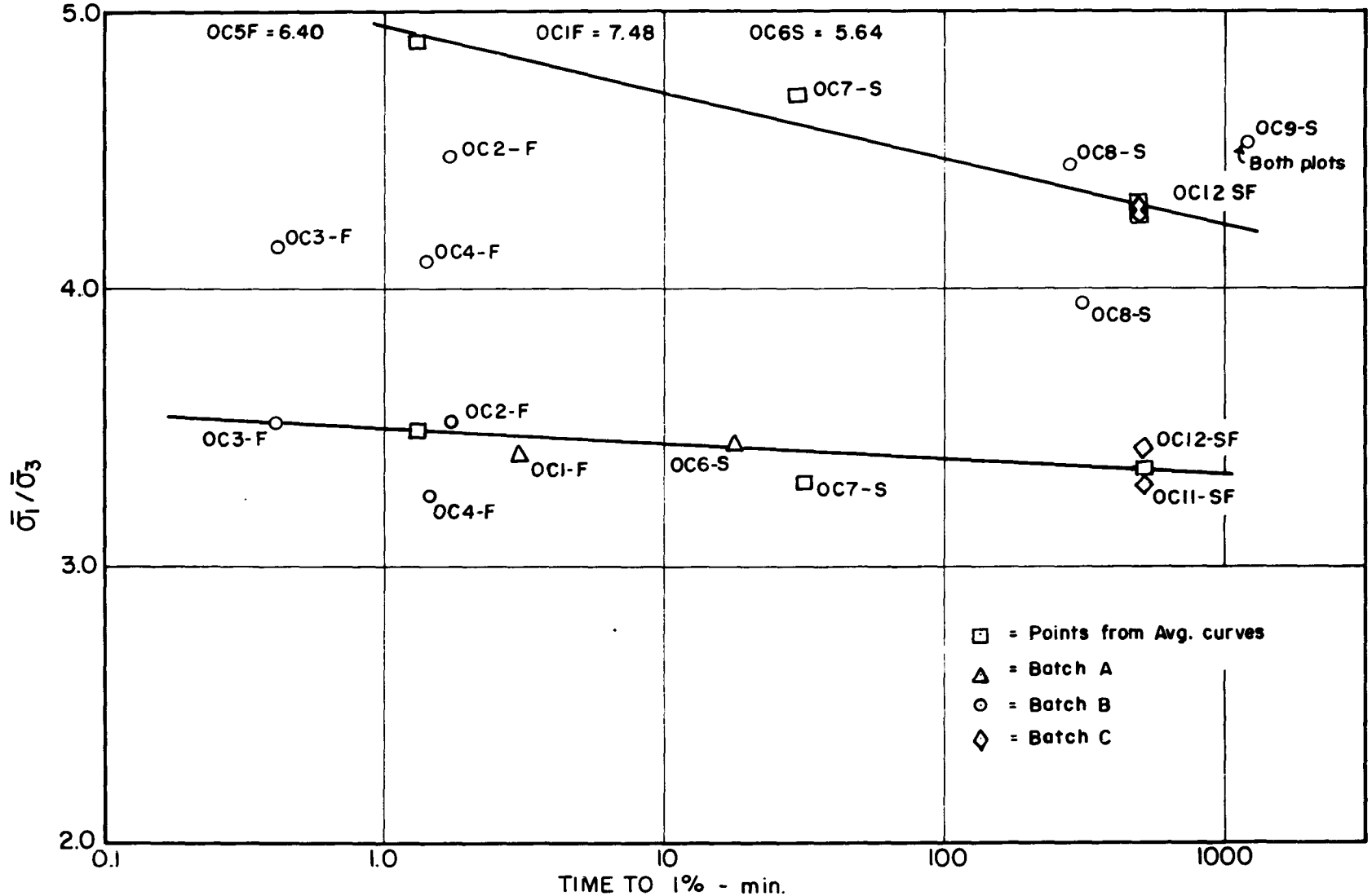

FIGURE 40 OBLIQUITY vs STRAIN RATE - OVERCONSOLIDATED SAMPLES

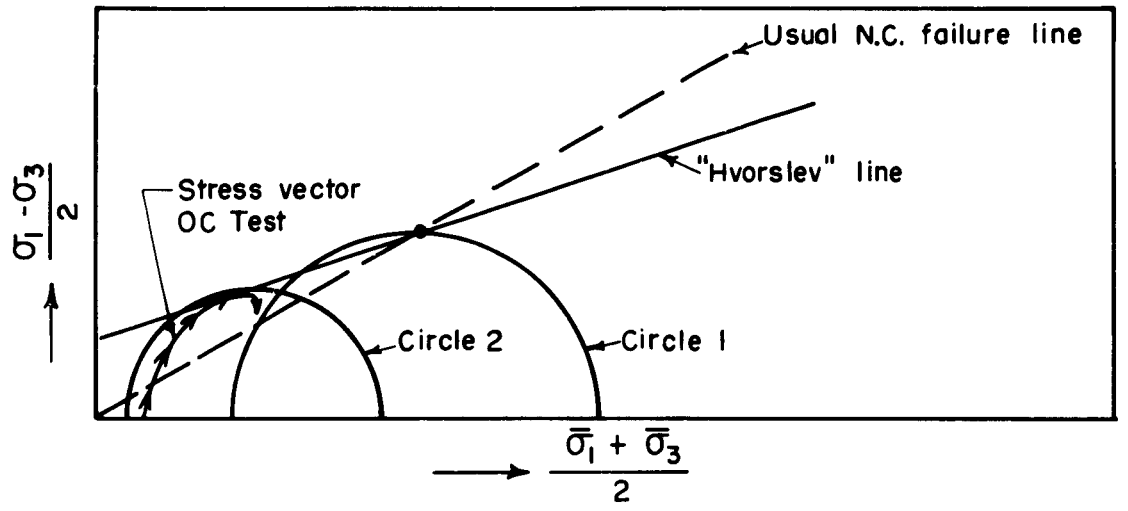

FIGRE 41 FAILURE ENVELOPES

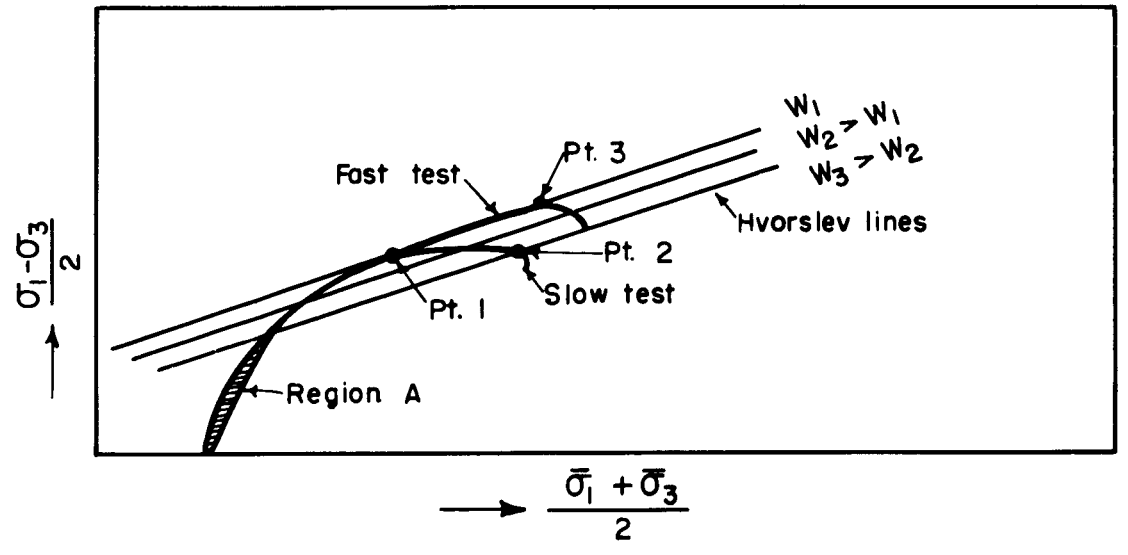

FIGURE 42 BEHAVIOR OF OVERCONSOLIDATED SAMPLES IN TERMS OF STRESS VECTORS

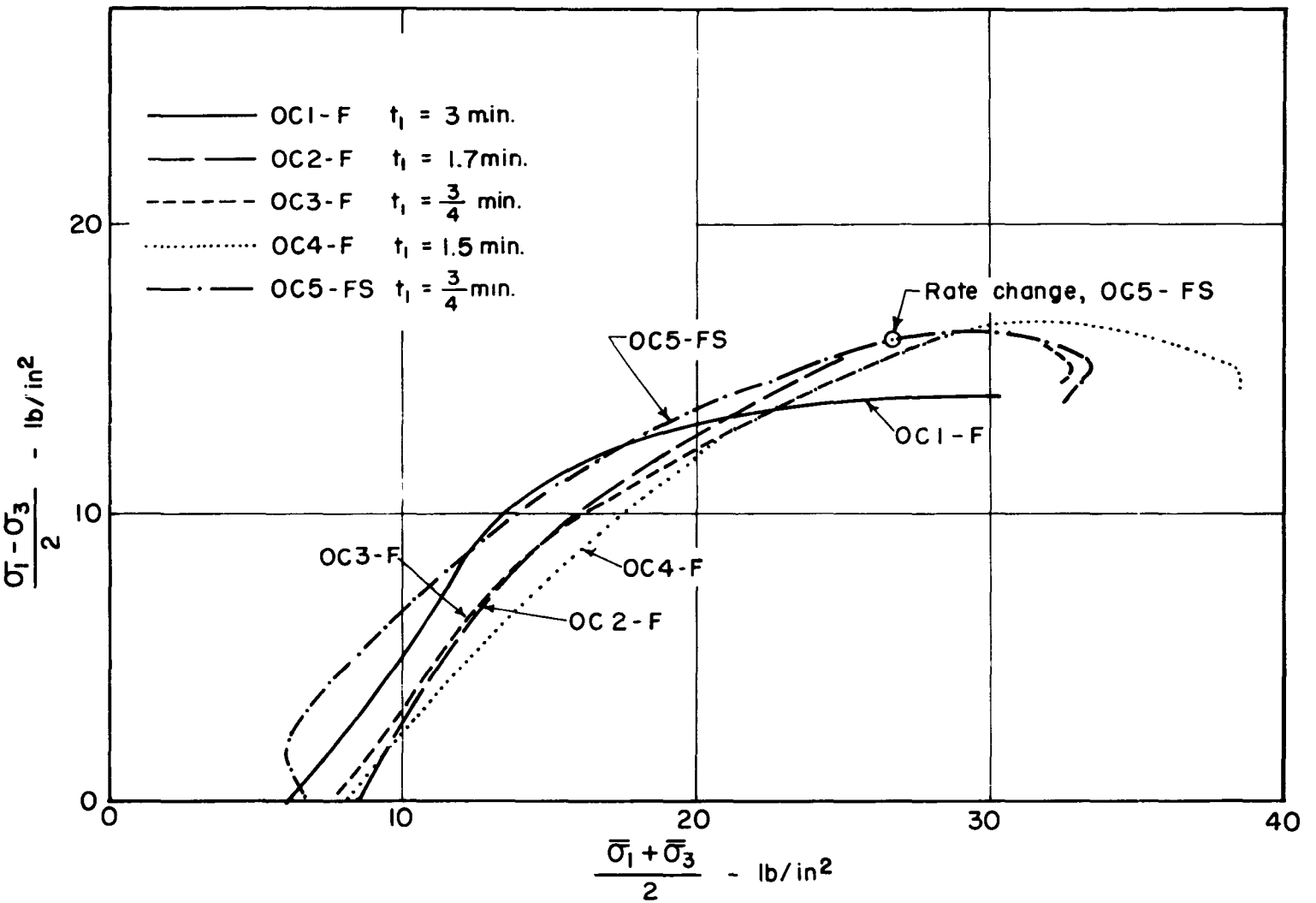

FIGURE 43 SUMMARY PLOT - STRESS VECTORS - FAST TESTS - OVERCONSOLIDATED SAMPLES

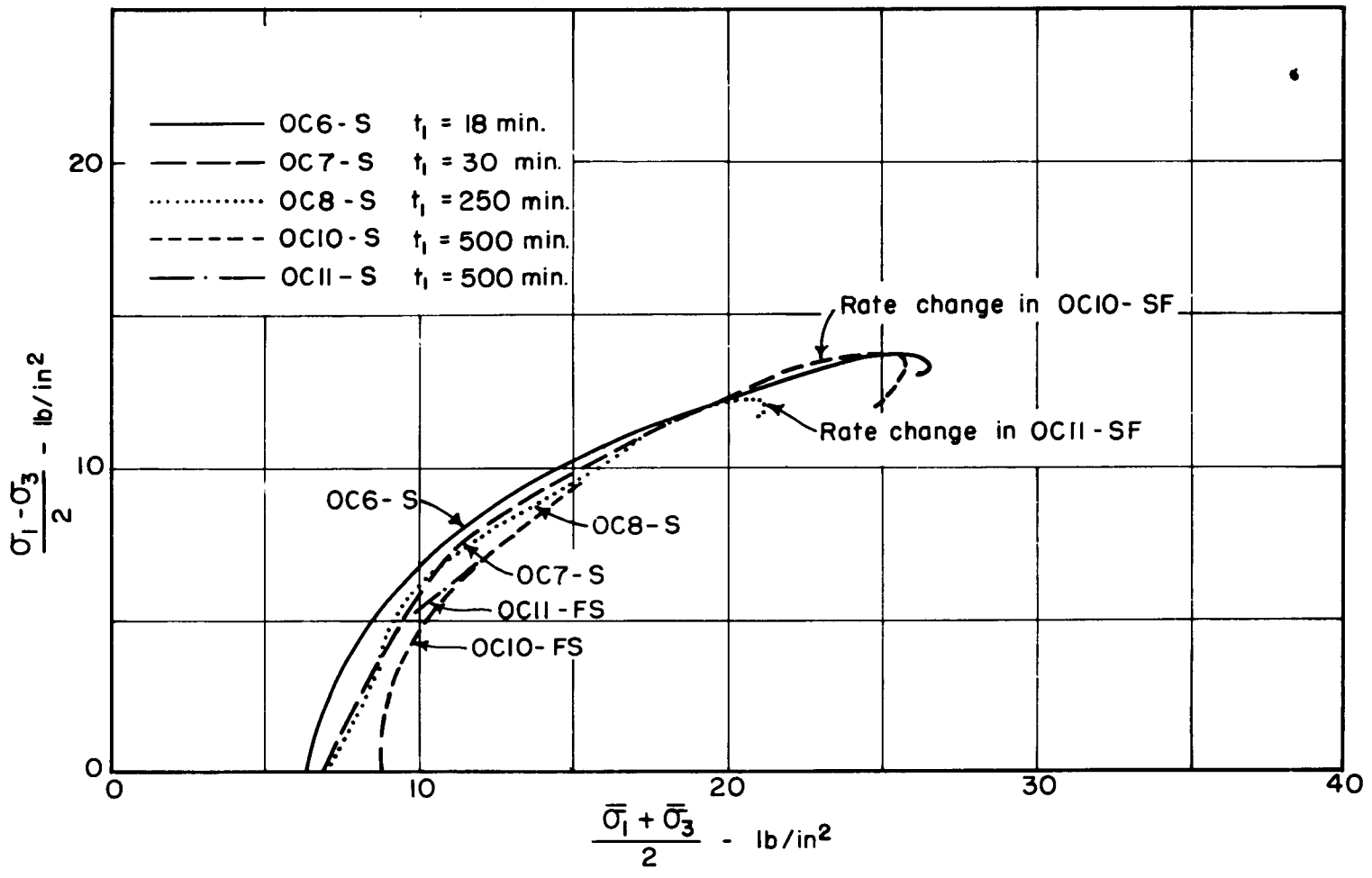

FIGURE 44 SUMMARY PLOT - STRESS VECTORS - SLOW TESTS - OVERCONSOLIDATED SAMPLES

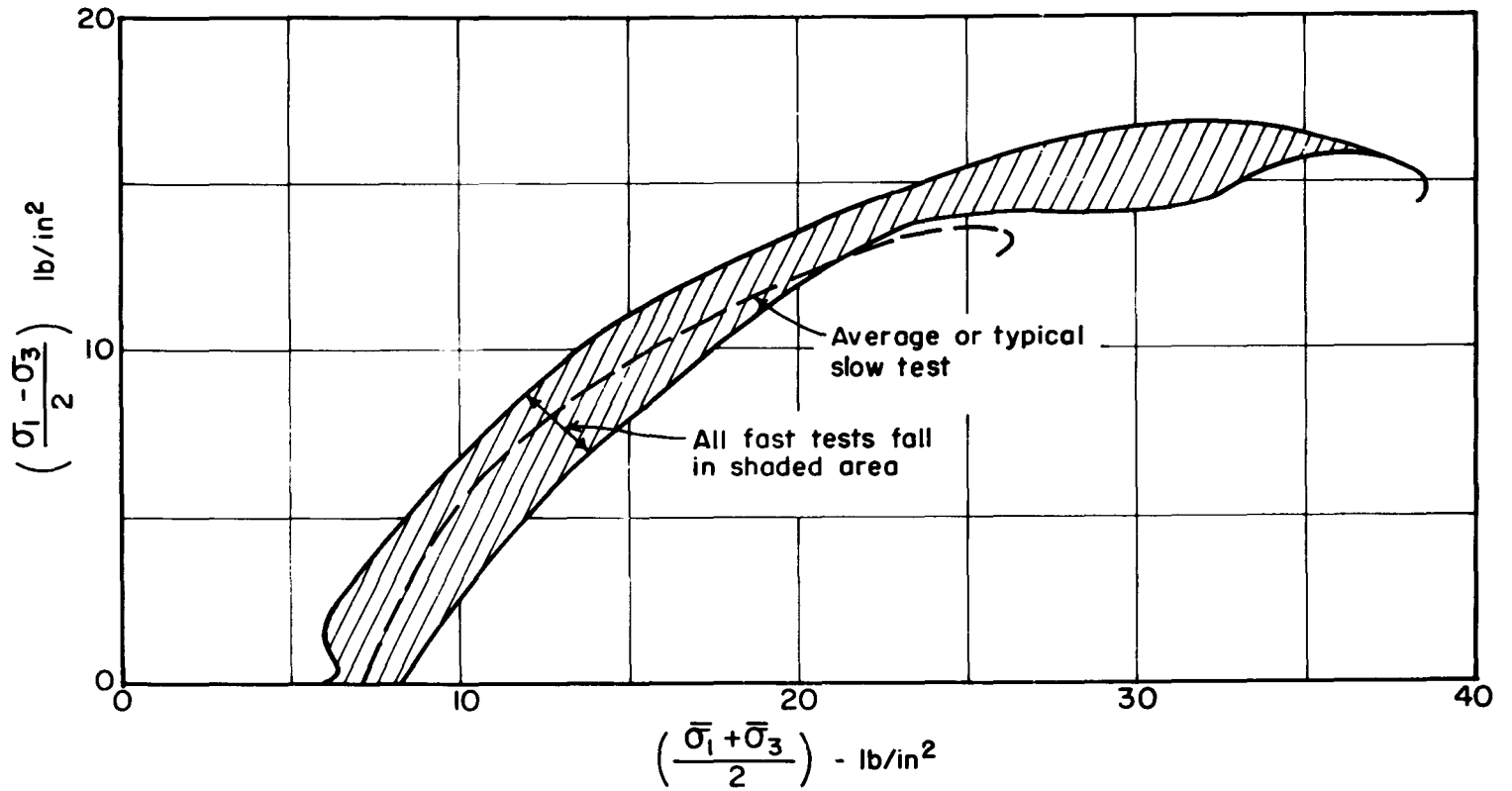

FIGURE 45 SUMMARY PLOT - ALL STRESS VECTORS - OVERCONSOLIDATED SAMPLES

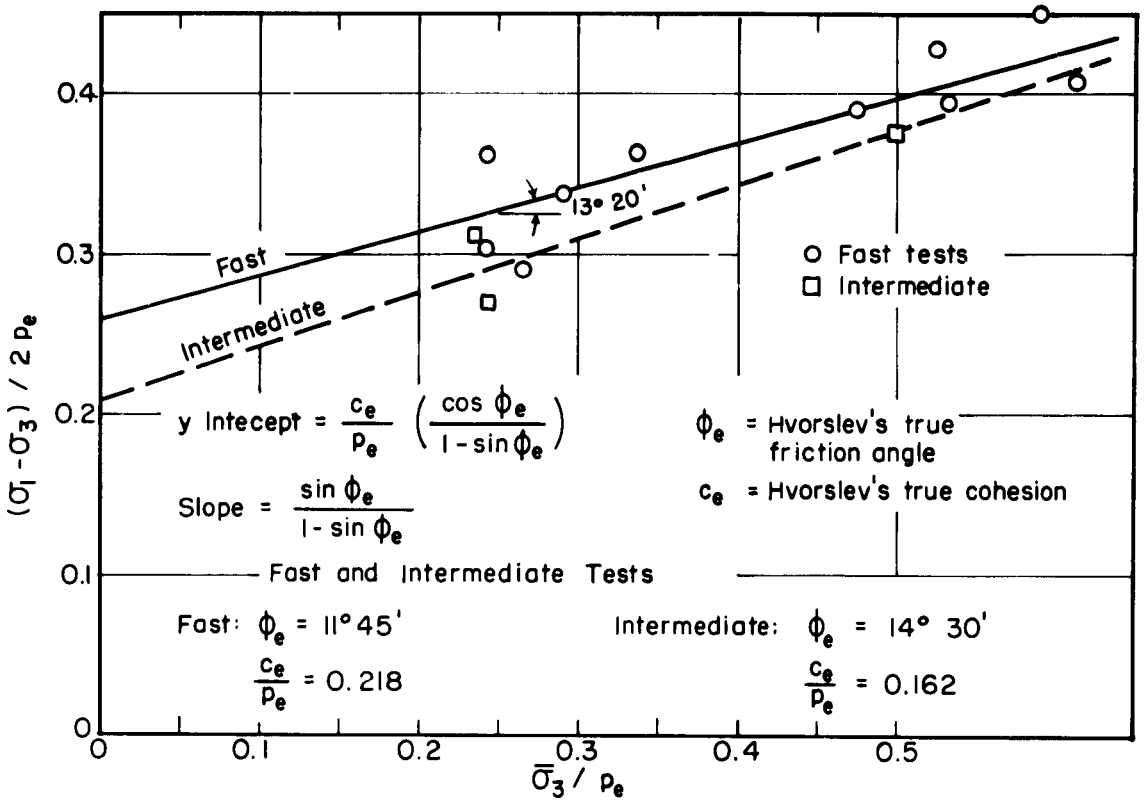

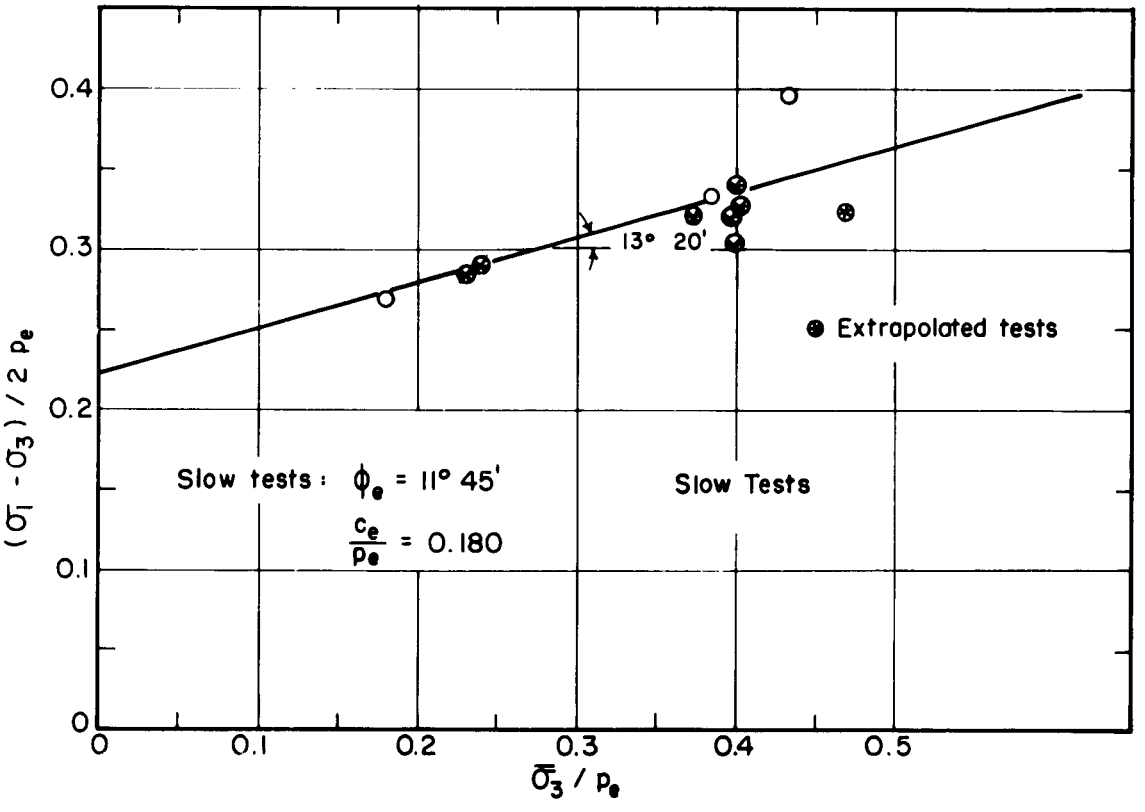

FIGURE 46 PLOT FOR DETERMINATION OF HVORSLEV PARAMETERS AT FAILURE

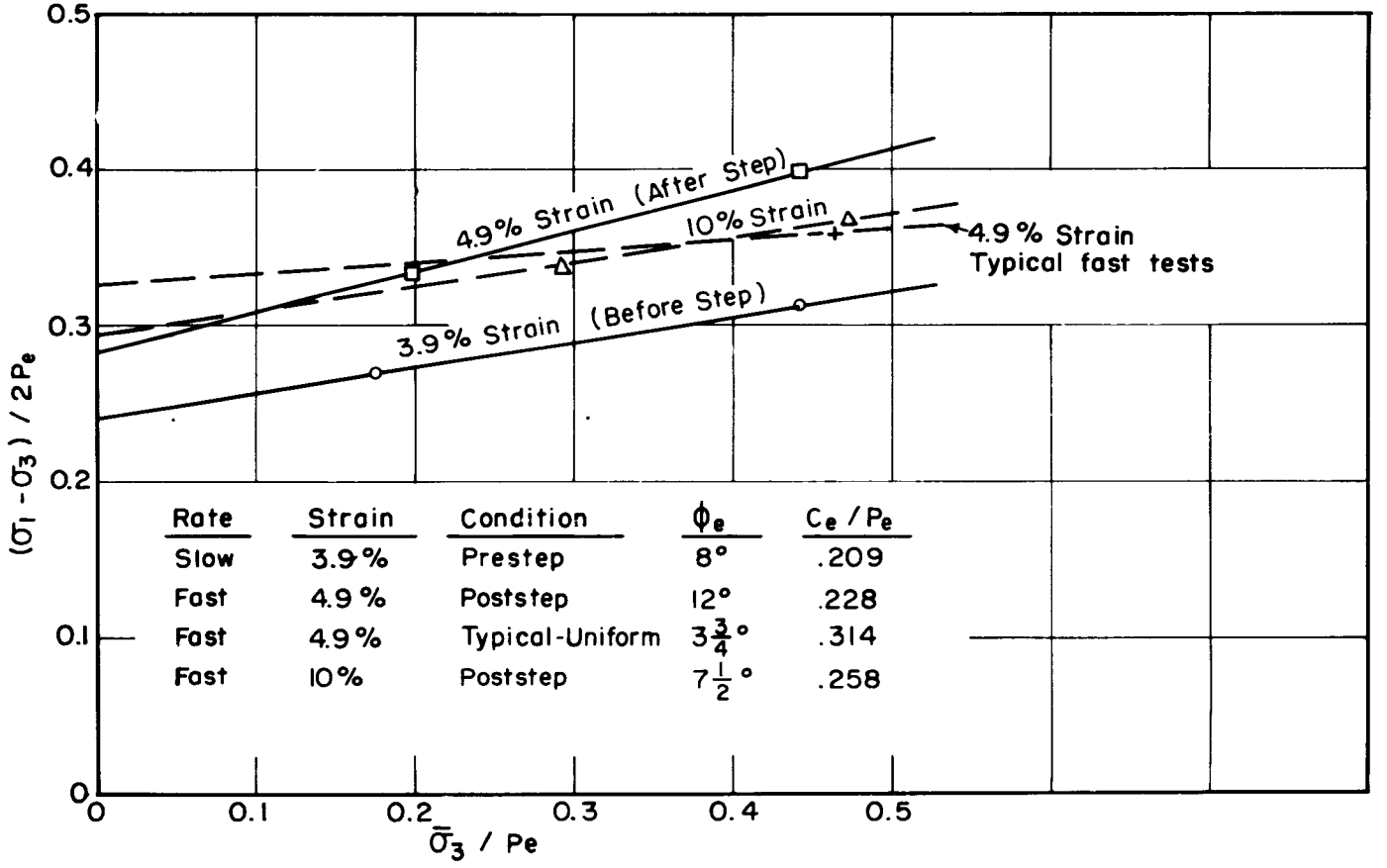

FIGURE 47 ANALYSIS OF STEP INCREASE IN STRAIN RATE IN TERMS OF HVORSLEV PARAMETERS

Appendix A

PORE PRESSURE MEASUREMENT: DEVICES, TECHNIQUES, AND PERFORMANCE

CONTENTS

LIST OF FIGURES

Appendix A

PORE PRESSURE MEASUREMENT: DEVICES, TECHNIQUES, AND PERFORMANCE

A. Introduction

The research described in the preceding chapters became possible only through the development of rapidly responding pore water pressure measuring devices and techniques for the utilization of these devices. This Appendix describes these devices in detail. In addition, the techniques employed in the successful utilization of these devices are described, and data supporting response claims are presented.

The basic element of the devices employed in measuring pore pressures in this research is an electric pressure transducer. This pressure transducer combines outstanding sensitivity with extreme rigidity and thus it was possible to develop a system having an exceptionally low compliance (i.e., very small volume change required to accurately measure pressures).

This pressure transducer was incorporated into two measuring systems, one allowing measurement of pore pressure in the triaxial compression specimen at the conventional specimen base location but with a rapidly responding electronic system. The other system provided measurement of the pore water pressure developed at the elevation of the sample mid-height by employing a small porous probe.

Both of these systems required the development of techniques for their successful application and the success of both these systems as applied to triaxial compression samples was the main experimental factor in this research.

B. Electric Pressure Transducer and Associated Instrumentation

The electric pressure transducer employed in this research was developed and is commercially available from the Dynisco Division of American Brake Shoe Company, 42 Carleton Street, Cambridge 42, Massachusetts, as Model PT-25. This "Dynisco" gage consists of a four-active-arm unbonded strain gage bridge which senses the deflection of a small, rigid diaphragm. It is accurate to better than 0.25 percent of its full scale output and exhibits a maximum non-linearity of less than 0.50% of its full scale output. The particular gages employed in this research had full scale ranges of 0 to 150 lb./in.^{2}. These gages have a compliance on the order of 3×10^{-6} cubic centimeters per pound per square inch pressure change which is less than the change in volume of the water in a typical triaxial compression specimen. (The cubic compressibility of water is 3.4×10^{-6} lb. per square inch. An 80 cc sample at a water content of 33% contains 20 cc of water which will compress 68×10^{-6} cc/lb./in.^{2} or 20 times the gage compliance.)

These gages were activated with an extremely accurate, 6 volt D.C. power supply of the type used to replace standard reference cells in accurate recording equipment (EvenVolt Power Supply, Instrulab Inc., 1205 Lamar Street, Dayton 4, Ohio). The power supply is insensitive to changes in ambient temperature, a factor influencing earlier tests employing a storage battery as a power supply.

The output of these pressure transducers is extremely small, being of the order of from 0 to 10 millivolts D.C., at the range of pressure changes represented by the tests performed during this research. This output was displayed against time on a Moseley X-Y plotter on which 10 millivolts represented about 10 inches, and thus the required precision of measurement was possible.

The final layout of the instrumentation is pictured schematically in Figure A-6. This layout featured a sampling switch

allowing both base and midplane pore pressure transducer output to be displayed on the same channel of the X-Y plotter. This was accomplished by switching input channels approximately 15 times per one percent strain of the specimen. Prior to the development of this apparatus, two X-Y plotters were employed when both midplane and base measurements were required.

C. Porous Probe and Connections for Midplane Measurements

The porous probe used for midplane pore water pressure measurements is shown in Figure A-4. Stones were cut from larger pieces of Norton grade 2120 porous stones with a hacksaw and hand-shaped with a file. Both the file and the hacksaw were destroyed in the process. The shaped porous probe was fitted to a small brass cap and fastened securely with small patches of epoxy cement.

The brass cap was drilled as shown to allow slipping the end of a length of teflon tubing into place. No cement was used at this connection and this connection was made prior to each installation of the probe.

The teflon tubing employed was purchased from the Supernant Manufacturing Company of Newton, Massachusetts, and is marketed as "spaghetti" insulation for wiring. The type used was insulation for #31 gage wire and had an I.D. of 0.01 inches and O.D. of 0.03 inches. Thus this shape can be classed as a thick walled tube. This tubing was found to combine the properties of sufficient flexibility with extremely low volume change due to pressure change.

This tubing led from the triaxial cell through a small hole in the specimen pedestal. In the Norwegian cells, one of the base drainage holes was utilized, but in the English cells, a small hole was drilled to allow this tubing to pass from the triaxial chamber. In both cases the holes were quite close to the edge of the specimen pedestal. This exit was securely sealed with a plug of epoxy cement around the tube.

The external free end of the tube was connected to the measuring chamber holding the pressure transducer by a small (27 gage) hypodermic needle inserted into the tubing as shown in Figure A-3. Since insertion of the needle into unprotected tubing tended to split the tubing, the tubing was first fitted with a split sleeve as shown in the detail in Figure A-3.

Figure A-2 shows the final modification of the specimen pedestal of the triaxial cells. The method of construction was as follows: (1) The porous base stone was cut out in the region of the tubing outlet hole as shown. A layer of grease was applied to this cut surface to prevent future adherence of the epoxy cement. The cut stone was clamped to the pedestal. (2) The tubing was roughened with emery paper in the region of passage through the pedestal and the tubing was passed through the pedestal. (3) Using a piece of oiled paper as a circumferential form, the cutout in the stone was filled with epoxy cement. Care was taken to insure bond with the specimen pedestal. After the epoxy had set, the oiled paper form and the porous stone could be removed, leaving the epoxy addition securely bonded to the specimen pedestal and thus sealing the tubing as it passes out of the triaxial cell. Care was taken to keep each stone with its respective triaxial cell.

The complete base measuring assembly then consisted of (1) the porous probe and its brass cap, (2) the length of teflon tubing fitted into the hole in the brass cap, spiraling around the specimen and passing out of the cell via the base pedestal, and (3) the transducer chamber connected to the teflon tubing by a hypodermic needle.

D. Technique for Installation of Midplane System

This section describes the procedure for setting up a triaxial sample using the midplane pore pressure measuring system. This setup was accomplished in the following manner:

1. The porous probe, the base stone, transducer chamber and washer, two hypodermic needles and a hypodermic syringe, were placed in boiling water in a large vacuum dessicator. The dessicator was fitted with a lid, evacuated and kept evacuated for 24 hours. The water, of course, boiled vigorously until cool.

2. An additional quantity of deaired water was prepared and transferred to a large plastic tray about 6 inches deep. The base of the triaxial cell was placed in this tray and air bubbles flushed from the base drainage hole.

3. The hypodermic syringe was fitted with a needle below water in the dessicator and filled with deaired water. This syringe was used to flush thoroughly the length of teflon tubing attached to the triaxial cell base. This flushing was done beneath the surface of the water in the plastic tray.

4. The porous probe and base stone were transferred to the plastic tray containing the triaxial cell base in a beaker of deaired water. At no time were they removed from deaired water.

5. The two membranes, in a rolled condition, were attached by "O" rings to the pedestal and the now saturated porous base stone fitted into place.

6. The teflon tubing was pushed into the hole in the brass end cap of the porous probe.

7. The specimen was trimmed. A horizontal hole slightly smaller in diameter and length than the porous probe was formed in the specimen at mid-height. In some soils this may be sufficient, but in the Vicksburg clay specimens splitting of the specimen in tension occurred upon immersion in water. The hole could be formed in the sample dry, but if a drop of water were placed in the hole, the sample would split.

8. To avoid this splitting, the sample was carefully and squarely cut into two pieces with a fine wire saw. This cut split the hole. Now the sample existed as two cylinders, the top of one and the bottom of the other having $\frac{1}{2}$ of the hole.

9. The bottom half of the specimen was placed on the pedestal of the triaxial cell. The water in the tray was deep enough to cover this half entirely. All adhering air bubbles were removed by flushing with water using the hypodermic syringe.

10. The teflon tubing was spiralled around the triaxial specimen and the probe fitted into the half-hole in the bottom portion of the specimen.

11. The top half of the specimen was fitted into place taking care to avoid any entrapment of air bubbles.

12. A rubber dam cut from a membrane and $\frac{1}{2}$ inch wide, was placed over the specimen and over the cut as shown in Figure A-1.

13. The filter strips were positioned, the top cap affixed on the specimen and the first membrane rolled up. The water level was then lowered to the level of the pedestal. Care was taken to avoid having either the loose end of the teflon tubing or the base drainage connections come above the water surface.

14. A layer of silicone grease was applied to the inner membrane, the outer membrane was rolled up, and both membranes fastened securely with "O" rings to the top cap.

15. The triaxial chamber was secured in place and fitted with deaired water. A burette to measure drainage from the sample was attached to the base drainage system and a chamber pressure of about one atmosphere was applied. The loose end of the teflon tubing was now clamped off with a pinch clamp and the triaxial cell removed from the water. The chamber pressure was raised to the desired level and consolidation proceeded. Note: If the teflon tubing is sealed prior to application of a chamber pressure, or left sealed as an over-

consolidated sample rebounds, cavitation of water in the tube will occur introducing air bubbles into the system. On the other hand, if the tubing is not sealed during consolidation, it may clog as some soil particles may wash out through the stone.

The the sample is to undergo rebound, the free end of the teflon tubing must be immersed in deaired water and opened prior to reduction of the chamber pressure.

After consolidation and immediately prior to testing, the transducer chamber was attached. This was accomplished in the following manner:

1. The transducer, washer, chamber and hypodermic needle were assembled beneath the surface of deaired water in the dessicator.

2. The triaxial cell was again placed in a plastic tray of deaired water.

3. The pinch clamp was removed from the teflon tubing and the free end clamped in the split sleeve with a small bit protruding. This protruding bit, damaged by the clamp, was cut off flush with the sleeve using a new razor blade.

4. The transducer chamber assembly was removed from the dessicator, keeping the tip of the needle immersed in a small beaker of deaired water. The transducer was connected to the readout devices and activated. After a warm-up period, the zero pressure reading was noted.

5. The hypodermic needle was inserted into the teflon tubing. The pressure developed by this operation commonly amounted to 1 to 3 lb./in.^{2} and decayed in a matter of minutes.

6. The base drainage was either sealed or a base measuring device attached, as will be described in a following section.

7. A chamber pressure of 10 lb./in.^{2} was applied and the response of the system (or systems) was noted. If this response was 100% in less than 60 seconds, as was usually the case, the 10 lb./in.^{2}

pressure was removed and testing proceeded. If the response was inadequate, this 10 lb./in.^{2} increase in chamber pressure was permitted to remain as a back pressure for 24 hours and the response to another 10 lb./in.^{2} increment noted. In a few instances a final back pressure of 30 lb./in.^{2} resulted before the response criterion was met.

E. Base Measuring Systems

The base measuring systems consisted of chambers holding the "Dynisco" transducer and fitted with adapters for connection either to the Clockhouse cells or the NGI cells. In addition, a bleeder valve arrangement permitted relief of any pressure developed during connection. These devices are illustrated in Figure A-5.

The block, washer, and transducer were saturated in the same manner as the midplane system (i.e., boiling in the evacuated dessicator). They were assembled under water and transferred under water to the plastic tray containing the triaxial chamber. Again electrical connection was made before installation and the zero reading noted.

The bleeder valve arrangement consisted of a small ball forced to seat in a conical seat by a thumbscrew. The threads were quite loose and thus drainage past the threads could take place. The transducer-block assembly was connected to the base drainage system with this bleeder valve open. Tightening was accomplished slowly so drainage past the bleeder valve would prevent the development of any pressure. The bleeder valve was then closed tightly. The pressure developed during this operation was monitored and amounted to on the order of 2 lb./in.^{2} which decayed in a minute or two.

The response of this system was checked as was the midplane system. Little trouble developed in the utilization of this system.

F. Response of Systems

Following consolidation of each specimen and prior to the performance of the actual triaxial test, the response of the measuring system (or systems) was determined. This was accomplished by applying, as rapidly as possible, an increment of chamber pressure (usually 10 lb./in.^{2}) and allowing this increment of chamber pressure to remain until complete response was attained. Figure A-7 presents response curves of the needle and base measuring systems from tests NC6S and OC3F which are typical of those of every test.

In no instance was the response less than 100%. In OC2F and OC7S the initial response time was slightly greater than 60 seconds, so an additional back pressure was applied and allowed to remain for a period of time. The response time following this back pressuring was less than 60 seconds.

In addition, the response of the systems to an increment of deviator stress was checked by assembling a dummy sample, consolidating it in the usual manner and connecting the pore pressure measuring apparatus following consolidation and adding dead weight loads to the piston of the triaxial cell.

Figure A-8 shows the results of such a test. In the upper figure the results of the application of an increment of chamber pressure ($\Delta\sigma_3$) are shown. In the lower figure is shown the response to an addition of an increment of deviator stress $[\Delta(\sigma_1 - \sigma_3)]$. The response of the base system to an increment of chamber pressure appeared to be more rapid than to an increment of deviator stress. However, the response of the needle system to an increment of deviator stress was about twice as fast as the response to an increment of chamber pressure.

As a result of this experiment it can be concluded that the pre-test criterion of full response to a chamber pressure increment in

60 seconds or less seems quite reasonable as an insurance of rapid system response.

G. Conclusions

As a result of this research, it has been shown that measurement of pore pressures with electronic pressure transducers is not only feasible, but is superior in ease of measurement, rapidity of measurement, and reliability of measurement to the conventional manual rule balance system. This can be said with confidence since the particular clay used in this research represents an extreme to the range of clays to be tested.

In addition, an electronic measuring system utilizing a sensitive millivoltmeter, such as the Daystrom-Weston Model No. 1477 instead of the relatively expensive X-Y plotter as a readout device would be economically competitive with the currently marketed manual systems.

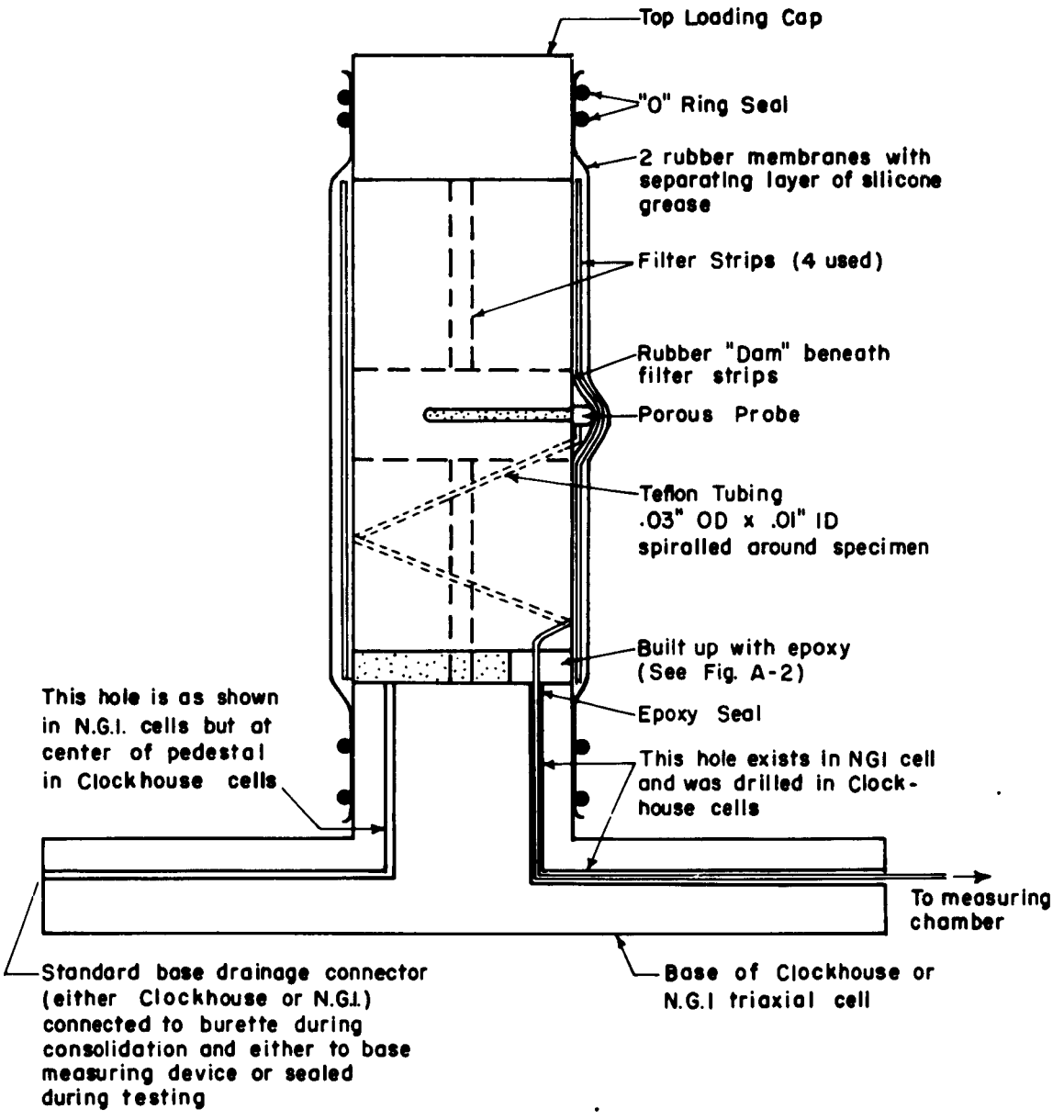

FIGURE A-1 FINAL METHOD OF INSTALLATION - MIDHEIGHT PORE PRESSURE MEASURING SYSTEM

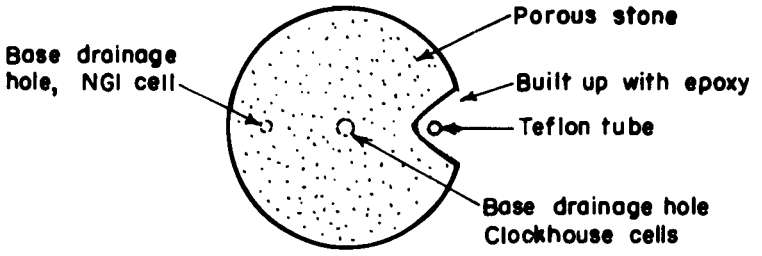

FIGURE A-2 TOP VIEW OF TRIAXIAL CELL PEDESTAL PRIOR TO PLACEMENT OF SPECIMEN

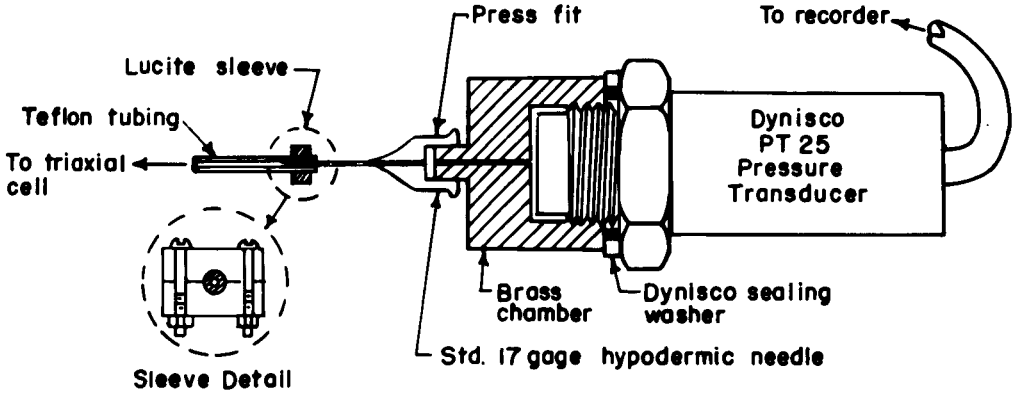

FIGURE A-3 FINAL ARRANGEMENT - CONNECTING CHAMBER - TEFLON TUBING TO PRESSURE TRANSDUCER

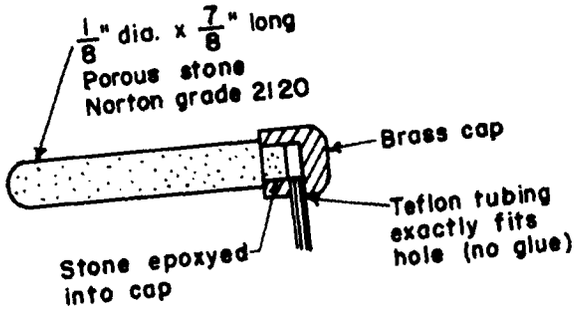

FIGURE A-4 DETAIL OF POROUS PROBE

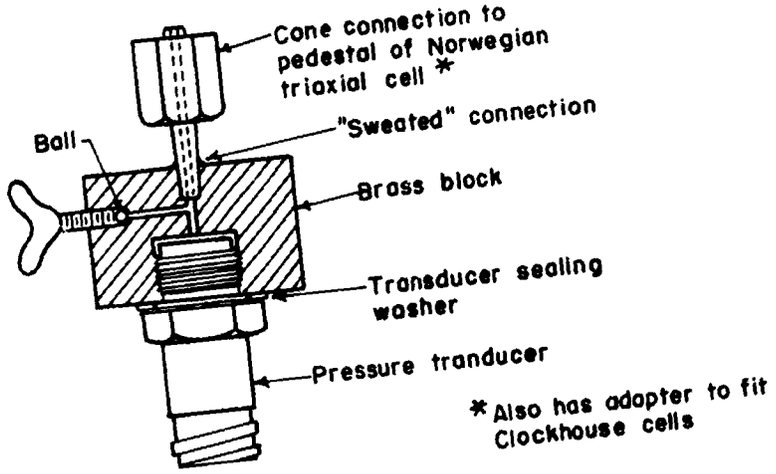

FIGURE A-5 BASE PRESSURE DEVICE

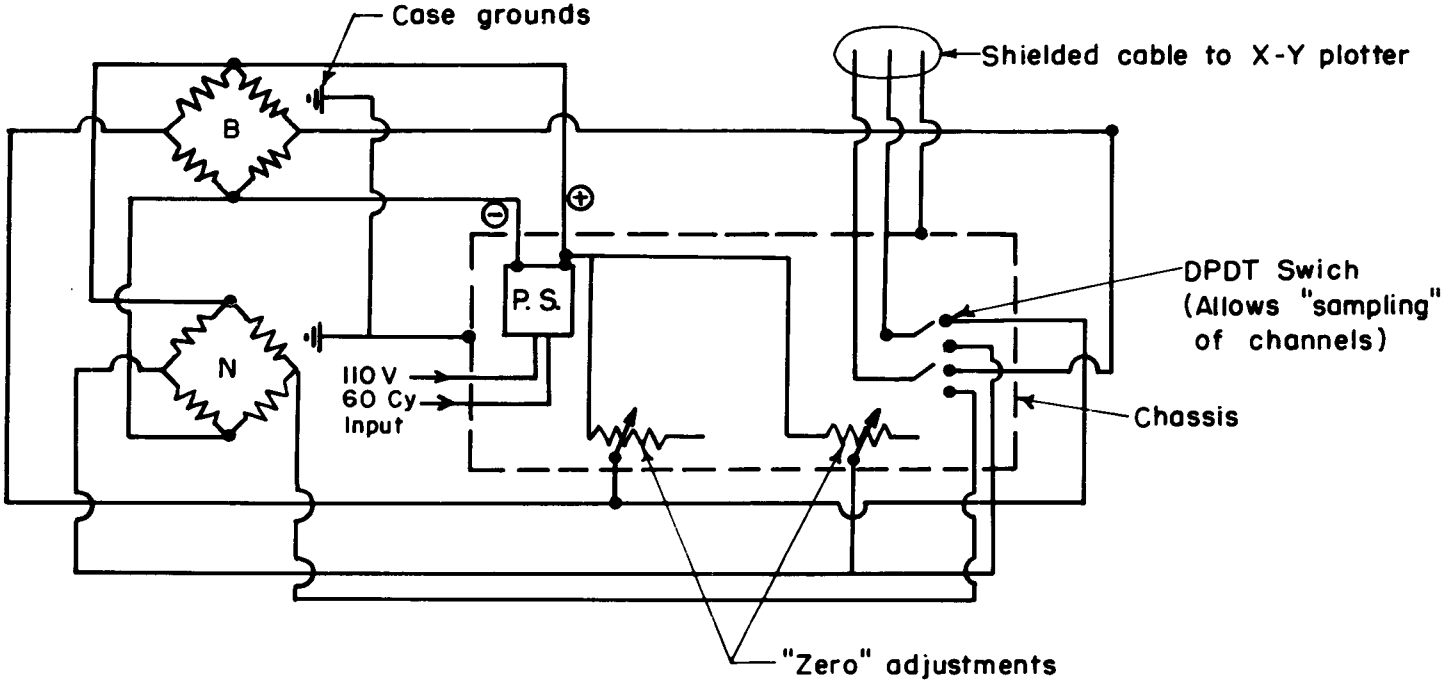

Notes:

B = Base transducer
N = Midplane transducer
4 Wire shielded cable from transducers to chassis
P.S. = Even volt 150 ma., 6V., DC power supply
Plotter and transducer cases grounded to chassis

FIGURE A-6 FINAL INSTRUMENTATION LAYOUT

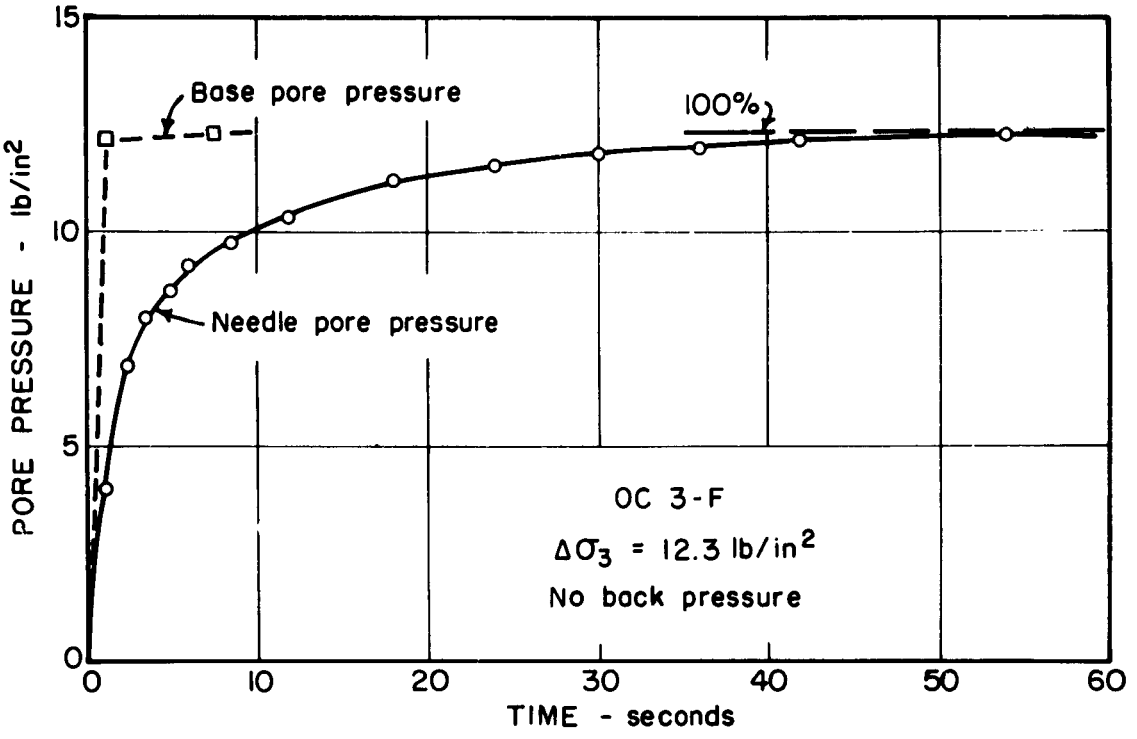

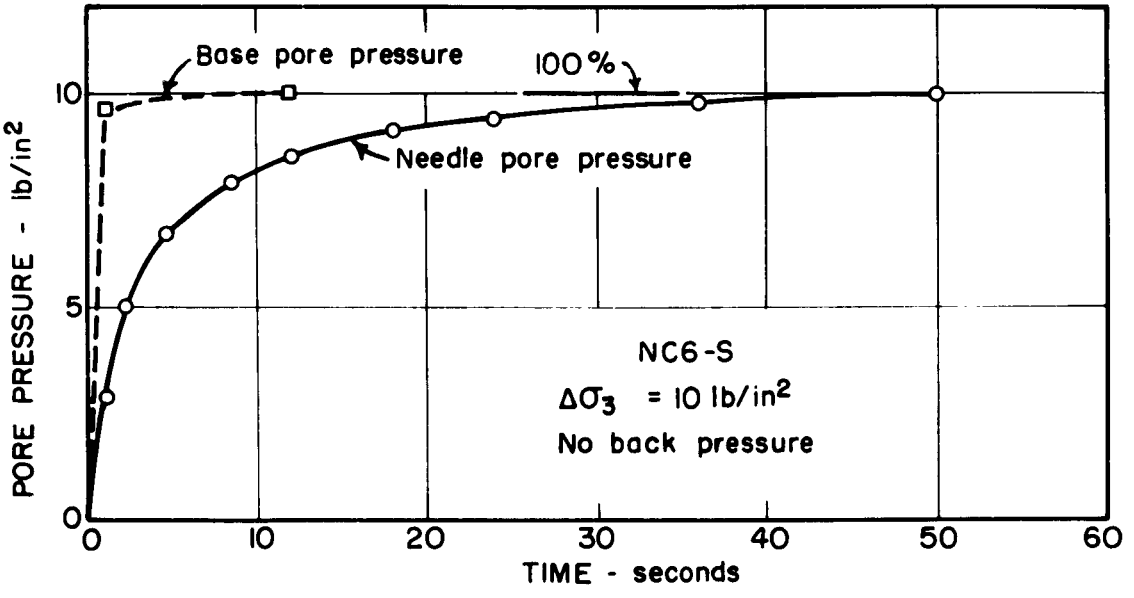

FIGURE A-7 TYPICAL RESPONSE - PORE PRESSURE SYSTEMS

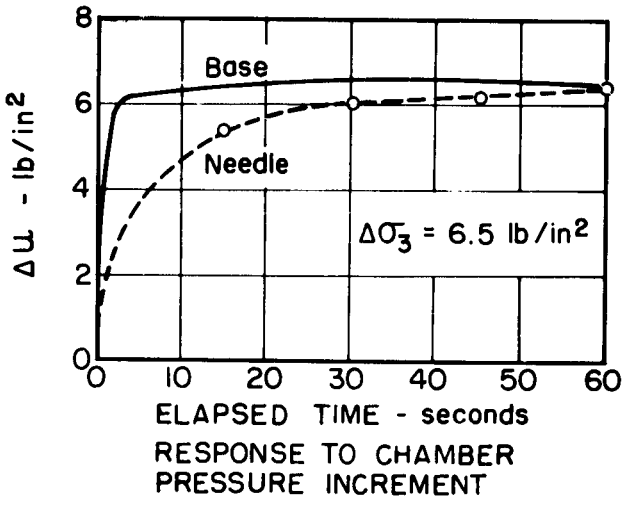

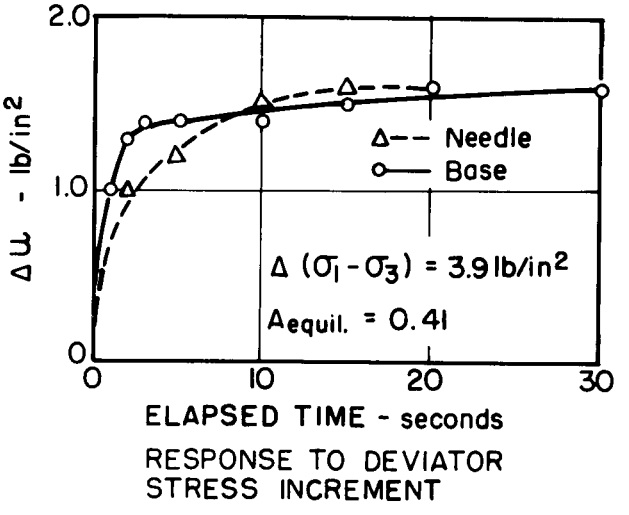

Also 30 min.

$(\sigma_1 - \sigma_3)_{before} = 0$

$(\sigma_1 - \sigma_3)_{after} = 3.9$ lb/in²

$u_o = 0$

$u_c = 1.6$ lb/in²

FIGURE A-8 RESPONSE TO DEVIATOR STRESS INCREMENT

Appendix B

PLOTS OF LABORATORY DATA

LIST OF FIGURES

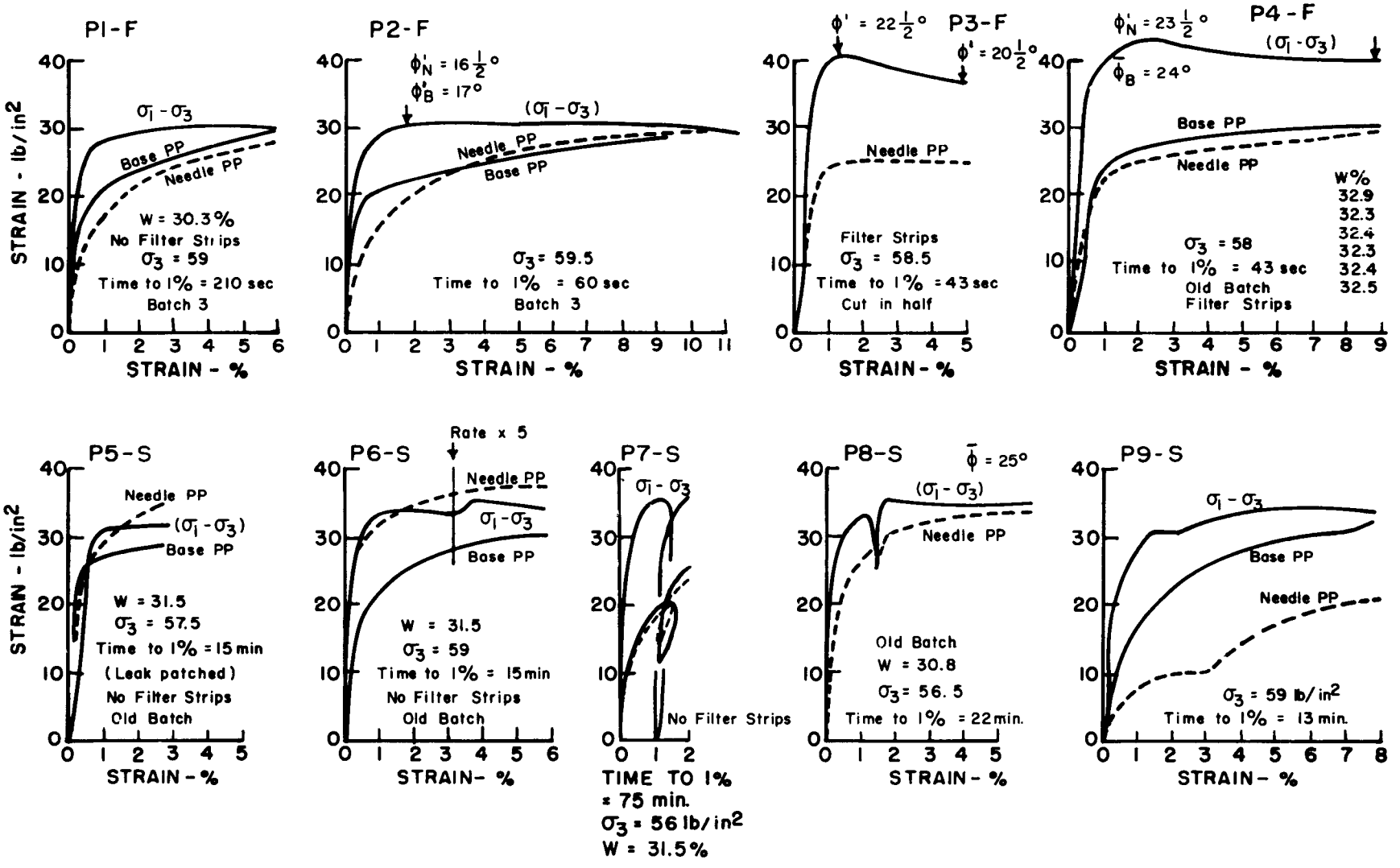

FIGURE B-1 RESULTS OF PRELIMINARY SERIES

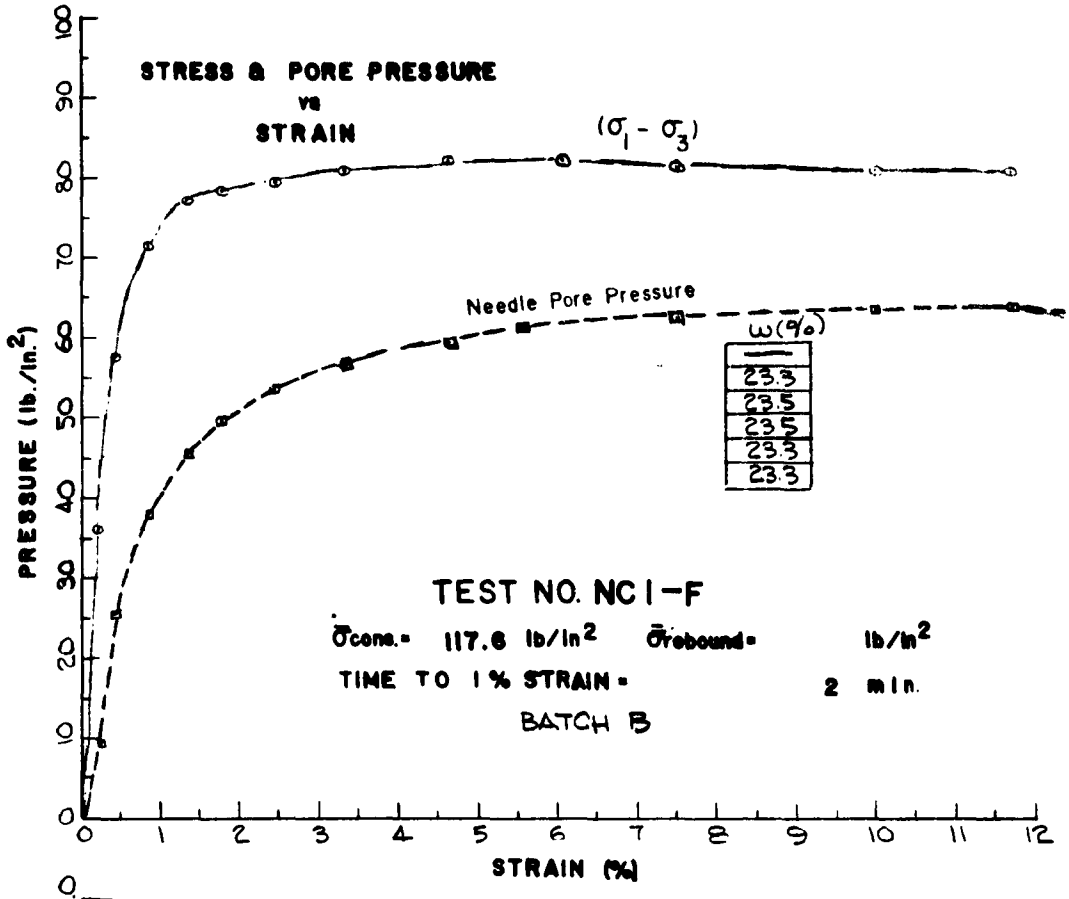

ω(%)
23.3
23.5
23.5
23.3
23.3

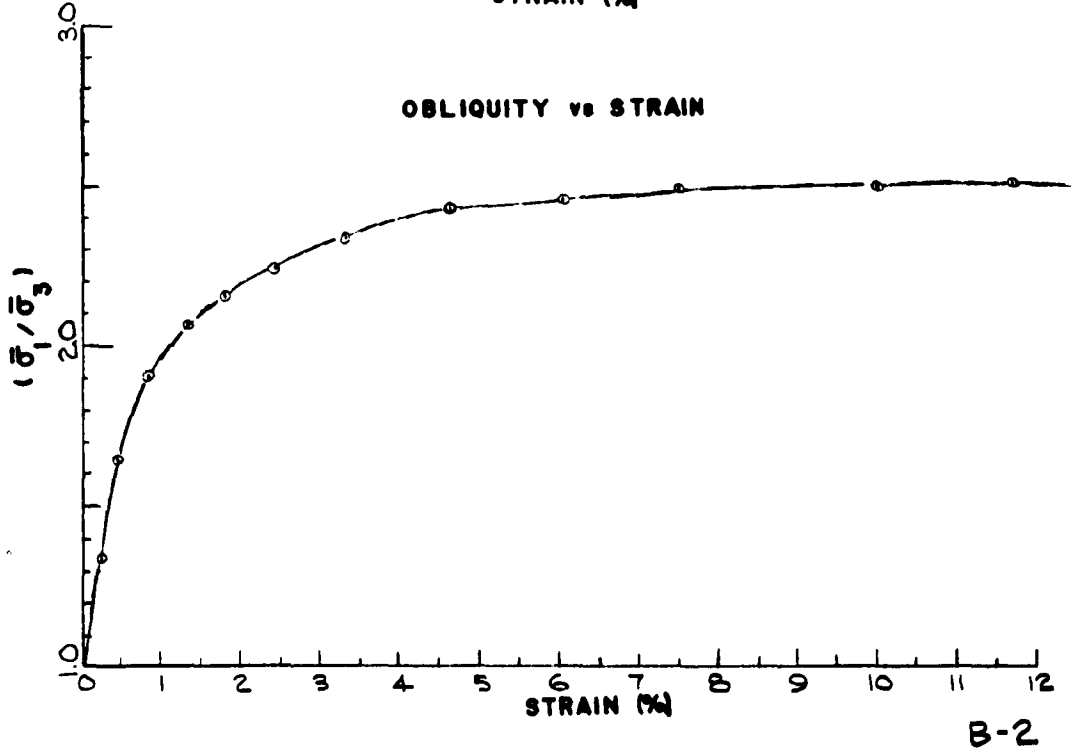

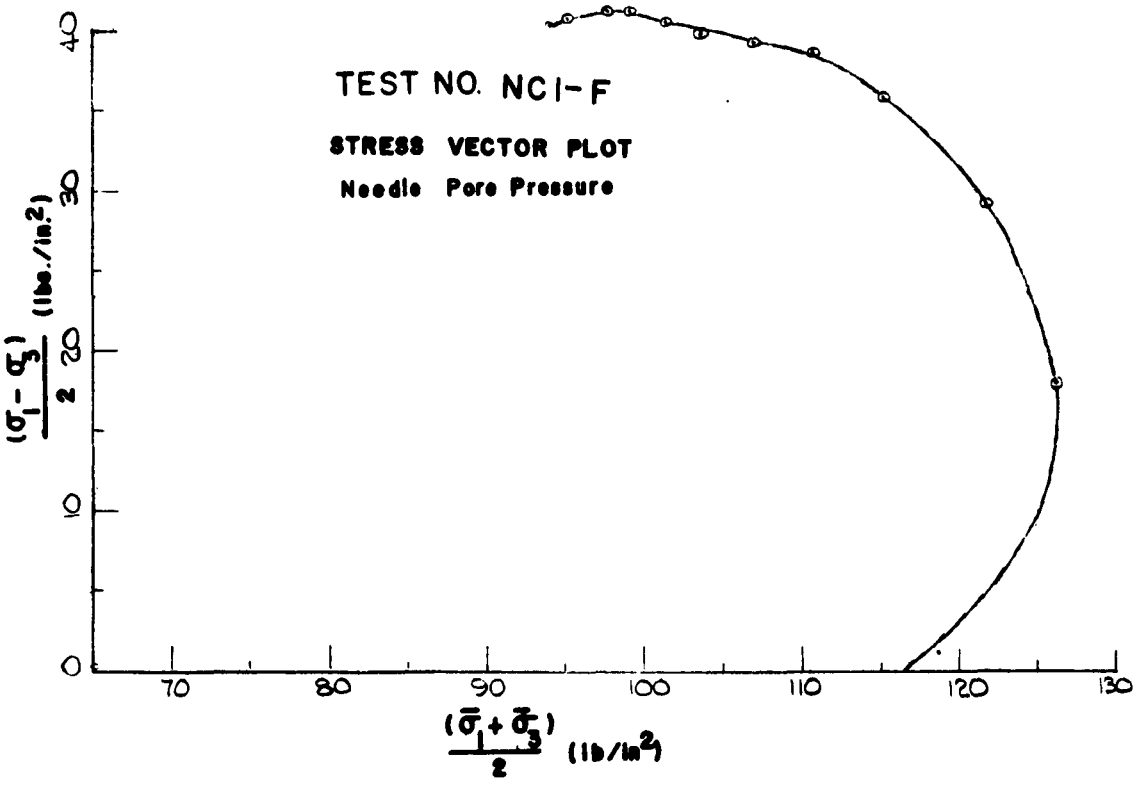
TEST NO. NC1-F
STRESS VECTOR PLOT
Needle Pore Pressure
$\frac{(\sigma_1 - \sigma_3)}{2}$ (lbs./in.^{2})
$\frac{(\bar{\sigma}_1 + \bar{\sigma}_3)}{2}$ (lb/in^2)
0
10
20
30
40
70
80
90
100
110
120
130

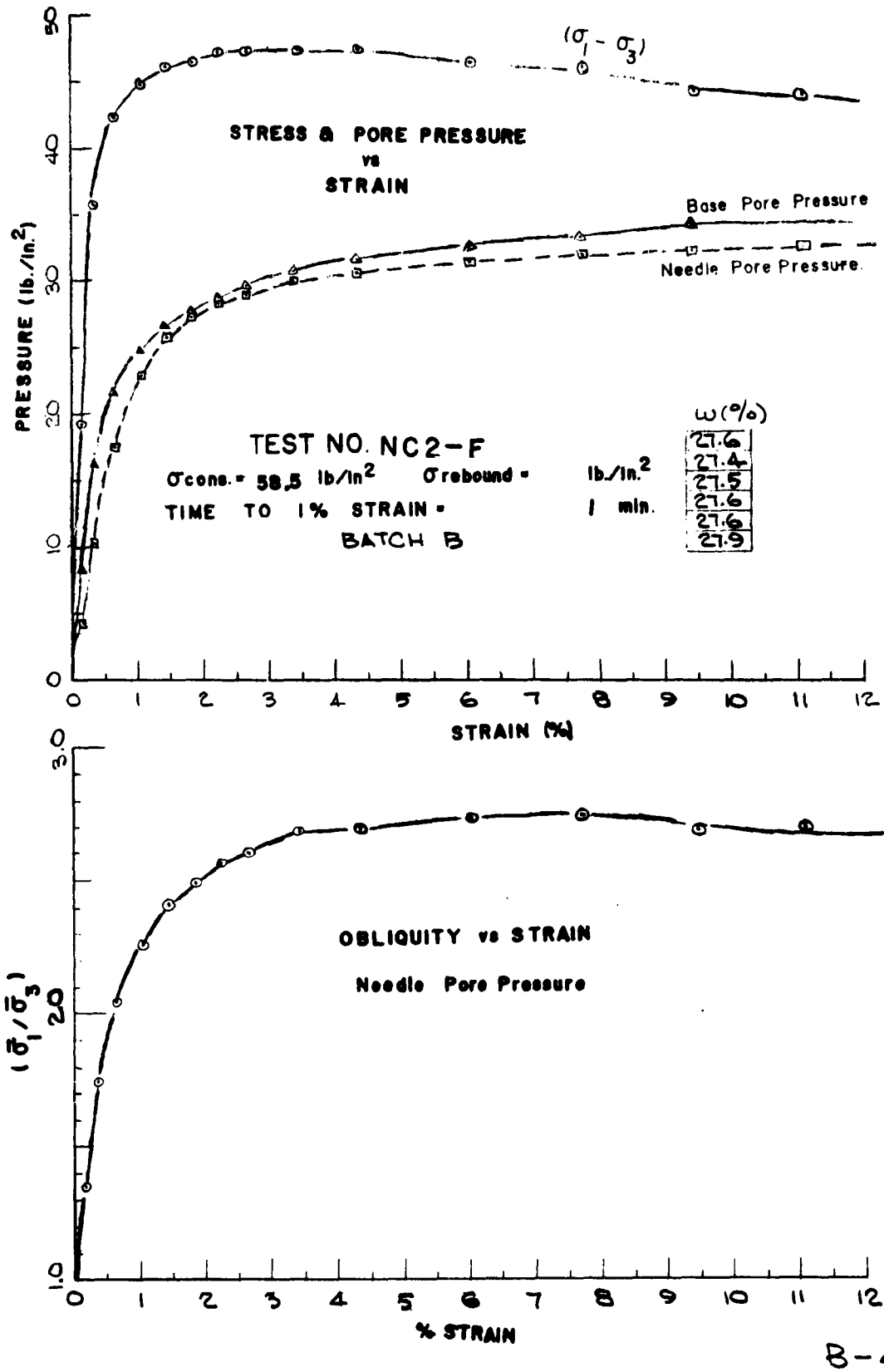
$(\sigma_1 - \sigma_3)$
STRESS & PORE PRESSURE
vs
STRAIN
Base Pore Pressure
Needle Pore Pressure
PRESSURE (lb./in.^{2})
TEST NO. NC2-F
σcons. = 58.5 lb/in^2 σrebound = lb./in.^{2}
TIME TO 1% STRAIN = 1 min.
BATCH B
ω(%)
27.6
27.4
27.5
27.6
27.6
27.9
STRAIN (%)
OBLIQUITY vs STRAIN
Needle Pore Pressure
$(\bar{\sigma}_1/\bar{\sigma}_3)$
% STRAIN

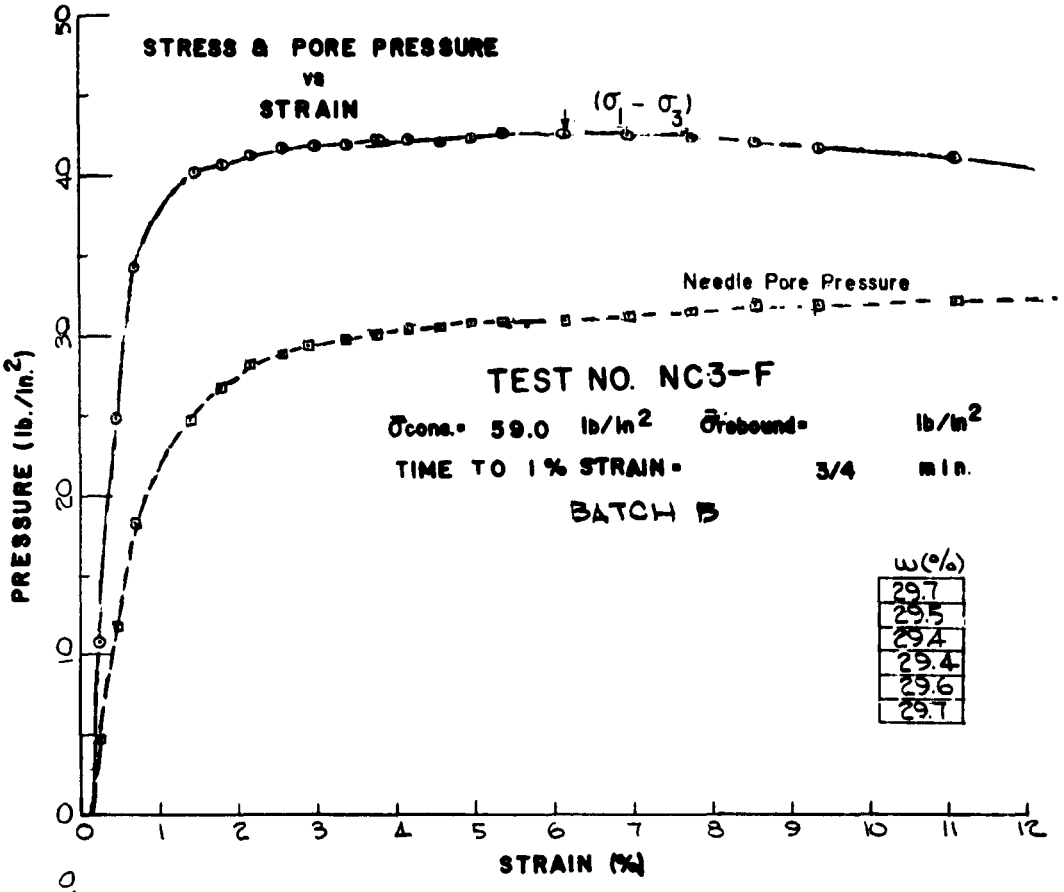
STRESS & PORE PRESSURE
vs
STRAIN
$(\sigma_1 - \sigma_3)$
Needle Pore Pressure
TEST NO. NC3-F
$\bar{\sigma}_{cons.}$ = 59.0 lb/in^2 $\bar{\sigma}_{rebound}$ = lb/in^2
TIME TO 1% STRAIN = 3/4 min.
BATCH B
ω(%)
29.7
29.5
29.4
29.4
29.6
29.7
PRESSURE (lb./in.^{2})
STRAIN (%)

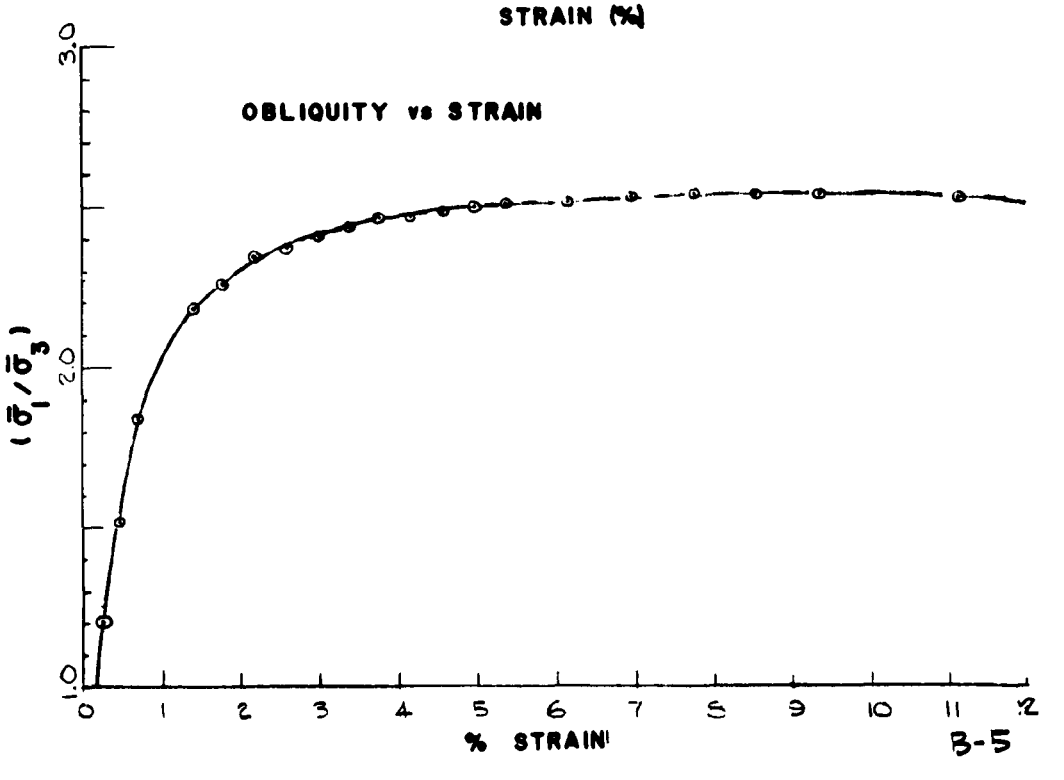
OBLIQUITY vs STRAIN
$(\bar{\sigma}_1/\bar{\sigma}_3)$
% STRAIN

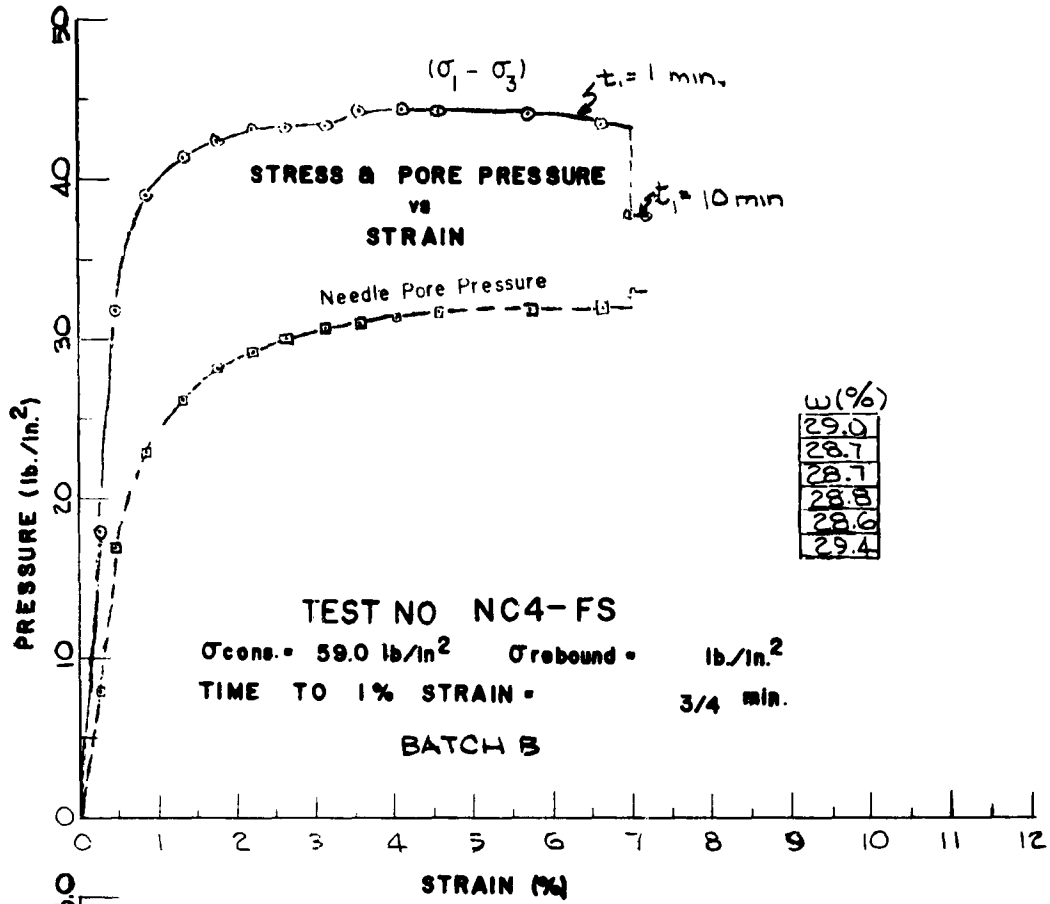
$(\sigma_1 - \sigma_3)$
t_1 = 1 min.
t_1 = 10 min
STRESS & PORE PRESSURE
vs
STRAIN
Needle Pore Pressure
PRESSURE (lb./in.^{2})
STRAIN (%)
ω(%)
29.0
28.7
28.7
28.8
28.6
29.4
TEST NO NC4-FS
$\sigma_{cons.}$ = 59.0 lb/in^2 $\sigma_{rebound}$ = lb./in.^{2}
TIME TO 1% STRAIN = 3/4 min.
BATCH B

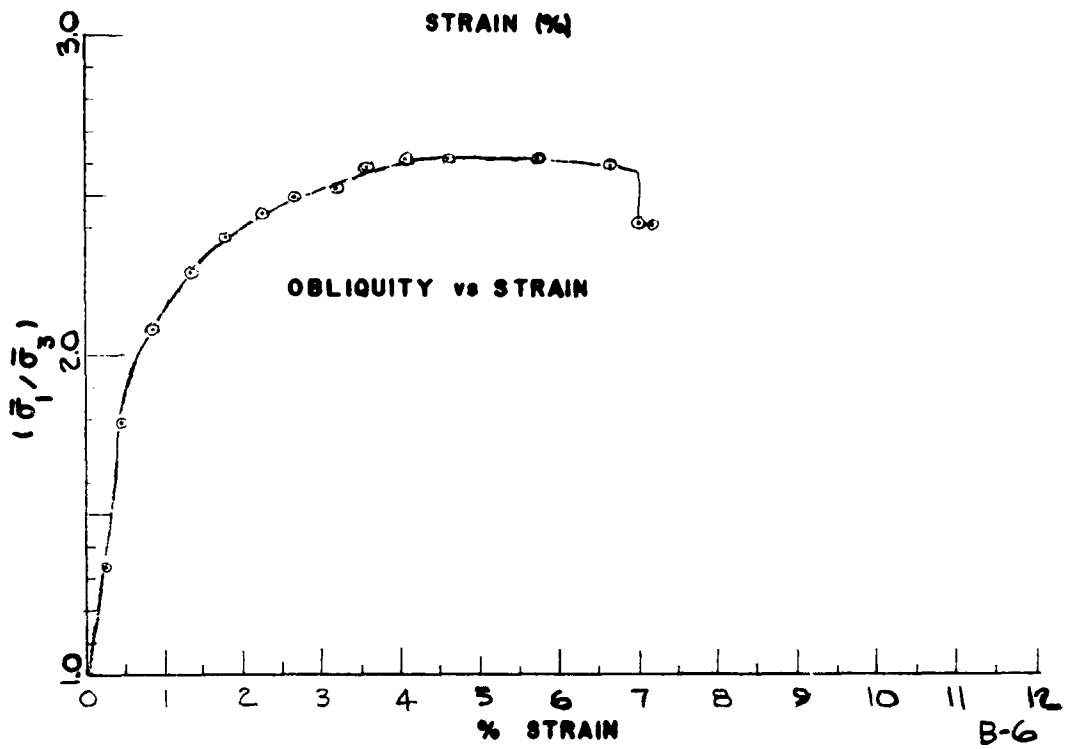
OBLIQUITY vs STRAIN
$(\bar{\sigma}_1 / \bar{\sigma}_3)$
% STRAIN

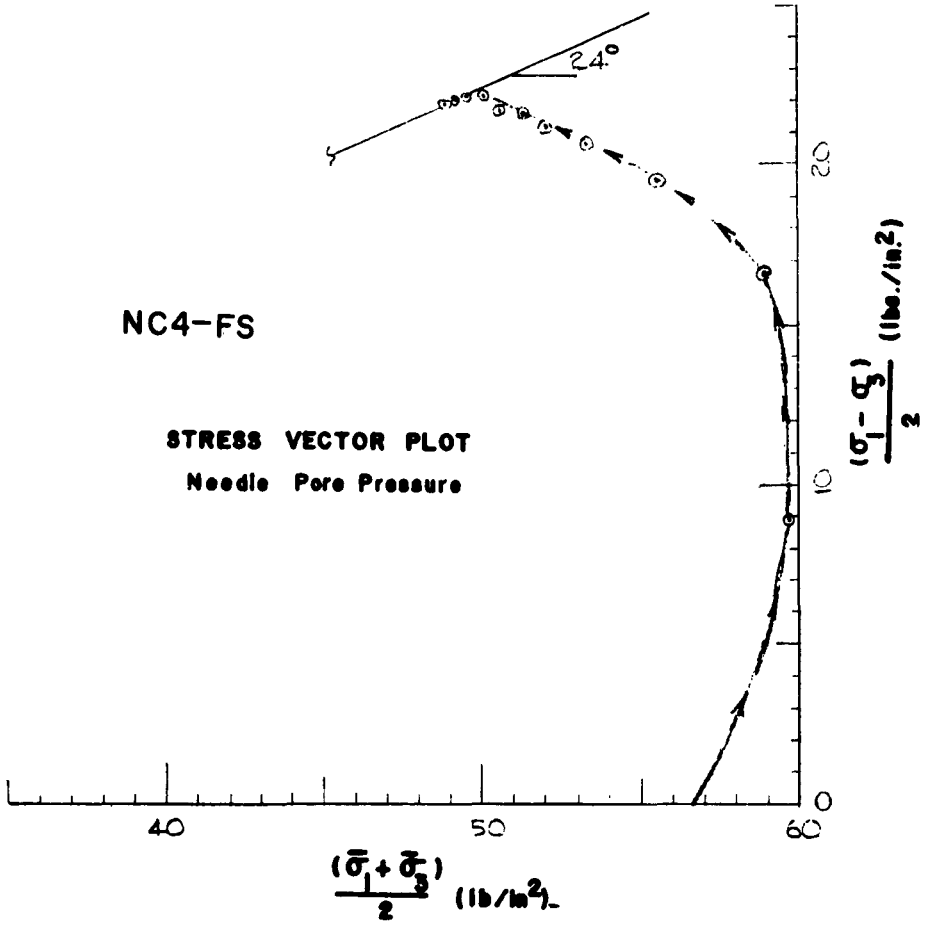
NC4-FS
STRESS VECTOR PLOT
Needle Pore Pressure
24°
0
10
20
40
50
60
$\frac{(\sigma_1 - \sigma_3)}{2}$ (lbs./in.^{2})
$\frac{(\bar{\sigma}_1 + \bar{\sigma}_3)}{2}$ (lb/in^2)

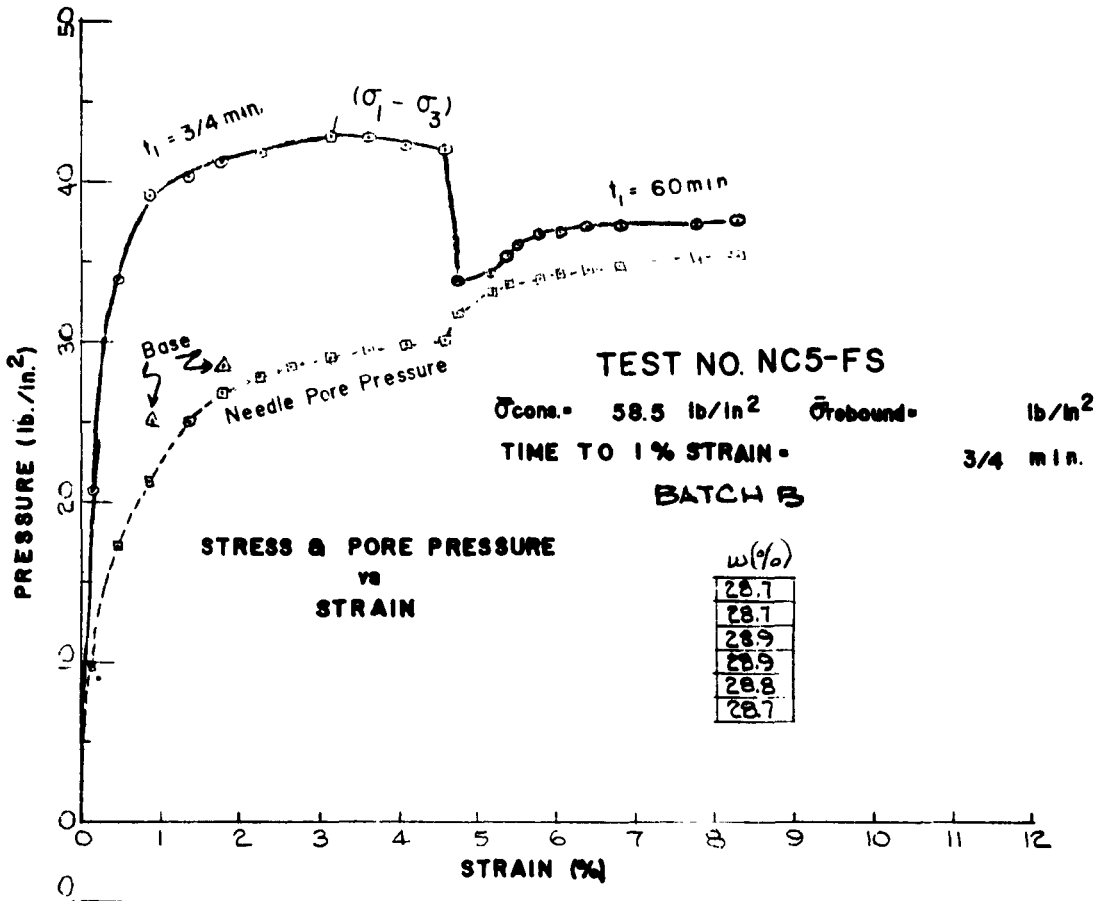
t_1 = 3/4 min.
$(\sigma_1 - \sigma_3)$
t_1 = 60min
Base
Needle Pore Pressure
PRESSURE (lb./in.^{2})
STRAIN (%)
TEST NO. NC5-FS
$\bar{\sigma}_{cons.}$ = 58.5 lb/in^2 $\bar{\sigma}_{rebound}$ = lb/in^2
TIME TO 1% STRAIN = 3/4 min.
BATCH B
STRESS & PORE PRESSURE
vs
STRAIN
w(%)
28.7
28.7
28.9
28.9
28.8
28.7

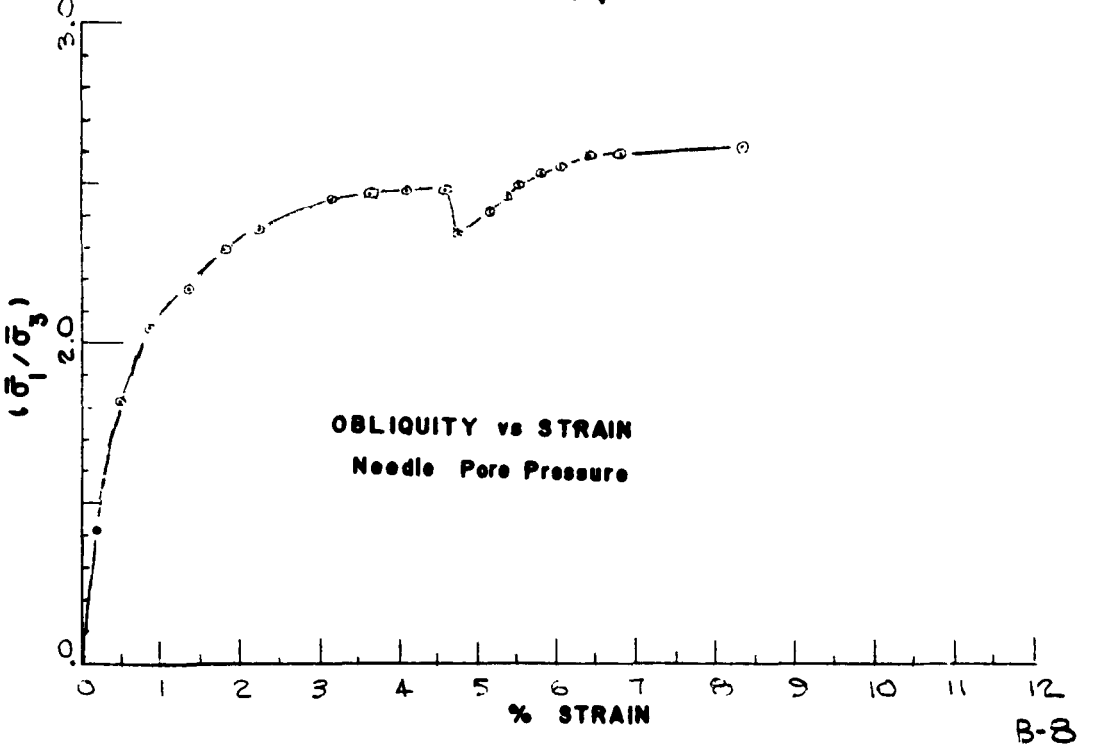
$(\bar{\sigma}_1/\bar{\sigma}_3)$
% STRAIN
OBLIQUITY vs STRAIN
Needle Pore Pressure

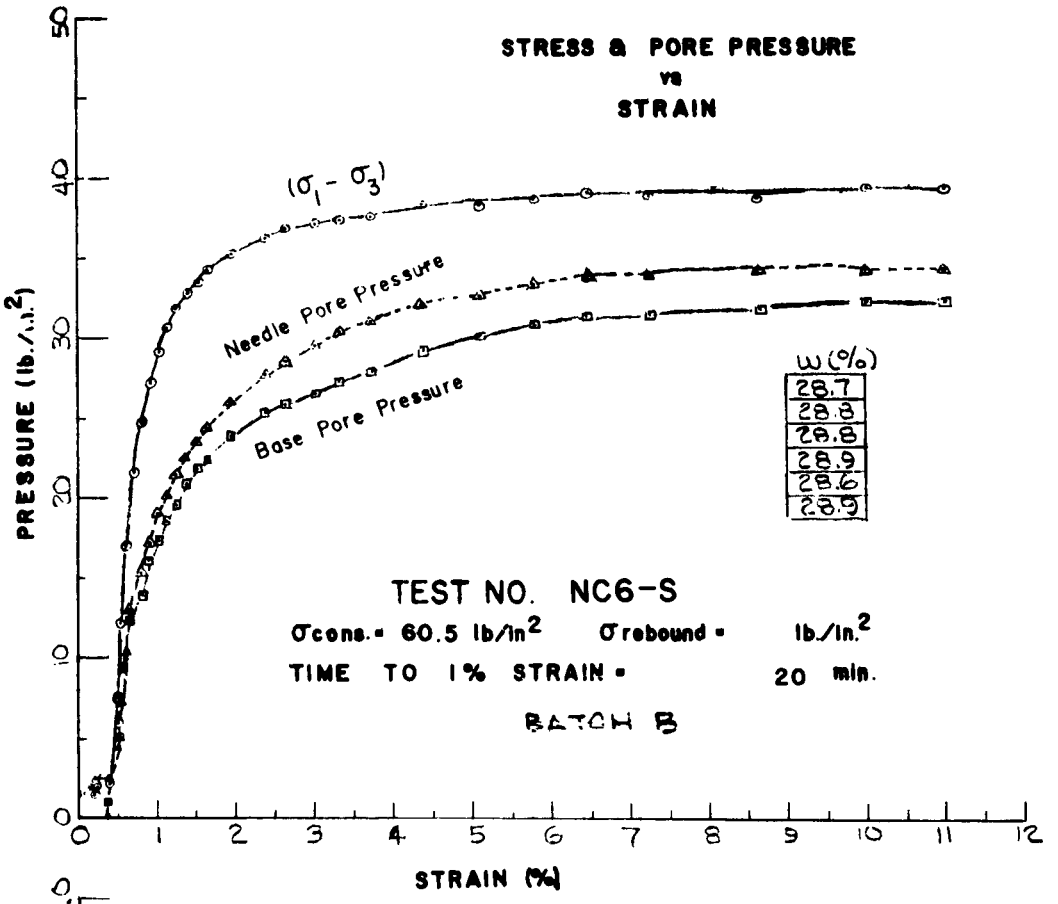
STRESS & PORE PRESSURE
vs
STRAIN
$(\sigma_1 - \sigma_3)$
Needle Pore Pressure
Base Pore Pressure
PRESSURE (lb./in.^{2})
w (%)
28.7
28.8
28.8
28.9
28.6
28.9
TEST NO. NC6-S
σcons. = 60.5 lb/in^2 σrebound = lb./in.^{2}
TIME TO 1% STRAIN = 20 min.
BATCH B
STRAIN (%)

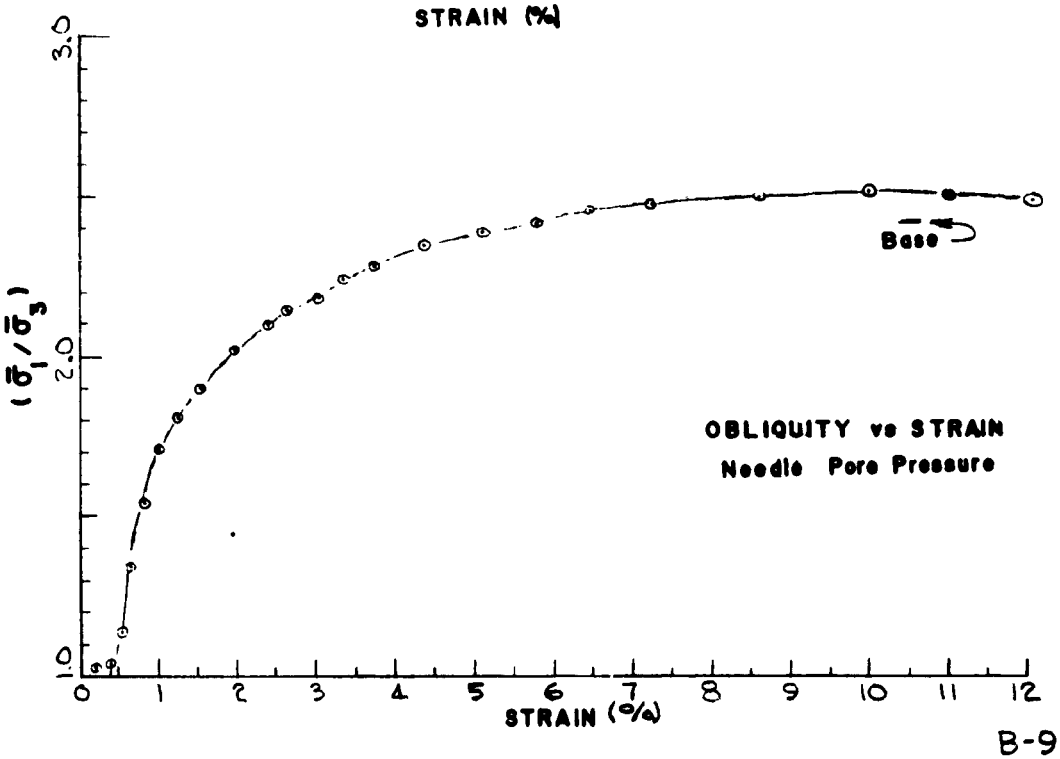
$(\bar{\sigma}_1 / \bar{\sigma}_3)$
Base
OBLIQUITY vs STRAIN
Needle Pore Pressure
STRAIN (%)

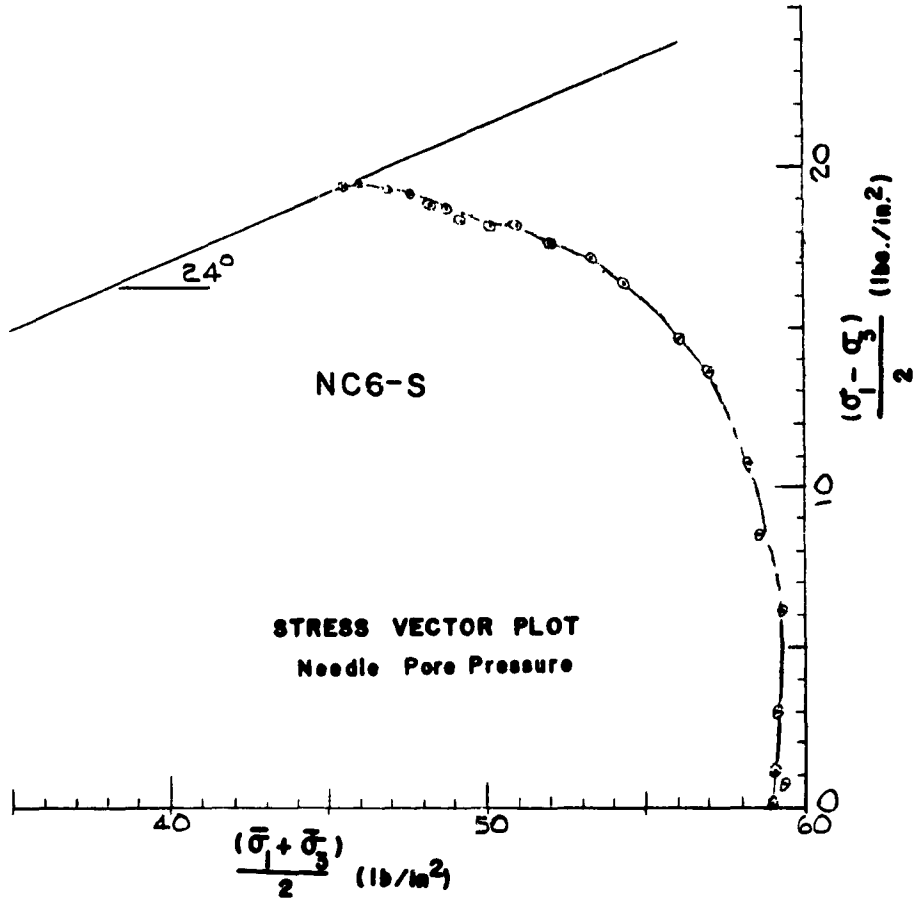
24°
NC6-S
STRESS VECTOR PLOT
Needle Pore Pressure
40
50
60
0
10
20
$\frac{(\bar{\sigma}_1 + \bar{\sigma}_3)}{2}$ (lb/in.^{2})
$\frac{(\sigma_1 - \sigma_3)}{2}$ (lbs./in.^{2})

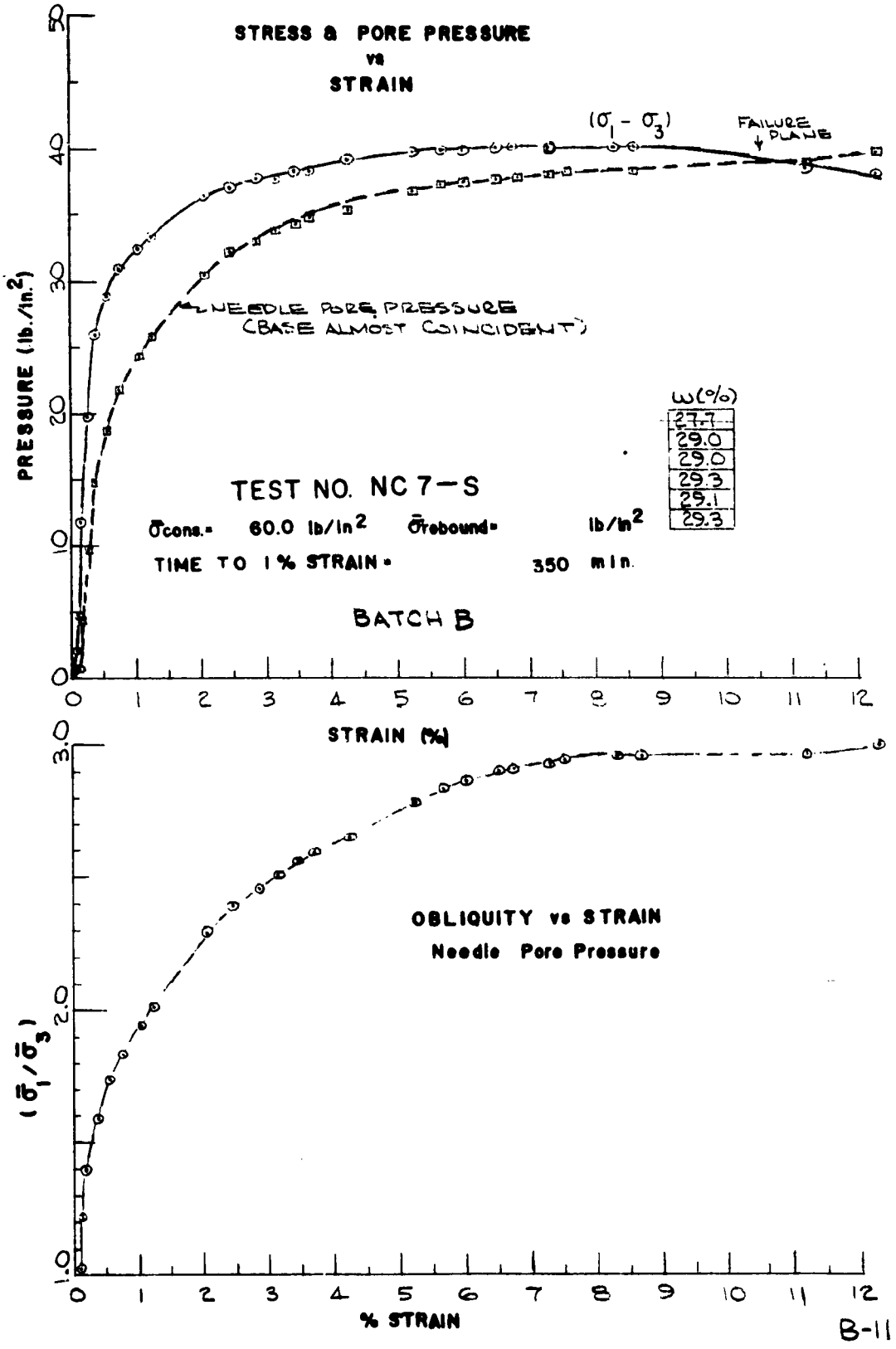
STRESS & PORE PRESSURE
vs
STRAIN
$(\sigma_1 - \sigma_3)$
FAILURE PLANE
NEEDLE PORE PRESSURE
(BASE ALMOST COINCIDENT)
PRESSURE (lb./in.^{2})
ω(%)
27.7
29.0
29.0
29.3
29.1
29.3
TEST NO. NC 7-S
$\bar{\sigma}_{cons.}$ = 60.0 lb/in^2 $\bar{\sigma}_{rebound}$ = lb/in^2
TIME TO 1% STRAIN = 350 min.
BATCH B
STRAIN (%)
OBLIQUITY vs STRAIN
Needle Pore Pressure
$(\bar{\sigma}_1/\bar{\sigma}_3)$
% STRAIN

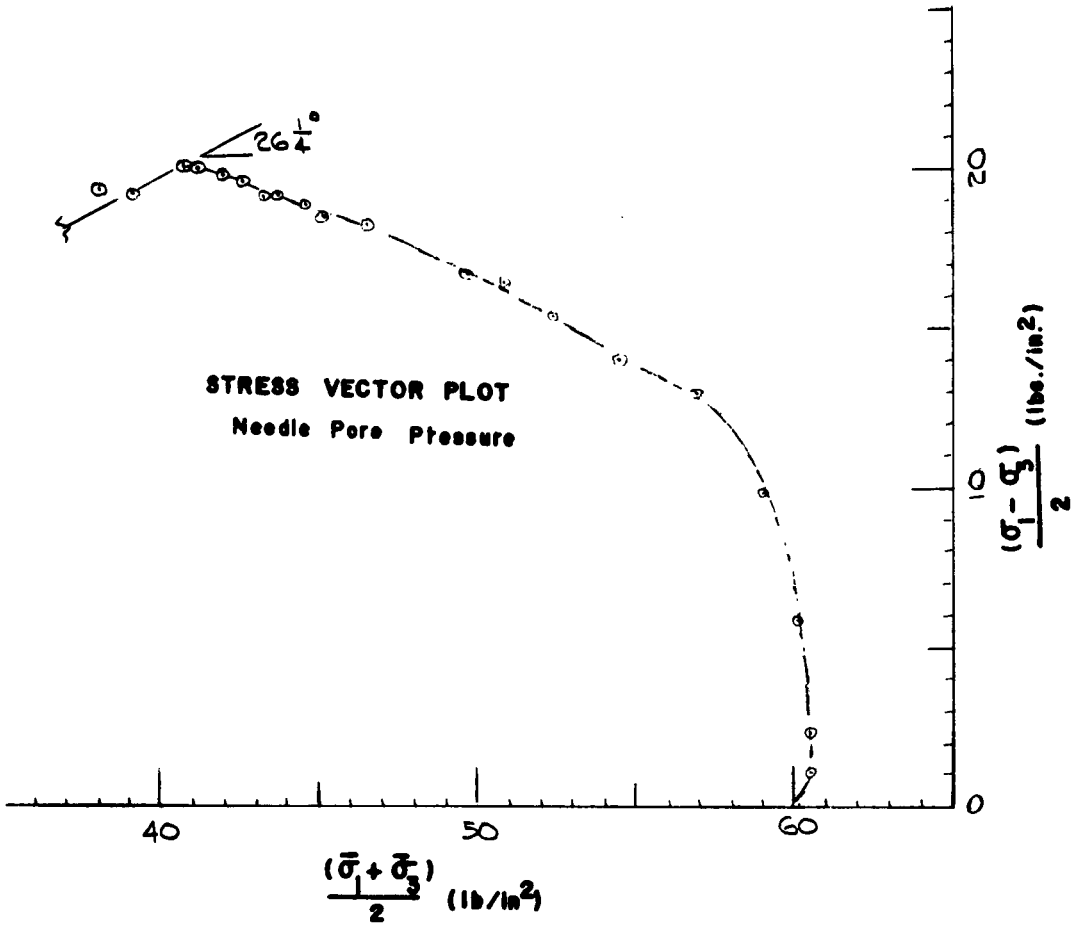
STRESS VECTOR PLOT
Needle Pore Pressure
26 1/4°
20
10
0
40
50
60
$\frac{(\sigma_1 - \sigma_3)}{2}$ (lbs./in.²)
$\frac{(\bar{\sigma}_1 + \bar{\sigma}_3)}{2}$ (lb/in²)

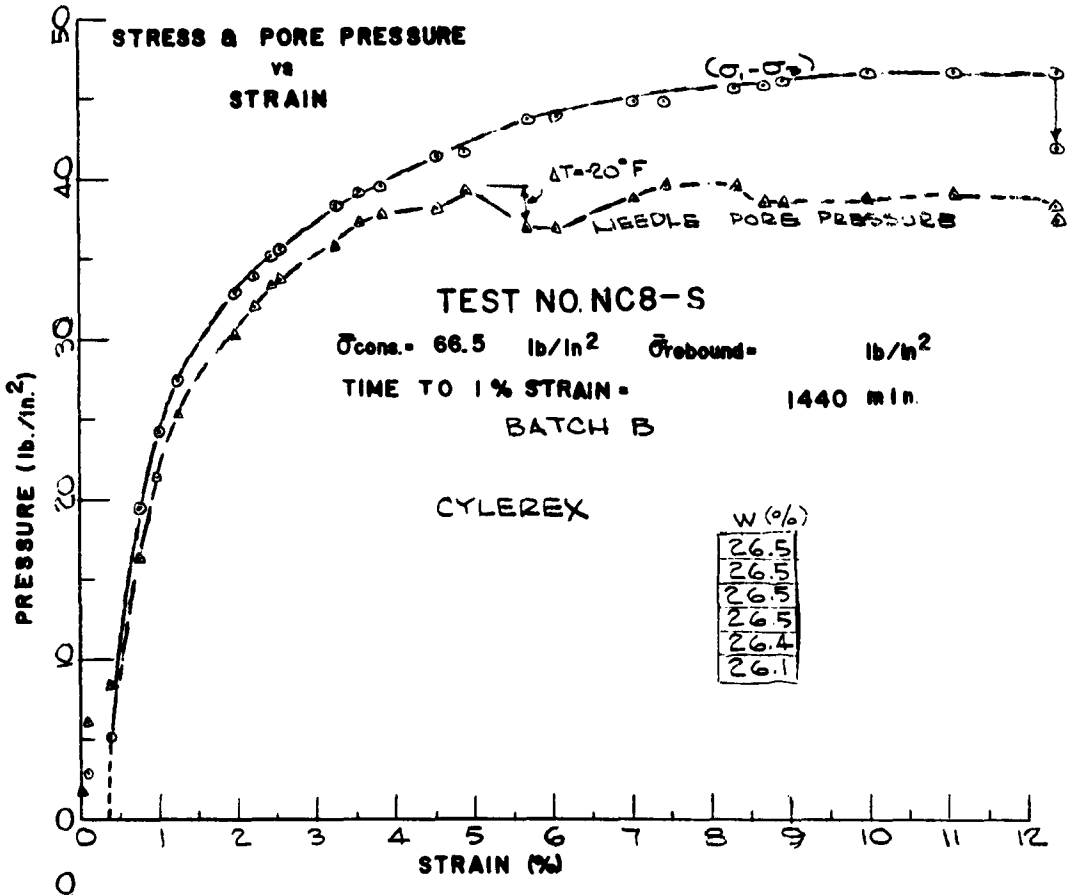
STRESS & PORE PRESSURE
vs
STRAIN
$(\sigma_1-\sigma_3)$
ΔT=20°F
NEEDLE PORE PRESSURE
TEST NO. NC8-S
$\bar{\sigma}_{cons.}$ = 66.5 lb/in²
$\bar{\sigma}_{rebound}$ = lb/in²
TIME TO 1% STRAIN = 1440 min.
BATCH B
CYLEREX
W (%)
26.5
26.5
26.5
26.5
26.4
26.1
PRESSURE (lb./in.²)
STRAIN (%)

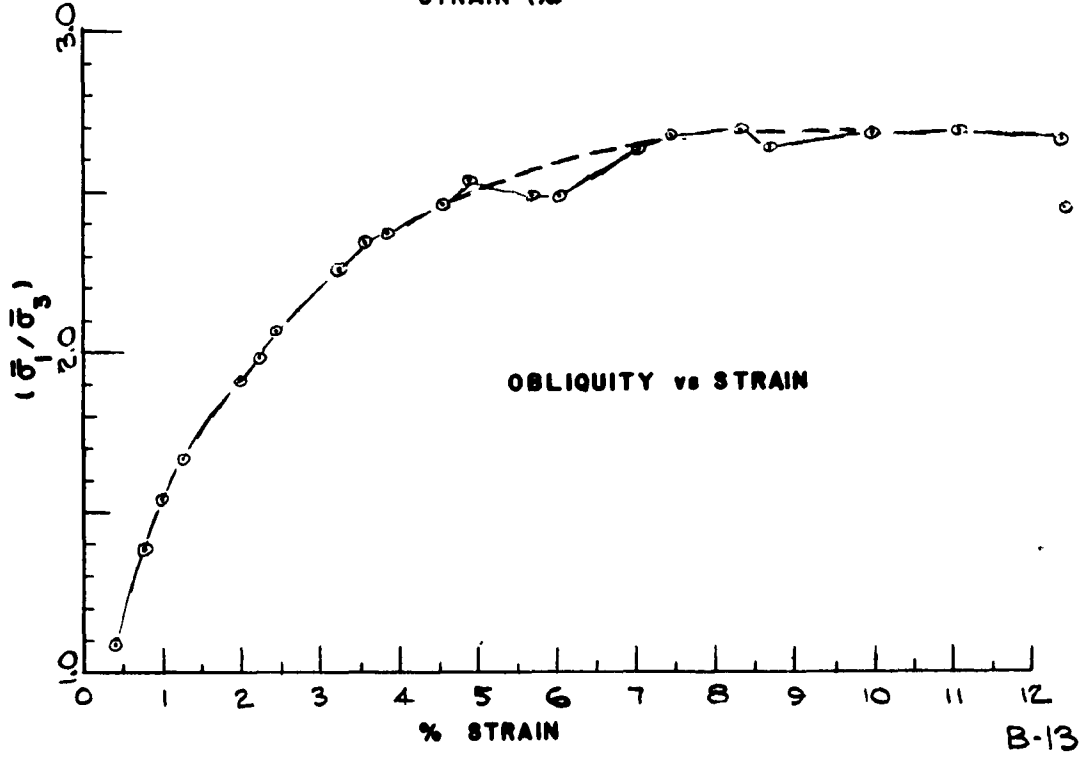
OBLIQUITY vs STRAIN
$(\bar{\sigma}_1/\bar{\sigma}_3)$
% STRAIN

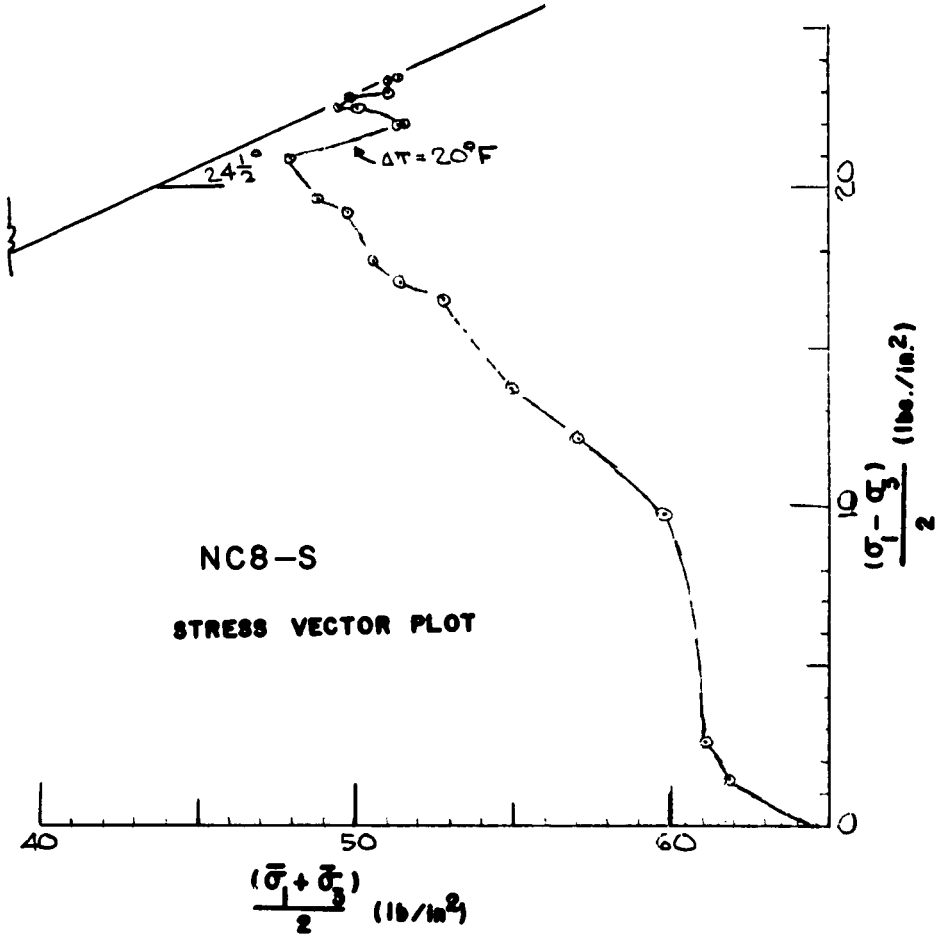
24½°
ΔT = 20°F
NC8–S
STRESS VECTOR PLOT
40
50
60
0
10
20
$\frac{(\bar{\sigma}_1 + \bar{\sigma}_3)}{2}$ (lb/in²)
$\frac{(\sigma_1 - \sigma_3)}{2}$ (lbs./in.²)

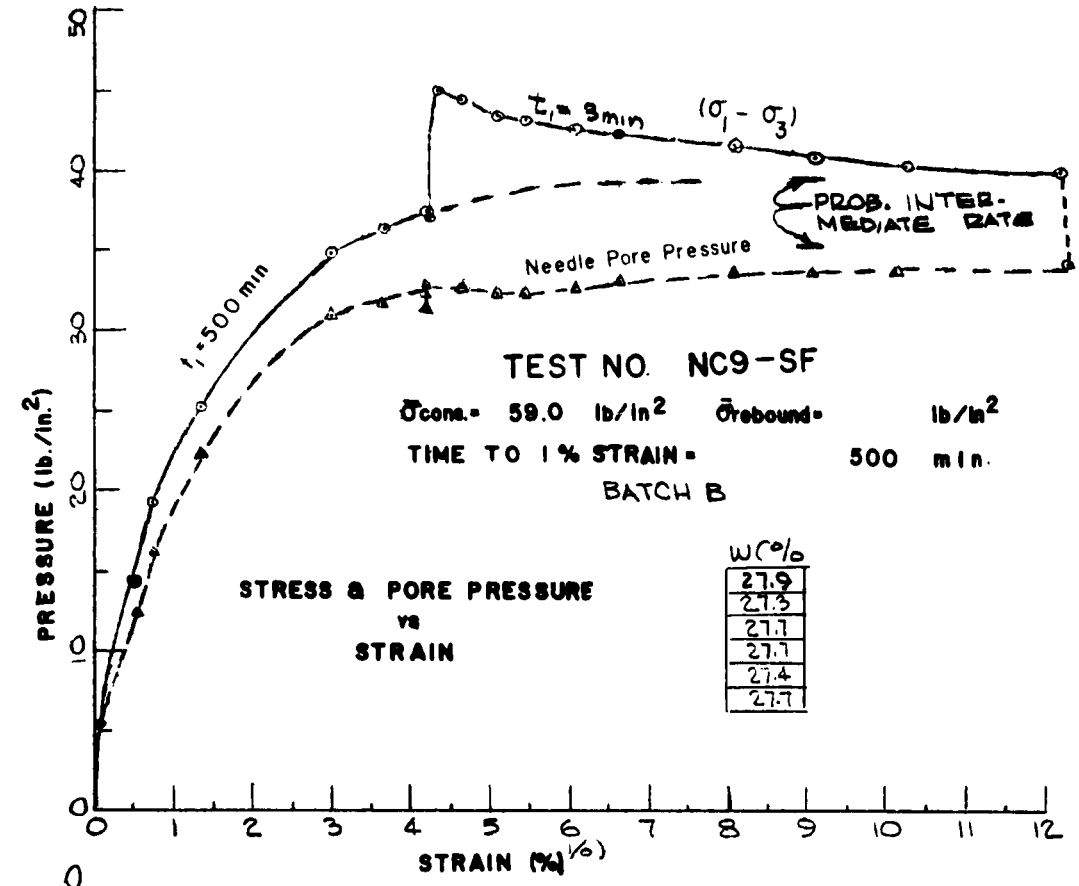
PRESSURE (lb./in.²)
STRAIN (%)^1/6
t_1 = 3 min
$(\sigma_1 - \sigma_3)$
PROB. INTER-MEDIATE RATE
Needle Pore Pressure
t_1 = 500 min
TEST NO. NC9-SF
$\bar{\sigma}_{cons.}$ = 59.0 lb/in²
$\bar{\sigma}_{rebound}$ = lb/in²
TIME TO 1% STRAIN = 500 min.
BATCH B
STRESS & PORE PRESSURE vs STRAIN
W.C% 27.9 27.3 27.7 27.7 27.4 27.7

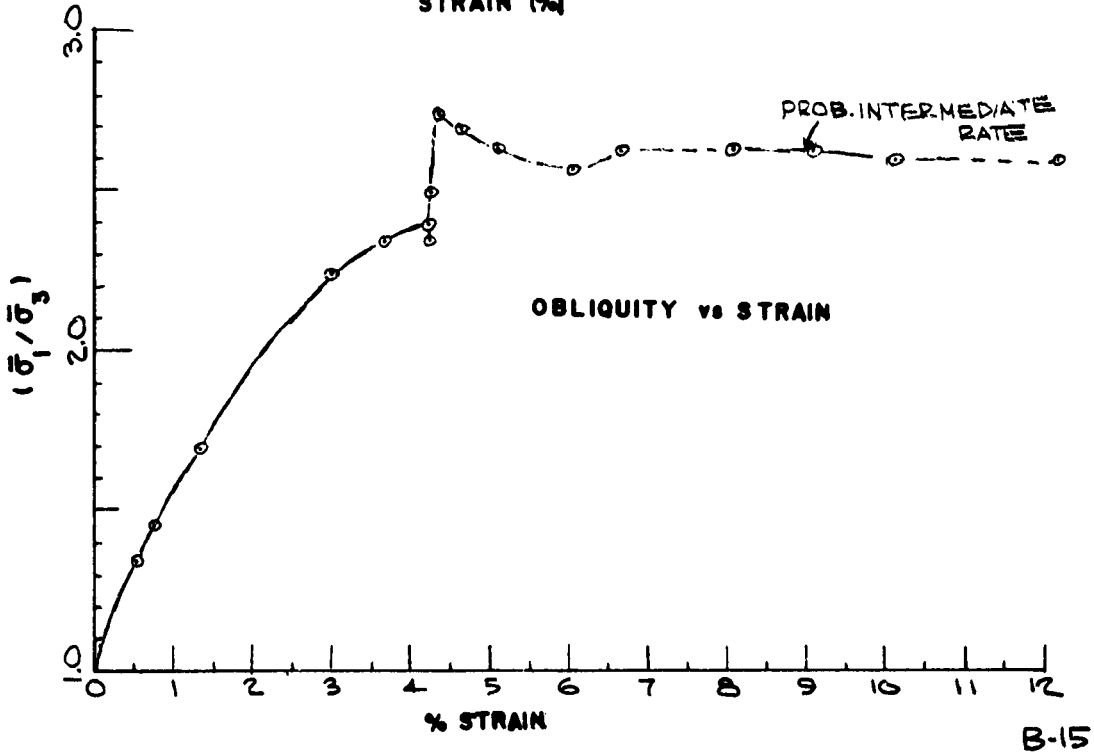
$(\bar{\sigma}_1/\bar{\sigma}_3)$
% STRAIN
PROB. INTERMEDIATE RATE
OBLIQUITY vs STRAIN

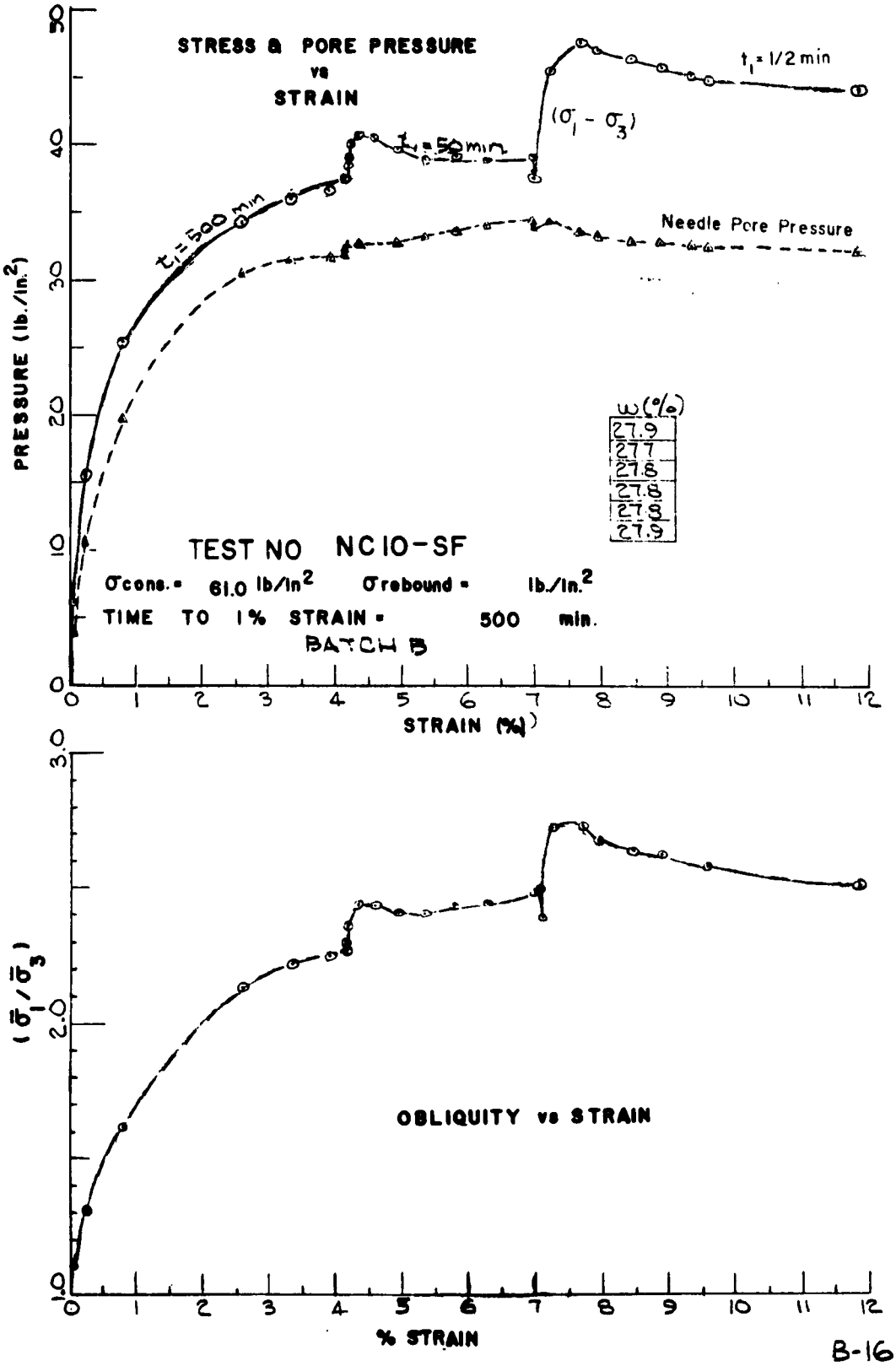
STRESS & PORE PRESSURE
vs
STRAIN
t_1 = 1/2 min
$(\sigma_1 - \sigma_3)$
t_1 = 50 min
t_1 = 500 min
Needle Pore Pressure
PRESSURE (lb./in.^{2})
w(%)
27.9
27.7
27.8
27.8
27.8
27.9
TEST NO NC10-SF
σcons. = 61.0 lb/in^2 σrebound = lb./in.^{2}
TIME TO 1% STRAIN = 500 min.
BATCH B
STRAIN (%)
$(\bar{\sigma}_1/\bar{\sigma}_3)$
OBLIQUITY vs STRAIN
% STRAIN

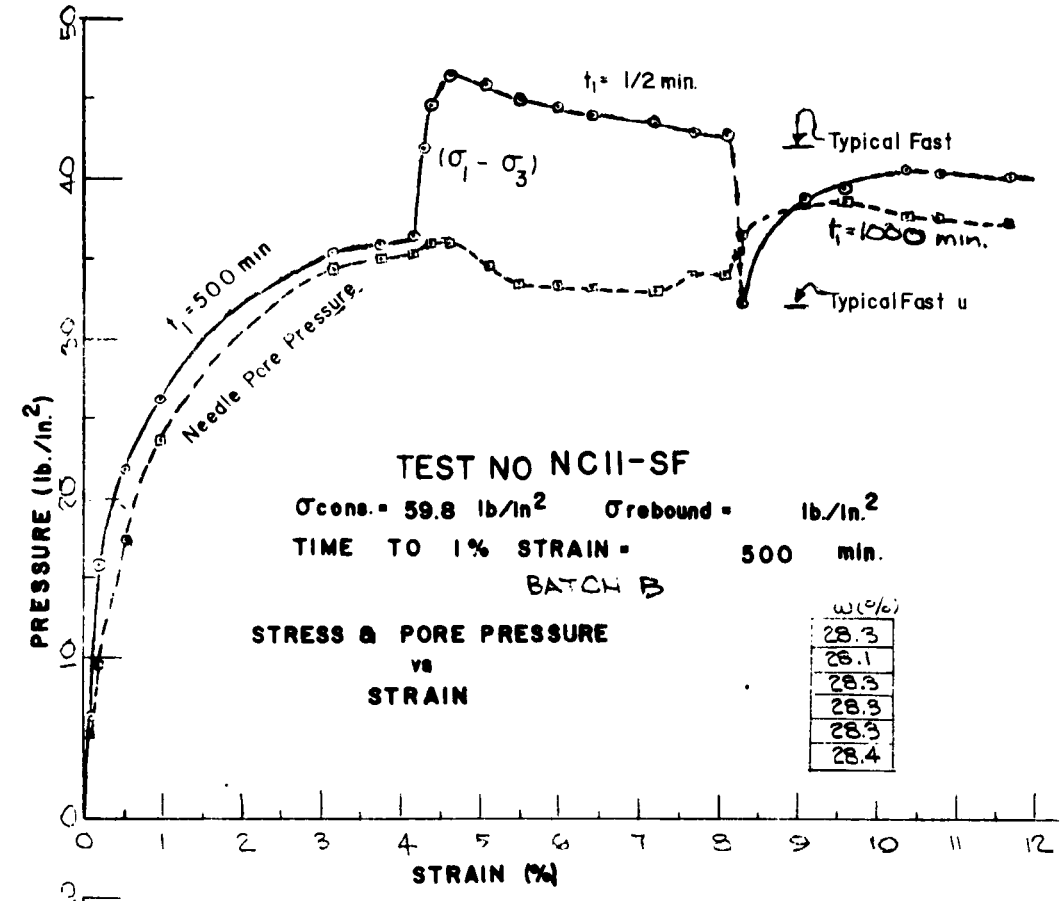
t_1 = 1/2 min.
$(\sigma_1 - \sigma_3)$
Typical Fast
t_1 = 1000 min.
Typical Fast u
t_1 = 500 min
Needle Pore Pressure
PRESSURE (lb./in.^{2})
TEST NO NC11-SF
σcons. = 59.8 lb/in^2 σrebound = lb./in.^{2}
TIME TO 1% STRAIN = 500 min.
BATCH B
STRESS & PORE PRESSURE
vs
STRAIN
ω(%)
28.3
28.1
28.3
28.3
28.3
28.4
STRAIN (%)

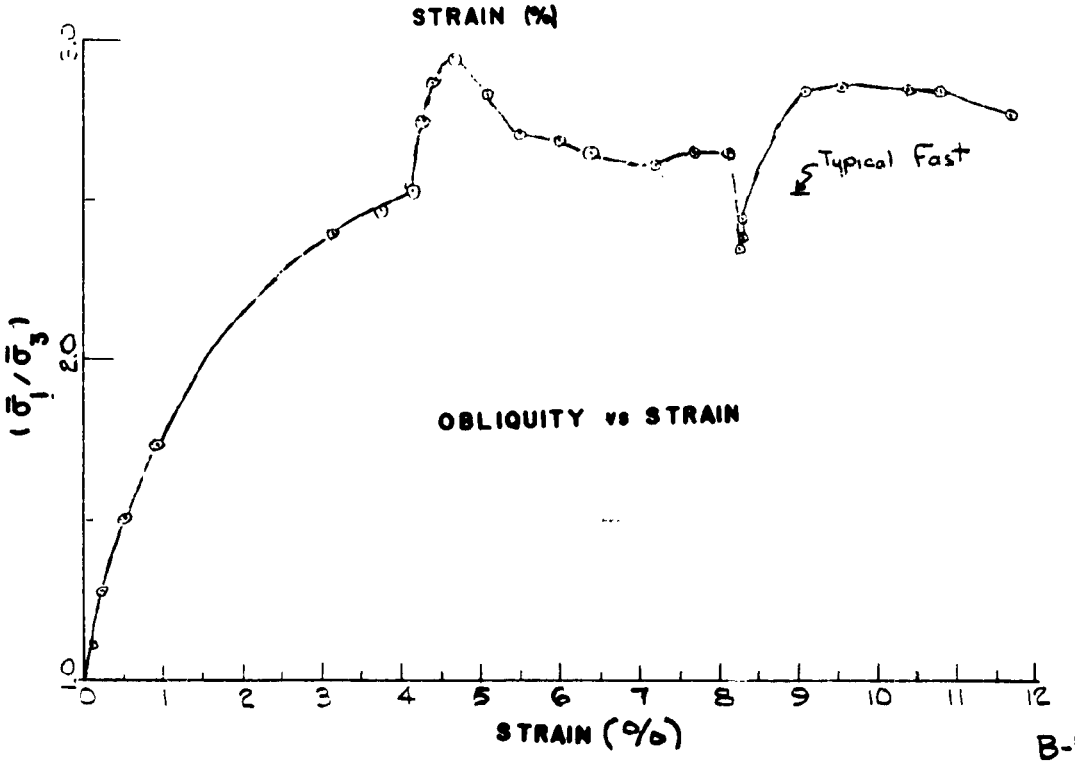
Typical Fast
$(\bar{\sigma}_1/\bar{\sigma}_3)$
OBLIQUITY vs STRAIN
STRAIN (%)

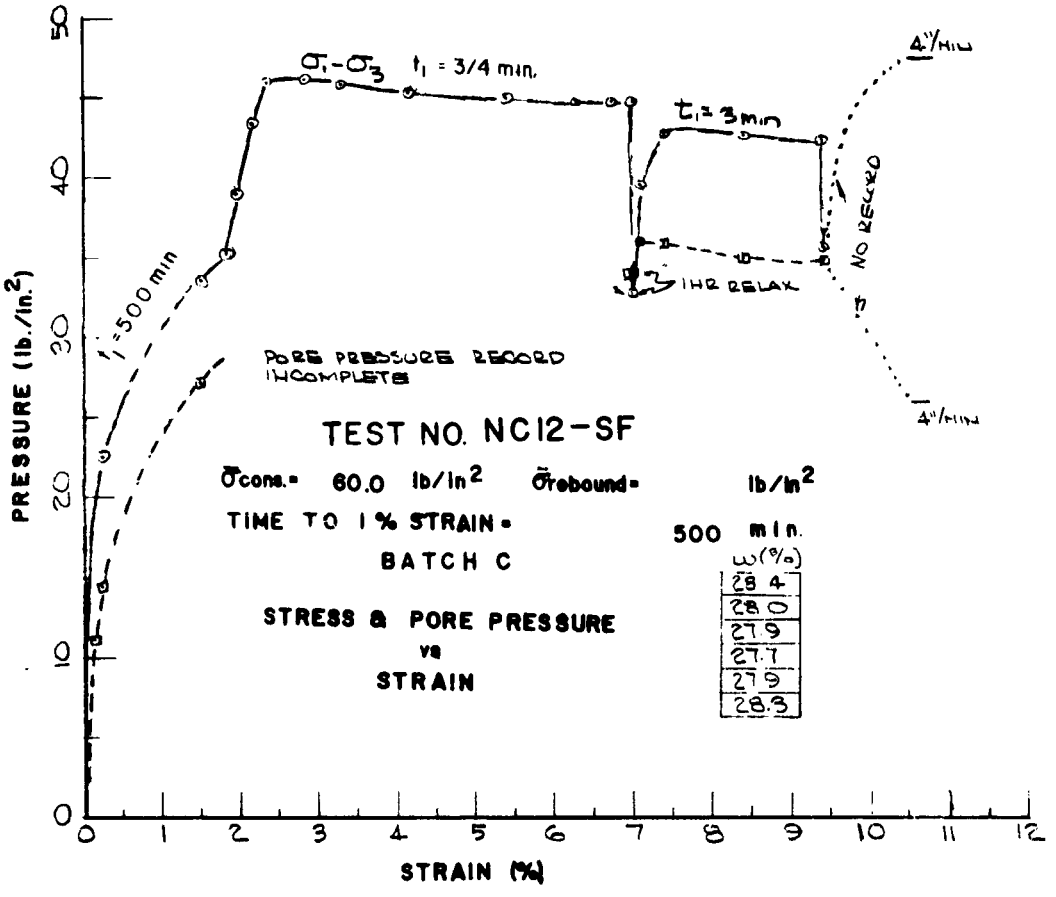
PRESSURE (lb./in.²)
STRAIN (%)
σ1-σ3
t1 = 3/4 min.
t1 = 3 min
4"/min
4"/min
NO RECORD
1HR RELAX
t = 500 min
PORE PRESSURE RECORD INCOMPLETE
TEST NO. NC12-SF
σcons.= 60.0 lb/in²
σrebound= lb/in²
TIME TO 1% STRAIN = 500 min.
BATCH C
STRESS & PORE PRESSURE vs STRAIN
ω(%)
28.4
28.0
27.9
27.7
27.9
28.3

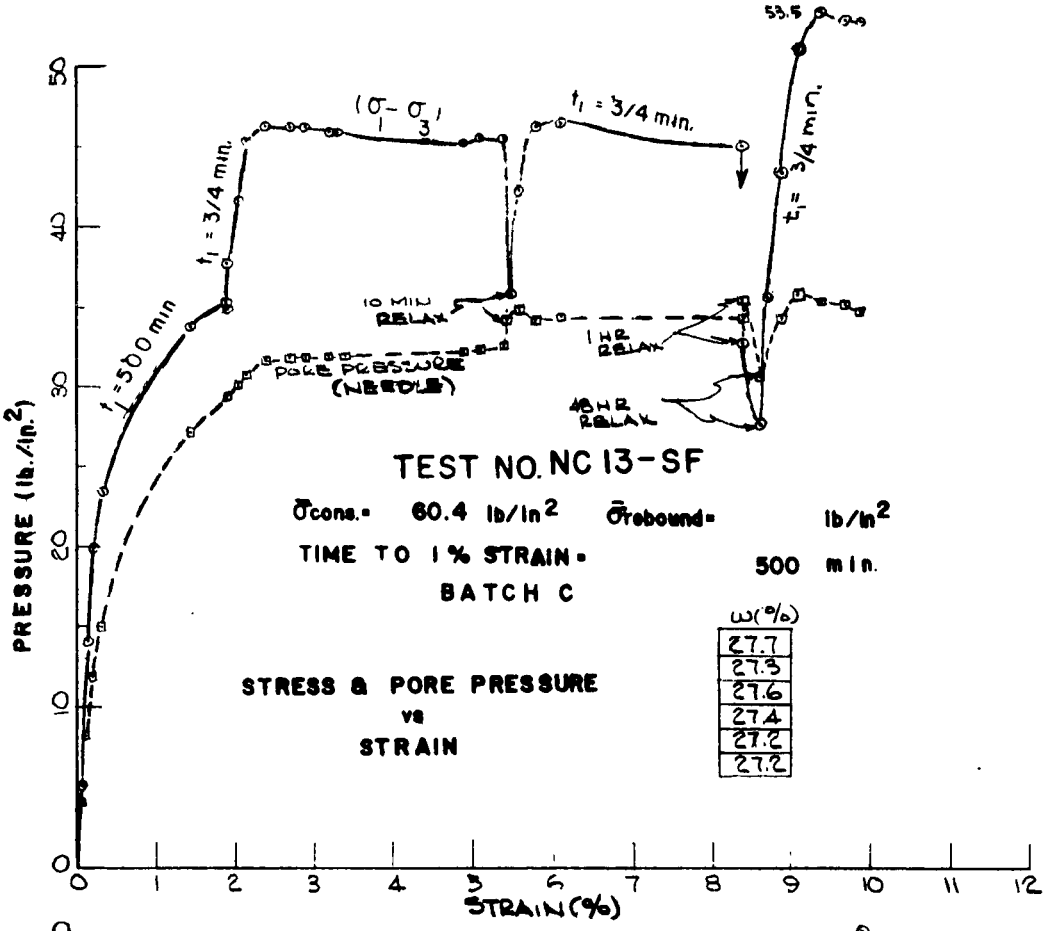
PRESSURE (lb./in.²)
STRAIN (%)
(σ1 - σ3)
t1 = 3/4 min.
t1 = 500 min
10 MIN RELAX
1 HR RELAX
48 HR RELAX
PORE PRESSURE (NEEDLE)
TEST NO. NC 13-SF
σcons. = 60.4 lb/in²
σrebound = lb/in²
TIME TO 1% STRAIN = 500 min.
BATCH C
ω(%)
27.7
27.3
27.6
27.4
27.2
27.2
STRESS & PORE PRESSURE vs STRAIN

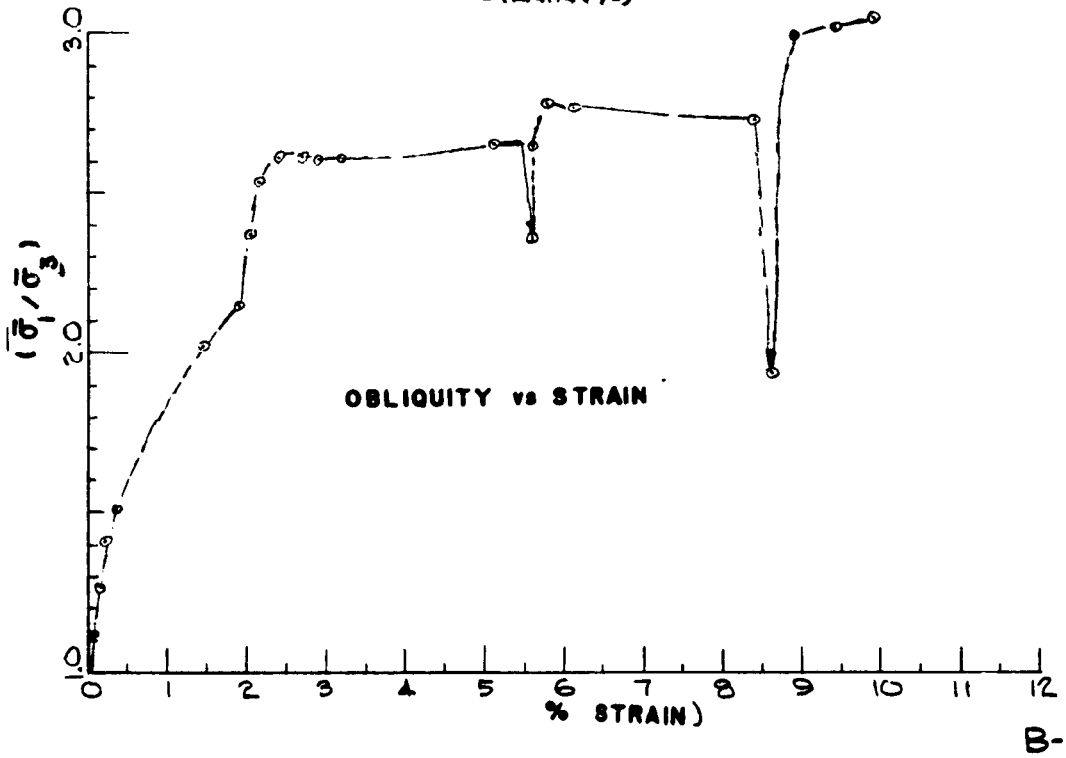
(σ̄1/σ̄3)
% STRAIN)
OBLIQUITY vs STRAIN

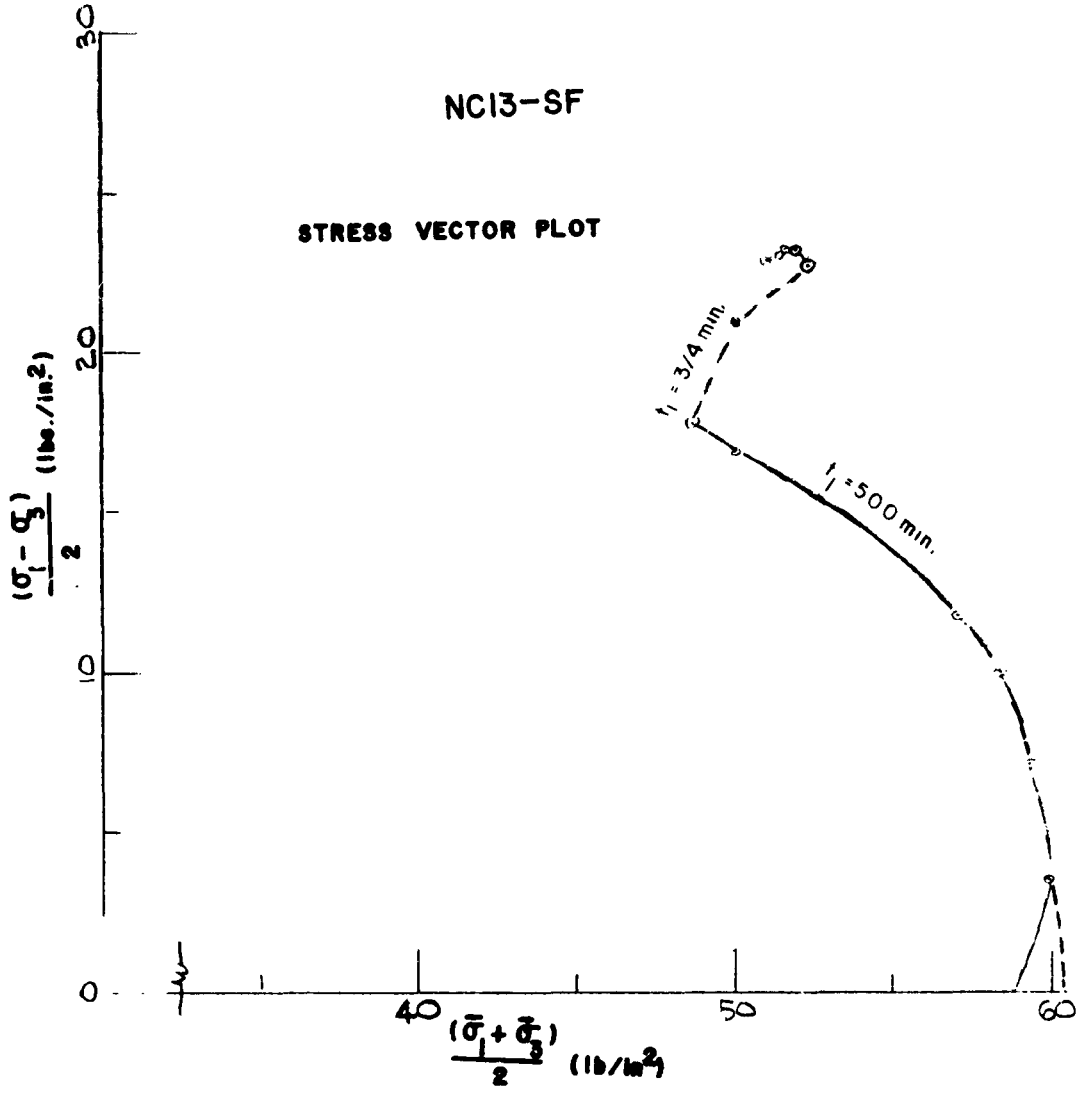
NC13-SF
STRESS VECTOR PLOT
t_1 = 3/4 min.
t_1 = 500 min.
$\frac{(\sigma_1 - \sigma_3)}{2}$ (lbs./in.²)
$\frac{(\bar{\sigma}_1 + \bar{\sigma}_3)}{2}$ (lb/in²)
30
20
10
0
40
50
60

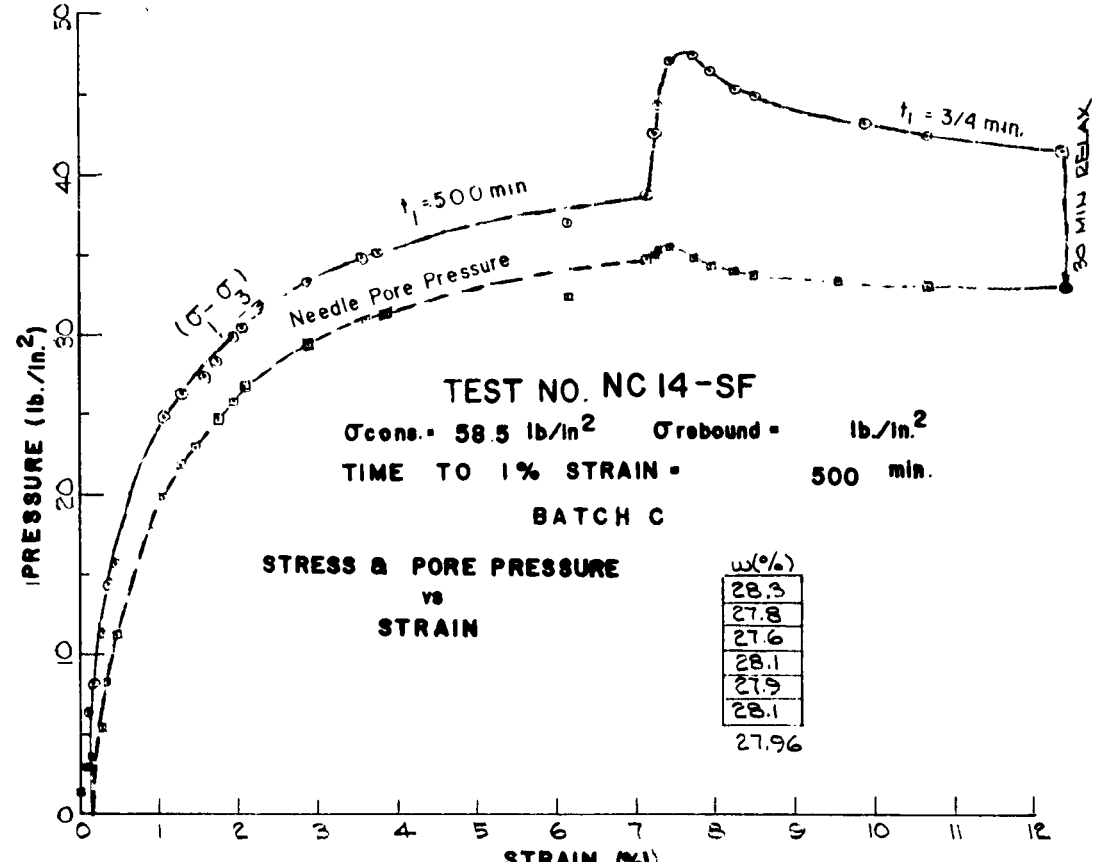
PRESSURE (lb./in.²)
STRAIN (%)
t_1 = 3/4 min.
t_1 = 500 min
$(\sigma_1 - \sigma_3)$
Needle Pore Pressure
30 MIN RELAX
TEST NO. NC 14-SF
σcons. = 58.5 lb/in²
σrebound =
lb./in.²
TIME TO 1% STRAIN =
500 min.
BATCH C
STRESS & PORE PRESSURE
vs
STRAIN
w(%)
28.3
27.8
27.6
28.1
27.9
28.1
27.96

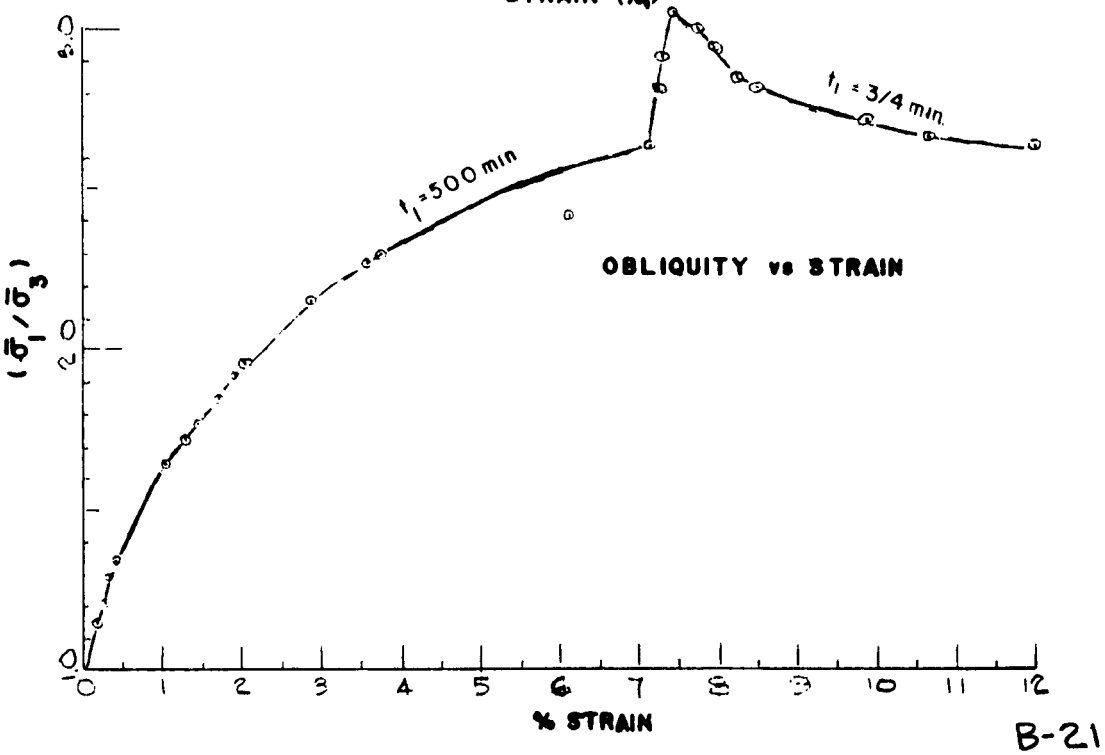
$(\bar{\sigma}_1 / \bar{\sigma}_3)$
% STRAIN
t_1 = 3/4 min.
t_1 = 500 min
OBLIQUITY vs STRAIN

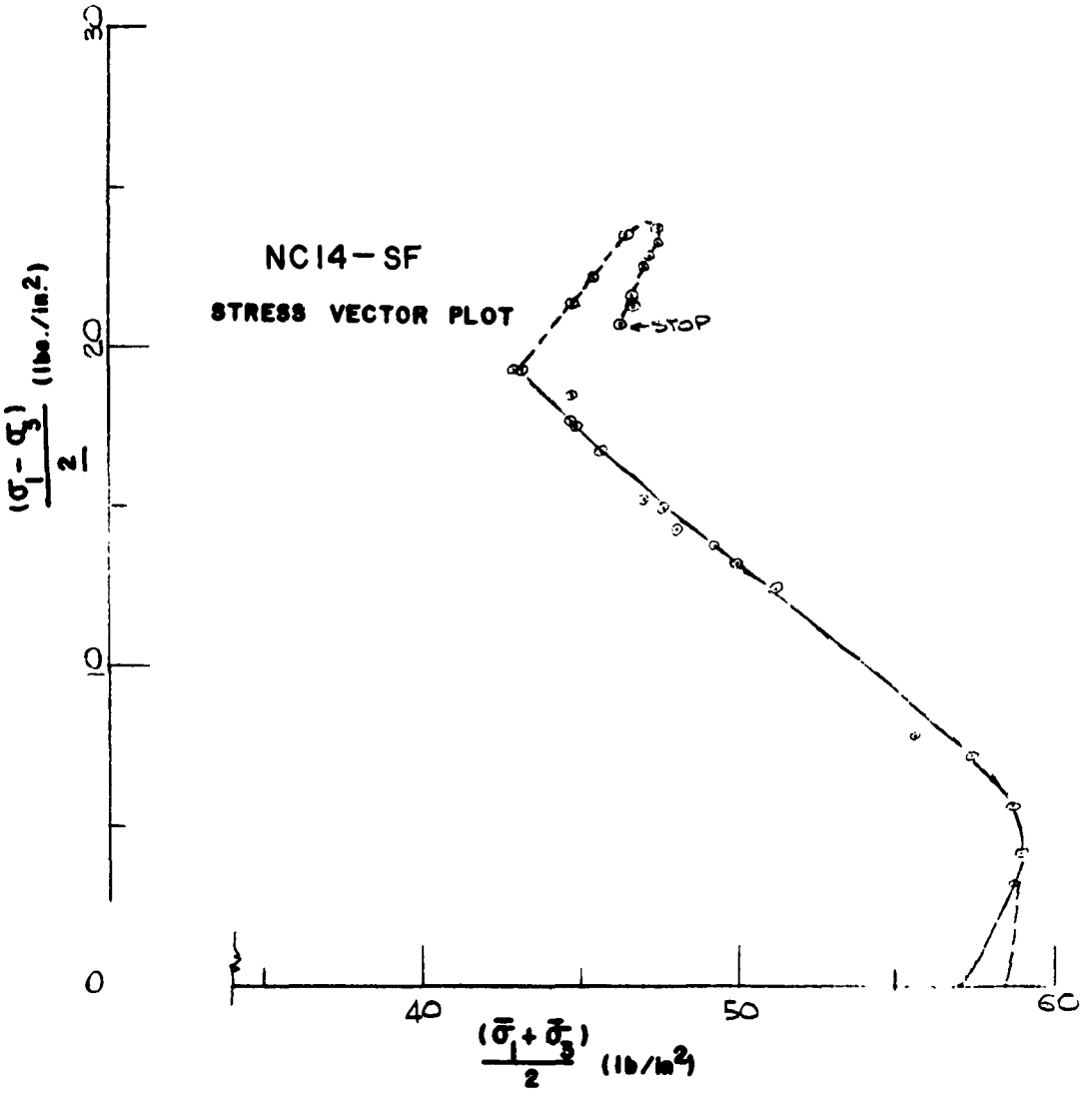
NC14 – SF
STRESS VECTOR PLOT
STOP
30
20
10
0
40
50
60
$\frac{(\sigma_1 - \sigma_3)}{2}$ (lbs./in.²)
$\frac{(\bar{\sigma}_1 + \bar{\sigma}_3)}{2}$ (lb/in²)

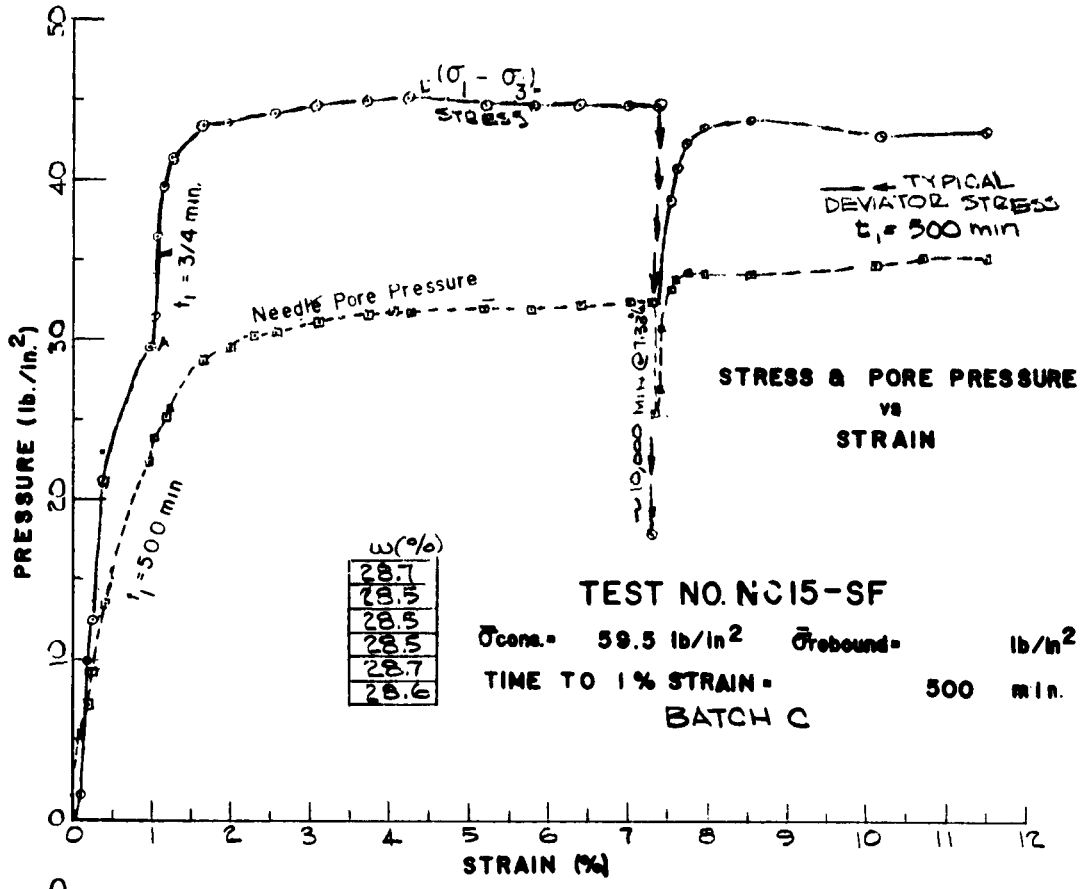
PRESSURE (lb./in.²)
STRAIN (%)
(σ1 - σ3)
STRESS
t1 = 3/4 min.
t1 = 500 min
Needle Pore Pressure
~10,000 min @ T: 3/4
TYPICAL
DEVIATOR STRESS
t1 = 500 min
STRESS & PORE PRESSURE
vs
STRAIN
w(%)
28.7
28.5
28.5
28.5
28.7
28.6
TEST NO. NC15-SF
σcons. = 59.5 lb/in²
σrebound =
lb/in²
TIME TO 1% STRAIN =
500 min.
BATCH C

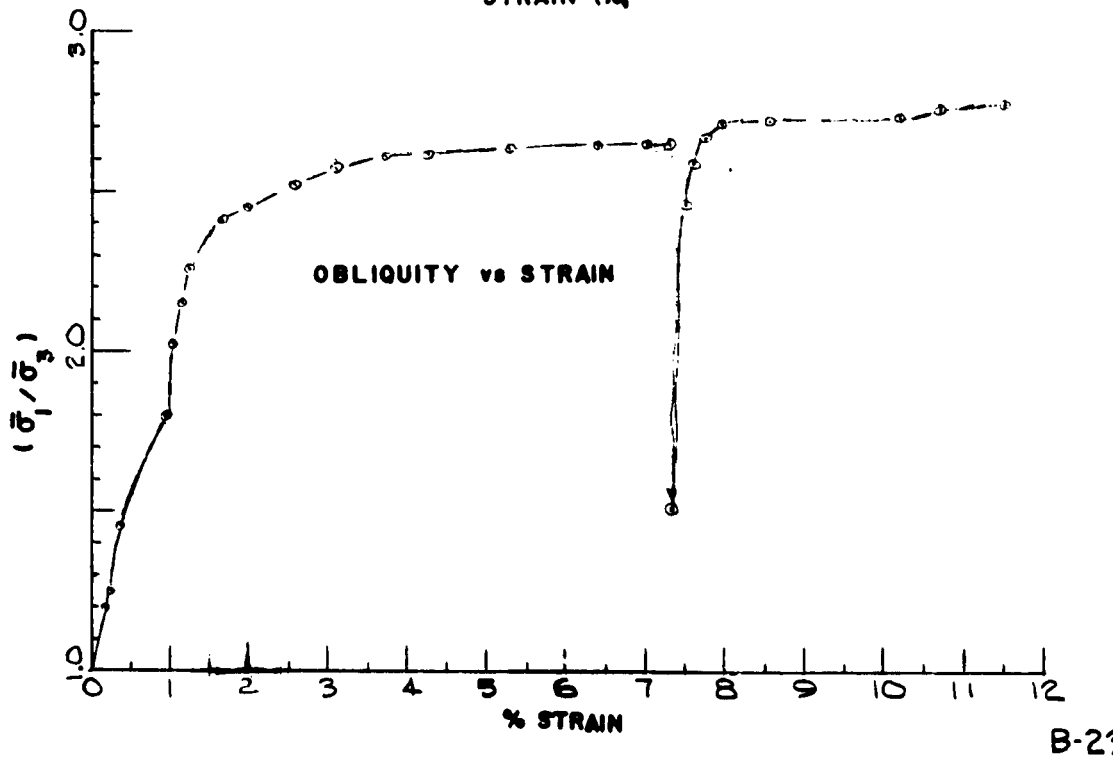
(σ̄1/σ̄3)
% STRAIN
OBLIQUITY vs STRAIN

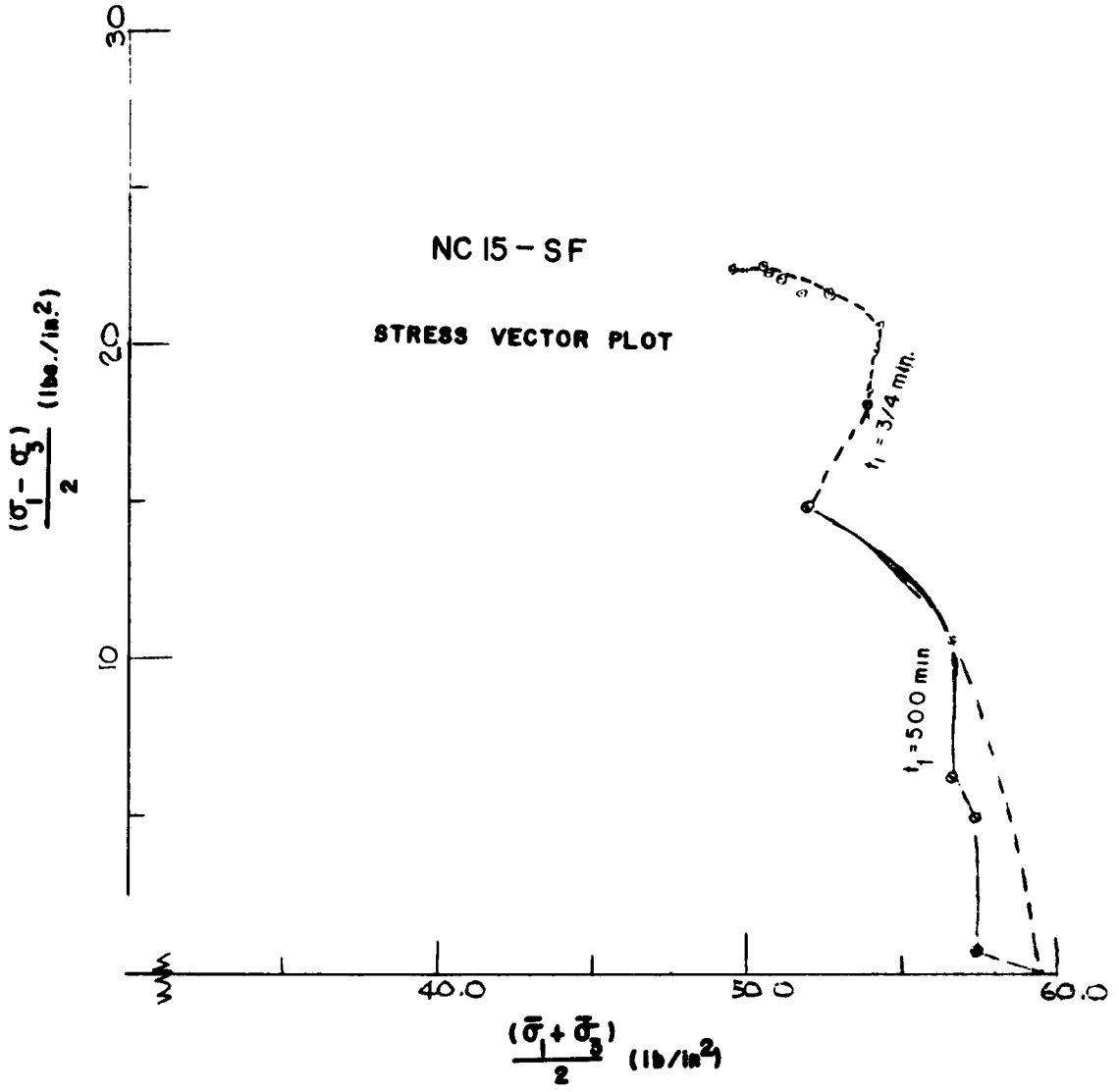
NC 15 – SF
STRESS VECTOR PLOT
$\frac{(\sigma_1 - \sigma_3)}{2}$ (lbs./in.2)
30
20
10
t_1 = 3/4 min.
t_1 = 500 min
40.0
50.0
60.0
$\frac{(\bar{\sigma}_1 + \bar{\sigma}_3)}{2}$ (lb/in2)

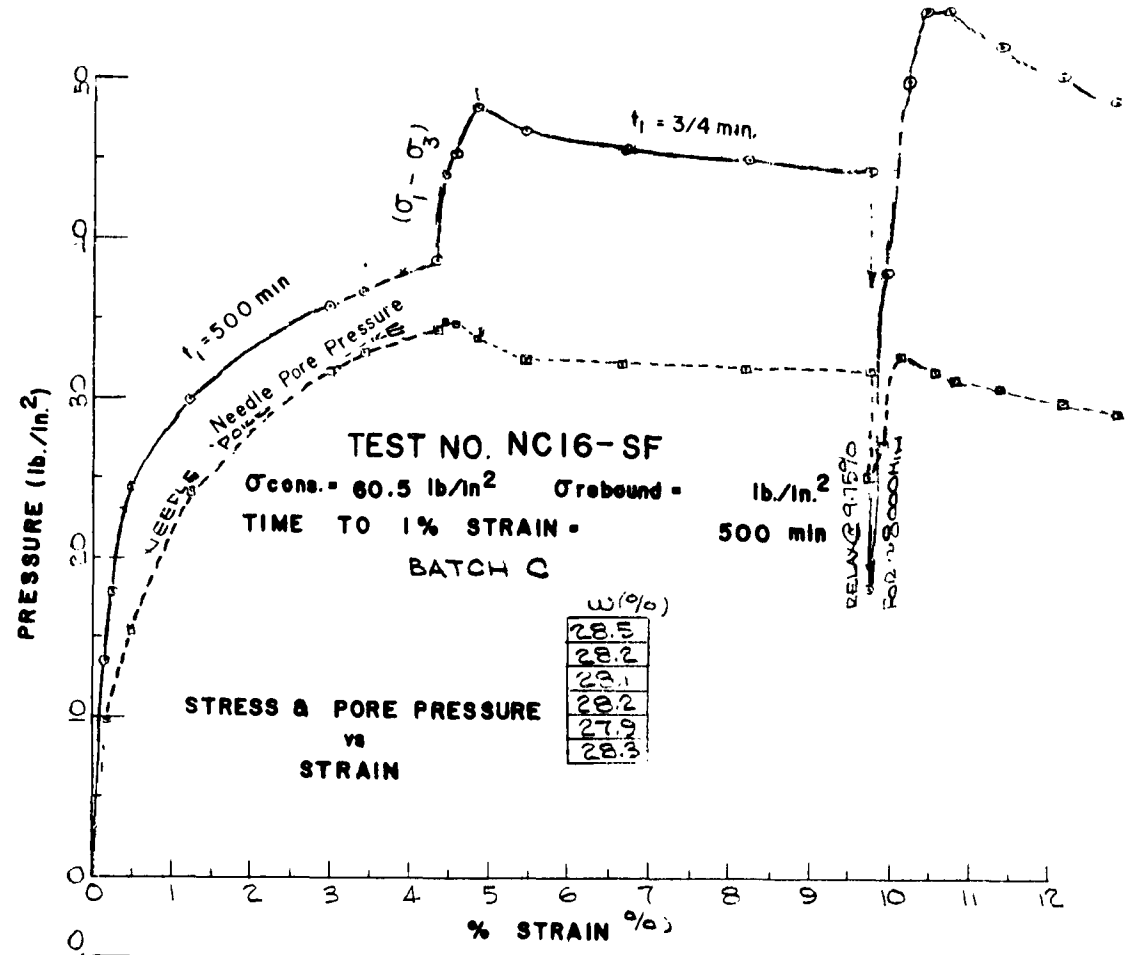
PRESSURE (lb./in.²)
$(\sigma_1 - \sigma_3)$
t_1 = 3/4 min.
t_1 = 500 min
Needle Pore Pressure
Veeps
TEST NO. NC16-SF
σcons. = 60.5 lb/in²
σrebound =
lb./in.²
TIME TO 1% STRAIN =
500 min
BATCH C
STRESS & PORE PRESSURE
vs
STRAIN
w(%)
28.5
28.2
29.1
28.2
27.9
28.3
% STRAIN %

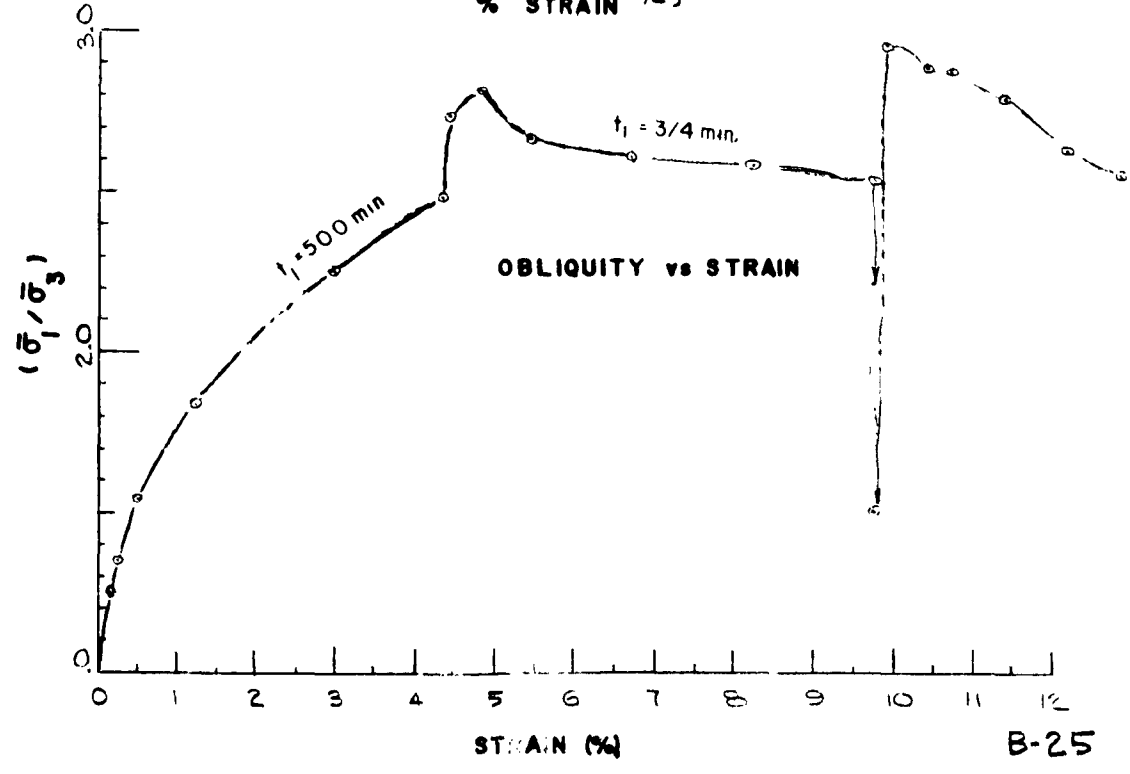
$(\bar{\sigma}_1 / \bar{\sigma}_3)$
t_1 = 3/4 min.
t_1 = 500 min
OBLIQUITY vs STRAIN
STRAIN (%)

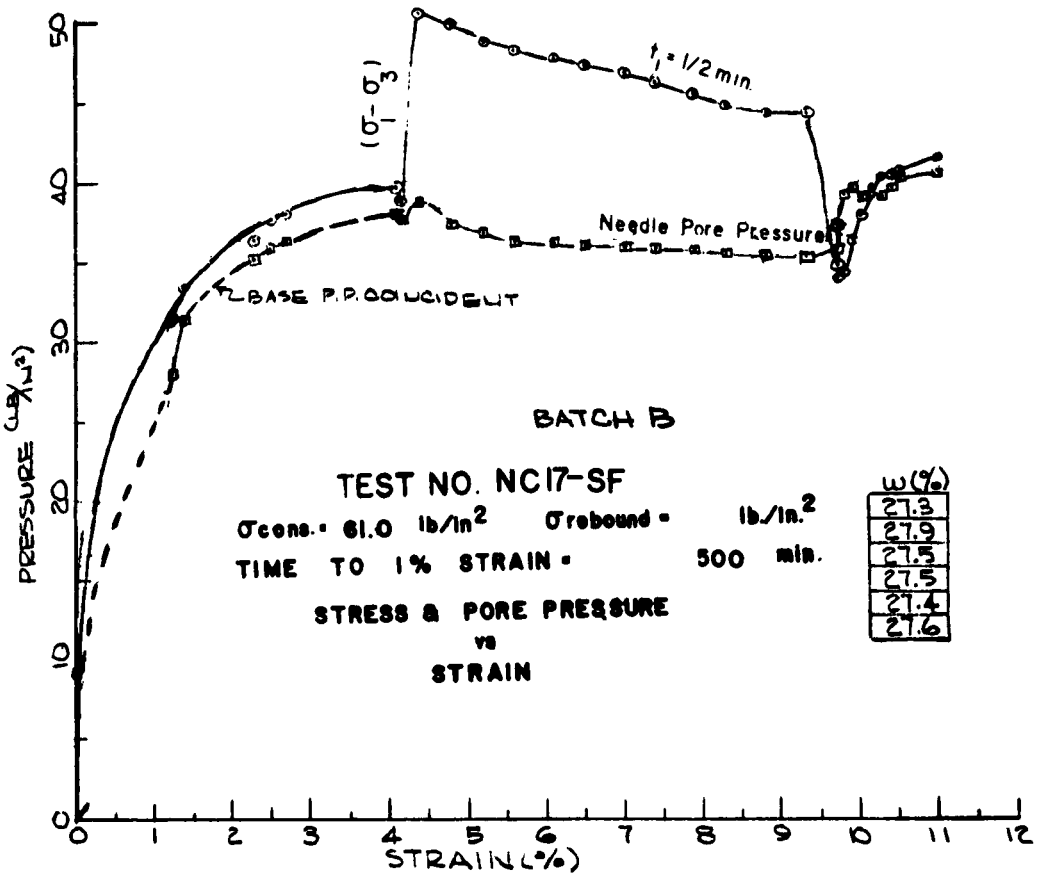
$(\sigma_1-\sigma_3)$
t_1 = 1/2 min.
Needle Pore Pressure
BASE P.P. COINCIDENT
BATCH B
TEST NO. NC17-SF
σcons. = 61.0 lb/in²
σrebound = lb./in.²
TIME TO 1% STRAIN = 500 min.
STRESS & PORE PRESSURE
vs
STRAIN
w(%)
27.3
27.9
27.5
27.5
27.4
27.6
PRESSURE (LB/IN²)
STRAIN (%)
0
10
20
30
40
50
0
1
2
3
4
5
6
7
8
9
10
11
12

NC 17– SF

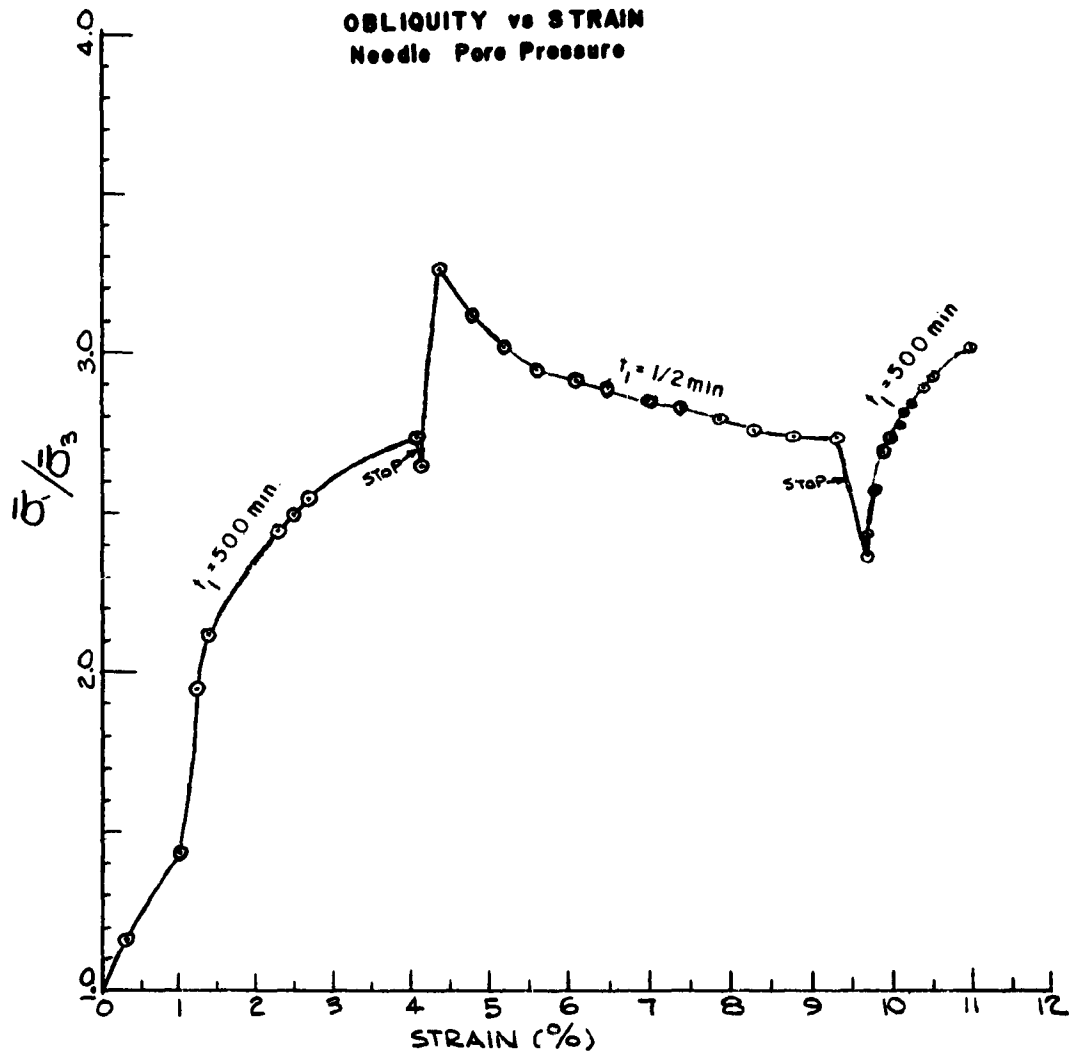
OBLIQUITY vs STRAIN
Needle Pore Pressure
$\bar{\sigma}_1/\bar{\sigma}_3$
4.0
3.0
2.0
1.0
0
1
2
3
4
5
6
7
8
9
10
11
12
STRAIN (%)
t_1 = 500 min
STOP
t_1 = 1/2 min
STOP
t_1 = 500 min

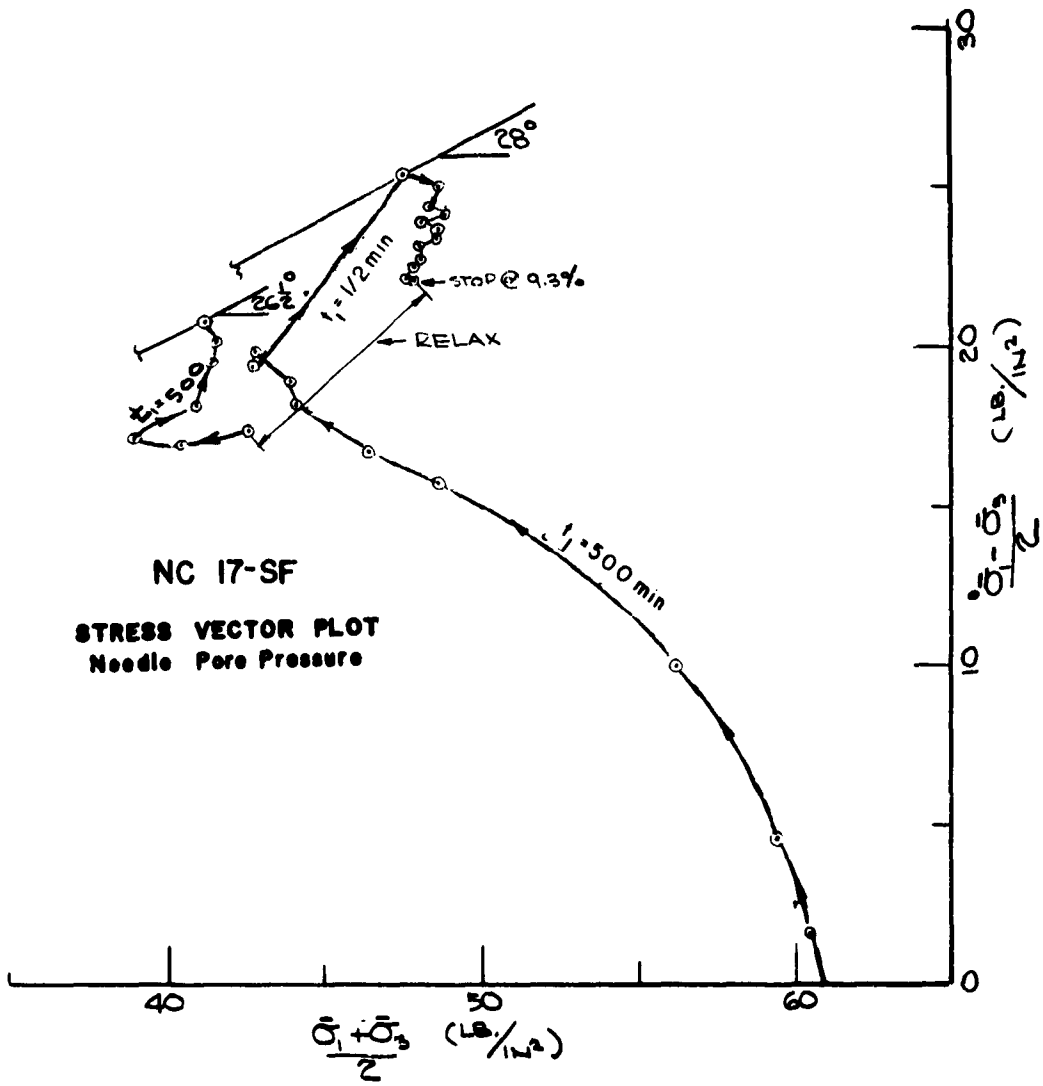
28°
26½°
t_f = 1/2 min
STOP @ 9.3%
RELAX
t_f = 500
t_f = 500 min
NC 17-SF
STRESS VECTOR PLOT
Needle Pore Pressure
40
50
60
0
10
20
30
$\frac{\bar{\sigma}_1 + \bar{\sigma}_3}{2}$ (lb./in²)
$\frac{\bar{\sigma}_1 - \bar{\sigma}_3}{2}$ (lb./in²)

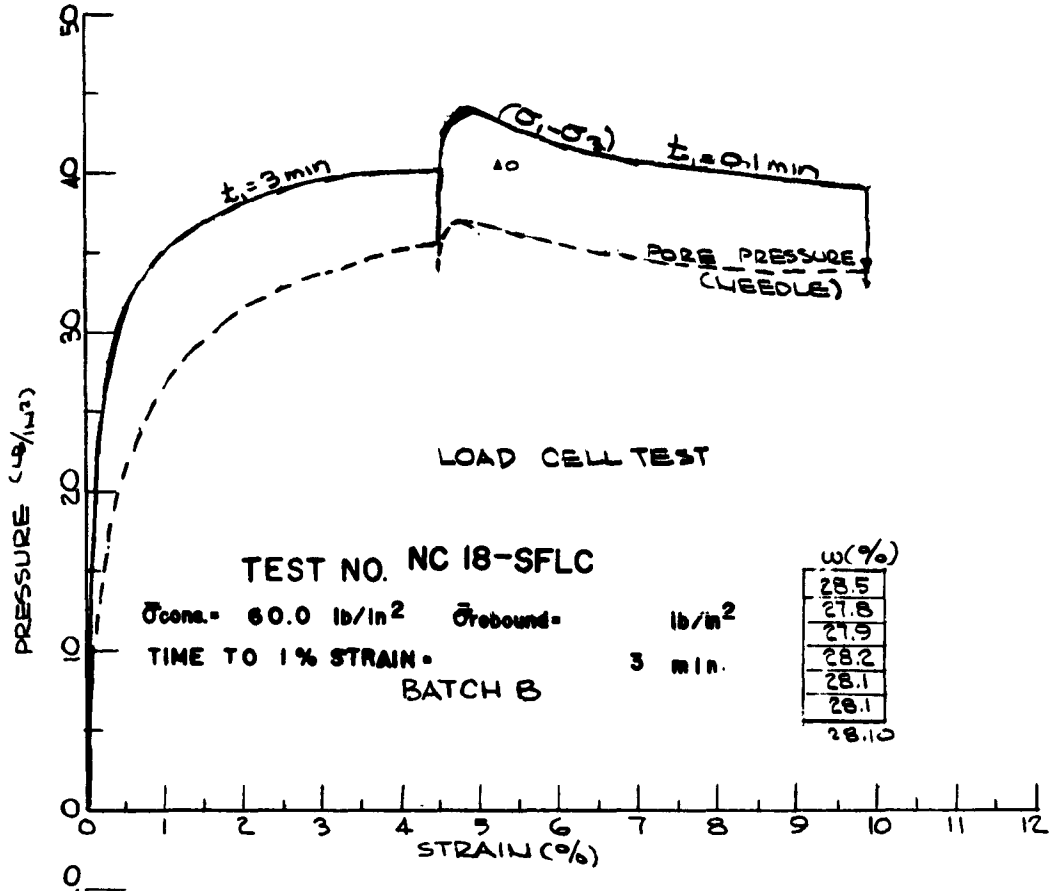
PRESSURE (lb/in²)
50
40
30
20
10
0
t_1 = 3 min
$(\sigma_1-\sigma_3)$
t_1 = 0.1 min
Δσ
PORE PRESSURE (NEEDLE)
LOAD CELL TEST
TEST NO. NC 18-SFLC
$\bar{\sigma}_{cons.}$ = 60.0 lb/in²
$\bar{\sigma}_{rebound}$ = lb/in²
TIME TO 1% STRAIN = 3 min.
BATCH B
ω(%)
28.5
27.8
27.9
28.2
28.1
28.1
28.10
0 1 2 3 4 5 6 7 8 9 10 11 12
STRAIN (%)

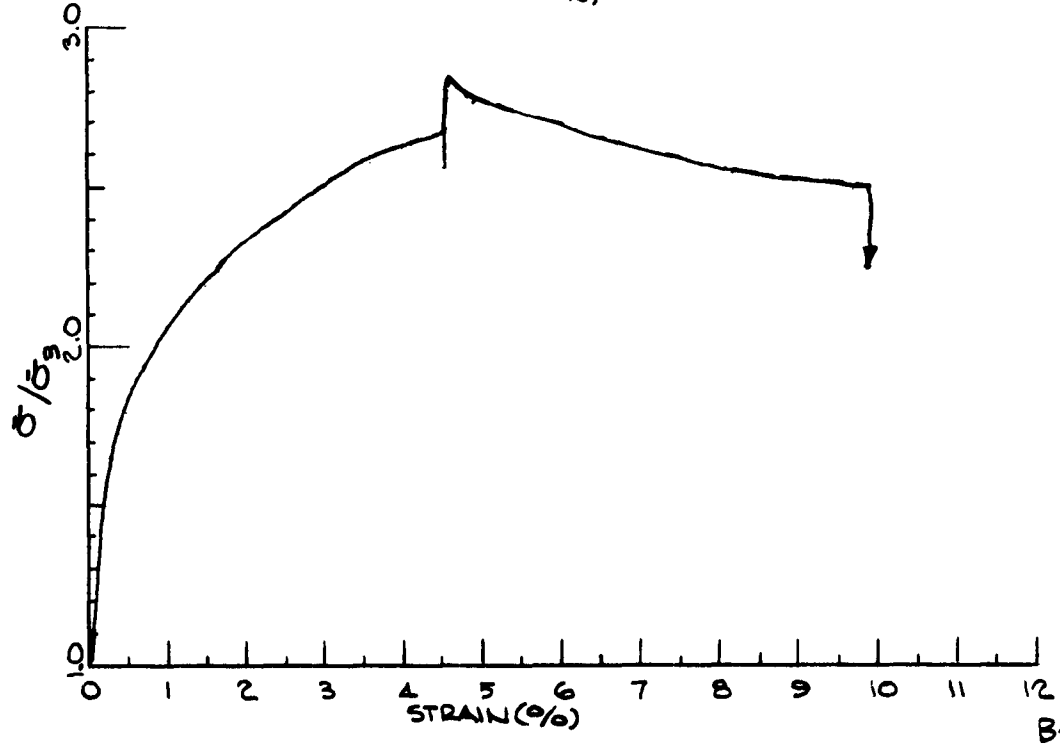
$\sigma/\bar{\sigma}_3$
3.0
2.0
1.0
0 1 2 3 4 5 6 7 8 9 10 11 12
STRAIN (%)

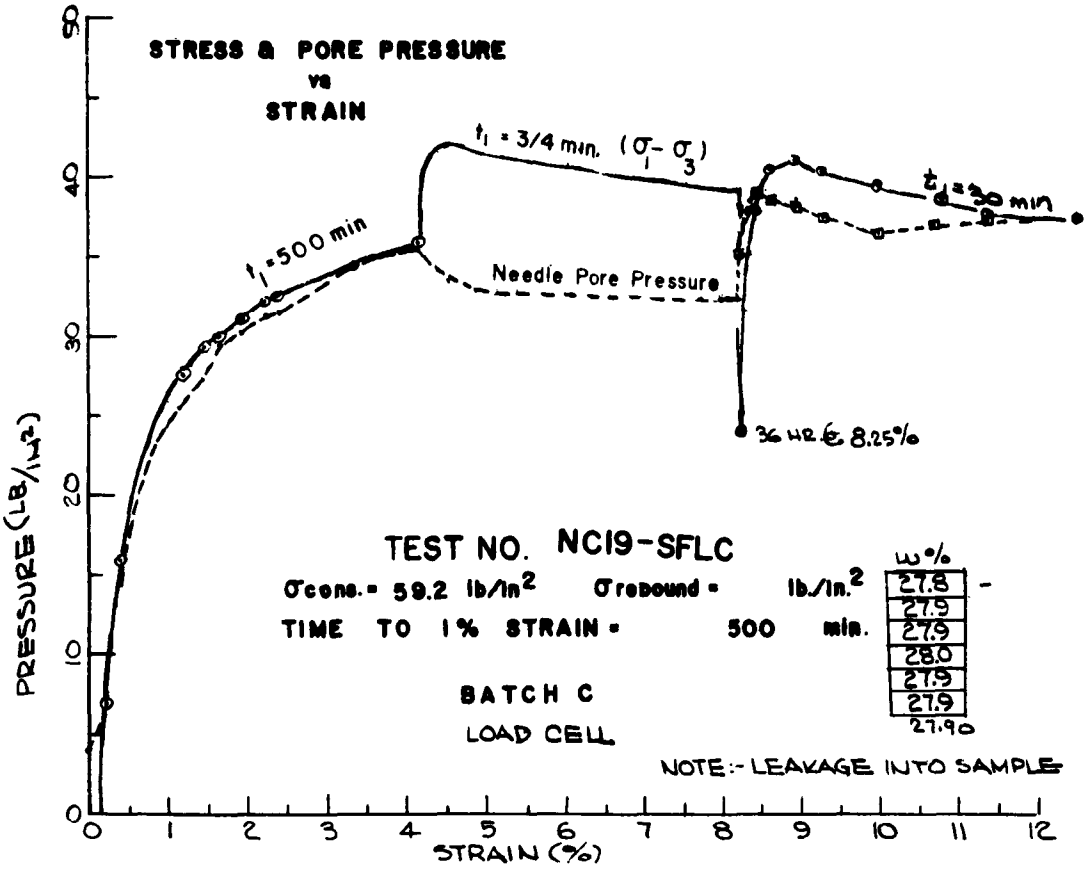
STRESS & PORE PRESSURE
vs
STRAIN
t_1 = 3/4 min. ($\sigma_1 - \sigma_3$)
t_1 = 500 min
t_1 = 30 min
Needle Pore Pressure
36 HR. @ 8.25%
TEST NO. NC19-SFLC
σcons. = 59.2 lb/in^2 σrebound = lb./in.^{2}
TIME TO 1% STRAIN = 500 min.
BATCH C
LOAD CELL
w%
27.8
27.9
27.9
28.0
27.9
27.9
27.90
NOTE:- LEAKAGE INTO SAMPLE
PRESSURE (LB/IN^2)
STRAIN (%)
0
10
20
30
40
50
0
1
2
3
4
5
6
7
8
9
10
11
12

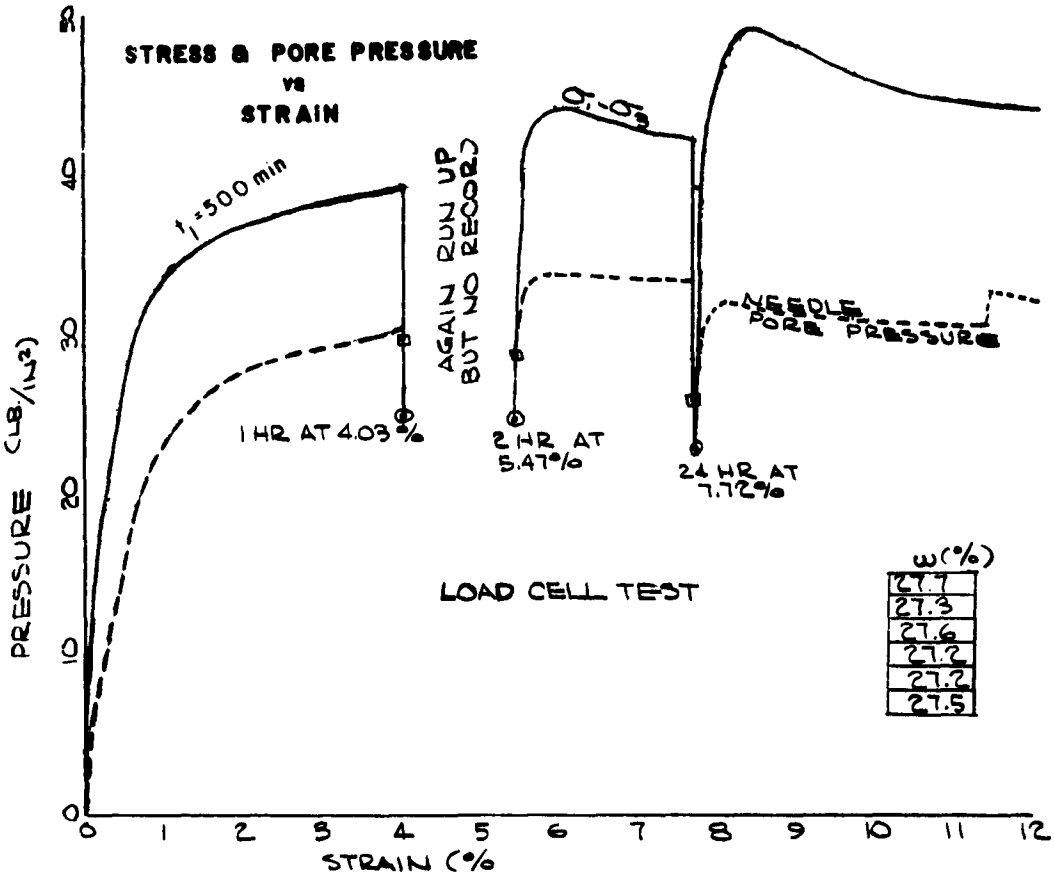

TEST NO. NC20-SFLC

$\sigma_{confs.}$ = 61.0 lb/in^2 $\sigma_{rebound}$ = lb./in.^{2}

TIME TO 1% STRAIN = 3/4 min

BATCH C

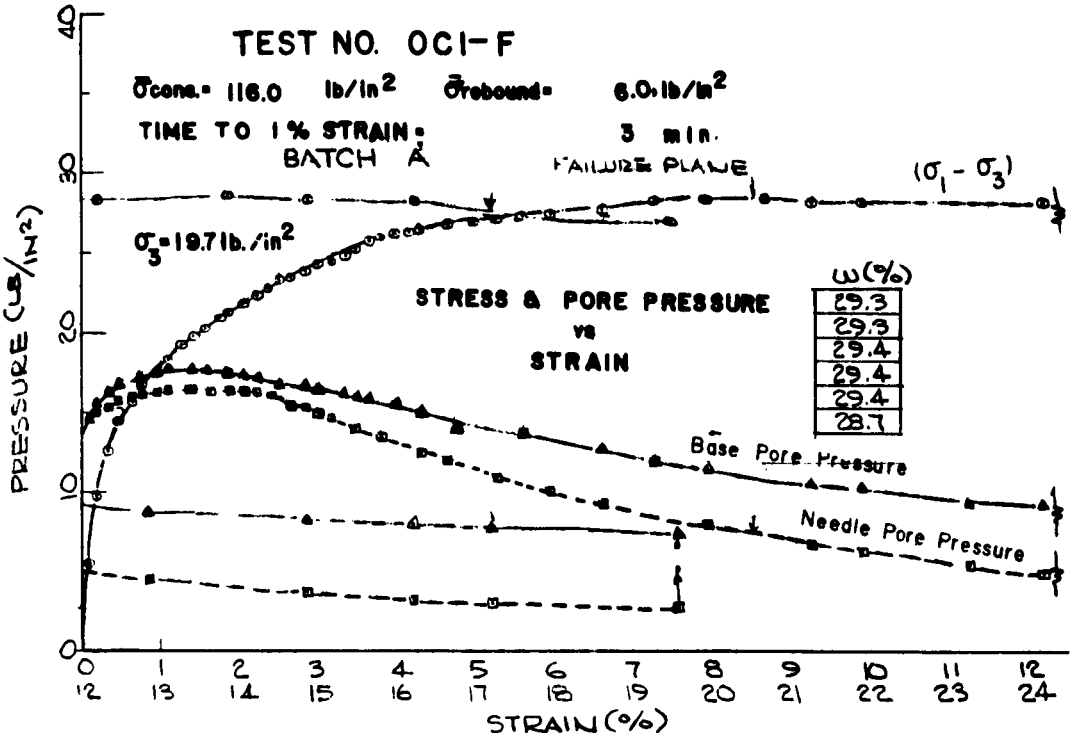
TEST NO. OCI-F
σ̄cons.= 116.0 lb/in²
σ̄rebound= 6.0 lb/in²
TIME TO 1% STRAIN= 3 min.
BATCH A
FAILURE PLANE
(σ1 - σ3)
σ3=19.7 lb./in²
STRESS & PORE PRESSURE
vs
STRAIN
w(%)
29.3
29.3
29.4
29.4
29.4
28.7
Base Pore Pressure
Needle Pore Pressure
PRESSURE (LB/IN²)
STRAIN (%)

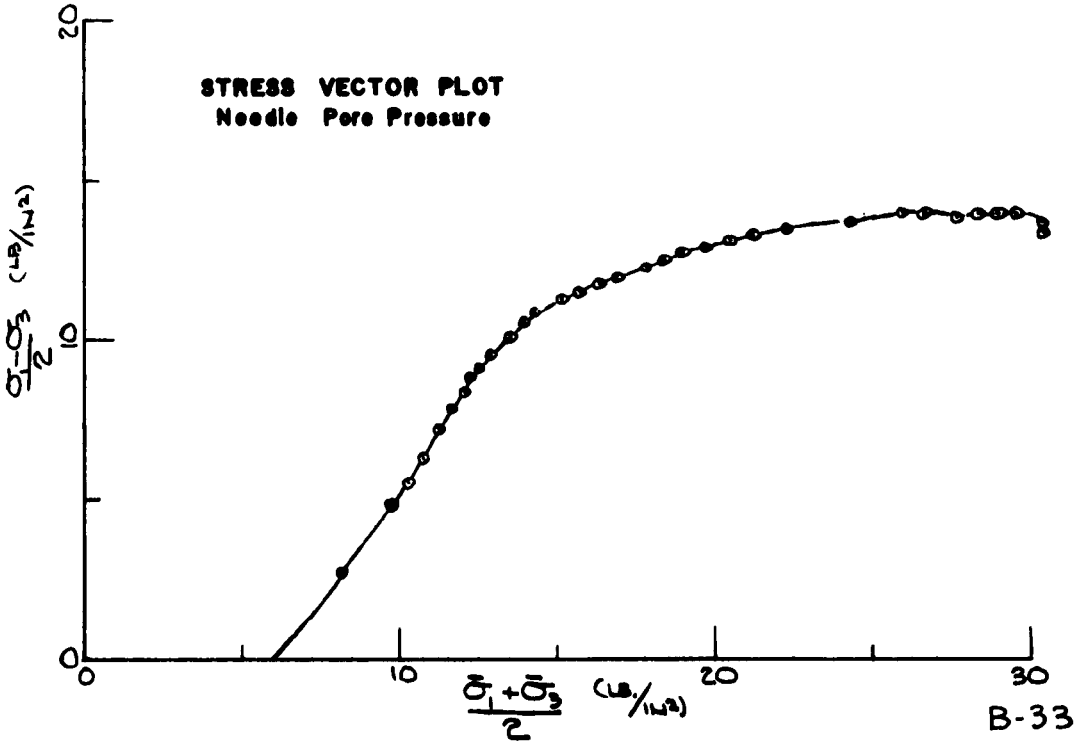
STRESS VECTOR PLOT
Needle Pore Pressure
(σ1-σ3)/2 (LB/IN²)
(σ1+σ3)/2 (LB./IN²)

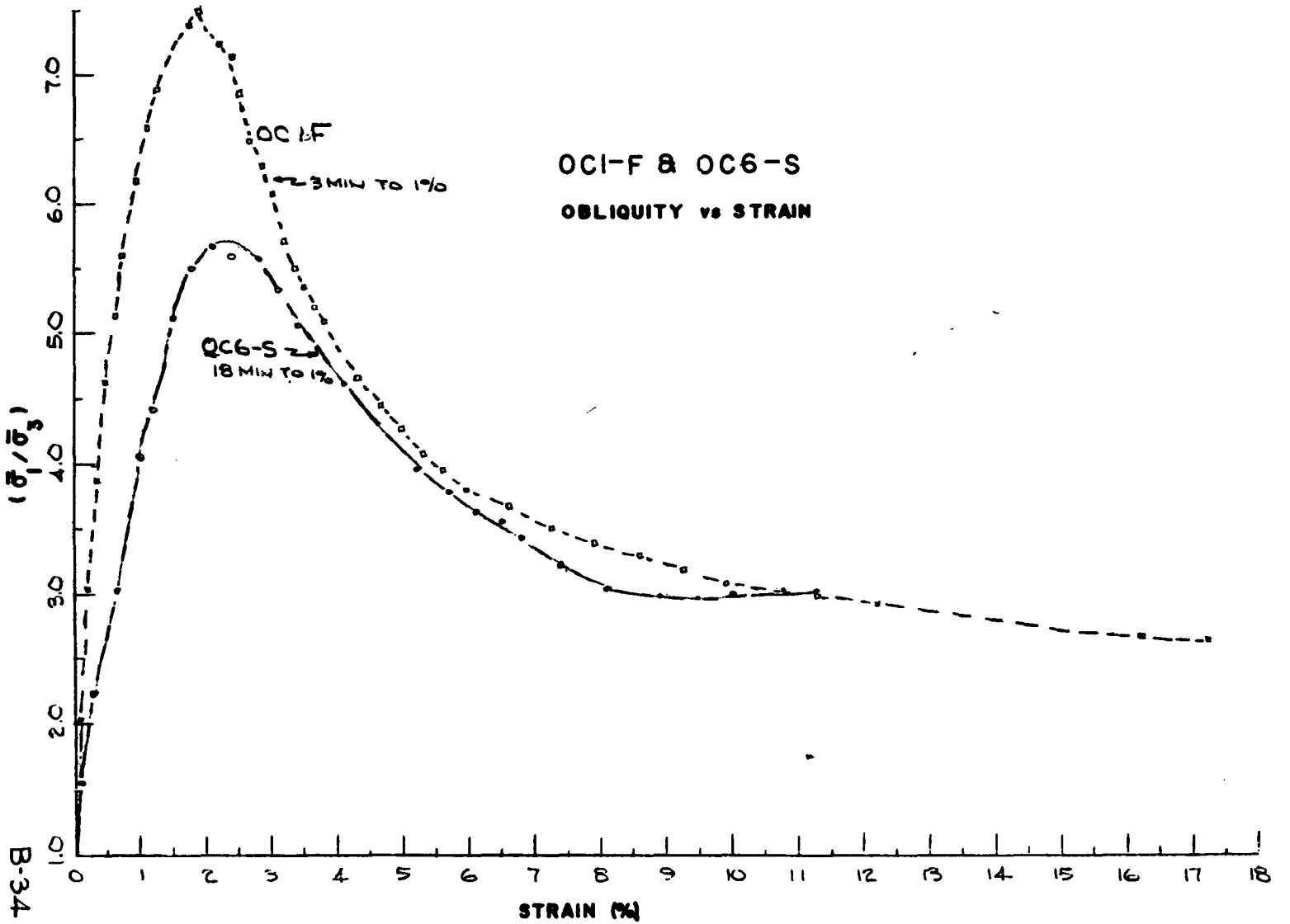
OC1-F & OC6-S
OBLIQUITY vs STRAIN
OC1-F
3 MIN TO 1%
OC6-S
18 MIN TO 1%
$(\bar{\sigma}_1/\bar{\sigma}_3)$
STRAIN (%)
1.0
2.0
3.0
4.0
5.0
6.0
7.0
0
1
2
3
4
5
6
7
8
9
10
11
12
13
14
15
16
17
18

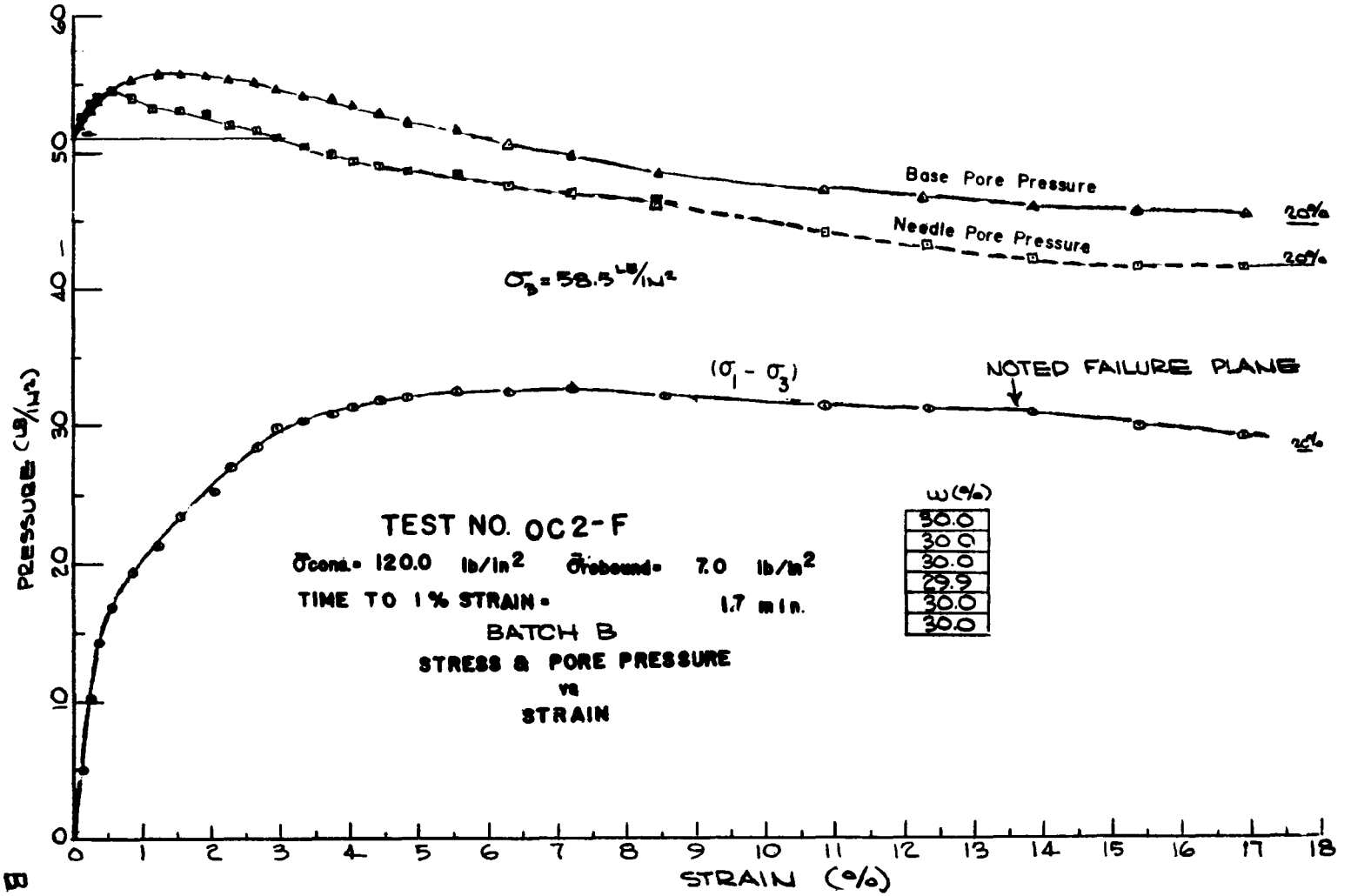
Base Pore Pressure
Needle Pore Pressure
$\sigma_3 = 58.5$ lb/in²
$(\sigma_1 - \sigma_3)$
NOTED FAILURE PLANE
TEST NO. OC2-F
$\bar{\sigma}_{cons.}$ = 120.0 lb/in² $\bar{\sigma}_{rebound}$ = 7.0 lb/in²
TIME TO 1% STRAIN = 1.7 min.
BATCH B
STRESS & PORE PRESSURE
vs
STRAIN
ω(%)
30.0
30.0
30.0
29.9
30.0
30.0
PRESSURE (lb/in²)
STRAIN (%)

OC2-F
OBLIQUITY vs STRAIN
$(\sigma_1-\sigma_3)_{MAX}$
σ_1/σ_3
1.0
2.0
3.0
4.0
5.0
0
1
2
3
4
5
6
7
8
9
10
11
12
13
14
15
16
17
18
STRAIN (%)

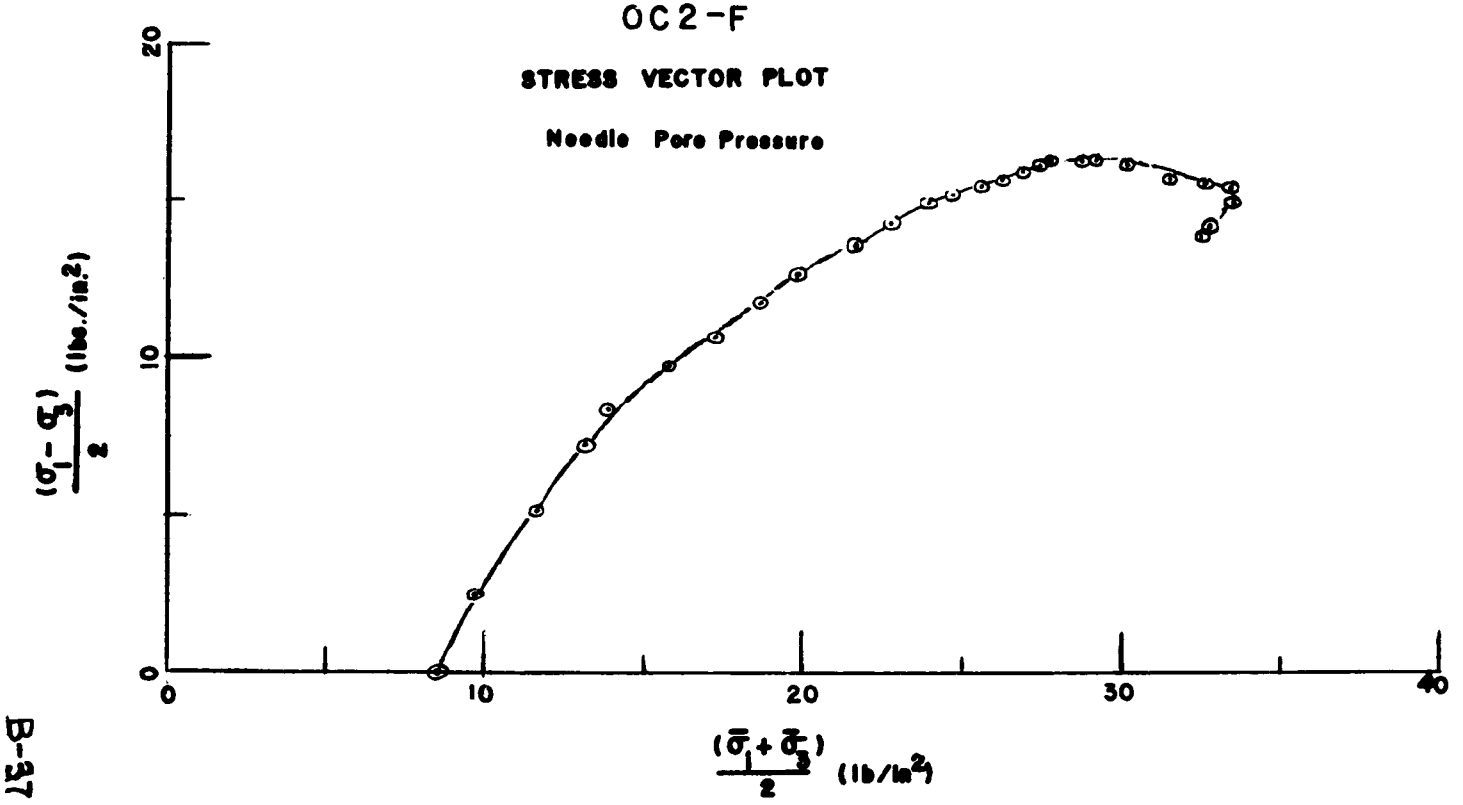
OC2-F
STRESS VECTOR PLOT
Needle Pore Pressure
$\frac{(\bar{\sigma}_1 - \bar{\sigma}_3)}{2}$ (lbs./in.^{2})
$\frac{(\bar{\sigma}_1 + \bar{\sigma}_3)}{2}$ (lb/in^2)
0
10
20
30
40

TEST NO. OC3-F

$\bar{\sigma}_{cons.}$ = 117.5 lb/in^2 $\bar{\sigma}_{rebound}$ = 7.2 lb/in^2

TIME TO 1% STRAIN = 3/4 min

BATCH B

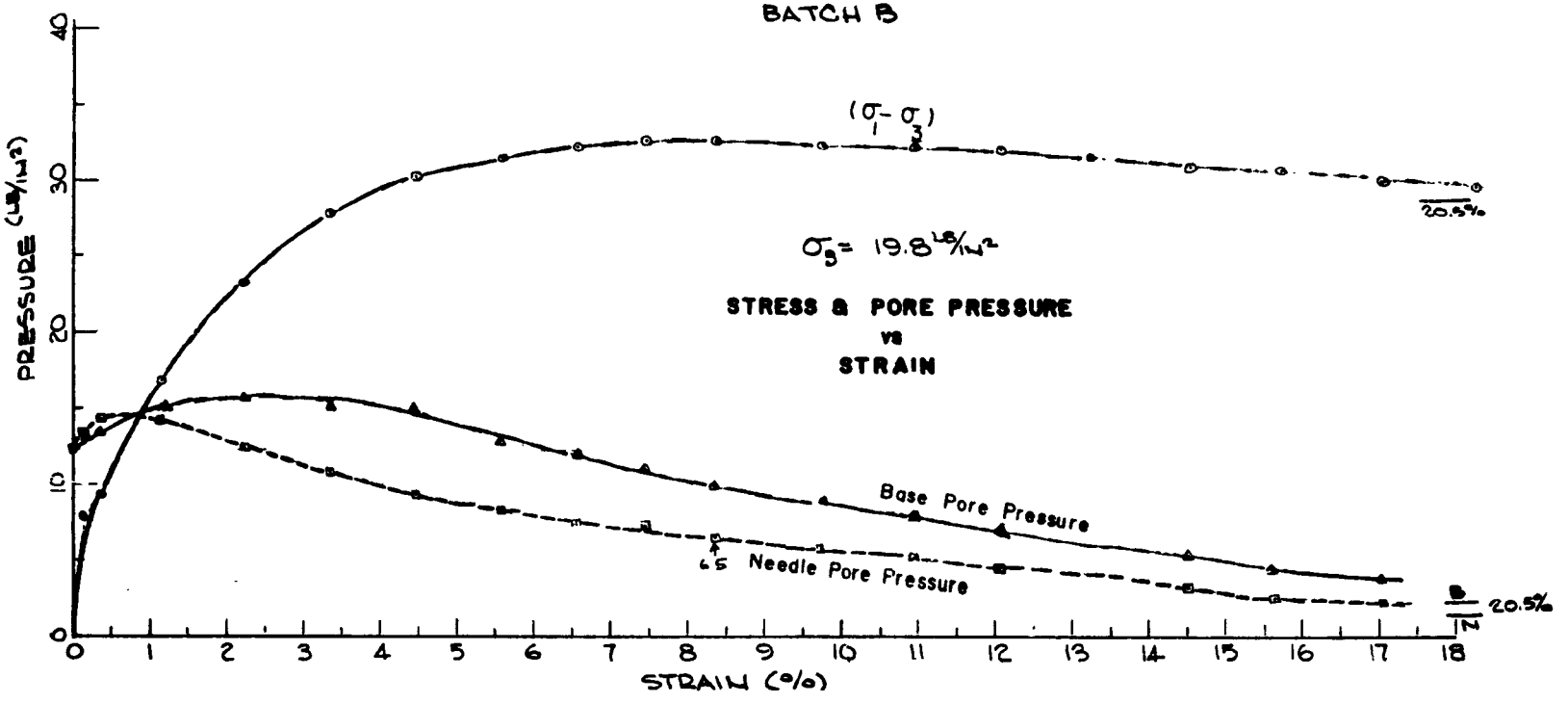

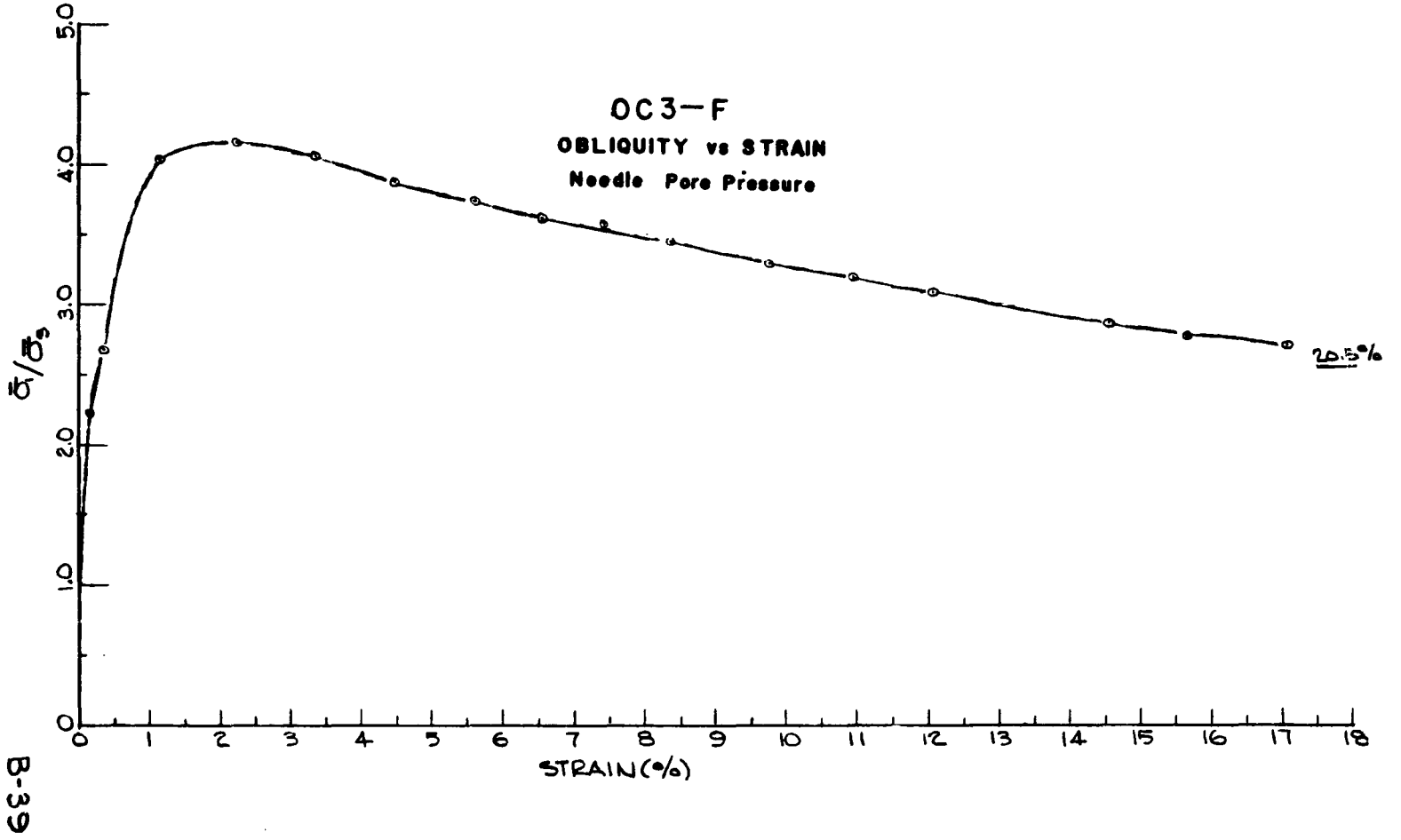
OC3—F
OBLIQUITY vs STRAIN
Needle Pore Pressure
$\bar{\sigma}_1/\bar{\sigma}_3$
STRAIN(%)
20.5%
0
1.0
2.0
3.0
4.0
5.0
0 1 2 3 4 5 6 7 8 9 10 11 12 13 14 15 16 17 18

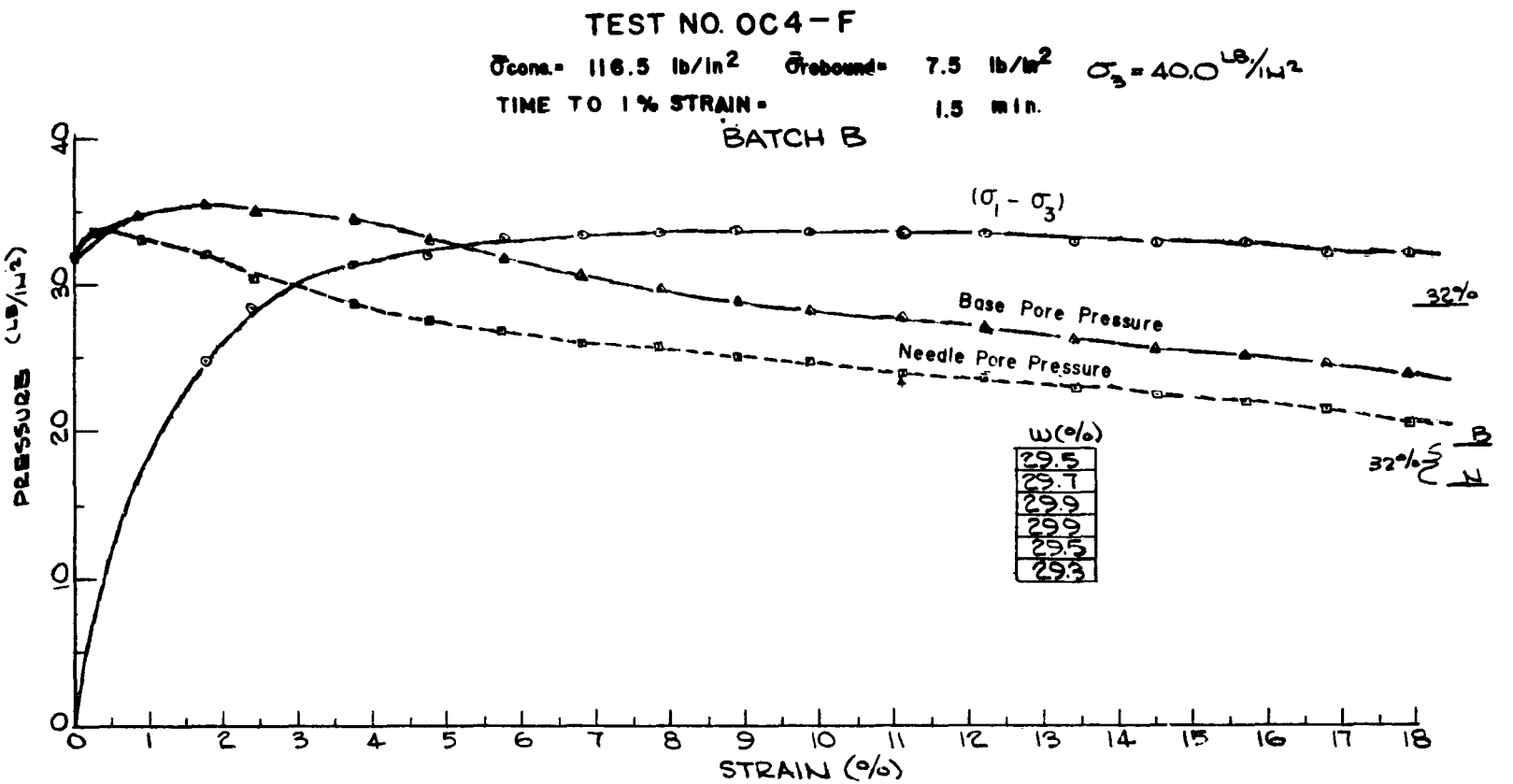
TEST NO. OC4-F
σ̄cons.= 116.5 lb/in² σ̄rebound= 7.5 lb/in² σ3 = 40.0 lb/in²
TIME TO 1% STRAIN = 1.5 min.
BATCH B
(σ1 - σ3)
Base Pore Pressure
Needle Pore Pressure
32%
B
32%
w(%)
29.5
29.7
29.9
29.9
29.5
29.3
PRESSURE (lb/in²)
STRAIN (%)
0
10
20
30
40
0 1 2 3 4 5 6 7 8 9 10 11 12 13 14 15 16 17 18

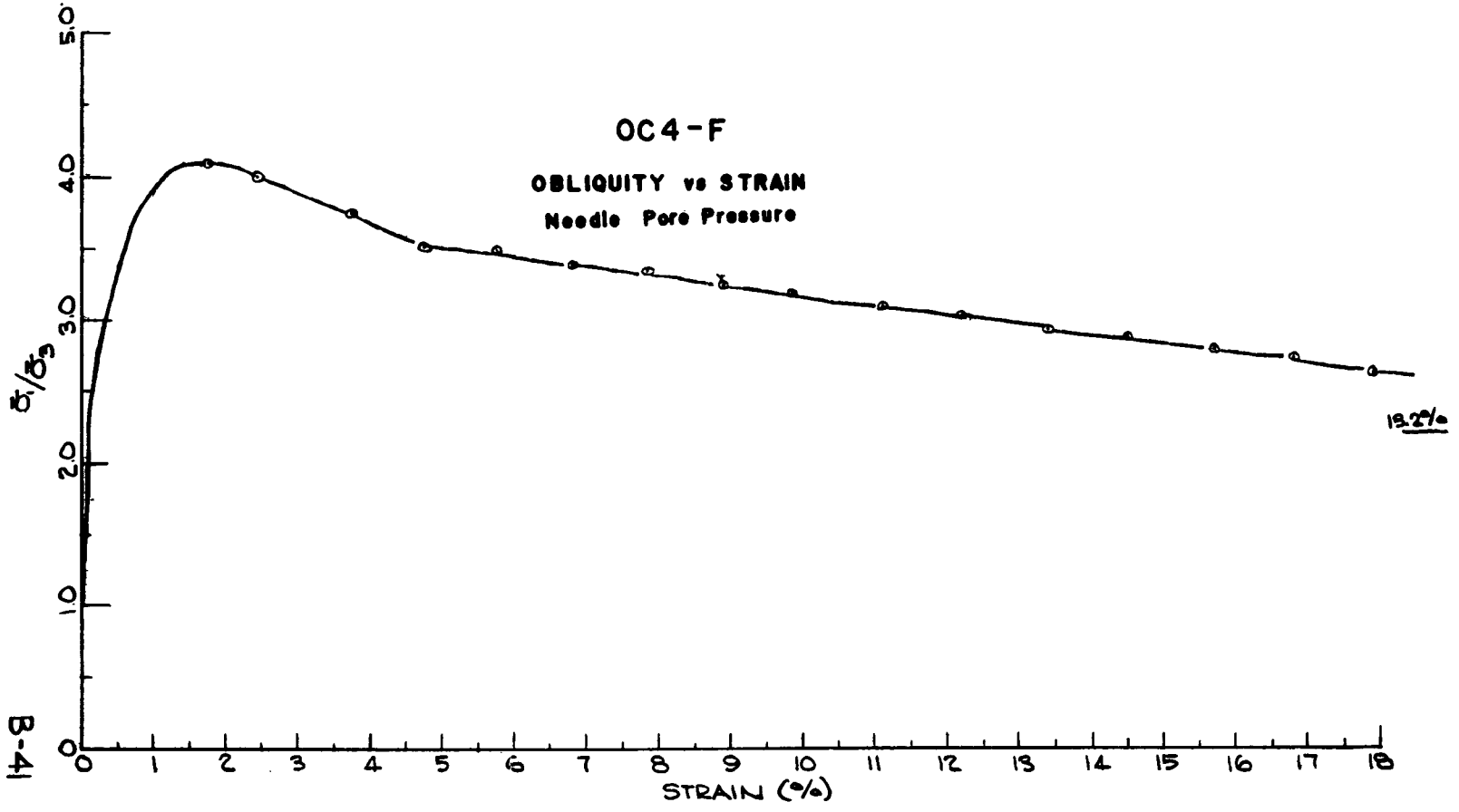
OC4-F
OBLIQUITY vs STRAIN
Needle Pore Pressure
σ_1/σ_3
STRAIN (%)
19.2%
0
1.0
2.0
3.0
4.0
5.0
0 1 2 3 4 5 6 7 8 9 10 11 12 13 14 15 16 17 18

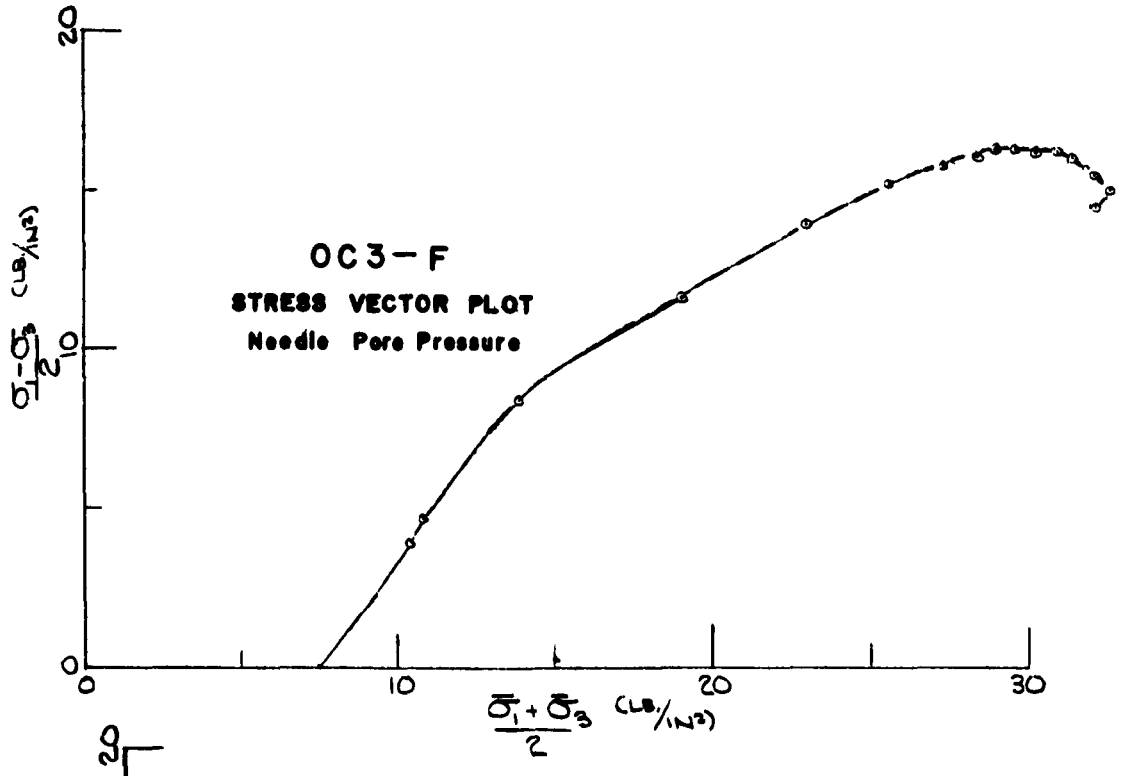
OC3-F
STRESS VECTOR PLOT
Needle Pore Pressure
$\frac{\sigma_1-\sigma_3}{2}$ (LB/IN²)
$\frac{\sigma_1+\sigma_3}{2}$ (LB/IN²)
0
10
20
30

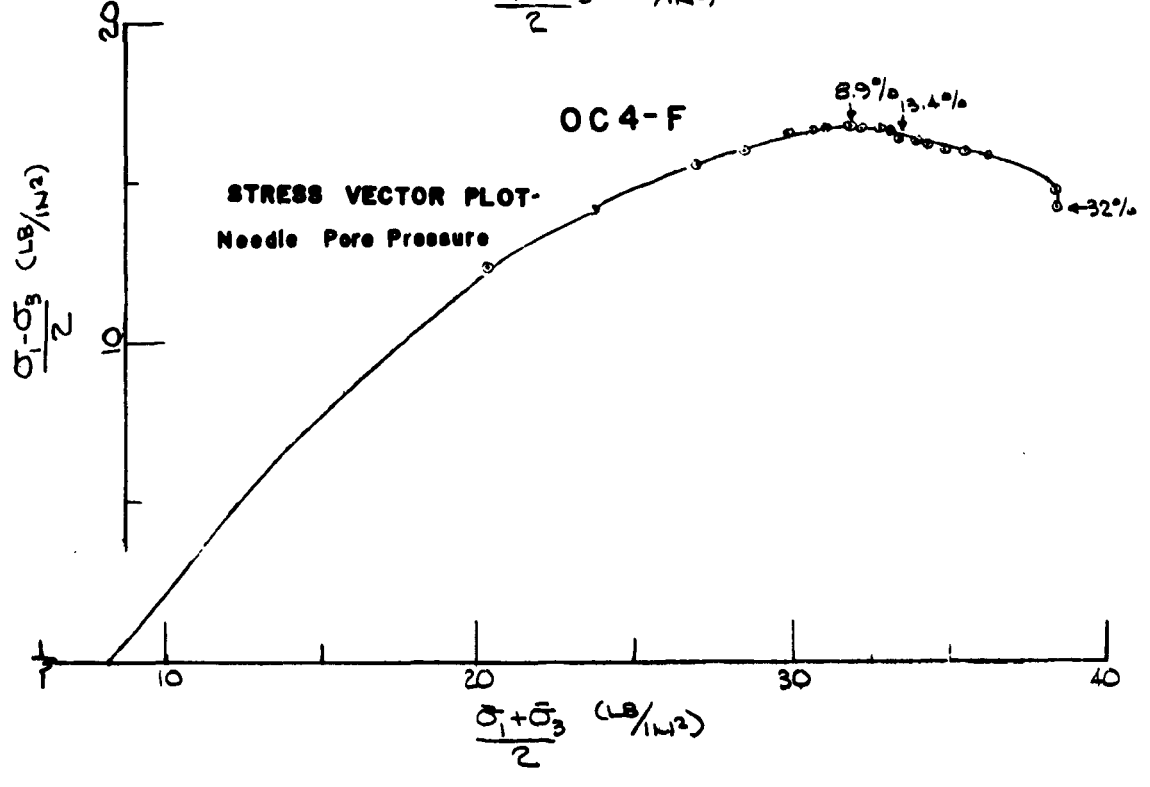
OC4-F
STRESS VECTOR PLOT-
Needle Pore Pressure
8.9%
13.4%
←32%
$\frac{\sigma_1-\sigma_3}{2}$ (LB/IN²)
$\frac{\sigma_1+\sigma_3}{2}$ (LB/IN²)
10
20
30
40

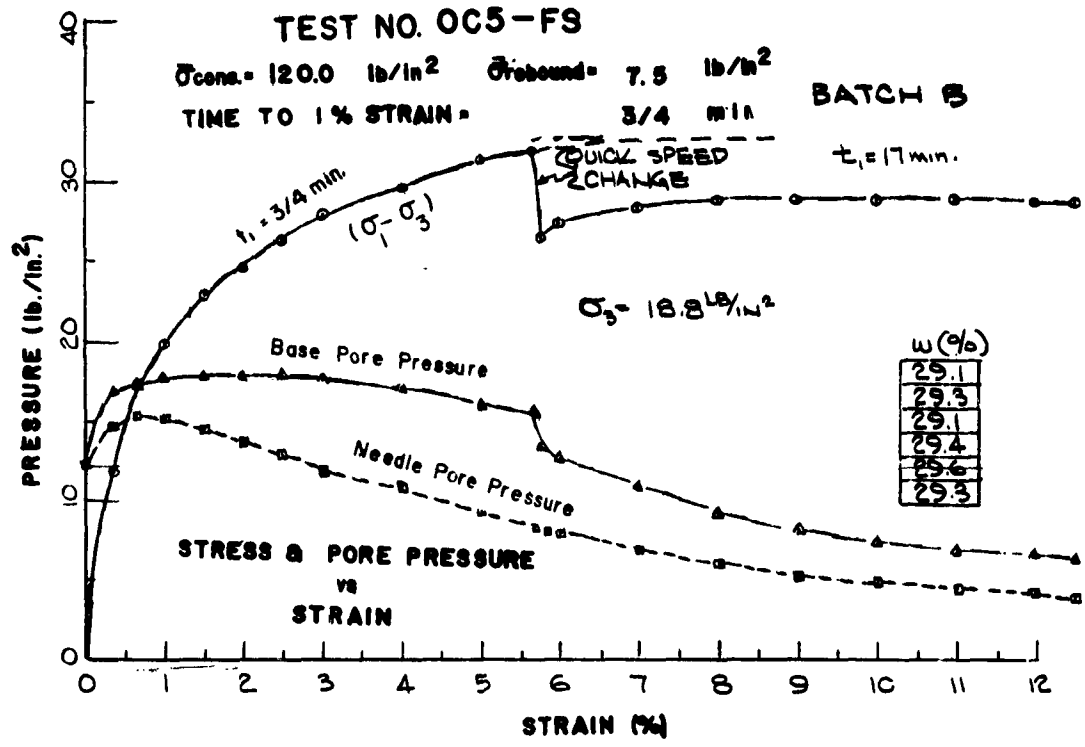
TEST NO. OC5-FS
$\bar{\sigma}_{cons.}$ = 120.0 lb/in^2 $\bar{\sigma}_{rebound}$ = 7.5 lb/in^2
TIME TO 1% STRAIN = 3/4 min
BATCH B
t_1 = 17 min.
QUICK SPEED CHANGE
t_1 = 3/4 min.
$(\sigma_1 - \sigma_3)$
σ_3 = 18.8 LB/IN^2
Base Pore Pressure
Needle Pore Pressure
STRESS & PORE PRESSURE vs STRAIN
w(%)
29.1
29.3
29.1
29.4
29.6
29.3
PRESSURE (lb./in.^{2})
STRAIN (%)

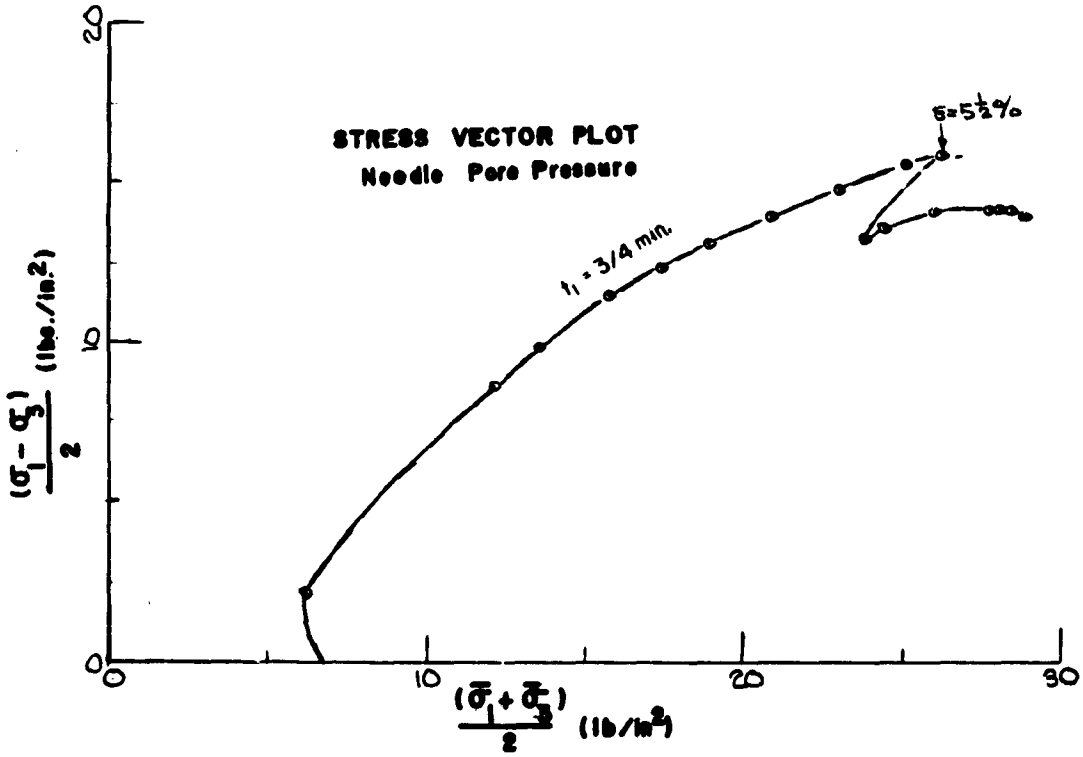
STRESS VECTOR PLOT
Needle Pore Pressure
t_1 = 3/4 min.
$\varepsilon = 5\frac{1}{2}\%$
$\frac{(\sigma_1 - \sigma_3)}{2}$ (lbs./in.^{2})
$\frac{(\bar{\sigma}_1 + \bar{\sigma}_3)}{2}$ (lb/in^2)

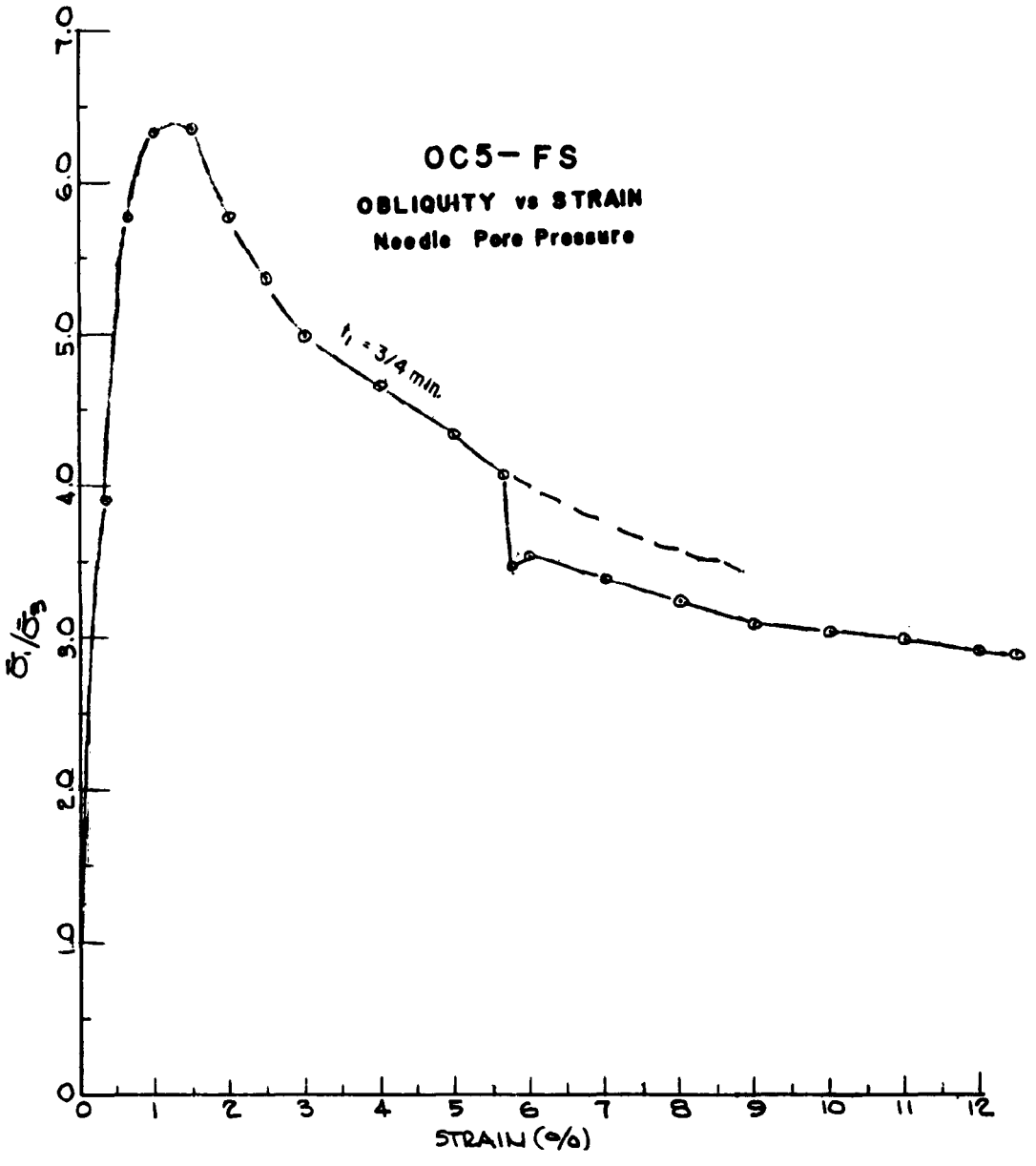
OC5-FS
OBLIQUITY vs STRAIN
Needle Pore Pressure
t_1 = 3/4 min.
$\bar{\sigma}_1/\bar{\sigma}_3$
STRAIN (%)
0
1.0
2.0
3.0
4.0
5.0
6.0
7.0
0
1
2
3
4
5
6
7
8
9
10
11
12

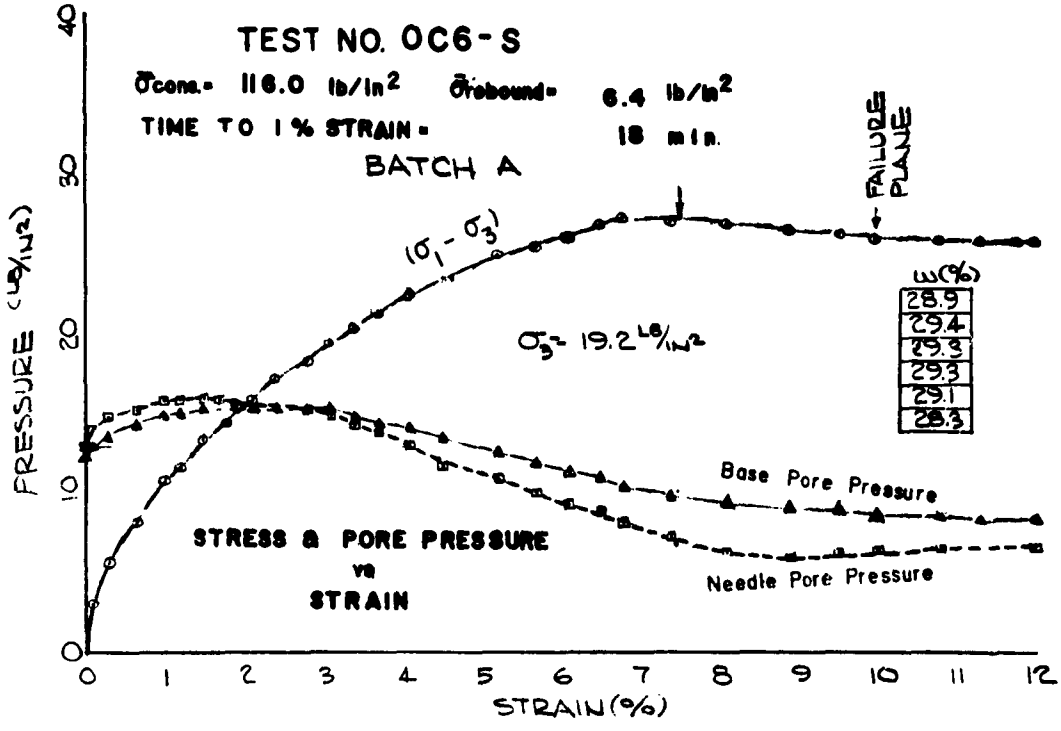
TEST NO. OC6-S
σ̄con.= 116.0 lb/in²
σ̄rebound= 6.4 lb/in²
TIME TO 1% STRAIN = 18 min.
BATCH A
FAILURE PLANE
(σ1 - σ3)
σ3 = 19.2 LB/IN²
w(%)
28.9
29.4
29.3
29.3
29.1
28.3
Base Pore Pressure
Needle Pore Pressure
STRESS & PORE PRESSURE
vs
STRAIN
PRESSURE (LB/IN2)
STRAIN (%)

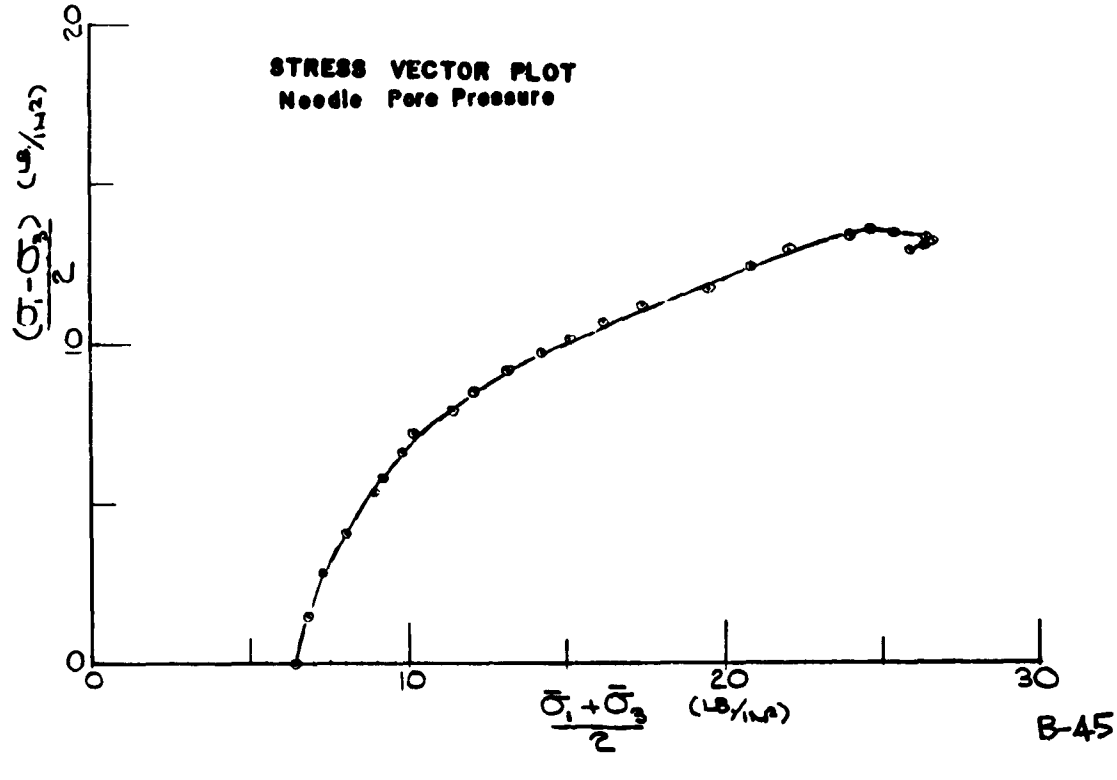
STRESS VECTOR PLOT
Needle Pore Pressure
(σ1 - σ3)/2 (LB/IN2)
(σ1 + σ3)/2 (LB/IN2)

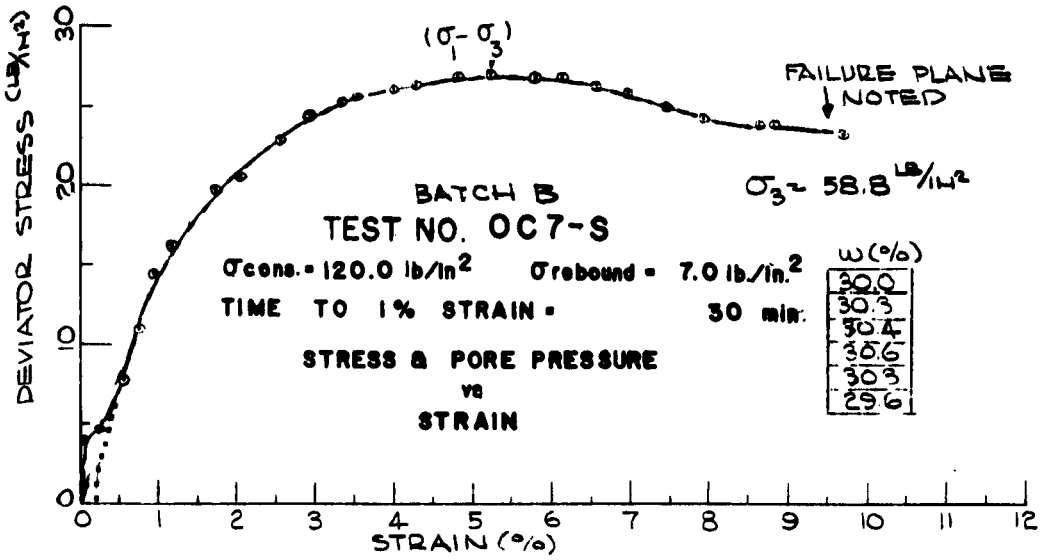
DEVIATOR STRESS (LB/IN²)
(σ1 - σ3)
FAILURE PLANE NOTED
BATCH B
TEST NO. OC7-S
σcons. = 120.0 lb/in²
σrebound = 7.0 lb./in.²
TIME TO 1% STRAIN = 30 min.
σ3 = 58.8 LB/IN²
STRESS & PORE PRESSURE
vs
STRAIN
w(%)
30.0
30.3
30.4
30.6
30.3
29.6
STRAIN (%)

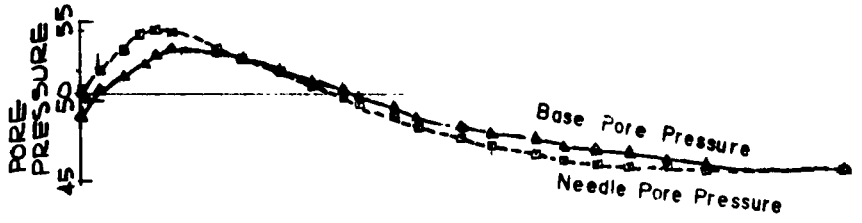
PORE PRESSURE
Base Pore Pressure
Needle Pore Pressure

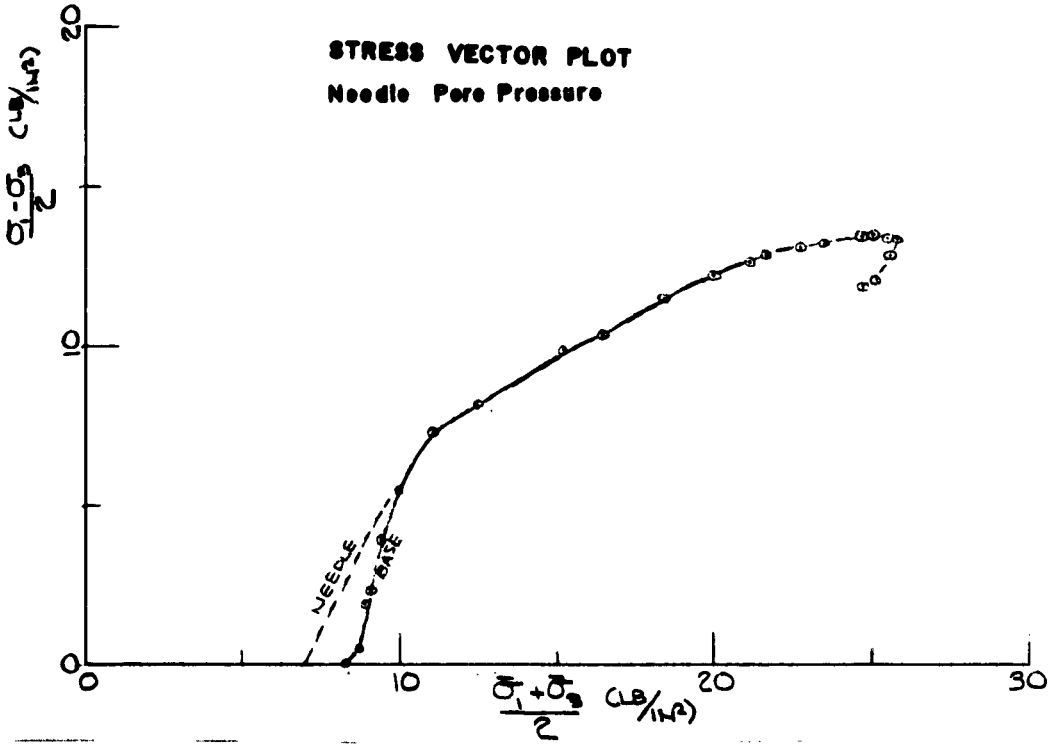
STRESS VECTOR PLOT
Needle Pore Pressure
(σ1 - σ3)/2 (LB/IN²)
NEEDLE
BASE
(σ1 + σ3)/2 (LB/IN²)

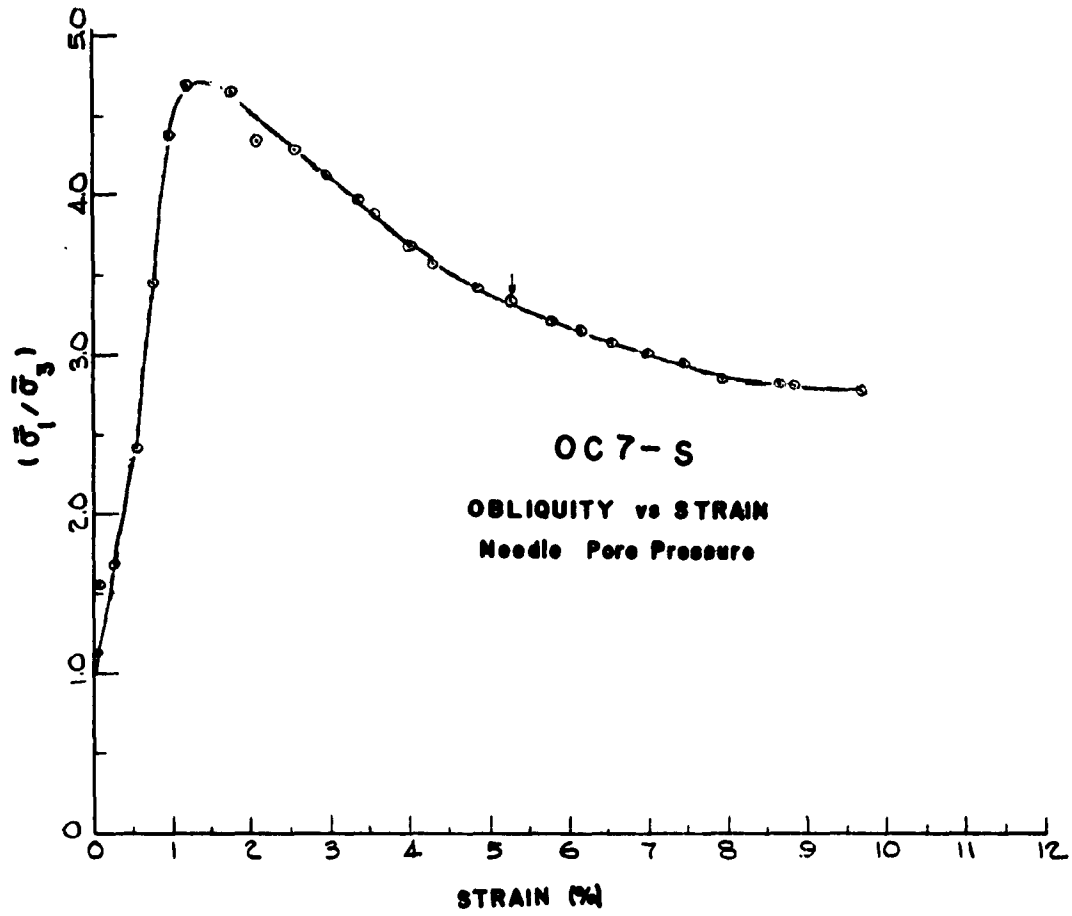
OC 7 - S
OBLIQUITY vs STRAIN
Needle Pore Pressure
$(\bar{\sigma}_1/\bar{\sigma}_3)$
STRAIN (%)
0
1.0
2.0
3.0
4.0
5.0
0
1
2
3
4
5
6
7
8
9
10
11
12

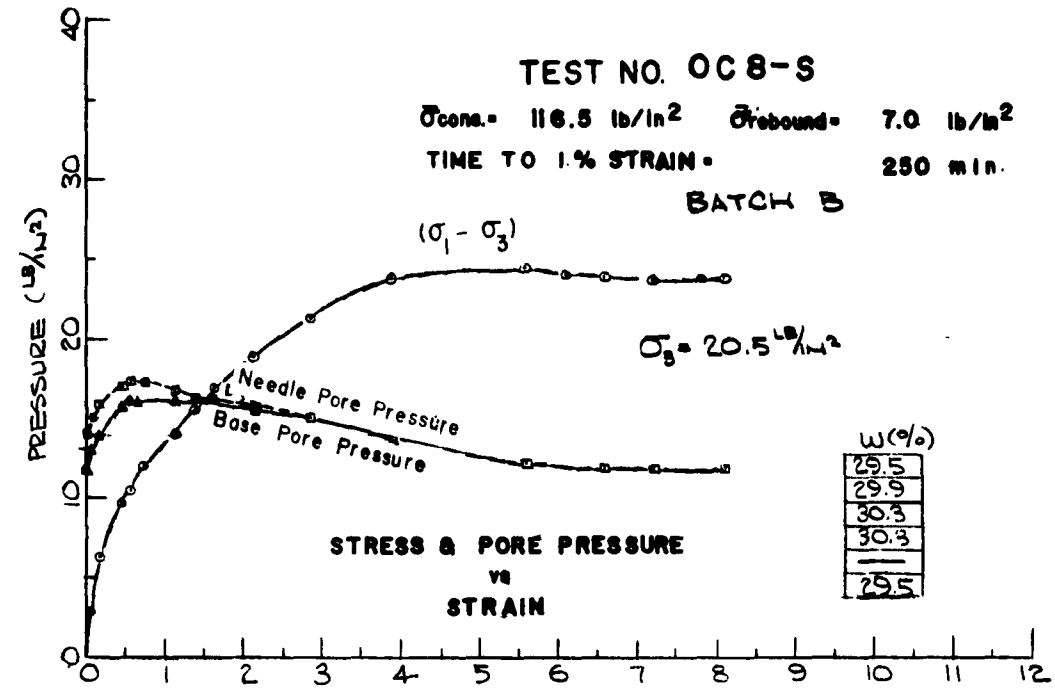
TEST NO. OC 8-S
σ̄cons.= 116.5 lb/in²
σ̄rebound= 7.0 lb/in²
TIME TO 1.% STRAIN = 250 min.
BATCH B
(σ1 - σ3)
σ3 = 20.5 LB/IN²
Needle Pore Pressure
Base Pore Pressure
W(%)
29.5
29.9
30.3
30.3
29.5
STRESS & PORE PRESSURE
vs
STRAIN
PRESSURE (LB/IN²)
0
10
20
30
40
0
1
2
3
4
5
6
7
8
9
10
11
12

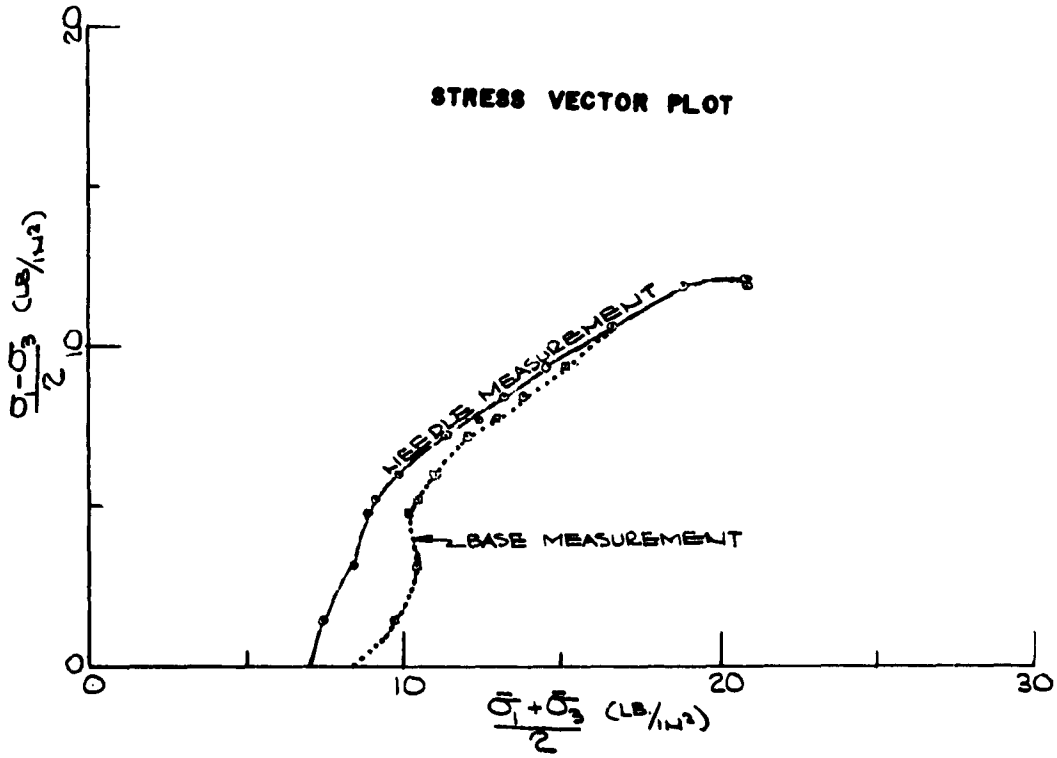
STRESS VECTOR PLOT
(σ1-σ3)/2 (LB/IN²)
NEEDLE MEASUREMENT
BASE MEASUREMENT
(σ1+σ3)/2 (LB/IN²)
0
10
20
30

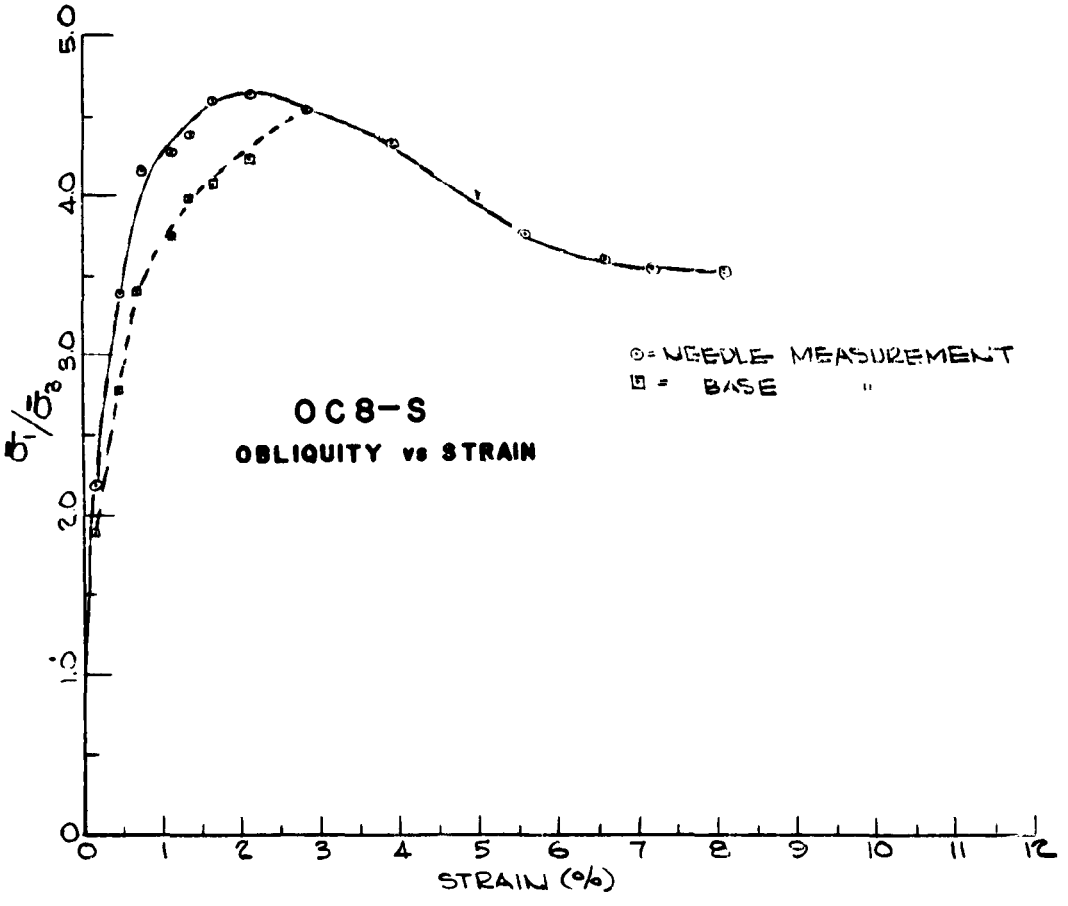
OC8-S
OBLIQUITY vs STRAIN
⊙= NEEDLE MEASUREMENT
□ = BASE "
$\bar{\sigma}_1/\bar{\sigma}_3$
STRAIN (%)
0
1.0
2.0
3.0
4.0
5.0
0 1 2 3 4 5 6 7 8 9 10 11 12

TEST NO. OC 9-S

$\bar{\sigma}_{cons.}$ = 116.5 lb/in^2 $\bar{\sigma}_{rebound}$ = 9.0 lb/in^2

BATCH B

NOTE:- THIS TEST WAS RUN AT RATE = .00001"/MIN
- IN CYLEREX
- WITH LOAD CELL
- CONSIDERABLE SEATING TROUBLE - PEDESTAL TO SHAFT OF LOAD CELL & CELL PISTON TO CAP
- ALSO ELECTRICITY OFF TO LOAD FRAME SPORADICALLY.
- DISTINCT FAILURE PLANE

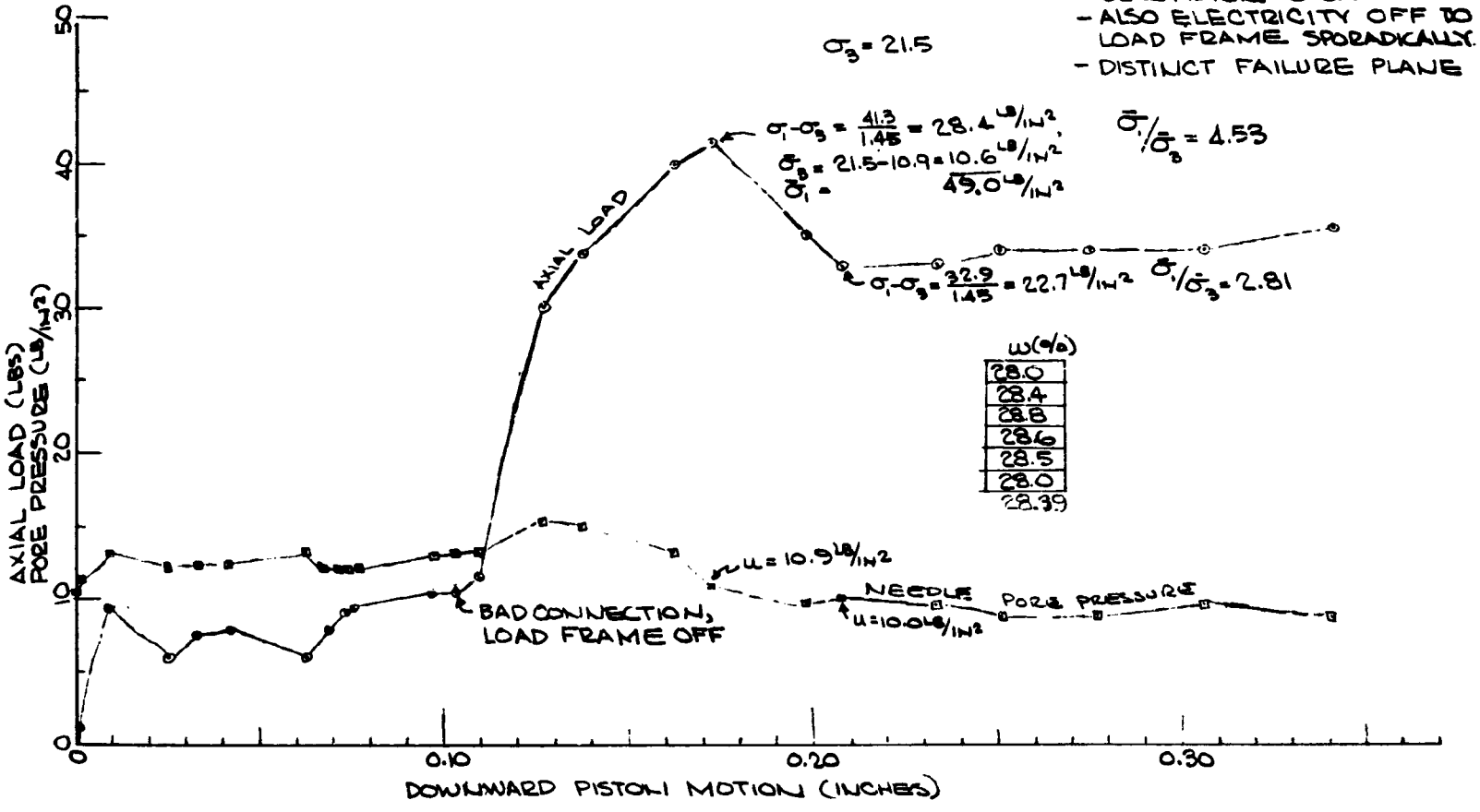

B-50

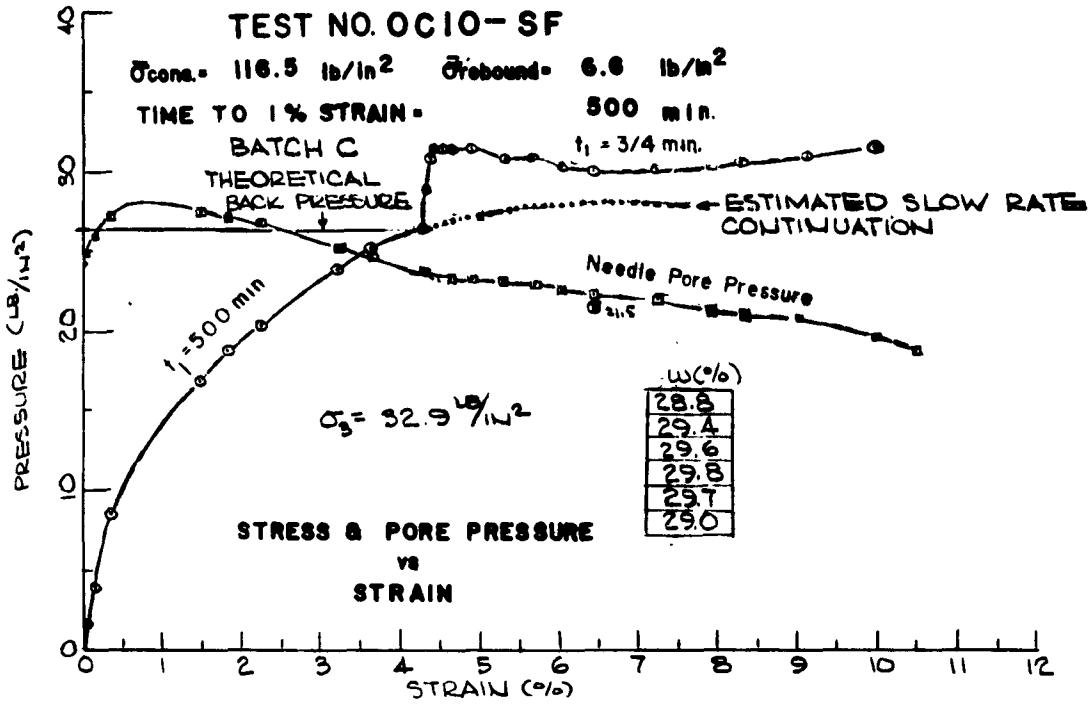
TEST NO. OC10-SF
$\bar{\sigma}_{cons.}$ = 116.5 lb/in^2 $\bar{\sigma}_{rebound}$ = 6.6 lb/in^2
TIME TO 1% STRAIN = 500 min.
BATCH C
THEORETICAL BACK PRESSURE
t_1 = 3/4 min.
ESTIMATED SLOW RATE CONTINUATION
Needle Pore Pressure
t_1 = 500 min
σ_3 = 32.9 lb/in^2
w(%)
28.8
29.4
29.6
29.8
29.7
29.0
STRESS & PORE PRESSURE vs STRAIN
PRESSURE (lb/in^2)
STRAIN (%)

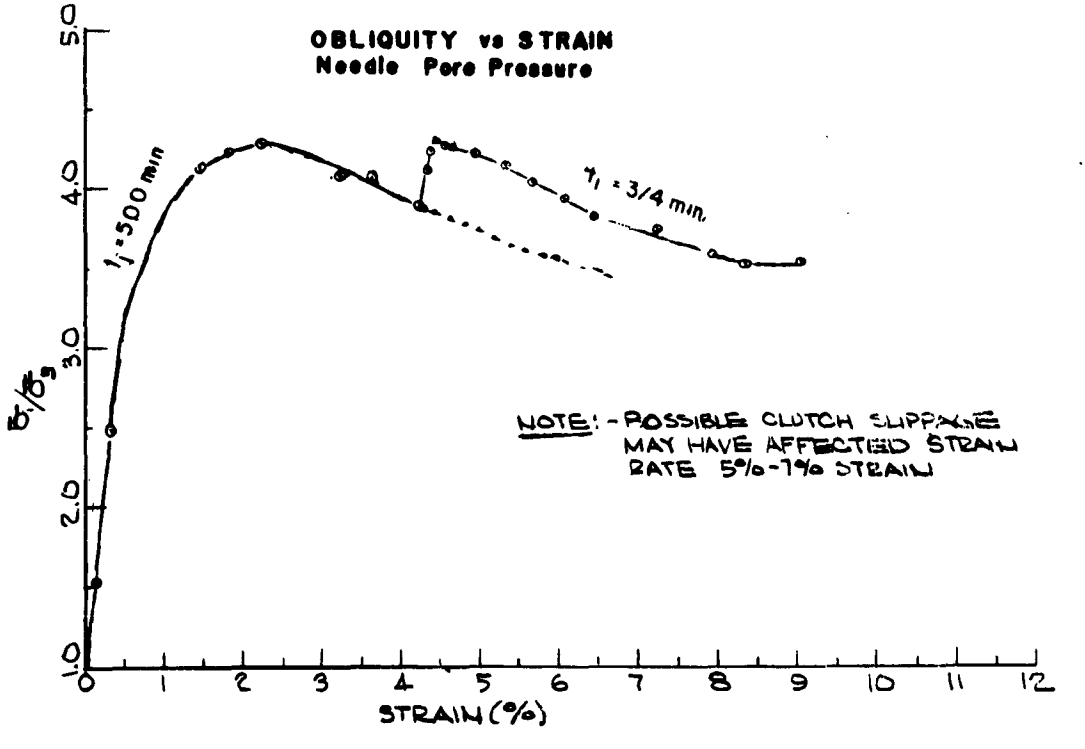
OBLIQUITY vs STRAIN
Needle Pore Pressure
t_1 = 500 min
t_1 = 3/4 min.
σ_1/σ_3
NOTE:- POSSIBLE CLUTCH SLIPPAGE MAY HAVE AFFECTED STRAIN RATE 5%-7% STRAIN
STRAIN (%)

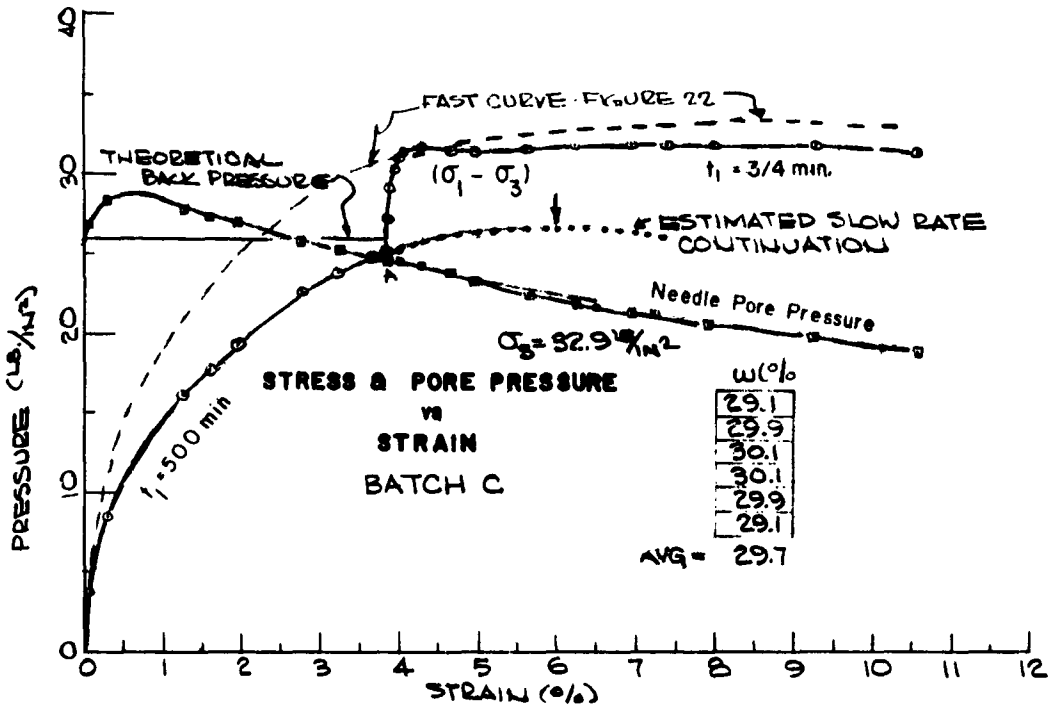
FAST CURVE - FIGURE 22
THEORETICAL BACK PRESSURE
$(\sigma_1 - \sigma_3)$
t_1 = 3/4 min.
ESTIMATED SLOW RATE COUNTINUATION
Needle Pore Pressure
σ_3 = 32.9 lb/in²
STRESS & PORE PRESSURE
vs
STRAIN
BATCH C
t_1 = 500 min
w(%)
29.1
29.9
30.1
30.1
29.9
29.1
AVG = 29.7
PRESSURE (lb/in²)
STRAIN (%)

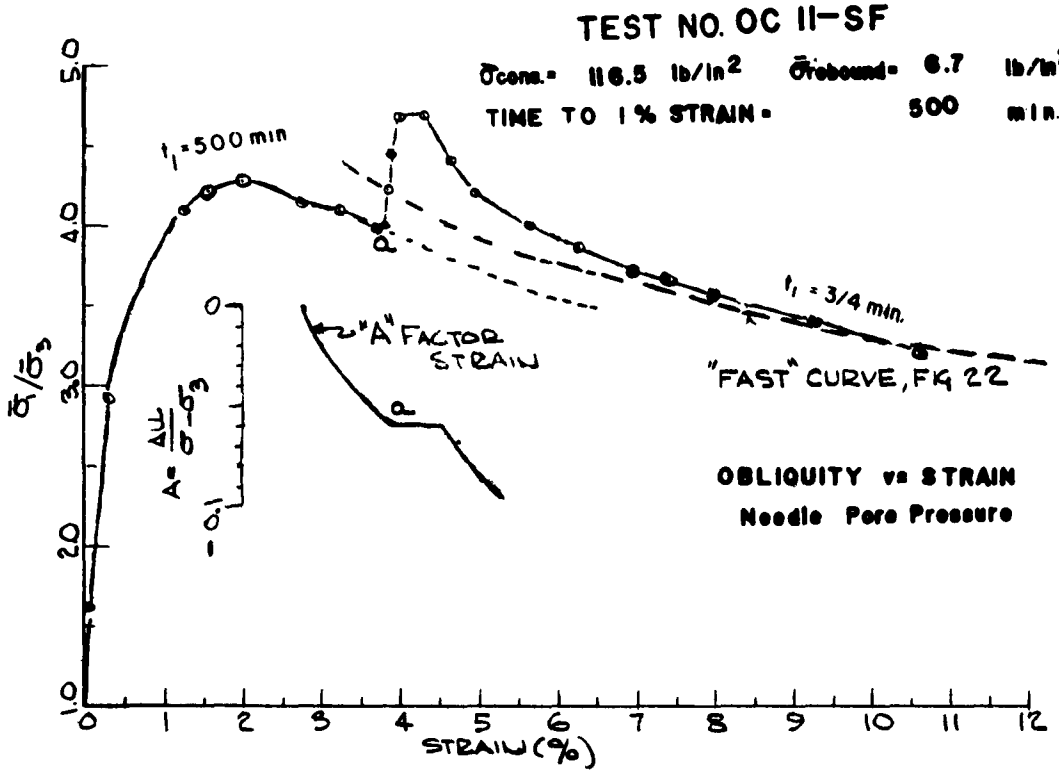
TEST NO. OC II-SF
$\bar{\sigma}_{cons.}$ = 116.5 lb/in²
$\bar{\sigma}_{rebound}$ = 6.7 lb/in²
TIME TO 1% STRAIN = 500 min.
t_1 = 500 min
t_1 = 3/4 min.
"A" FACTOR STRAIN
"FAST" CURVE, FIG 22
OBLIQUITY vs STRAIN
Needle Pore Pressure
$\bar{\sigma}_1/\bar{\sigma}_3$
$A = \frac{\Delta u}{\bar{\sigma}_1 - \bar{\sigma}_3}$
STRAIN (%)

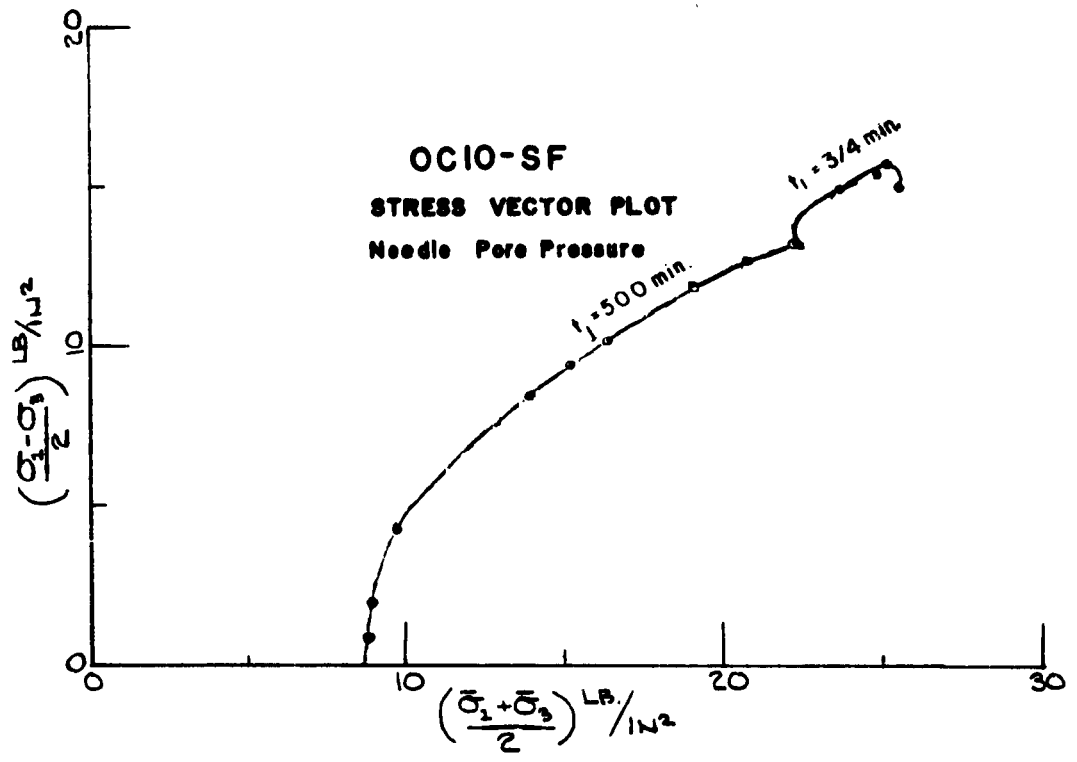
OC10-SF
STRESS VECTOR PLOT
Needle Pore Pressure
t_1 = 3/4 min.
t_1 = 500 min.
$\left(\frac{\bar{\sigma}_1-\bar{\sigma}_3}{2}\right)$ LB/IN²
$\left(\frac{\bar{\sigma}_1+\bar{\sigma}_3}{2}\right)$ LB./IN²
0
10
20
30

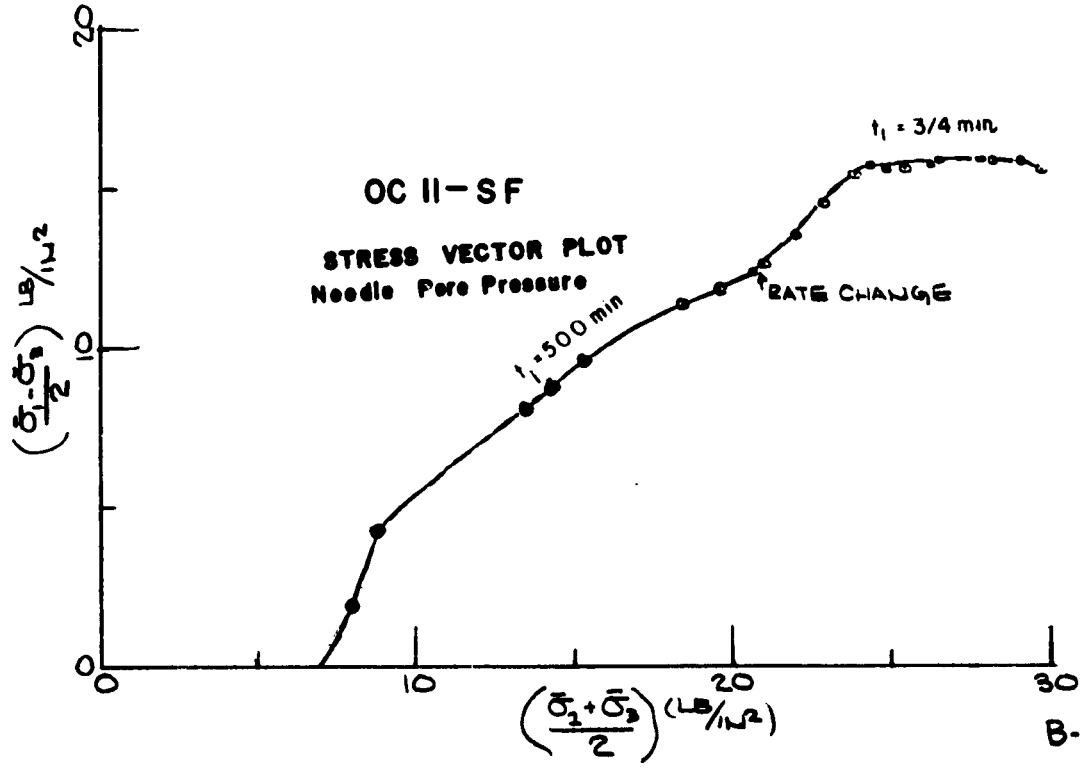
OC 11-SF
STRESS VECTOR PLOT
Needle Pore Pressure
t_1 = 3/4 min
t_1 = 500 min
RATE CHANGE
$\left(\frac{\bar{\sigma}_1-\bar{\sigma}_3}{2}\right)$ LB/IN²
$\left(\frac{\bar{\sigma}_1+\bar{\sigma}_3}{2}\right)$ (LB/IN²)
0
10
20
30

DISTRIBUTION LIST

Addresses	No. of Copies
Bureau of Mines, Washington, D. C., Attn: J. E. Crawford	1
Chief, Bureau of Yards and Docks, ND, Washington 25, D. C. Attn: D-440	1
Chief, Defense Atomic Support Agency, Washington 25, D. C. Attn: Document Library Attn: Major Vickery	12 1
Chief of Engineers, Department of the Army, Washington 25, D. C. Attn: ENGTE-E Attn: ENGMC-EB	1 2
Chief of Naval Operations, ND, Washington, D. C. Attn: Op-75	1
Chief of Research and Development, DA, Washington 25, D.C. Attn: Atomic Division	1
Commander, Air Force Ballistic Missile Division, Air Research and Development Command, Attn: WDFN, P. O. Box 262, Inglewood 49, California	1
Commander, Armed Services Technical Information Agency (ASTIA), Arlington Hall Station, Arlington 12, Va.	20
Commander, Air Force Special Weapons Center, Kirtland Air Force Base, Albuquerque, N. M., Attn: SWRS	4
Commander, Wright Air Development Center, Wright-Patterson Air Force Base, Ohio, Attn: WCOSI	1
Command General, U. S. Army Materiel Command, Attn: AMCRD-RS-ES, Room 2507, Building T-7, Washington 25, D. C.	3
Commanding Officer and Director, U. S. Naval Civil Engineering Laboratory, Port Hueneme, Calif.	1
Director, Weapons Systems Evaluation Group OSD, Room 1E880, The Pentagon, Washington 25, D. C.	1

Director, U. S. Army Engineer Waterways Experiment Station, P. O. Box 631, Vicksburg, Miss. 25

Director of Civil Engineering, Headquarters, U. S. Air Force, Washington 25, D. C., Attn: AFOCE

Director of Defense Research and Engineering, Washington 25, D. C., Attn: Technical Library 1

Headquarters, U. S. Air Force, Washington 25, D. C., Attn: AFTAC, C. F. Romney 2

Space Technology Laboratory, Inglewood, Calif., Attn: B. Sussholz 1

U. S. Coast and Geodetic Survey, Washington, D. C. Attn: D. S. Gardner 1

U. S. Coast and Geodetic Survey, San Francisco, Calif. Attn: W. K. Cloud 1

U. S. Geological Survey, Washington, D. C., Attn: J. R. Balsley 1

California Institute of Technology, Pasadena, Calif.
Attn: F. Press 1
Attn: R. Benioff 1

Columbia University, New York, N.Y., Attn: J. E. Oliver 1

Pennsylvania State College, Atomic Defense Engineering Dept., State College, Pa., Attn: Prof. Albright 1

Stanford Research Institute, Physical Sciences Division Menlo Park, Calif., Attn: Dr. R. B. Vaille, Jr. 2

American Machine and Foundry, 7501 North Natchez Avenue, Niles 48, Ill., Attn: Mr. Tom Morrison 1

Barry Wright Corporation, 700 Pleasant St., Watertown 72, Mass., Attn: Mr. Cavanaugh 1

Holmes and Narvey, Los Angeles, Calif., Attn: S. B. Smith 1

Dr. Harold Brode, RAND Corporation, 1700 Main Street, Santa Monica, Calif. 1

Dr. N. M. Newmark, Civil Engineering Hall, University of Illinois, Urbana, Illinois 1

Dr. T. H. Schiffman, Armour Research Foundation, Illinois Institute of Technology, Technology Center, Chicago 16, Ill. 1

Prof. F. E. Richart, Jr., Dept. of Civil Engineering, University of Michigan, Ann Arbor, Michigan 1

Prof. Robert L. Kondner, The Technological Institute, Northwestern University, Evanston, Ill. 1

Prof. Gerald A. Leonards, School of Civil Engineering Purdue University, Lafayette, Indiana 1

Prof. H. Bolton Seed, Dept. of Civil Engineering, University of California, Berkeley, Calif. 1

Prof. H. Neils Thompson, Civil Engineering Dept., University of Texas, Austin 12, Texas 1

Mr. Kenneth Kaplan, United Research Services 1811 Trousdale Drive, Burlingame, Calif. 1

Mr. W. R. Perret, 5112, Sandia Corporation, Sandia Base, Albuquerque, N. M. 1

Mr. Fred Sauer, Physics Department, Stanford Research Institute, Menlo Park, Calif. 1

Mr. A. A. Thompson, Terminal Ballistics Laboratory, Aberdeen Proving Ground, Aberdeen, Md. 1

Mr. C. J. Nuttall of Wilson, Nuttall, Raimond Engineers, Inc., Chestertown, Md. 1

Dr. Grover L. Rogers, Recon, Inc., Box 3622 MSS, Tallahassee, Florida 1